

United Arab Emirates University

**Scholarworks@UAEU**

---

Dissertations

Electronic Theses and Dissertations

---

4-2020

**ACTIVATED CARBON NANOFIBERS FROM RENEWABLE (LIGNIN)  
AND WASTE RESOURCES (RECYCLED PET) AND THEIR  
ADSORPTION CAPACITY OF REFRACTORY SULFUR COMPOUNDS  
FROM FOSSIL FUELS**

Efstratios Svinterikos

Follow this and additional works at: [https://scholarworks.uaeu.ac.ae/all\\_dissertations](https://scholarworks.uaeu.ac.ae/all_dissertations)



Part of the [Computer Sciences Commons](#)

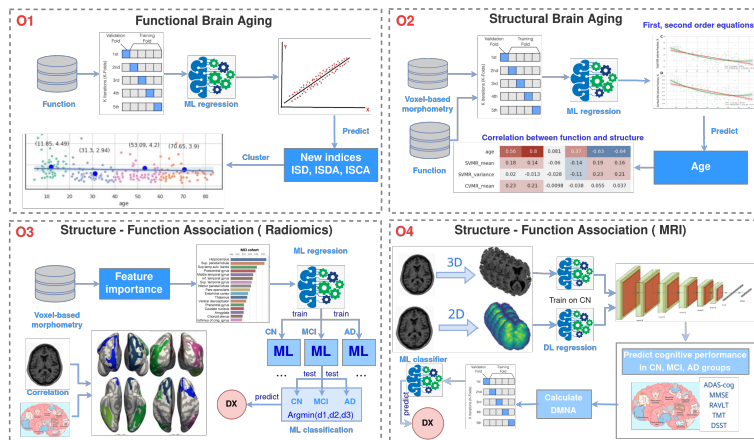
---

DOCTORATE DISSERTATION NO. 2022: 9

College of Information Technology

# DIAGNOSTICS OF DEMENTIA FROM STRUCTURAL AND FUNCTIONAL MARKERS OF BRAIN ATROPHY WITH MACHINE LEARNING

*Tetiana Habuza*



June 2022

United Arab Emirates University

College of Information Technology

**DIAGNOSTICS OF DEMENTIA FROM STRUCTURAL AND  
FUNCTIONAL MARKERS OF BRAIN ATROPHY WITH  
MACHINE LEARNING**

Tetiana Habuza

This dissertation is submitted in partial fulfillment of the requirements for  
the degree of Doctor of Philosophy in Informatics and Computing

June 2022

**United Arab Emirates University Doctorate Dissertation**

**2022: 9**

Cover: Image regarding Information and Communication Technology in this study

(Photo: By Tetiana Habuza)

©2022 Copyright Tetiana Habuza, Al Ain, UAE


All Rights Reserved

Print: University Print Service, UAEU 2022



## Declaration of Original Work

I, Tetiana Habuza, the undersigned, a graduate student at the United Arab Emirates University (UAEU), and the author of this dissertation, entitled "*Diagnostics of Dementia from Structural and Functional Markers of Brain Atrophy with Machine Learning*", hereby, solemnly declare that this the original research work that has been done by me under the supervision of Prof. Nazar Zaki, in the College of Information Technology at the UAEU. This work has not previously been presented or published, or formed the basis for the award of any academic degree, diploma or a similar title at this or any other university. Any materials borrowed from other sources (whether published or unpublished) and relied upon or included in my dissertation have been properly cited and acknowledged in accordance with appropriate academic conventions. I further declare that there is no potential conflict of interest with respect to the research, data collection, authorship, presentation and/or publication of this dissertation.

Student's Signature:  \_\_\_\_\_

Date: 18.06.2022

## **Advisory Committee**

1) Advisor: Nazar Zaki

Title: Professor

Department of Computer Science and Software Engineering

College of Information Technology

2) Member: Yauhen Statsenko

Title: Associate Professor

Department of Radiology

College of Medicine and Health Sciences

3) Member: Abdelkader Nasreddine Belkacem

Title: Assistant Professor

Department of Computer Science and Software Engineering

College of Information Technology

## Approval of the Doctorate Dissertation


This Doctorate Dissertation is approved by the following Examining Committee Members:

1) Advisor (Committee Chair): Nazar Zaki

Title: Professor

Department of Computer Science and Software Engineering

College of Information Technology

Signature  Date 18.06.2022

2) Member: Amir Ahmad

Title: Associate Professor

Department of Information Systems & Security

College of Information Technology

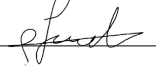
Signature  Date 18.06.2022

3) Member: Fady Alnajjar

Title: Associate Professor

Department of Computer Science and Software Engineering

College of Information Technology

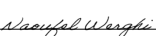
Signature  Date 18.06.2022

4) Member (External Examiner): Naoufel Werghi

Title: Professor

Department of Electrical Engineering and Computer Science

College of Engineering, Khalifa University, UAE

Signature  Date 18.06.2022

This Doctorate Dissertation is accepted by:

Dean of the College of Information Technology: Professor Taieb Znati

Signature Taieb Znati

Date 24/07/2022

Dean of the College of Graduate Studies: Professor Ali Al-Marzouqi

Signature Ali Hassan

Date 27/07/2022

## Abstract

Dementia is a condition in which higher mental functions are disrupted. It currently affects an estimated 57 million people throughout the world. Dementia diagnosis is difficult since neither anatomical indicators nor functional testing are currently sufficiently sensitive or specific. There remains a long list of outstanding issues that must be addressed. First, multimodal diagnosis has yet to be introduced into the early stages of dementia screening. Second, there is no accurate instrument for predicting the progression of pre-dementia. Third, non-invasive testing cannot be used to provide differential diagnoses. By creating ML models of normal and accelerated brain aging, we intend to better understand brain development. The combined analysis of distinct imaging and functional modalities will improve diagnostics of accelerated decline with advanced data science techniques, which is the main objective of our study. Hypothetically, an association between brain structural changes and cognitive performance differs between normal and accelerated aging. We propose using brain MRI scans to estimate the cognitive status of the cognitively preserved examinee and develop a structure-function model with machine learning (ML). Accelerated aging is suspected when a scanned individual's findings do not align with the usual paradigm. We calculate the deviation from the model of normal aging (DMNA) as the error of cognitive score prediction. Then the obtained data may be compared with the results of conducted cognitive tests. The greater the difference between the expected and observed values, the greater the risk of dementia. DMNA can discern between cognitively normal and mild cognitive impairment (MCI) patients. The model was proven to perform well in the MCI-versus-Alzheimer's disease (AD) categorization. DMNA is a potential diagnostic marker of dementia and its types.

**Keywords:** Convolutional Neural Network, Structural-Functional Association, Dementia, Neurodegeneration, Deviation from Model of Normal Aging.

## تشخيص الخرف من خلال العلامات الوظيفية و الهيكلية لضمور الدماغ باستخدام التعلم الآلي.

### الملخص

الخرف هو حالة مرضية تتعطل فيها الوظائف العقلية للشخص، و يؤثر مرض الخرف حالياً على ما يقدر بنحو ٥٧ مليون شخص حول العالم. ويعد تشخيص الخرف صعباً بسبب عدم كفاءة المؤشرات التشخيصية و الاختبارات الوظيفية الحالية، حيث أنه لا يزال هناك العديد من القضايا المعلقة التي يجب معالجتها مثل، ادخال الوسائط المتعددة لتشخيص المراحل المبكرة من مرض الخرف و عدم وجود اداة دقيقة للتنبؤ بمرض الخرف قبل تطوره، و اخيراً أنه لا يمكن استخدام الاختبار غير الجراحي لتوفير التشخيص التفريقي للمرض. الهدف الرئيسي لهذه الدراسة هو التمكن من إنشاء نماذج التعلم الآلي لشيخوخة الدماغ الطبيعية والمتسارعة، حيث سنتمكن من فهم نمو الدماغ بشكل أفضل، وسيؤدي التحليل المشترك للتصوير المتميز والطرائق الوظيفية إلى تحسين تشخيص التدهور المتسارع، وذلك باستخدام تقنيات علوم البيانات المتقدمة. نظرياً، يختلف الارتباط بين التغيرات الهيكلية للدماغ والأداء المعرفي بين الشيخوخة الطبيعية والمتسارعة. و نقترح في هذه الدراسة استخدام فحوصات التصوير بالرنين المغناطيسي (MRI) للدماغ لتقدير الحالة المعرفية للممتحن المحفوظ معرفياً وتطوير نموذج هيكل وظيفي باستخدام خاصية التعلم الآلي، وعادةً ما يُشتبه في حدوث الشيخوخة المتسارعة عندما لا تتوافق نتائج الفرد الذي تم فحصه مع النموذج. و يتم حساب الانحراف عن نموذج الشيخوخة الطبيعية (DMNA) كخطأ في توقع النتيجة المعرفية. ثم يتم مقارنة البيانات التي تم الحصول عليها بنتائج الاختبارات المعرفية التي تم إجراؤها. كلما زاد الاختلاف بين القيم المتوقعة و التي تم ملاحظتها، زاد خطر الإصابة بالخرف. يمكن لحساب الانحراف عن نموذج الشيخوخة الطبيعية (DMNA) التمييز بين مرضى ضعف الإدراك المتوسط (بثي) وبين مرضى ضعف الإدراك العادي. وقد أثبتت الأبحاث أن النموذج يعمل بشكل جيد في تصنيف ضعف

الادراك الخفيف مقابل مرض الزهايمر. لذلك يعتبر حساب الانحراف عن نموذج الشيخوخة الطبيعية (DMNA) علامة تشخيصية محتملة للخرف وأنواعه.

**مفاهيم البحث الرئيسية:** الشبكة العصبية التلافيفية، رابطة هيكلية وظيفية، مرض الخرف، التنكس العصبي، الانحراف عن نموذج الشيخوخة الطبيعية.

## **Author's Contribution**

Tetiana Habuza made multiple valuable contributions to the dissertation. She addressed all of the dissertation's goals in detail. She proposed a new way to research age-related changes in cognitive subdomains by measuring the balance between cognitive functional activities during distinct psychophysiological tasks. Through the use of ML, she developed a detailed description of brain anatomical changes in normal aging and discovered patterns of brain structure-function relationship that are suggestive of MCI. She built an ensemble ML model to apply the concept of brain structure-function association patterns to clinical diagnostics. She also presented a dependable marker of disease-related cognitive loss to satisfy the study's principal goal by creating a predictive model and evaluating its performance. Physicians can use this method to improve MCI and dementia screening and prognosticate MCI progression.

The author assisted in the planning of the project, data collection and processing, experimentation, and analysis of the results. She was exclusively responsible for formulating the study's objectives and design, justifying the choice of research techniques, describing the findings, and supporting the outcomes with an advanced literature review.



## Author Profile

Tetiana Habuza received her bachelor's degree in Applied Mathematics and Master's degree in Informatics from Yuriy Fedkovych Chernivtsi National University, Chernivtsi, Ukraine in 2004 and 2005, respectively. Her research interest is in the fields of artificial intelligence, machine learning (deep learning), bioinformatics, and control theory. In 2018, having a strong interest in Data Science and research, she returned to academia and joined the Computer Science Ph.D. program at the UAEU. Currently, she mainly focuses on using advanced machine learning techniques to automatically detect valuable biomarkers from medical images. She has more than ten years of research experience. As a result of her current research activity, Tetiana was awarded for best research work in the second forum for women in research (QUWA): Empowering Women in Research & Innovation (UAE, Sharjah), work title "Diagnostics of dementia from structural and functional markers of brain atrophy with deep learning". During her PhD studies she published ten papers in Q1 journals on Computer Engineering, Neuroscience, Clinical Microbiology and Immunology, Clinical medicine. She has also worked in AI&Robotics Lab and big data analytics center at UAE university.

### Contact information:

Email            tetiana.habuza@gmail.com

Phone            +971569176530

PO box           15551

Department    Department of CS and Software Engineering

College           College of IT, UAEU

## **Acknowledgements**

I would like to express my sincere gratitude to my supervisor Professor Nazar Zaki and co-advisor Professor Yauhen Statsenko for their continuous support during my PhD study and related research, for their patience, motivation, and immense knowledge. Their guidance helped me in all the time of research, complete and write this dissertation. I could not have imagined having better mentors for my PhD study.

I would also like to thank all the faculty members of College of Information Technology at UAEU for their support and cooperation during my study. My thanks should go to my colleagues and friends, especially Balqis Mubarak Al Breiki, Alramzana Nujum Navaz, Faiza Hashim, and Zeid Moh'd Monther Shukfah for support, discussions, and suggestions. It was an honour to me being a part of our PhD cohort.

This work was generously supported by UAE University. I am grateful to the UAE University that granted me a scholarship to pursue my PhD study.

I take this opportunity to express my sincere love and warmest gratitude to my family: my great parents (Mr Vasyl Gabuza and Mrs Olga Gabuza), my husband (Eng. Volodymyr Puiul), my children (Volodymyr and Olga). Special thanks go to my sister Nadia Kozak and her family. I would have never accomplished this work without their continuous support and encouragements.

## Dedication

*To my great parents, my beloved husband and my lovely kids*

## Table of Contents

Title . . . . .	i
Declaration of Original Work . . . . .	iii
Advisory Committee . . . . .	iv
Approval of the Doctorate Dissertation . . . . .	v
Abstract . . . . .	vii
Title and Abstract (in Arabic) . . . . .	viii
Author's Contribution . . . . .	x
Author Profile . . . . .	xi
Acknowledgments . . . . .	xii
Dedication . . . . .	xiii
Table of Contents . . . . .	xiv
List of Tables . . . . .	xvii
List of Figures . . . . .	xix
List of Abbreviations . . . . .	xxiv
Chapter 1: Introduction . . . . .	1
1.1 Problem Statement . . . . .	4
1.2 Objectives . . . . .	6
1.3 Literature Review . . . . .	8
1.3.1 The Relevance of Researching Cognitive Decline in a Healthy Population . . . . .	10
1.3.2 Processes Behind Neutocognitive Slowing . . . . .	14
1.3.3 Normal Brain Aging . . . . .	19
1.3.4 AD Dementia . . . . .	22
1.3.5 Other Types of Dementia . . . . .	24
1.3.6 Structure-Function Association . . . . .	26
1.3.7 Functional Tests for Cognitive Assessment . . . . .	28
1.3.8 Brain Morphology Studies with MRI . . . . .	29
1.3.9 Machine Learning Methods . . . . .	30
Chapter 2: Materials and Methods . . . . .	33
2.1 Data Collection . . . . .	33

2.1.1 Alzheimer's Disease Neuroimaging Initiative Dataset . . . . .	33
2.1.2 Psychophysiological Outcomes of Brain Atrophy Dataset . . . . .	34
2.2 Research Design . . . . .	35
2.2.1 Development of Machine Learning Models of Age-Related Cognitive Decline, Study of Changes in Cognitive Subdomains . . . . .	35
2.2.2 Patterns of Brain Structural Changes in Normal Aging . . . . .	39
2.2.3 Patterns of Brain Structure-Function Association Indicative of Mild Cognitive Impairment and Dementia . . . . .	42
2.2.4 Improving Screening for MCI and Dementia . . . . .	44
2.3 Methods . . . . .	47
2.3.1 MRI Acquisition and Brain Morphometry . . . . .	47
2.3.2 Data Pre-processing . . . . .	49
2.3.3 Psychophysiological Tests . . . . .	51
2.3.4 Cognitive Tests . . . . .	53
2.3.5 Machine Learning . . . . .	55
Chapter 3: Results and Discussions . . . . .	60
3.1 ML Models of Age-Related Cognitive Decline . . . . .	60
3.1.1 Estimates of the Proportional and Disproportional Changes in Cognitive Domains . . . . .	60
3.1.2 Optimal Number of Age Cohorts . . . . .	64
3.1.3 Proportional Changes in the Cognitive Domains with Age . . . . .	68
3.2 Patterns of Structural Changes in Normal Aging . . . . .	75
3.2.1 Age Related Brain Morphometry Changes . . . . .	75
3.2.2 Mathematical Models of Age-Related Changes . . . . .	94
3.2.3 Comparison of Dynamics of Psychophysiological Performance with Brain Structural Changes . . . . .	99

3.3 Patterns of Brain Structure-Function	
Association Indicative of MCI and Dementia . . . . .	102
3.3.1 Dynamics of Performance in Cognitive and Neurophysiological Tests in Patients with MCI and Dementia . . . . .	102
3.3.2 Models of Brain Structure-Function Associations in Cognitively Normal Individuals, Patients with MCI or Dementia . . . . .	107
3.3.3 Classification of Examinees Into Cohorts According to the Pattern of SFA Association . . . . .	126
3.4 Deviation From Model of Normal Aging: Application of Deep Learning to Structural MRI and Cognitive Scores . . . . .	130
3.4.1 Association of Cognitive Tests and Structural Data . . . . .	130
3.4.2 Proposed Marker of Disease-Related Cognitive Decline . . . . .	134
3.4.3 Justification of DMNA as Marker of Dementia . . . .	136
3.4.4 Prediction of Progressive MCI. Differentiation Between Alzheimer's Disease and Other Neurodegenerative Diseases . . . .	139
Chapter 4: Conclusion . . . . .	142
References . . . . .	147
List of Publications . . . . .	184
Appendices . . . . .	187
Appendix A: Definitions . . . . .	187
Appendix B: Evaluation Measures . . . . .	188
Appendix C: Development of a CAD System . . . . .	190

## List of Tables

Table 1.1:	Reliability and shortcomings of dementia diagnostic methods . . . . .	11
Table 1.2:	Recent papers about diagnostics of MCI and AD . . . . .	32
Table 3.1:	Clusters based on distribution of samples over age and proposed indices . . . . .	66
Table 3.2:	Comparative analysis of results in PTs . . . . .	71
Table 3.3:	Outcomes of the classification and regression models on POBA dataset . . . . .	72
Table 3.4:	Brain morphometry with regard to the age group and sex . . . . .	81
Table 3.5:	Prediction quality of the first-order and second-order ML regression models for predicting results of psychophysiological tests out of age . . . . .	95
Table 3.6:	Importance of psychophysiological and morphological variables based on performance of the linear and quadratic models . . .	96
Table 3.7:	Performance of models trained on cognitively preserved population, subjects diagnosed with MCI or dementia with adjustment to the maximal score of the scales (MAE/range, %) . . . . .	108
Table 3.8:	Metrics of models trained on cognitively preserved population, subjects diagnosed with MCI or dementia (MAE) . . . . .	109
Table 3.9:	Demographics, cognitive performance and volumes of brain parts in studied groups . . . . .	131

Table 3.10:	Mean absolute error of voting regression ensemble model trained on structural brain images averaged along axial, coronal and sagittal axes . . . . .	135
Table 3.11:	Performance of models trained on cognitively preserved population and tested on three different cohorts (MAE) . . . . .	135
Table 3.12:	Classification model performance reported in recent studies . . . . .	138
Table 3.13:	Threshold values of the DMNA markers in binary classification . . . . .	138
Table 3.14:	Performance of binary classification model to distinguish between stable and progressive MCI . . . . .	140
Table 3.15:	Absolute values of DMNA according to A/T/N classification system . . . . .	140
Table A1:	Strengths and limitations of CAD systems to assist doctors in diagnosis of NDs . . . . .	193



## List of Figures

Figure 1.1:	Most common causes of dementia . . . . .	2
Figure 1.2:	The use of machine learning within clinical practice .	2
Figure 1.3:	Different modalities of dementia's biomarkers, including neuroimaging, genomics, CSF, and peripheral systems . . . . .	3
Figure 2.1:	Overview of the suggested methodology . . . . .	36
Figure 2.2:	Simple and complex visual-motor task estimates, and the cognitive functions they describe during the lifespan . . . . .	37
Figure 2.3:	Preparation and application of the proposed SFA model to clinical practice . . . . .	46
Figure 2.4:	Pipeline of proposed framework . . . . .	47
Figure 2.5:	Brain MRI changes throughout 4 stages marked from A to D: adolescence, early adulthood, middle, and old age. T1w sequence with isometric (3D) voxel is used to reconstruct sagittal and coronal views; FLAIR sequence is used to retrieve axial images . . . . .	48
Figure 2.6:	Skull-stripped images averaged along axial (a), coronal (b), and sagittal (c) axes . . . . .	51
Figure 3.1:	Elbow approach with the knee point detection algorithm to select the best number of clusters for the ISCA index . . . . .	65
Figure 3.2:	Distribution of ISD values throughout life . . . . .	68
Figure 3.3:	Distribution of ISDA values throughout life . . . . .	69
Figure 3.4:	Distribution of ISCA values throughout life . . . . .	70
Figure 3.5:	Pairwise distribution of reaction time and age in RMO test . . . . .	70

Figure 3.6: Distribution of MAE to range of index values in different age cohorts . . . . .	73
Figure 3.7: Voxel-based brain morphometry results throughout lifespan. Linear trends with 95% CI highlighted in red, second-order trends are drawn in green . . . . .	76
Figure 3.8: Changes in indices of brain morphometry throughout lifespan (A-D) and in four age groups (E-H). Linear trends with 95% CI highlighted in red, second-order trends are drawn in green . . . . .	78
Figure 3.9: Trendlines displaying differences in voxel-based brain morphometry across four age groups . . . . .	80
Figure 3.10: Distribution of DMT and RT with its variance in SVMR and CVMR tasks . . . . .	82
Figure 3.11: Studies of attention with (B, D) and without interference (A,C). Distribution of mean reaction time with its variance and time delay because of distraction . . . . .	84
Figure 3.12: Distribution of RT and its variance in responding to moving object test (A-B). Linear trendlines of performance in responding to moving object in age groups (C) . . .	85
Figure 3.13: Linear dependencies of performance in PTs across lifespan . . . . .	87
Figure 3.14: Coefficients of correlation between PTs results and volumes of major brain compartments . .	100
Figure 3.15: MMSE scores in the group of cognitively normal adults and patients with MCI or dementia . .	103
Figure 3.16: ADAS13 in the group of cognitively normal adults and patients with MCI or dementia . .	104

Figure 3.17: Results in RAVLT test in the group of  
cognitively normal adults and patients  
with MCI or dementia . . . . . 105

Figure 3.18: Performance in DSST in the group of  
cognitively normal adults and patients  
with MCI or dementia . . . . . 106

Figure 3.19: Executive functioning assessed with TMT  
test in the group of cognitively normal  
adults and patients with MCI or dementia . . . . . 106

Figure 3.20: Gray matter volume in the group of  
cognitively normal adults and patients  
with MCI or dementia . . . . . 107

Figure 3.21: Brain structures ranked according to  
information gain value for MMSE score  
prediction. Inflated cortical  
representations showing significant  
correlations between cortical volumes and  
test score . . . . . 113

Figure 3.22: Brain structures ranked according to  
information gain value for ADAS13 score  
prediction. Inflated cortical  
representations showing significant  
correlations between cortical volumes and  
test score . . . . . 114

Figure 3.23: Brain structures ranked according to  
information gain value for RAVLT score  
prediction. Inflated cortical  
representations showing significant  
correlations between cortical volumes and  
test score . . . . . 115

Figure 3.24: Brain structures ranked according to information gain value for DSST score prediction. Inflated cortical representations showing significant correlations between cortical volumes and test score . . . . .	116
Figure 3.25: Brain structures ranked according to information gain value for TMT score prediction. Inflated cortical representations showing significant correlations between cortical volumes and test score. . . . .	117
Figure 3.26: Confusion matrix of multigroup classification based on MMSE prediction from VBM data . . . . .	127
Figure 3.27: Confusion matrix of multigroup classification based on MMSE prediction from SBM data . . . . .	128
Figure 3.28: Confusion matrix of multigroup classification based on MMSE prediction from SBM and VBM data . . . . .	128
Figure 3.29: Confusion matrix of multigroup classification based on MMSE, ADAS and RAVLT prediction from VBM data . . . . .	129
Figure 3.30: Confusion matrix of multigroup classification based on MMSE, ADAS and RAVLT prediction from SBM data . . . . .	129
Figure 3.31: Confusion matrix of multigroup classification based on MMSE, ADAS and RAVLT prediction from SBM and VBM data . . . .	130

Figure 3.32: Associations of results in cognitive tests with age, functional and structural features in healthy cohort (a), patients with MCI (b) and AD (c). Association is reported in terms of Pearson’s correlation coefficient. Cross-mark overlays non-significant relationships between features ( $p > 0.05$ ). . . . . 133

Figure 3.33: Distribution of deviation from model of normal aging among study cohorts . . . . . 136

Figure 3.34: Performance of Random Forest model classifying cases into healthy and AD groups. DMNA values are input to the model . . . . 137

Figure 3.35: Performance of Random Forest model classifying cases into CN and MCI cohorts (a); patients with MCI and AD (b). DMNA values are input to model . . . . . 137

Figure A1: High-level pipeline of the proposed web-based CAD system . . . . . 194

Figure A2: Entity relation diagram of the database of the proposed CAD system . . . . . 195

Figure A3: Sample of expected visualization of the brain structures segmented by the proposed CAD tool using T1w images . . . . . 196

Figure A4: Sample of the expected output from proposed web-based CAD tool for relative hippocampus volume to show the separability measure between cognitively normal group and cohort diagnosed with dementia . . 197

## **List of Abbreviations**

Acc	Accuracy
AC	Asymmetry Coefficient
AD	Alzheimer's Disease
ADAS-cog	Alzheimer's Disease Assessment Scale
ADNI	Alzheimer's Disease Neuroimaging Initiative
AI	Artificial Intelligence
AST	Attention Study Technique
AUC	Area Under the Curve
BAC	Balanced Accuracy
BET	Brain Extraction Tool
CAD	Computer-Aided Diagnosis System
CDR	Clinical Dementia Rating
CI	Confidence Interval
CN	Cognitively Normal (Healthy subject)
CNN	Convolutional Neural Network
CT	Computed Tomography
EF	Executive Functioning
CSF	Cerebrospinal Fluid
iCSF	Inner Cerebrospinal Fluid
CVMR	Complex Visual-Motor Reaction
DALY	Disability-Adjusted Life Year
DMNA	Deviation from Model of Normal Aging
DMT	Decision-Making Time
GM	Gray Matter
cGM	Cortical Gray Matter
DL	Deep Learning
DSST	Digit Symbol Substitution Test
IES	Inverse Efficiency Score
IRT	Interference Resilience Technique
ISD	Index of Simple Reaction Time to Decision-making Time
ISCA	Index of performance in Simple and Complex Visual-Motor Reaction with Account for Accuracy

ISDA	Index of Simple Reaction Time to Decision-Making Time with the Accuracy Performance
IQR	Interquartile Range
LR	Linear Regression
MAE	Mean Absolute Error
MCI	Mild Cognitive Impairment
MoCA	Montreal Cognitive Assessment
MMSE	Mini Mental State Examination
ML	Machine Learning
MRI	Magnetic Resonance Imaging
ND	Neurodegenerative Disorder
OLS	Ordinary Least Squares
PET-CT	Positron Emission Tomography-Computed Tomography
POBA	Psychophysiological Outcomes of Brain Atrophy
PT	Psychophysiological Test
RAVLT	Rey Auditory-Verbal Learning Test
RMO	Reaction to a Moving Object
RMSE	Root Mean Square Error
ROC	Receiver Operating Characteristic Curve
RT	Reaction Time
$R^2$	Coefficient of Determination
SBM	Surface-Based Morphometry
SD	Standard Deviation
SFA	Structure-Function Association
Sens	Sensitivity
Spec	Specificity
SVMR	Simple Visual-Motor Reaction
T1w	T1-weighted
TIV	Total Intracranial Volume
TMT	Trail Making Test
TPR	True Positive Rate
VBM	Voxel Based Morphometry
WM	White Matter
WMHs	White Matter Hyperintensities





## Chapter 1: Introduction

Any society's primary priority should be public health. A typical public health strategy should aim to reduce the burden on medical staff and equipment by screening the entire community. The screening programs enable the early detection and diagnosis of those at risk of diseases. Risk stratification can help determine the likelihood of a patient's health deteriorating. It aids in the planning and management of clinic resources, among other things.

Risk stratification potentially determines a probability of worsening of a patient's health. It helps, among others, to improve the resources planning and management in clinics. Elder risk assessment [1], dementia risk score, cognitive testing, and chronic comorbidity count [2], to mention a few, are some of the procedures used to identify high-risk patients. Those strategies are solely based on comorbidity analysis. An optimal solution should be able to precisely diagnose an illness and predict how the disease will progress [3, 4, 5].

According to the World Health Organization guidelines, there are three ways to assess the disease's burden:

- the disability-adjusted life year (DALY).
- the number of years of life lost of dying early.
- the number of years of life lived with disability as the disease consequence.

One DALY represents the loss of the equivalent of one year of full health. In high-income countries, the number of DALYs (expressed per 100 000 population) for neurodegenerative disorders (NDs) is extremely

high. In the UK, it was 1088.9 for Alzheimer’s disease (AD) and 123.0 for Parkinson’s disease in 2019, whereas in the US, it was 3837.1 and 513.1. Between 2000 and 2019, the number of DALYs for Alzheimer’s disease roughly doubled.

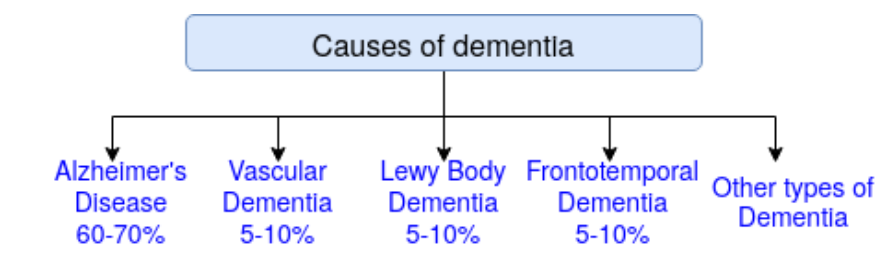


Figure 1.1: Most common causes of dementia

NDs are incurable conditions that result in death of neurons and a progressive deterioration, i.e. dementia. Higher mental functions, such as reasoning, planning, judgment, and memorization, are disrupted in dementia. AD is the most frequent cause of dementia (Figure 1.1). Currently, 57 million people worldwide suffer from dementia. By 2050, this figure is expected to triple, reaching 152 million instances [6].

Screening	Diagnostics	Treatment
Assessing a risk of having a disease  Identification of high-risk groups	Differential diagnosis  Assessing the risk of worsening the patient	Predicting disease outcomes  Predict disease complications

Figure 1.2: The use of machine learning within clinical practice

The reason for such an exponential increment in dementia is societal

aging, which leads to the rise of the incidence of NDs that manifest with dementia. In the UAE for instance, the life expectancy has increased from 74.3 in 2000 to 78.32 in 2022 [7]. Brain atrophy (BA) is a morphological basis of both aging and NDs. Therefore, it is important to identify markers of specific types of brain atrophy, i.e. to segregate pathology versus age-related conditions (Figure 1.2).

Dementia diagnosis is difficult due to the lack of a standardized test. Several approaches may aid in the detection of dementia. Brain imaging may act as a subtle biomarker of the disease, thanks to recent developments in computing resources and technologies (Figure 1.3).

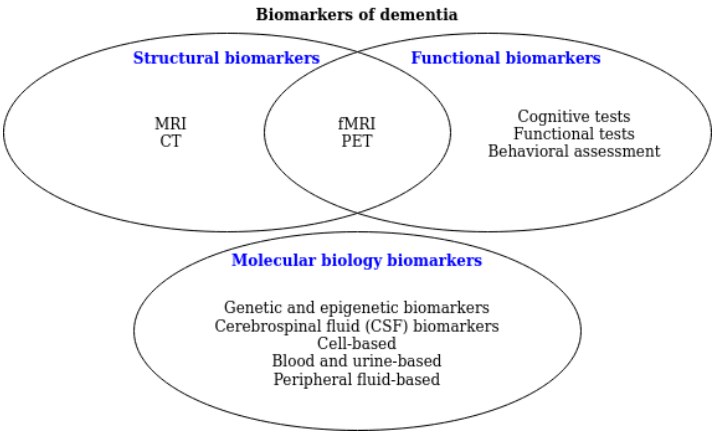


Figure 1.3: Different modalities of dementia’s biomarkers, including neuroimaging, genomics, CSF, and peripheral systems

Unfortunately, there are no particular radiological indications of NDs. However, deep learning (DL) algorithms show significant promise in the processing of visual modalities. DL has made great progress in medical image classification, detection, and segmentation problems. It outperformed even the most expert picture readers. Non-linear patterns concealed in data

can be extracted using advanced machine learning (ML) and DL techniques such as convolutional neural networks (CNN). Learning adaptability is stronger in CNN models than in models with hand-crafted features. As a result, scientists use CNN models to classify a patient's diagnosis based on diagnostic photographs (e.g., brain MRI, CT, PET-CT).

Clinical datasets collect a large amount of data, such as structural attributes (image modalities), functional data (cognitive test results), laboratory findings, demographic features (age, gender, ethnicity, family anamnesis), and so on. They could be a source of accurate diagnostic models, if properly analyzed using ML. Application of ML and DL to neurology, for example, could aid in the early diagnosis and prognostication of NDs.

## **1.1 Problem Statement**

The relationship between brain structural changes and man's functional performance is complicated. Neural plasticity accounts for this phenomenon. Plasticity is a specific feature of biological systems to adjust to pathology. However, the process of adjusting the system may cause diminishing to the potential outcomes of the disease. As a result, clinical appearance may not reflect a true structural impairment, and vice versa. In AD and mild cognitive impairment (MCI), for example, there is no apparent association between functional performance and structural abnormalities. Furthermore, despite the progression of today's neuroscience, pathophysiological mechanisms are complex and so remain unstudied. Future diagnostics should include a wide range of diagnostic modalities and clinical data, such as structural and functional characteristics, risk factors,

demographics, etc. These features can be used in conjunction with ML algorithms to validate the diagnosis and forecast the development of the disease (e.g., disease severity, outcomes, a response to therapy).

New findings may have valuable impact on earlier detection, diagnosis and treatment of age-related degenerative diseases. Many researchers have created methods to identify the diagnosis using structural data as DL progressed. They employed both cognitively preserved and demented patients to train their models. However, such models' application and therapeutic utility are restricted. To that purpose, we identified outstanding concerns and questions that must be addressed to facilitate the risk assessment of ND and its severity:

1. The normal aging of the brain is still poorly understood.
2. It is difficult to correctly pinpoint the onset of age-related deterioration in intellectual performance.
3. Proportionality of changes in cognitive domains and sub-domains are not yet studied.
4. Neurology lacks a tool for assessing the risk of early cognitive retardation. The optimal tool should be non-invasive and reliable. A multimodal approach based on functional and anatomical brain properties can be used to develop such a tool.
5. Association between the brain structure, cognitive status and executive functioning (EF) is an issue of ongoing studies. It is not yet clear how the association evolves in pathology.
6. Physicians lack a viable computer-aided diagnostic (CAD) system for ND screening.

## 1.2 Objectives

We intend to get an insight into the normal and accelerated brain aging by developing ML models. The AI approach to the analysis of medical data allows us to apply multimodal diagnostics to clinical practice. The combined analysis of distinct imaging and functional modalities improves diagnostics of NDs with advanced data science techniques, which is the main objective of our study.

Hypothetically, there are different types of age- and diseases-linked changes in brain morphometry, cognitive performance and their association. We will identify these patterns by comparing the diagnostic images and the results of psychophysiological and cognitive assessment with ML and DL techniques.

If there is no distinct patterns there should be a common mode of structural deterioration and cognitive decline reflecting brain atrophy with some threshold level indicative of the disease. ML can allow us to distinguish normal aging from pathology with the help of a classification model.

We devised the tasks mentioned above for addressing the objective:

1. Develop ML models of age-related cognitive decline and study age-related changes in cognitive subdomains:
  - (a) Create new indices that measure the ratio of cognitive functioning activity during the completion of psychophysiological tasks.
  - (b) Study results in psychophysiological tests (PTs) and split the examined cohort into an ideal number of age groups. Search for potential biomarkers of age-group identification by exploring

the metrics of the unsupervised ML model.

- (c) Examine any probable links between age and the newly suggested scores, as well as the predictive power of PTs in determining the values of the indices developed.
2. Create an accurate model describing brain morphologic changes throughout life:
- (a) Use ML to analyze structural changes in main brain compartments and simulate neurofunctional performance at different ages.
  - (b) Choose the mathematical model that best describes the progression of anatomical and functional changes in the brain throughout lifespan.
  - (c) Compare the dynamics in brain volumetry with psychophysiological performance across the life.
3. Identify patterns of brain structure-function association (SFA) indicative of MCI and dementia:
- (a) Study the dynamics of the performance in cognitive and neurophysiological tests in patients with MCI and dementia.
  - (b) Build models of brain SFAs in cognitively normal individuals and patients with MCI or dementia.
  - (c) Create a method for categorizing the examinees into two groups based on the pattern of SFAs: cognitively normal seniors and patients with MCI or dementia.
4. Improve screening for MCI and dementia and prognosticate progression of MCI:
- (a) Conduct an exploratory analysis of structural and functional

changes in cognitively preserved population and patients with MCI or dementia.

- (b) Propose a reliable marker of disease-related cognitive decline.
- (c) Justify the proposed marker as a screening tool for MCI and dementia.
- (d) Assess the novel marker's diagnostic capability in distinguishing stable from progressing MCI and Alzheimer's amyloidopathy from other types of NDs.

### **1.3 Literature Review**

Diagnosing dementia in its preliminary phase is hampered by the shortcomings of reliable screening methods within neuroscience (see Table 1.1). These persisting limitations can delay the accurate clinical diagnosis by more than 12 months, inevitably eliminating the intended benefit of early treatment, such as memory enhancement, reduced anxiety, and social activity engagement [8, 9].

Diagnostics of NDs can be enhanced through:

- Identification of the dementia onset with a multi-modal approach.
- An informant-based assessment. This method is favoured by scientists and medical professionals as it provides fundamental insight into the patient's personality, which is critical during initial diagnostics. Panegyres et al. reported that this method is more dependable than the mini-mental state examination (MMSE) [10].
- Evolution of the screening strategy to the point where it can be incorporated into routine clinical diagnostics. Brain aging should be the foundation of this novel test. The predominant solution consists



of three steps: 1) researching the new potential origin of brain aging; 2) evaluating the reliability of the test in an unaffected population; and 3) similarly evaluating the tests' reliability in dementia patients.

The cognitive changes of the aging brain have been attracting increasing interest from researchers, which has led to an accumulation of data that present partial insights regarding changes in reaction time (RT), working memory [11, 12], executive functions [13, 14], memory, linguistic skills, and cognition [15, 16]. To delineate the procedure of cognitive decline associated with advancing age, scientists have conceptualised brain reserve and cognitive reserve. These concepts alleviate the repercussions of head trauma, senescence and NDs [17]. Nevertheless, a comprehensive theory for medical practitioners remains absent. Hence, this set of unanswered questions remain:

- Cognitive and brain reserves are not exhaustively studied. Brain reserve is predicted by anatomical quantification (cranial volume, height, and length) [18]. However, [19] stated that the list of brain reserve predictors should include the total number of neurons, synapses, and dendrites. In addition to these structural discoveries, the cognitive reserve consists of psychological factors and various lifestyle activities during a lifespan [18]. Nevertheless, [20] suggested that neural reserve and compensation constitute cognitive reserve.
- The brain's resilience against cognitive decline is not entirely understood. Research has suggested that the primary defence is the brain reserve and that it defines the cognitive reserve's potential [21]. Hence, the potential onset of dementia is delayed in patients with more neurons, compared to patients with a lower brain reserve [22].

On the other hand, neuroplasticity is determined by intelligence preceding the onset of dementia, the level of education, and individual lifestyle (cognitive reserve). Hence, patients cope better with dementia if they have had a higher level of education and higher intellect. Furthermore, symptoms of dementia are independently moderated by cognitive and brain reserves [23]. The need for additional research regarding the brain reserve and cognitive reserve relationship persists.

- Presently, the widely used PTs in the assessment of cognitive domains remain understudied and under-established regarding their accuracy and association. A meta-analysis study reviewing cognitive tests reported that the frequently used MMSE presented the lowest sensitivity during MCI diagnostics [24]. This finding is further supported by an additional review stating that the limited predictive power associated with MMSE and Montreal Cognitive Assessment (MoCA) exceeds that of recall tests [25].

### *1.3.1 The Relevance of Researching Cognitive Decline in a Healthy Population*

Novelty in research regarding age-related changes in cognitive subdomains: Numerous studies focused on comparing NDs patients to a cognitively normal population [26, 27], however, considering that the normal aging process is understudied. Hence, such a comparison is of little value [28, 29, 30]. These studies fail particularly to address the pathophysiological changes associated with aging. Age-related cognitive decline seems to be controlled by fundamental neurobiological changes, for example vascular changes and buildup of neuropathology [31, 32, 33].

Table 1.1: Reliability and shortcomings of dementia diagnostic methods

Method		Diseases investigated	Sens,%	Spec,%	Ref	Shortcomings
MRI		Progression of MCI	87	66	[34]	It is crucial to avoid coming across as over confident, since imaging features are not pathognomonic in most cases [34, 35, 26, 36, 37, 38]
		Parkinson's Disease	61	68	[26]	
		Multiple sclerosis	93	81	[36]	
Tractography		Amnesic MCI	96	94.2	[37]	
		Parkinson's disease	40-86	41-94	[38]	
fMRI		mild AD	77.3	70	[39]	Altered BOLD signals found in AD/MCI patients indicate potential impairments in haemodynamic processes apart from alterations in neuronal activity [39, 40]
PET		AD vs FTLT	69.4	93.2	[41]	Irrespective of the auspicious reliability and accuracy, the implementation of PET/MRI remains predominantly research-based, due to its unique radiotracer requirements [41, 42, 43, 44]
		AD vs MCI	81.8	86	[43]	
		Amyotrophic lateral sclerosis	94.8	80	[44]	
Angiography		Dementia with Lewy bodies (DLB)	93	87	[45]	During this method patients are exposed to radiations, as well as potential kidney function impairment and an allergic reaction, associated with the iodinated contrast
Brain perfusion	MRI	AD vs FTLT	69	68	[46]	Assessing the damaged brain function in FTLT, through ASL perfusion, can fluctuate regionally despite extensive atrophy [46, 47, 48, 49, 50]
	SPECT	Dementia	61	70	[48]	
		DLB vs AD	87-100	90-96	[49]	
	SPECT + MMSE	DLB vs AD	81	85	[50]	
Cognitive tests	FBI	FTLT	90	100	[51]	This method may present insensitivity to elusive brain abnormalities. Transferring the test outcome between varying cognitive impairments should be done attentively [51, 52, 53, 54, 53, 55]
	Mini-Cog	Cognitive Impairment	60	90	[54]	
	MoCA	Vascular dementia	77 vs 85	97 vs 88	[53]	
	MMSE		88 vs 84	70 vs 86	[55]	
	full vs short MoCA	MCI vs dementia	88 vs 79	74 vs 80	[55]	

\* AD - Alzheimer's disease;  
 BOLD - blood-oxygen-level-dependent  
 DLB - Dementia with Lewy bodies;  
 FBI - Frontal Behavioral Inventory;

FTLT - fronto-temporal lobe dementia;  
 MCI - mild cognitive impairment;  
 MMSE - Mini Mental State Examination;  
 MoCA - Montreal Cognitive Assessment;

The increasing support for an alternative purposing explanation regarding the estimations of the cognitive change in the elderly might have been unfavourably influenced by pathologies commonly associated with older age, especially NDs such as AD [56]. Research regarding accelerated brain aging is rendered of little value in the persisting absence of scientific data describing what can be considered as regular cognitive changes [57]. These studies have recurrent restrictions and a disarranged bias. Differentiating between pathological cognitive declines and normal cognitive aging remains problematic in these studies, especially regarding the age group above 65 years [58, 59, 60].

There are numerous NDs and classification models [61], for example, a neuropathological based classification enumerates more than 10 groups with various nosologies associated with each group [62]. Scientists experience difficulty when considering this substantial amount of diseases within a consolidated system. Clinical impression, together with non-invasive diagnostics, does not provide adequate details to discriminate between these diseases. High number of invasive neuropathological examination is required [62]. Granted, in this situation, comparative studies can incorporate the entire scope of NDs. For this reason, scientists prefer non-invasive methods, such as cognitive tests and MRI, to investigate the normal process of aging [32, 58, 63, 64, 65, 66, 67, 68]. Brain aging researchers have not investigated the comparison between healthy adults and patients suffering from neurodegeneration. The point of focus is not on identifying the specific disease. Instead, the researcher focuses on permitted changes within a healthy population, leading to a conjecture regarding accelerated brain aging in noticeable cases. In our earlier research, we

mirrored this approach [69, 70, 71, 72]. The rate of information processing speed and its change related to age is a subject of ongoing research [73, 74, 75]. The vast interest in information processing speed is based on its correlation to functional abilities in older adults [74, 76]. However, the current formulated research questions regarding this field are inadequate. The correlation of structural and biochemical changes to information processing has been a recent research topic of interest. For instance, a recent study on normal decline found an inverse correlation between the interleukin-6 level and information processing speed. As well as an inverse relationship between the fractional anisotropy of corpus and information processing speed [77, 78]. Furthermore, an additional study underlined the correlation between a substantial volume of corpus callosum, decreased levels in insulin and the inflammatory markers, and intact older adults self-reporting an increase in physical activity [79].

Research has ascribed the decline of white matter (WM) integrity to the age-related decrease in cognitive speed [75, 80, 81]. However, the main contributing factors to WM changes remain unclear. A sufficient explanation for observing neurocognitive slowing associated with aging is still absent. Continuing research aims to establish the cause of change in information processing speed during normal aging. Patients with neurodegeneration can be compared to a healthy population to underline risk factors associated with neurodegeneration. Risk factors include genetics [82] and changes in WM [83]. Studying aging in a healthy population could benefit future identification and differentiation of the preliminary signs associated with NDs.

Depending on the conducted assignments, inconsistent findings

have been reported regarding changes in the information processing speed related to age. For example, younger adults were more proficient in coding and symbol searching assignments, while on the other hand, older adults were more skilled in inspection time assignments [84]. A satisfactory explanation has not been produced for this finding. A parallel study reported that the slowing of performance speed occurs over the lifespan [85]. However, research has reported that the decrease in sensory function is linked to the decline in processing speed [86, 87]. Furthermore, studies have also claimed that the general cognitive status in adults above 40 years is predicted by the cognitive processing speed. However, this is not the case in adults younger than 40 years. Additional research is required to verify the findings [32].

### *1.3.2 Processes Behind Neurocognitive Slowing*

A few processes contribute to neurocognitive slowing, such as atrophy and neuroplasticity. However, these two processes have been reported as direct theoretical opposition [88]. Brain atrophy has been linked to numerous factors such as vascular factors [89], inflammation [90], diet [91], metabolic disorders [92], and dysbiosis [90]. These factors provide insight into dementia-related mechanisms and uphold the notion of cognitive impairment management through manipulation of these factors. Contradictory to this is the idea of neuroplasticity. According to the idea, cognitive and low-intensity physical training can reduce noticeable brain aging and delay the appearance of dementia [77, 88].

Concurrent changes in cognitive domains associated with aging: Declines could vary according to cognitive domains. Numerous declines

progressively worsen over time, while some remain stable, such as language. Generally, the change in reaction speed related to age is linked to numerous changes in the cognitive domains [67]. EF, the cognitive domain accounting for individual goal-directed behaviour, is affected by decreased information processing. Two explanations are offered for this finding. Firstly, relevant operations cannot be performed within a predetermined time interval. Secondly, slow processing reduces the amount of information which is concurrently available. Hence, the delayed supply of information leads to the collapsing of the higher-level processing [93]. Consequently, EF deficit can potentially affect performance in numerous cognitive variables, this inducing cognitive decline [67].

Research has proposed numerous interdependent cognitive aging mechanisms. Irrespective of commonality among findings presented by various speed-based tasks, the decline in abilities is not a general factor of cognitive slowing [88, 94]. For instance, working memory is responsible for task-recall, which is associated with reasoning. It is logical to conclude that its impairment will have a significant impact on older adults' cognitive performance.

EF and cognitive control: Cognitive control is the capability to arrange our thoughts and actions according to internal goals [77]. EF is an umbrella term under which EF and cognitive control fall. Furthermore, it also covers a set of higher-order (cognitive) processes associated with arranging conscious behaviour during an unfamiliar situation [95]. EF consist of three subdomains: inhibitory control, which includes the prevention of insignificant information and prohibiting prepotent responses; task switching, which is the capability to switch between mental sets

effortlessly. Finally, it is updating, the continuous monitoring and instantaneous addition/deletion of content to the working memory. Age-related cognitive decline is associated with declining inhibitory control [96]. Moving between different assignments requires working memory in the absence of a cue, and a decrease in the memory domain over time might impact this EF [97, 98].

Attention is commonly split into two comprehensive subdomains. The first subdomain is selective attention, for example, concentration, while the second subdomain is sustained attention or vigilance, for example, divided attention [99]. A declining capability in paying attention to selected stimuli is associated with the elderly. Age-related declines in selective attention interact with other cognitive domains and other changes related to age [77, 100].

There are additional attention subsystems. For example, it has been proven that the relationship between goal-guided attention and habitual spatial attention is affected by aging [101]. The authors of this study interpret habitual spatial attention as the attention attracted regularly to a target, such as a space with a heightened possibility of triggering stimuli. Older adults experience difficulty with interrupted goal-guided attention, yet they are relatively unhampered in utilising spatial attention through coincidental habit-based learning. Therefore, the decrease in certain attention subdomains can be counterbalanced through teaching searching habits to older adults. Age-related decline influences attention since attention skills have EF elements [99]. A deficiency in obstructing insignificant information is associated with older adults, which could be attributed to changes in the prefrontal cortex [100].



Memory, as a cognitive domain, could be subjected to influence from multiple processes such as working memory, executive control operations, speed, and sensory declines. The loss of memory could originate from an inadequate capability to pay attention and move between functional brain networks. Change in older adults' structural and functional brains causes them to experience difficulty disregarding distractions, which leads to significant and insignificant information being co-encoded. Inevitably this causes an overload on the limited cognitive resources [100].

Irrespective of the well-known fact that with age, memory performance decreases, it is interesting that all memory aspects are not equally impaired [102]. The procedural memory is manifested automatically without intentionally recalling past events, while on the other hand the declarative memory depends on intentionally recalling past experiences. It includes episodic memories of specific experiences and the semantic memories, which mirror our common comprehension of facts and the definitions of words. Generally, the older adults experience the most severe memory loss in long-term episodic memory due to its significant attention demand. Negligible age-related changes are generated in the sensory, semantic, and procedural memory due to their small attention demand [100, 102].

Memory is mediated with other cognitive domains. Semantic memory can be seen as an arranged data storage of words or concepts - "nodes". These nodes are linked through associative pathways [77]. When a node is activated by a person paying attention, it initiates an escalation within the network, which ultimately activates various nodes and enables processing [102].

Working memory acts as a buffer. It stores data for cognitive processing and is subjected to age-related changes such as the decline in capacity and processing speed. A decrease in the processing speed and disintegration of primary control processes is responsible for the change in working memory. Primary control processes in this context refer to resistance to unwanted influence, memory updating, binding, assignment coordination, top-down control. This knowledge derived from neuroimaging data. Furthermore, age-related changes in working memory have a more significant influence on spatial material than on the verbal [11].

Perceptual and sensory deficiency worsens cognitive decline as well as increases the difficulty of fulfilling cognitive assignments. Declines in these domains are associated with a decreased capability to identify a stimulus from the sensory modalities and limit the process and incorporating the obtained information. Clinically, older adults can experience various challenges when using their five sensory modalities. For example agnosia is when experiencing difficulty in identifying formally recognisable objects [99]. Other domains are impacted by the age-related cognitive changes in the sensation and perception domains. For example, auditory memory and language comprehension issues result from a hearing deficit [88]. However, the intervention of decreasing perceptual processes is also possible. Davis's "posterior-to-anterior shift in aging" model proposes intervening in the decrease of perceptual processes linked to the occipital regions through increasing prefrontal activities. However, this assumes that task performance in young and older adults can be compared, even though the process depends on different neural mechanisms [100].

Motor skills are defined as the primary components of motor activity and construction is defined as the capability to duplicate or create sketches of ordinary objects. Motor skills and construction could be compromised in critical dementia cases, nondominant hemisphere trauma, or by parietal cortex lesions [99]. It has been reported that cognitive processes linked to language remain constant or even enhances up to the age of mid-70s [88]. Language deficits could be linked to an EF deficit (for example, the capability to retrieve semantic storage effectively) or to a decreased processing speed [99]. A crucial element in comprehensive impairment is a primary lag of the neurologic response. Furthermore, change in attention and declined memory influence speech comprehension [103]. Intercorrelation and inseparability of cognitive domains: One should not consider the intercorrelation of cognitive domains as an insufficient cogency. Compelling evidence has indicated that common domains of cognitive dysfunction are inseparable in in a variety of patient groups, including individuals with schizophrenia and bipolar illness [99].

### *1.3.3 Normal Brain Aging*

Normal brain aging can be described in terms of the brain atrophy and neurocognitive slowing. The first term covers the brain structural changes across the life. The second term denotes the functional outcomes of the process. Atrophy is a process by which the size or number of cells in response to a stimulus [104] is decreased. Brain atrophy is a common feature of brain aging and of numerous diseases that affect the brain. Macroscopically, BA results in brain shrinkage, and compensatory enlargement of cerebrospinal fluid spaces, the ventricles and the

subarachnoid space. Ventricular volume trajectory shows a strong association with age and pathologic measurement because it is a summary marker of atrophy, both of gray matter and white matter (as a result of glial, myelin, axonal and/or neuronal loss) [105]. But there is no simple, sensitive quantitative marker which is well associated with the extent of cognitive impairment or highly specific to any particular ND.

Features of brain atrophy: Normally, decreasing of brain size does not automatically lead to cognitive impairment until the age of 65 years [106]. MRI allows researchers to accurately quantify the atrophy of cortical and subcortical gray matter regions (in terms of volume loss, macro-morphological changes and cortical thinning), and to evaluate white matter structural damage [106]. Ventricular volume trajectory is significantly associated with age, the presence of infarcts, neurofibrillary tangles and neuritic plaque scores, the presence of some gene alleles and dementia diagnosis. The total brain volume trajectory is significantly associated with age and mild cognitive impairment diagnosis. The hippocampal volume trajectory is significantly associated with amyloid angiopathy [105].

Brain atrophy is an authentic subject of relevant research due to the tendencies of the world-wide civilization, such as the aging of population accompanied with the increasingly high rate of NDs. Many publications state the issue of either the structural changes or the functional impairment of the nervous system (e.g., cognitive decline). Unfortunately, it is still unclear, to what degree brain atrophy contributes to the malfunctioning of the nervous system. Structural MRI studies have revealed that the extent of age-related brain changes varies markedly across individuals [107]. Other studies of

brain functioning based inconsistencies in both onset and the rate of episodic memory loss in the elderly cohort, which accounts for different inherited and life-style factors [108]. However, there is no evidence of a direct link between structural and functional impairment.

Brain atrophy is observed overall in (normal) brain aging and neurodegeneration. Regarding normal brain aging, there were some attempts to establish structural-functional association, but the evidence provided us with inconsistent data. For example, the association was significant for older participants (65–80 years) but not middle-aged (55–60 years) participants [106]. However, findings show that brain atrophy starts almost after puberty. What may account for these discrepancies? Does a compensation of functioning take place? If so, in what way? Therefore, does the process last typically until the age of 60 years?

Some studies have demonstrated that brain atrophy in normal aging participants is characterized by several trends. Firstly, in the volumetric reduction within the human cortex. The second is the shrinking of the neuronal networks suddenly, from a more distributed arrangement to a more localized topology in the middle-aged group (30–58 years). Afterwards, it maintains this localized topology in the older participant group. The researchers concluded that there are variations in topological organization of neuronal networks during normal ageing [109]. Therefore, they specifically describe such components of brain atrophy as volume reduction, structural and functional connectivity impairment. However, this still fails to provide us with evidence of how the structural changes and the disconnected state affect simple physiological reactions. To clarify these issues, it is imperative that new research should be conducted and

concluded.

#### *1.3.4 AD Dementia*

Alzheimer's disease accounts for more than half cases of dementia which can be defined as an acquired and persistent generalized disturbance of higher mental functions, such as reasoning, planning, judgment, memory and additional thought processes, in an otherwise alert person [104]. According to the age of onset and leading etiological factors, it can be classified into several categories. The senile dementia's typical onset is after 65 years of age. It is an age-related condition; however, it can hardly be distinguished from the vascular dementia. The pre-senile cases of dementia refer to such causes as NDs, cerebrovascular disease, infections, acute or chronic traumatic brain damage, metabolic diseases, toxic and chronic alcoholism, nutritional deficiency, myelin disorders, primary or secondary brain tumours, occlusive hydrocephalus.

ND is a term surrounding a wide variety of disorders that are characterized by the progressive dysfunction and/or death of glial / nerve cells. This leads to a typically slow and progressive disease with variable, gradual neurologic dysfunction. Numerous classifications have been described in the past. However, the better NDs are understood, the more classifications shift towards focusing on changes at the biochemical level [35]. Tau proteins (or  $\tau$  proteins) – proteins that stabilize microtubules (a part of the cytoskeleton which provides structure and shape to the cytoplasm of cells) [110]. In pathological conditions of tauopathy, tau is hyperphosphorylated. Other modifications include acetylation, nitration, glycation, conformational change and C-terminal truncation [111].

Tauopathies are a class of ND characterized by neuronal and/or glial inclusions composed of the microtubule-binding protein, tau [111]. These NDs derive from the pathological pathway which leads from soluble and monomeric to hyperphosphorylated, insoluble and filamentous tau protein. They could be inherited (mutations of genes encoding tau protein), however there are generally non-inherited forms. Apart from molecule structure differences, tauopathies vary in the cell types (neurons or glia) and anatomical regions (i.e. limbic/neocortex, basal ganglia and brainstem) most vulnerable to tau-mediated neurodegeneration. Clinically, tauopathies can present with a range of phenotypes that include both movement- and cognitive/behavioral-disorders or non-specific amnesic symptoms in advanced age [111]. The distribution of pathologic accumulations of tau proteins in ND defines the clinical symptoms: e.g., Alzheimer's disease is a dementing illness and Parkinson's disease is namely a movement disorder [110]. A major limitation for pharmacologic prevention of pathological tau transmission is the inability to readily detect tauopathies [111].

AD is the ND which accounts for approximately 70% of all cases of dementia. For this reason, NDs are usually classified into AD and non-AD forms [104, 106]. MRI-derived structural patterns of cortical atrophy have been shown to accurately track disease progression and seem to be promising in distinguishing AD subtypes. Disease progression has also been associated with changes in white matter tracts. Recent studies have revealed two areas often overlooked in AD, namely the striatum and basal forebrain with more focal atrophy, although the impact of these changes regarding cognition is still unclear [106].

Brain atrophy assessed on structural magnetic resonance imaging

(MRI) has been demonstrated as a valid marker of AD-related neurodegeneration at the late stages of the disease [106]. However, reliable means of identifying cognitively-normal individuals at higher risk to develop AD are more likely to derive from psychophysiological testing (e.g., event-related potentials) [112]. So, the full understanding of the pathophysiological mechanisms underlying AD- and MS-related functional impairment of the brain and its structural bases remains incomplete [113].

### *1.3.5 Other Types of Dementia*

Dementia with Lewy bodies (or Lewy body dementia) is the second most common type of progressive dementia after Alzheimer's disease dementia. Protein deposits, called Lewy bodies, develop in nerve cells in the brain regions involved in thinking, memory and movement (motor control) [114].

Parkinson disease is a ND which mainly affects the motor system. It is more common in men (1:3.5) and women have a lower rate of decline. The official data by the department of measurement and health information of the World Health Organization (WHO) allow us to compare the burden which Parkinson's disease (PD) and AD put on the society. For instance, in the UAE, age-standardized disability-adjusted life year was 584 for AD and 61.1 for Parkinson's Disease in 2016 [115]. From the 2016 annual report of the GBD 2016 Dementia Collaborators, high-income countries such as the United States of America (USA) and the United Kingdom (UK) had a higher rate of AD per 100 000 population: 1278 in the UK; 1247 in the USA. In the UAE, the rate of the disease was 110 per 100 000 people [116]. For PD, the prevalence was just 26 in the UAE, 176 in the UK and 218 in the USA per



per 100 000 population in the same year [117].

Life expectancy is constantly increasing in the UAE [118]. This contributes to the rise of ND morbidity, but the summary death statistics do not claim NDs as a common cause of death. Both dementia and PD are rated to 0.7 cases of death per 100 000 population according to the Global Burden of Disease study in 2016 [119]. The numbers for the UK are 46.7 and 9.09 respectively. However, even drug use disorders which are non-typical for the population of the UAE are responsible for much more cases of mortality according to the same source of the statistical data: 8 cases per 100 000 [119].

Frontotemporal dementia (FTD) is a class of disorders characterized by the loss of nerve cells in the frontal and temporal lobes of the brain. These lobes decrease in volume and as a result behavior, demeanor, language, and mobility can all be affected by FTD [120]. Depending on whatever section of the brain is affected, the signs and symptoms will differ. Some patients with FTD have major personality changes, becoming socially inept, impetuous, or emotionally apathetic, while others lose their capacity to communicate effectively [120]. FTD is sometimes misdiagnosed as a mental illness or AD. FTD, on the other hand, tends to strike at a younger age than AD. FTD usually develops between the ages of 40 and 65, however it can sometimes develop later in life. FTD is responsible for 10% to 20% of all dementia cases [120]. There are common types of FTD, such as Frontal variant (affects behavior and personality) and primary progressive aphasia (affects ability to communicate or understand the language).

Myelin disorders (e.g., multiple sclerosis, leukodystrophy) are myelin sheath abnormalities or a myelin breakdown (demyelination)

resulting either from a primary attack on myelin sheath or the oligodendrocyte or simultaneously [121]. Cognitive decline also occurs at the late stages of the diseases.

Vascular dementia – is a general term describing dementia caused by impaired blood flow to the brain, e.g., multi-infarct dementia, arteriosclerotic dementia, global hypoxia/hypoperfusion, vasculitis [104].

Dementia Resulting From Traumatic Brain Injury is a long-term consequence of traumatic brain injury. According to estimates, 2% of the US population has long-term disability as a result of a previous traumatic brain injury, with percentages significantly higher in underdeveloped nations [122]. Multiple epidemiologic studies demonstrate that having a traumatic brain injury in early or midlife is related with an elevated risk of dementia in later life, making dementia one of the most feared long-term outcomes of traumatic brain injuries [122].

### *1.3.6 Structure-Function Association*

Studying the relationship between a system's structure and actions provides an understanding of the normal brain and body function, enabling more effective diagnostics and treatment of abnormal or disease states. To enhance the diagnostics one may use an innovative approach to data analysis by incorporating newly developed ML methods into computer-aided diagnosis systems. This may give an insight into the importance of specific data features and calculate the weights of potential predictors. The proposed solution should be based on state-of-the-art methods, which will allow us to assess overall functioning at the level of organ systems and the whole body. To become a popular tool for screening

dementia, a test must comply with physiology of brain changes across the life. The optimal solution consists of the following steps. The first one is investigating possible new causes of aging. The second step is testing reliability in a healthy population. And the third step is testing in patients with emergent dementia [77].

Researchers have gathered diverse information, but have not yet been able to develop a general theory. They have concentrated on diverse aspects of cognitive aging that focus on changes in EF, memory, and linguistic abilities and knowledge. However, all these processes cannot be addressed in a single study. To date, no systematic analysis or review has produced a well-defined theoretical approach that could be easily put into practice. The diagnostics of NDs is challenging, since neither structural signs nor functional tests are sensitive enough or specific. Thus, a long list of unresolved issues remains to be covered. First, despite the well-known advantages of multimodal diagnostics it has not yet been incorporated into screening for early-stage dementia. Second, there is no reliable tool to predict whether pre-dementia will progress. Third, it is impossible to perform the differential diagnostics of exact ND with non-invasive tests. For instance, the early differential diagnosis between MCI due to AD and MCI due to other ND conditions is particularly challenging in clinical settings. To improve the current situation, we propose a combined analysis of structural findings and functional data. The best way to carry out such analysis is to apply ML [123]. The strengths and limitations of brain structural and functional assessment are briefly discussed below. As seen from the references, there is no agreement between authors on which non-invasive diagnostic modality is most promising for screening purposes.

We chose to focus on multimodal diagnostics to benefit from both types of data.

### *1.3.7 Functional Tests for Cognitive Assessment*

Physicians can use functional tests to improve early diagnostics of NDs, but such tests have multiple disadvantages. They are time-consuming; they require a special testing environment to keep the subject focused; and there is no understanding of the pathophysiological mechanisms underlying cognitive decline whose structural bases are not studied well [124]. However, psychophysiological, and cognitive tests and evoked potential studies can detect purely pre-symptomatic stages of dementia. Many models of developing dementia include cognitive test scores as predictors [125]. The most widely employed cognitive tests are the MMSE [126], Alzheimer's disease assessment scale cognitive subscale (ADAS-cog) [127], Rey auditory-verbal learning test (RAVLT) [128], digit symbol substitution test (DSST) [129], trail making test (TMT) [130], clinical dementia rating (CDR) [131], logical memory tests, and immediate and delayed recall test [132].

When combined with structural data to form a multimodal diagnostic tool, cognitive tests identify NDs more reliably [133, 134]. Few studies have focused on the prediction of cognitive status from brain structural images (see Table 1.2). Some authors have predicted MMSE scores from resting state functional MRI scans of patients with AD [135]. Others have calculated MMSE, ADAS-cog, and CDR scores from structural MRI images [136]. Prediction of results in tests that reflect a lower number of cognitive domains (e.g., RAVLT) was less accurate than in tests covering

a larger set of domains (ADAS or MMSE). One research team predicted MMSE and ADAS-cog scores with a model which integrated spatial-temporal features of the brain received from MRI findings [137]. Recent studies have provided an insight into the neurophysiological and morphological characteristics of the brain in patients with dementia [133, 134, 135, 136, 137]. However, the clinical utility of the proposed models remains limited.

### *1.3.8 Brain Morphology Studies with MRI*

Structural MRI is a valid marker of the late stages of AD [138], however, at an early stage, it is not particularly revealing of the difference in the brain's structural change in normal and accelerated aging. For this reason, some authors believe that electrophysiological diagnostics (e.g., event-related potentials) can be used to reliably identify those at risk of AD [125, 139]. Contrarily, there is evidence that neuropathological changes can be detected through neuroimaging much earlier than cognitive decline becomes apparent [140]. The level of age-related brain change differs markedly between people, according to structural MRI studies [141]. Inconsistencies in the onset and rate of episodic memory loss in the elderly have been discovered in studies on brain functioning. Inherited and lifestyle factors may account for these discrepancies. There is no direct link between structural and functional impairment. Researchers have attempted to discover the structure-function relationship in the brain through advanced methods of neuroimaging and have shown the importance of visual rating scales, volumetric assessment, and structured reporting [124, 142].

A few brain regions are vulnerable to atrophy in NDs, namely the

hippocampus, amygdala, entorhinal cortex, fusiform gyrus, putamen, and medial temporal lobe. The aforementioned structures are neural centers responsible for learning, memory, navigation, processing information, emotions, behavior and time perception. Some authors have studied the brain at the macrostructural level. With MRI, they have assessed the enlargement of gray matter (GM), WM, ventricles, and accumulation of WM lesions that show up as hyperintense areas in the T2-weighted sequence [143, 144]. Other research has focused on the microstructural effects of NDs, such as neuronal death and the accumulation of  $\beta$ -amyloid and  $\tau$ -protein in the hippocampus [145, 146]. The macrostructural characteristics of the brain (tissue volumes) can be identified with MRI and used for screening for NDs. Microstructural characteristics (tissue organization) serve as the gold standards of diagnostics.

### *1.3.9 Machine Learning Methods*

Processing biomedical images with ML techniques is a field of ongoing study [147]. It has already been demonstrated that ML may be used to investigate the link between morphological and functional changes in the brain. [123]. Numerous conventional ML and DL methods have been proposed to distinguish AD patients from cognitively preserved people using structural MRI data [8]. For instance, Altaf et al. used a combination of textures (i.e., a gray level co-occurrence matrix) and clinical features (i.e., MMSE) to predict the final diagnosis [148]. Ahmed et al. resorted to the bag-of-visual-words approach to generate a unique signature of an individual brain from the hippocampus and posterior cingulate cortex [149]. Khedher et al. analyzed tissue-segmented MRI (i.e., WM and GM images)

to diagnose AD at early stages [150]. Other authors have used slices or 2D patches extracted from T1-weighted (T1w) MRI as predictors in designed 2DCNN models [151, 152, 153, 154]. Recently, 3D patches extracted from MRI were used to segregate healthy individuals from patients with MCI or AD [155]. The authors extracted voxels corresponding to the hippocampus and used them as an input to a 3DCNN classification model [156]. 3D images of the whole brain also served as an input to 3D subject-level CNNs [152, 157, 158, 159, 160, 161, 162, 163]. Qiao et al. used a 3DCNN with sharing weights to extract the features from MRI, followed by multiple sub-networks which transformed the MMSE regression models into a series of binary classification models[162]. We presume that new findings on the brain SFA may foster further research on earlier detection and treatment of NDs. The multimodal diagnostics that we are developing with ML brings together the advantages of both morphological and functional findings.

All the methods discussed are summarized in Table 1.2. In contrast to previous studies, we intend in the current research to find a difference in the SFA of the brain of the healthy population and cognitively impaired individuals. The finding may serve diagnostic purposes. The brain SFA may have features that are specific either to cognitive deterioration in a disease or to normal neurocognitive slowing in aging. We propose to predict a cognitive status of the examinee from the brain MRI data and compare the prediction with an actual result of cognitive testing. We hypothesize that the larger the gap between the predicted and observed values, the higher the risk of dementia. We name the difference “deviation from the model of normal aging” (DMNA). It is supposed that this change in SFA patterns may serve as an early sign of ND.

Table 1.2: Recent papers about diagnostics of MCI and AD

Reference	Year	Dataset	Image modality	Training dataset	Prediction		Cognitive tests						
					Diagnosis	SFA	ADAS	MMSE	RAVLT	CDR	DSST	TMT	
Stonnington et al. [136]	2010	ADNI + in-house	MRI	CN+AD		✓							
Liu et al. [164]	2013	ADNI	MRI	CN+MCI+AD	✓		✓	✓	✓				
Gupta et al. [151]	2013	ADNI	MRI	CN+MCI+AD	✓								
Payan and Montana [152]	2015	ADNI	MRI	CN+MCI+AD	✓								
Ahmed et al. [149]	2015	ADNI	MRI	CN+MCI+AD	✓								
		ADNI +											
Sorensen et al. [165]	2015	AIBL[166] + Metropolit[167]	MRI	CN+MCI+AD	✓	✓		✓					
Li et al. [168]	2015	ADNI	MRI	CN+MCI+AD	✓		✓	✓					
Khedher et al. [150]	2015	ADNI	MRI	CN+MCI+AD	✓								
Hosseini-Asl et al. [169]	2016	ADNI	MRI	CN+MCI+AD	✓								
Suk et al. [170]	2016	ADNI	MRI	CN+MCI+AD	✓								
Gao et al. [171]	2017	Navy General Hospital ( China)	CT	CN+MCI+AD	✓								
Zhang et al. [172]	2017	ADNI	MRI	CN+MCI+AD	✓								
Korolev et al. [157]	2017	ADNI	MRI	CN+MCI+AD	✓								
Cui and Liu [156]	2018	ADNI	MRI	CN+MCI+AD	✓								
Billones et al. [160]	2017	ADNI	MRI	CN+MCI+AD	✓								
Liu et al. [173]	2018	ADNI	MRI + PET	CN+MCI+AD	✓								
Altaf et al. [148]	2018	ADNI	MRI + PET	CN+MCI+AD	✓								
Lee et al. [153]	2019	ADNI	MRI	CN+MCI+AD	✓								
Lahrimi and Shmuel [134]	2019	ADNI	MRI + tests	CN+AD	✓		✓	✓					
Basaia et al. [158]	2019	ADNI + in-house	MRI	CN+MCI+AD	✓								
Lei et al. [137]	2019	ADNI	MRI	CN+MCI+AD		✓	✓	✓					
Fang et al. [174]	2019	ADNI	MRI	CN+MCI+AD	✓								
Liu et al. [155]	2020	ADNI	MRI	CN+MCI+AD	✓								
Wang et al. [159]	2020	ADNI	MRI	CN+MCI+AD	✓								
Duc et al.[135]	2020	In-house	rs-fMRI	CN+AD	✓	✓		✓					
Zhang et al. [175]	2021	ADNI	MRI	CN+MCI+AD	✓								
Sathiyamoorthi et al. [176]	2021	ADNI	MRI	NC+MCI+AD	✓								
Qiu et al. [177]	2022	ADNI+OASIS	MRI	CN+MCI+AD	✓								
Soliman et al. [161]	2022	ADNI	MRI	CN+AD	✓								
Qiao et al. [162]	2022	ADNI	MRI	CN+MCI+AD		✓		✓					
Gao et al. [163]	2022	ADNI	MRI	CN+AD	✓								
Proposed		ADNI	MRI	CN	✓	✓	✓	✓	✓		✓	✓	

CDR - clinical dementia rating score [131]



## Chapter 2: Materials and Methods

### 2.1 Data Collection

#### 2.1.1 *Alzheimer's Disease Neuroimaging Initiative Dataset*

The data used in this study were obtained from the Alzheimer's disease neuroimaging initiative (ADNI) dataset [178]. ADNI1 covers 400 subjects diagnosed with MCI, 200 subjects with early AD and 200 elderly control subjects with an age range of 55 to 90 years. For more information about ADNI datasets, please visit the link <https://adni.loni.usc.edu/> (see inclusion and exclusion criteria at [179]). In this study, we acquired MRI and clinical information on all the cases collected from the ADNI dataset in a cross-sectional and longitudinal study design. This provided us with a total of 1,421 study cases from 800 subjects (CN/MCI/AD: 28.56/25.97/45.67%; male/female: 59.47/40.53%). We collected the following information:

- Clinical data on the final diagnosis.
- Demographic data (i.e., age, gender, ethnicity).
- Morphometric data (i.e., volumes of brain areas mostly affected by ND).
- Results of cognitive assessment generated using the MMSE, RAVLT, TMT (part B), DSST, and ADAS-cog tests.
- Pre-processed T1w MRI files.

ADNI data availability and ethical issues: The dataset can be downloaded from [adni.loni.usc.edu](https://adni.loni.usc.edu). The use agreement form was signed to allow us access to the data.

### *2.1.2 Psychophysiological Outcomes of Brain Atrophy Dataset*

Psychophysiological outcomes of brain atrophy (POBA) repository is a set of results in a battery of PTs. The battery was proposed by Charykova et al. to screen maladjustment in athletes [180]. We examined 231 people with cerebral MRI and asked them to pass PTs. The age of the study participant ranged from 4 to 84 years. Examinees with periodic headaches and concern about having organic brain abnormalities were not included in the study. Literacy was used as an inclusion criterion, which meant that only adults who had completed at least one professional course after graduating general education were considered. Organic brain pathology, mental problems, head injuries, and radiological indicators of NDs based on MRI findings were all considered exclusion criteria. The year ranges within the age groups are described below. The number of full years of life for the Adolescents class was less than 20 years. Young adults were 20-39 years old. The range of years of Midlife adults was from 40 to 60 years. Finally, the age of Older adults was 60 years and over. From the comprehensive POBA dataset we acquired the following data:

- Demographic data (i.e., age, gender).
- EF testing ( simple (SVMR) and complex (CVMR) visual-motor reaction; technique: "Reaction to a moving object").
- Wrist dynamometry and asymmetry coefficient (left and right hands maximum muscular strength, asymmetry coefficient or a fraction of the maximum muscular strength of the contralateral arms).
- Psychological testing (attention study technique (AST) and interference resilience technique(IRT) with response time to visual

interference).

- Raw T1w and FLAIR MRI scans.

POBA data availability and ethical issues: The UAEU Human Research Ethics Committee granted ethical approval for the retrospective analysis of data provided as standard of care (Notice Number: ERH\_2019\_4006 19\_11). No potentially identifiable personal information is presented in the study. The POBA dataset is available on request from the link <https://bi-dac.com>.

## **2.2 Research Design**

Figure 2.1 offers an overview of the suggested methodology. Research design developed for each objective is described in the following sections.

### *2.2.1 Development of Machine Learning Models of Age-Related Cognitive Decline, Study of Changes in Cognitive Subdomains*

For the primary objective, we sought to improve the diagnostics of age-related alterations in cognitive processes. The goal was to ascertain if different executive functions deteriorate in proportion to age. By assessing individuals without dementia, we created a series of experiments and generated an open-access POBA dataset. The assessments and their dependent output variables represent cognitive subdomain performance (e.g., switching and inhibitory control, information processing speed, etc.). Cognitive functions are hypothetically linked, and the rate of their age-related decrease is assumed to be relatively similar. Furthermore, there is a theory that links normal neurocognitive decline to slowed core or computational processing, which is universal to all cognitive functions

[181, 182]. Disproportional alterations, on the other hand, could suggest faster brain aging.

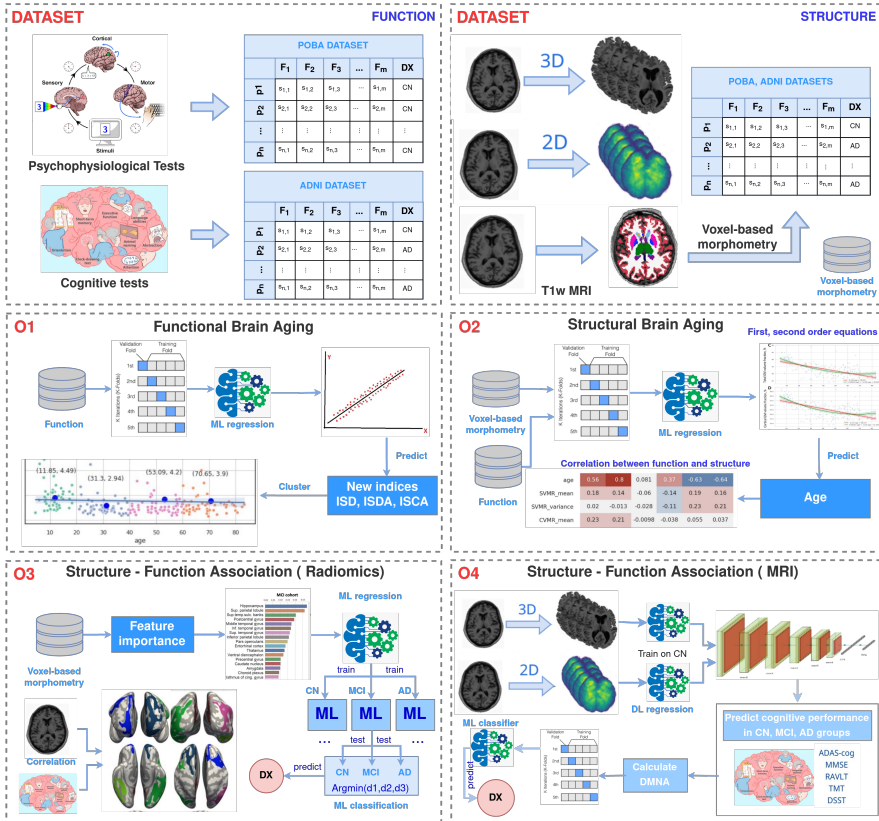


Figure 2.1: Overview of the suggested methodology

The first sub-objective was to create new indices that measure the ratio of functional cognitive processes during the completion of psychophysiological tasks. We looked at the structure of the CVMR, also known as the choice reaction, to come up with a suitable solution. The choice reaction, like SVMR, has sensory acquisition (visual perception) and motor responding elements. CVMR also includes the decision-making aspect that is involved in processing an inhibitory condition that is provided

in the task (see Figure 2.2). There is a time delay (DMT) as a result of this procedure. In a recent study, we looked at the age-related heterogeneity of DMT. We focused on the fraction between DMT (the switching and inhibitory control estimate) and SVMR (the information processing speed estimate) in this section of the investigation. The age-related dynamics of the dependent variable of the reaction to a moving object (RMO) test, which indicates the coordinated involvement of numerous cognitive domains, were also examined.

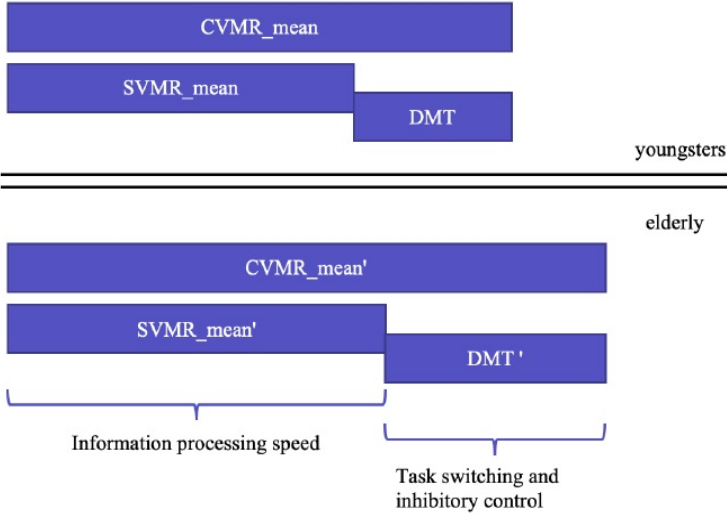


Figure 2.2: Simple and complex visual-motor task estimates, and the cognitive functions they describe during the lifespan

The second sub-objective was to determine the best number  $k$  of separate nonoverlapping age divisions. To accomplish this, we used a heuristic strategy based on the elbow method. The K-means algorithm used the distortion score, or the sum of squared distances from each point to its associated centroid, as an assessment metric for each chosen  $k$ . The

minimal distortion score matched the ideal cutoff  $k$  value. After determining the ideal  $k$ , we used the K-means clustering approach to evaluate the separability measure by age group. Each cluster had a centroid, and we calculated the number of relevant and irrelevant data points in each group.

In the third sub-objective, we employed ML classification methods to predict an individual's age group based on their performance in PTs. The 40-year-old age limit was taken into account. This age is justified as a cutoff value for the cognitive deterioration that may be detected by test performance, according to our recent study [32]. In this case, we used conventional ML (Gaussian NB, Gradient Boosting, Random Forest, AdaBoost, linear and non-linear SVM, Ridge, Lasso) classification models and trained them in the stratified 10-fold cross-validation technique.

The projected results in each fold were blended and subsequently averaged to determine the models' ultimate accuracy. We compared the model performance with and without indices to predict age by evaluating and comparing the model performance measures. We created an averaged receiver operating characteristic (ROC) curve to assess the performance of the predictive model. The mean area under the ROC curve (AUC), specificity (Spec), sensitivity (Sens), and accuracy (Acc) values were also computed. Because the sample was uniformly distributed across age groups, these performance measures were deemed to be appropriate. For each index used as a predictor we calculated  $Mean \pm SD$  to average the accuracy of the framework. Finally, we employed the Kruskal-Wallis test to ascertain if the variation of accuracy for one index was significantly different ( $p < 0.05$ ) from that of other indices.

In the fourth sub-objective, we examined if the proposed indices could be utilized to produce a summary of the results of individual psychophysiological testing. As a result, we employed ML regression models to forecast the new indices' values. We used all of the features in the POBA dataset as predictors, excluding those that can be used to derive the values of the indices. With the exception of the SVMR\_IES variable, we utilized the same predictors to estimate the value of the index of performance in an SVMR and CVMR with account for accuracy (ISCA). These features were eliminated because ISCA can be obtained using SVMR\_IES. We used mean absolute error (MAE), root mean squared error (RMSE), and a fraction of MAE to a range of values ( $max - min$ ) to assess the quality of the regressor outcome.

### 2.2.2 *Patterns of Brain Structural Changes in Normal Aging*

We started with the first sub-objective which was to use ML approach (regression) for the assessment of the structural alterations of the major brain regions and to find the patterns of neurofunctional performance in different age groups. We looked at a pairwise distribution of voxel-based brain morphometry (VBM) results (Subsection 2.3.1) over different age groups to achieve this sub-objective. Formulae 2.1-2.5 were used to adapt the data to the individual's full skull volume. We investigated variables related to attention, reaction speed, and task switching using pairwise distributions of psychophysiological attributes across ages. For each age cohort and gender we presented the VBM and PT results as *IQR*, *Mean  $\pm$  SD*, and conducted the Kruskal-Wallis test to compare the distribution of the group data across the overall cohort.

$$CSF\% = CSF / TIV \quad (2.1)$$

$$iCSF\% = iCSF / TIV \quad (2.2)$$

$$GM\% = GM / TIV \quad (2.3)$$

$$WM\% = WM / TIV \quad (2.4)$$

$$WMH\% = WMH / TIV \quad (2.5)$$

The Ridge Regression model with a linear least-squares optimization function and L2-norm regularisation was used to examine the association between anatomical brain features and functional performance across time in different life periods. We evaluated the derived linear models for significant age-related dynamics using the t-test (a zero slope value was taken as the null hypothesis). If the p-value for the slope was less than 0.05, the dynamics of a variable in a given age cohort were deemed to be significant.

In the second sub-objective, we chose the mathematical model that best reflects the progression of anatomical and functional changes in the brain throughout time. Several tasks were included in this sub-objective. We looked at the relationship between the VBM, the findings of the PT, and age. The underlying assumption was that performance in some cognitive domains would fall linearly with age, whereas performance in other domains would exhibit a non-linear relationship with age.

In the first part of sub-objective two, we studied both linear and non-linear (polynomial) relationships between age, VBM, and PTs.



$$feature = f(age) \quad (2.6)$$

As an independent variable, we employed the age exponent:

$$feature = A \cdot age + B \quad (2.7)$$

$$feature = A \cdot age^2 + B \cdot age + C \quad (2.8)$$

where the feature is a value of either the functional (DMT, SVMR\_mean, CVMR\_mean, IRT\_mean, AST\_mean, TRVI, and RMO\_mean) or the structural (e.g., the volume of CSF, GM, WM) attribute;  $A, B, C \in \mathbb{R}$ .

A regression model given in Formula 2.8 is non-linear with respect to age. Despite this, the model remains linear for the dataset-estimated parameters  $A$ ,  $B$ , and  $C$ . As a result, we could use a linear regression (LR) approach to fit the data for both linear and non-linear functions (refer to Formulae 2.7-2.8). We generated a new feature matrix using polynomial features to determine the optimal parameters for the non-linear function. The constructed matrix was then fed into the LR model. Despite the fact that this technique allowed us to employ high-dimensional feature spaces, we limited the analysis to first- and second-order relationships.

In the second part of sub-objective two, we looked at algorithm performance indicators to ascertain which model best fit the data. To communicate changes in VBM and PTs throughout life, we employed linear and non-linear (polynomial kernel) regression models. The 95% confidence intervals (CIs) for both the parabolic and the linear trendline functions were

determined using the bootstrap approach. We performed a comparison of the linear and polynomial models for generalization purposes. We used MAE, RMSE, and R2 metrics to evaluate the model's performance.

The third sub-objective was to contrast the kinetics of functional and structural changes in the brain across different age cohorts. We began by looking at the relationship between cognitive performance and volumetric brain data. We did this by calculating correlation coefficients across the full study cohort's data. Subsequently, using the t-test, we looked for statistical difference between the slopes in age cohorts in the linear models of brain anatomical and functional changes.

### *2.2.3 Patterns of Brain Structure-Function Association Indicative of Mild Cognitive Impairment and Dementia*

First sub-objective: We assessed changes in the cognitive and neurophysiological test scores in normal and accelerated aging. We explored the age-related variability of cognitive scores in the tests most commonly used either to diagnose MCI and dementia or improve the accuracy of multimodal diagnostics. The first group of tests included MMSE and ADAS-cog which reflect global cognitive functioning. The second group of tests covered a few cognitive domains, i.e., information processing in DSST, memory in RAVLT, and information processing in TMT (part B). To present the change in test scores with disease progression, we built linear trendlines for the cognitively preserved group and patients with MCI or dementia.

Second sub-objective: We built regression models predicting functional performance in cognitive tests from brain radiomics. The vulnerability of distinct neuronal cells to atrophy in accelerated aging

differs among cell groups and brain regions. Reasonably, SFA are considered to have pathology-specific features. Therefore, we trained the regression models on each study cohort separately. The input to the model was the data acquired from VBM and surface-based brain morphometry (SBM). The VBM is a computational approach to neuroanatomy that measures the differences in local concentrations of brain tissue through a voxel-wise comparison of multiple brain images. The SBM is a complementary structural imaging analysis for quantifying GM abnormalities. The feature selection technique allowed us to identify the most valuable structural neuroimaging measures. The models reflect SFA patterns which are unique for each study cohort. We also looked for significant correlations between cortical parcellation volumes and test scores in the cohorts to investigate neuroanatomical differences in relation to cognitive status.

The third sub-objective was to assess the diagnostic value of the proposed models. We classified individual findings according to the model which best described the case, i.e., the model with the minimal absolute error in prediction in identifying the CN, MCI, or dementia group. In this case, the ML model trained on the cases of CN, MCI or Dementia groups describes a disease-specific SFA pattern. The pattern serves as a unique "stamp" of the disease on which the model was trained. Therefore, one can find the "stamp" which best fits the case. To boost the performance of the multigroup classification, we employed the model blending technique. As an ensemble algorithm, we chose the majority voting method. Since it required an odd number of constituent classifiers, we selected the three most accurate models which predict results in MMSE, ADAS and RAVLT.

#### 2.2.4 Improving Screening for MCI and Dementia

The first objective was to conduct a comparative analysis of the brain structure and function in CN subjects, and MCI and AD groups. We used non-parametric statistical methods to assess the separability of the three groups, namely the Kruskal-Wallis test for continuous data and the Chi-square test for quantitative features.

The second sub-objective was to propose a new marker of accelerated cognitive decline. In line with the hypothesis of this objective, we proposed to predict the cognitive status of a cognitively preserved examinee from brain MRI data and used the SFA model. Then we applied the SFA model to the findings of the study group. When the findings of a scanned individual did not fit the standard SFA model, accelerated aging was suspected. We calculated the deviation from the model of normal aging (DMNA) as the error of cognitive score prediction (see Formula 2.9).

$$DMNA = y_{predicted} - y_{actual} \quad (2.9)$$

where  $y$  is a result of the cognitive test.

Modeling cognitive performance from MRI is a complex problem. To reduce its computational complexity, we transformed MRI images into two-dimensional data (see Subsection 2.3.2). Then we designed a CNN model and trained it on images of CN individuals. To generalize the model to a true rate error, we utilized the five-fold cross-validation technique. As an input, we used the pre-processed MRI data, both 3D and 2D ( $D_{axial}^{(CN)}$ ,  $D_{coronal}^{(CN)}$ ,  $D_{sagittal}^{(CN)}$ ). The output variables were the results of the following

cognitive tests: MMSE, RAVLT, TMT (part B), DSST, and ADAS-cog. After the prediction of cognitive performance we calculated DMNA (see Formula 2.9).

The third sub-objective was to justify the reliability of DMNA. It was a three-fold task. First, we employed non-parametric statistical tests to compare the DMNA values of the CN group with those of MCI and AD patients. Second, we created ML models that distinguished the following study cohorts by DMNA values: CN people from patients with MCI, and the latter from those with AD. The models were trained with the ten-fold cross-validation technique. Finally, we evaluated their performance. The performance of the regression models was expressed as MAE. The accuracy of the classification model was assessed with Sens, Spec, F-measure, ROC, AUC, Acc and balanced accuracy (BAC).

The fourth sub-objective was two-fold. In the first part of sub-objective four, we tested whether the proposed marker could prognosticate the conversion of pre-dementia to dementia. To find the cases of stable and progressive MCI, we carried out an exhaustive search of all longitudinal studies: ADNI1, ADNI2, ADNI-GO, and ADNI3. Then, we built the conventional ML model segregating the cases according to stability/progression. We used DMNA in MMSE and ADAS-cog as more reliable predictors because the tests covered the global cognition functioning. To compare the distribution of DMNA in two groups, we applied the non-parametric Kruskal-Wallis test. We also assessed the Sens and Spec of the model, classifying MCI cases as stable or progressive. The second part of sub-objective four was to check whether DMNA could differentiate cognitive decline due to AD from other NDs. To address the

research question, we used ATN criteria [183] and adopted a two-step analysis. Firstly, we dichotomized each biomarker category as either normal (-) or abnormal (+) with the following cutoff thresholds. A case was considered as A- if the CSF concentration of  $\beta$ -amyloid was higher than 81/ml [184, 185], as T- if the level of  $\tau$ -protein was less than 56 pg/ml [184, 186], and as N- if the uptake of fluorine-18 deoxyglucose was larger than 1.21 [187]. Secondly, we classified all the cases with MCI and dementia into groups and calculated mean values of DMNA for them. Finally, we identified the difference in DMNA between demented individuals with Alzheimer's continuum (A+) and those with either normal AD biomarkers or non-AD pathologic change (A-). Figure 2.3 shows the general idea of the proposed SFA model, and Figure 2.4 illustrates the proposed framework.

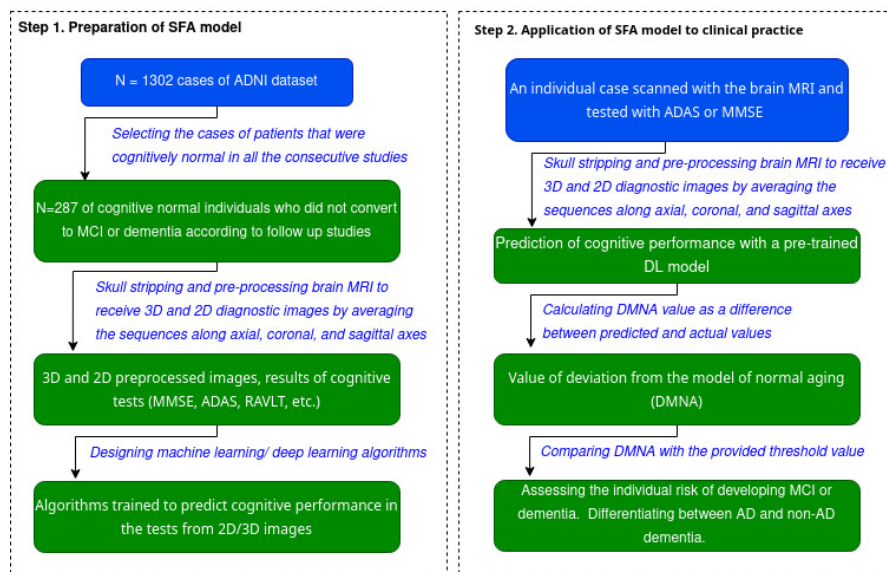


Figure 2.3: Preparation and application of the proposed SFA model to clinical practice

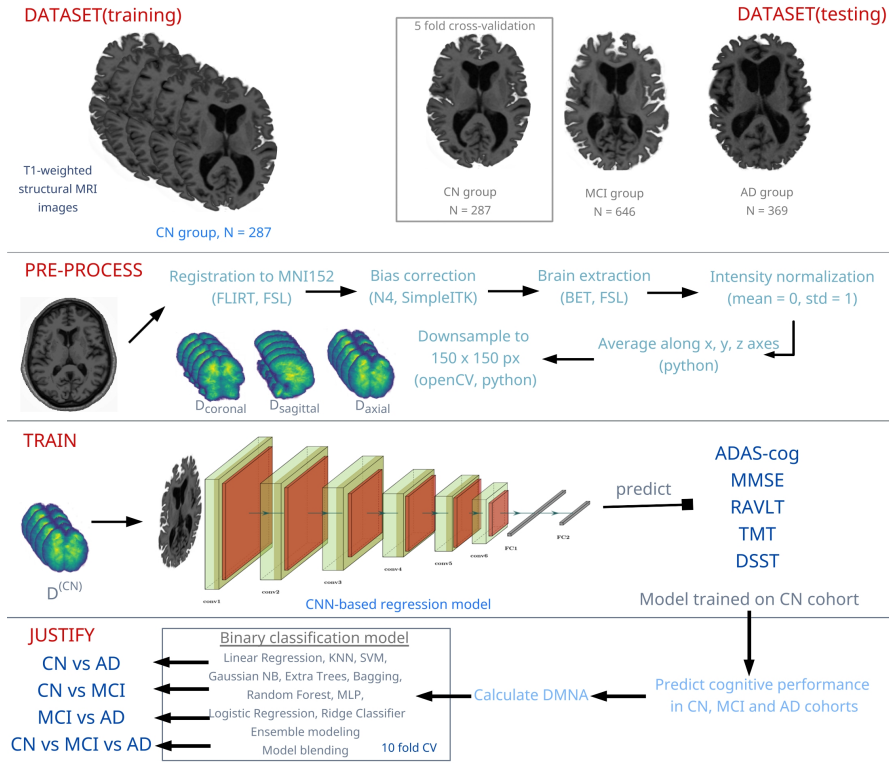


Figure 2.4: Pipeline of proposed framework

## 2.3 Methods

### 2.3.1 MRI Acquisition and Brain Morphometry

In ADNI dataset brain images were obtained with 1.5 or 3 Tesla scanners. The detailed information about MRI acquisition can be found from the link <http://adni.loni.usc.edu/methods/mri-tool/mri-acquisition>. In POBA dataset brain images were acquired with a 1.5T MRI scanner. The structural acquisition settings were as follows. 3D-T1w images had 1 mm voxel size. The scanning matrix was  $224 \times 256$ . TE was 6.21 ms, and TR - 13 ms [188]. The FLAIR sequence had a 4mm slice thickness. The scanning grid was  $260 \times 320$ . TE was 104 ms, and TR - 9,130 ms. We used FLAIR for measuring

WM hyperintensities (WMHs) (see Figure 2.5).

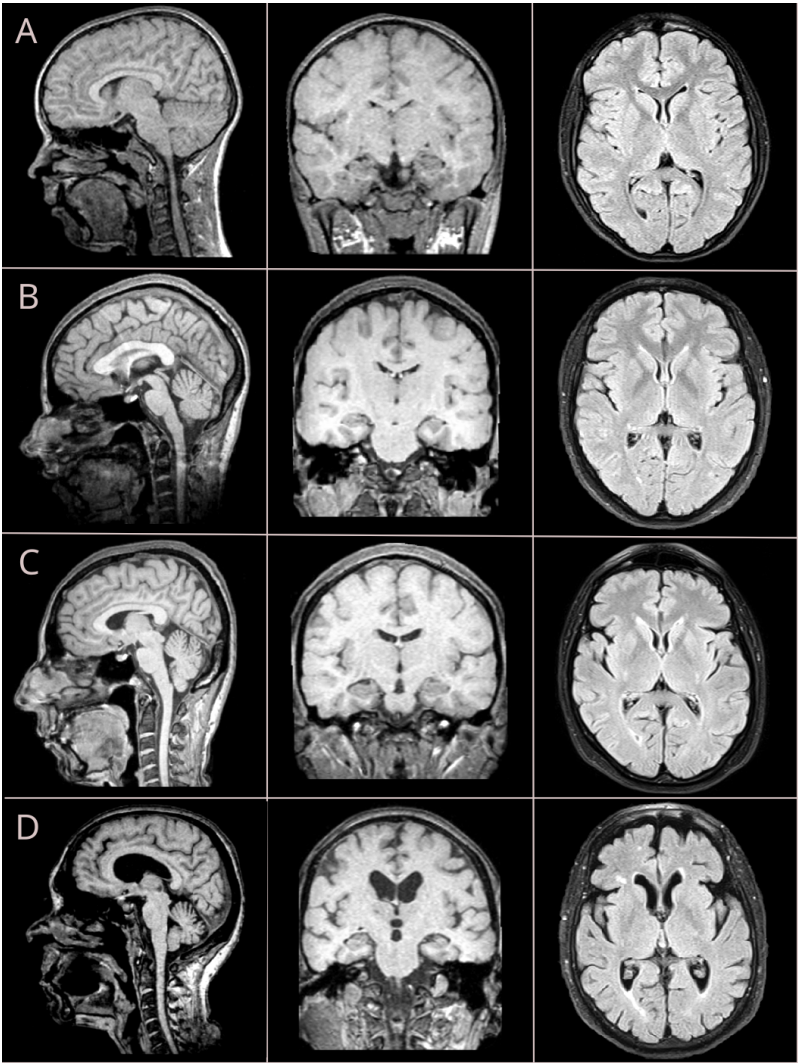


Figure 2.5: Brain MRI changes throughout 4 stages marked from A to D: adolescence, early adulthood, middle, and old age. T1w sequence with isometric (3D) vowel is used to reconstruct sagittal and coronal views; FLAIR sequence is used to retrieve axial images

VBM was employed to quantify the brain structural changes. Then we calculated volumes of WM hyperintensities and the following



structures: interventricular CSF, hippocampus, putamen, caudate nucleus, amygdala, WM, enthorinal cortex, fusiform gyrus, middle temporal lobe, GM, cortical GM and total intracranial volume. The segmentation of the brain into its major compartments (WM and GM, SCF) was done as below. We applied the 12-th version of the computational anatomy toolbox (<http://www.neuro.uni-jena.de/cat/>) for the statistical parametric mapping software (<http://www.fil.ion.ucl.ac.uk/spm/>) [188]. We resorted to the lesion segmentation toolbox LST v2.0 to segment the changes in FLAIR-hyperintense WM lesions [189, 190]. Subcortical, cortical and parcellation volumes were computed with FreeSurfer 7.1.0 software [191]. We resorted to Desikan/Killiany atlas as a reference. All morphometric features were expressed as percentage to the total intracranial volume and used as an input to the ML model predicting the cognitive scores.

### 2.3.2 *Data Pre-processing*

All the retrieved images passed through grad-warping and intensity correction and were scaled to gradient drift with the phantom data (for more details, see [178]). The pre-processed T1w structural MRI images were downloaded in NIFTI format. We also retrieved the corresponding clinical data from the dataset. Then the images were registered to an MNI152 space with FLIRT tool from FSL package [192]. As brains differ in size and shape, each brain image was translated into a common reference space (normalized) to ensure consistency of orientation. To correct low-frequency intensity non-uniformity, we used N4 bias field correction algorithm [193]. Then we normalized the voxel intensities by scaling them to the standard normal distribution parameters. To enhance the predictive performance, we

extracted the brain parenchyma with Brain Extraction Tool from FSL package [192]. Pre-processed 3D T1w images were downsampled to the size of 64 by 64 by 64 pixels and used as an input to the 3DCNN models. One of the major challenges of studies on MRI is a high dimensionality of data [194]. We used the following approach to reduce the dimensionality. An MRI image was defined as

$$I = \{(v_x, v_y, v_z) : x = \overline{1, X}, y = \overline{1, Y}, z = \overline{1, Z}\}, \quad (2.10)$$

where  $X, Y, Z$  were the dimensions of the MRI scan in axes  $x, y$  and  $z$ .

Then the  $j^{th}$  sagittal, coronal or axial slice  $s$  of the  $I$  image could be defined as:

$$s_{sagittal}^{(j)} = (j, v_y, v_z), s_{coronal}^{(j)} = (v_x, j, v_z), s_{axial}^{(j)} = (v_x, v_y, j) \quad (2.11)$$

The corresponding averaged images were generated as follows:

$$I_{sagittal} = \frac{1}{X} \sum_{i=1}^X s_{sagittal}^{(i)}$$

$$I_{coronal} = \frac{1}{Y} \sum_{i=1}^Y s_{coronal}^{(i)}$$

$$I_{axial} = \frac{1}{Z} \sum_{i=1}^Z s_{axial}^{(i)}$$

In this way, we averaged voxel intensities along the sagittal, coronal and axial axes and created two-dimensional datasets  $D_{axial}, D_{sagittal}$ ,

and  $D_{coronal}$ :

$$D_{axial} = \{I_{axial}^1, I_{axial}^2, \dots, I_{axial}^N\}$$

$$D_{sagittal} = \{I_{sagittal}^1, I_{sagittal}^2, \dots, I_{sagittal}^N\}$$

$$D_{coronal} = \{I_{coronal}^1, I_{coronal}^2, \dots, I_{coronal}^N\}$$

Then, we removed the background by cropping the image to the size of the brain mask. We downsampled brain images with nearest-neighbor interpolation to 150 by 150 pixels, normalized them to the values between 0 and 1, and saved in JPEG format as shown in Figure 2.6. To unify the pre-processing workflow, we used Nipype which is an open-source community-developed initiative under the umbrella of NiPy [195]. To automate the deployment of the applications within the software containers, we installed Neurodocker which wraps up the aforementioned software in a complete file system.

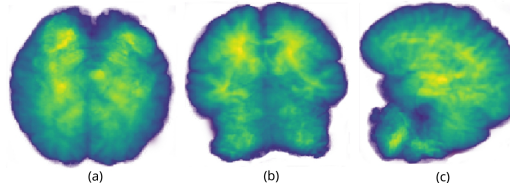


Figure 2.6: Skull-stripped images averaged along axial (a), coronal (b), and sagittal (c) axes

### 2.3.3 Psychophysiological Tests

To assess individual psychophysiological status, we used a battery of neurophysiological tests [180]. The battery included a variety of tasks that tested cognitive areas such as attention and EF, with an emphasis on the

inhibitory control and task switching and subdomains. The tests facilitated an evaluation of information processing speed. We modelled changes in the dependent variables listed below throughout the course of a lifetime [188]:

- Simple visual-motor reaction (SVMR) is a test in which the only way to respond is to look at a single form of visual stimulus. The information processing speed is reflected by the mean reaction time. SVMR\_mean is calculated in a group of successive attempts.
- Complex visual-motor reaction (CVMR) is a “go/no-go” test. In this test the participant must choose between two different types of triggering stimuli. The mean reaction time is typically longer than in the previous test ( $CVMR\_mean > SVMR\_mean$ ). One can calculate the decision-making time (DMT) by subtracting the SVMR\_mean from the CVMR\_mean (see Formula 2.12). Task switching and inhibitory control is reflected by DMT.
- Attention study technique (AST) is a variant of SVMR that includes the attention domain. In AST, however, the participant must maintain a constant gaze on the display screen because triggering stimuli are delivered at various times. The average reaction time (AST mean) is recorded by the tester.
- Interference resilience technique (IRT). The participant is instructed to reply to targeted stimuli while ignoring interfering stimuli. The last ones overlay and obscure the target. The average reaction time is recorded by the tester - IRT\_mean – of a set of attempts. Formula 2.13 determines time delay because of visual interference value. Its acronym is TRVI. TRVI reflects inhibitory control and task switching.

- Reaction to a moving object (RMO) is a method for determining a balance of inhibition and excitation in the central nervous system. The test's mean reaction time (RMO\_mean) reveals whether the excitatory or inhibitory processes are dominant. We also looked at the variance in reaction time across attempts (RMO\_variance).
- To determine the maximum muscular strength of the hands we employed wrist dynamometry. Asymmetry coefficient (AC) was computed as the ratio of the maximum muscular strength of the right wrist (WDR\_MMS) and the left (WDL\_MMS) wrist (see Formula 2.14).

$$DMT = CVMR\_mean - SVMR\_mean \quad (2.12)$$

$$TRVI = IRT\_mean - AST\_mean \quad (2.13)$$

$$AC = \frac{WDR\_MMS}{WDL\_MMS} \quad (2.14)$$

#### 2.3.4 Cognitive Tests

The purely pre-symptomatic and early stages of dementia are likely to be identified by PT. The existing dementia risk models mainly comprise demographics, subjective cognitive complaints, lifestyle factors, health state estimates, and other variables [125]. Cognitive test scores or neuropsychological test batteries are incorporated as predictors into many models of developing dementia.

Alzheimer's disease assessment scale, cognitive subscale (ADAS-cog). ADAS-cog is an informative tool for monitoring the progression of

ND in clinical routine practice [196]. The test distinguishes between MCI and mild AD with a sensitivity of 0.86 and a specificity – 0.89 [197]. It can also identify “questionable dementia,” as its results in immediate recall and object naming tasks correlate with performance in the Category Verbal Fluency Test [198]).

The Mini-mental state examination (MMSE) is the most common method of diagnosing cognitive impairment in a single domain or multiple domains [199]. Although it detects various types of dementia with a high sensitivity and specificity (over 90%), the test should be accompanied by a full and detailed assessment of the patients [200]. For this, clinicians use neurophysiological tests (e.g., TMT, DSST) [201].

Trial making test (TMT). The primary purpose of the TMT is to provide information about neurophysiological conditions; therefore, it is used to diagnose NDs in combination with other tests and diagnostic modalities [201, 202, 203]. Its clinical implication is multifold. First, TMT helps to define the impaired cognitive domain and improves the assessment made with MMSE or MoCA [201]. Second, there is evidence that the inclusion of TMT (part B) boosts the performance of the models discriminating AD from non-AD MCI based on CSF and structural biomarkers [204]. Third, the test can sensitively distinguish a case of mild AD from amnesic MCI and healthy aging [205].

The Rey auditory verbal learning test (RAVLT) examines verbal learning and memory. It is capable of detecting cognitive impairment in multiple sclerosis [206]. The test differentiates between AD dementia and behavioral variants of fronto-temporal dementia [207] with a high sensitivity and specificity (over 81%). It also helps physicians to distinguish

AD from Lewy body dementia [208].

The Digit symbol substitution test (DSST) identifies early stages of dementia [209] and MCI by detecting working memory impairment and multimodal amnesia [210]. It also shows significantly impaired performance in early Lewy body dementia [211].

### 2.3.5 *Machine Learning*

Objective 1: To determine the best number  $k$  of separate nonoverlapping age divisions we used a heuristic strategy based on the elbow method. The K-means algorithm used the distortion score, or the sum of squared distances from each point to its associated centroid, as an assessment metric for each chosen  $k$ . The minimal distortion score matched the ideal cutoff  $k$  value. After determining the ideal  $k$ , we used the K-means clustering approach to evaluate the separability measure by age group. Each cluster had a centroid, and we calculated the number of relevant and irrelevant data points in each group. To predict an individual's age group based on their performance in PTs we used several classification algorithms, such as support vector machines [212] with linear and nonlinear (radial basis function) kernels, Gaussian Naive Bayes [213], Bagging meta-estimator [214], an extra-trees classifier [215], a random forest classifier [216], Gradient Boosting [217], AdaBoost [218]. Classification models were trained with the stratified 10-fold cross-validation technique.

Objective 2: The Ridge Regression model with a linear least-squares optimization function and L2-norm regularisation was used to examine the association between anatomical brain features and functional performance across time in different life periods. A regression model given in Formula 2.8

is non-linear with respect to age. Despite this, the model remains linear for the dataset-estimated parameters  $A$ ,  $B$ , and  $C$ . As a result, we could use a linear regression (LR) approach to fit the data for both linear and non-linear functions (refer to Formulae 2.7-2.8). We generated a new feature matrix using polynomial features to determine the optimal parameters for the non-linear function.

Objective 3: We employ conventional ML regression models predicting functional performance in cognitive tests from brain radiomics. We trained the regression models on the three study cohorts separately (CN, MCI, dementia). The predictors of the model were the data acquired from voxel- and surface-based brain morphometry. The models reflect SFA patterns specific for each study cohort. We also looked for significant correlations between cortical parcellation volumes and test scores in the cohorts to investigate neuroanatomical differences in relation to cognitive status. Finally, to assess the diagnostic value of the proposed models classified individual findings according to the model which describes the case best. The idea was that the ML model, when trained on the cases of this of that group, describes a disease-specific SFA pattern. The pattern serves as a "stamp" of the disease on which the model was trained. Therefore, one can find the "stamp" which fits the case best. We employed the majority voting technique to assess the performance of the multigroup classification.

Objective 4: To predict cognitive scores from structural data, we developed 2D CNN and 3D CNN regression models. 2D CNN: In the proposed CNN regression model, six convolution layers were followed by two fully connected dense layers. L2 regularization technique with penalty



and  $\alpha = 0.0001$  was employed. Network was trained for 200 epochs or until convergence with RMSProp optimizer. To optimize a learning rate hyperparameter we monitored the validation loss during the training process. When the metric stopped improving for 10 continuous epochs, we reduced the learning rate value by a factor of 0.2. To optimize the training time, we also monitored the validation loss. If it did not decrease for 20 continuous epochs, we terminated the training process. In this case, 20% of the training data were used for validation purposes. The model was trained on the CN cohort in the five-fold cross-validation technique. There were several arguments in favor of the necessity to train the models of SFA on non-demented cases exceptionally. As the model reflected the brain SFA of the healthy controls, it could be used as a reference norm. If trained on a mixed cohort of healthy individuals and patients, the model would fail to identify patients out of the reference range and would lose its diagnostic value. The trained model from the last fold was tested on MCI and AD groups.

For each case we obtained 2D images by averaging brain MRI in three planes: axial (A), coronal (B), and sagittal (C). We could use these either separately or in combination. For the combined approach we used both options: data and model blending. The first was fusing predictions, which was an ensemble estimator or voting regressor that averaged model outcomes. The second was model blending. We trained the LR model on the outcomes of three CNN models trained on axial, coronal, and sagittal averaged images. As an input, we used the pre-processed MRI data ( $D_{axial}^{(CN)}$ ,  $D_{coronal}^{(CN)}$ ,  $D_{sagittal}^{(CN)}$ ). The output variables were the results of the following cognitive tests: MMSE, RAVLT, TMT (part B), DSST, ADAS-cog.

3D CNN: We also developed a 3D CNN model and trained it on images of CN individuals from the ADNI dataset. Pre-processed 3D T1w images were downsampled to the size of 64 by 64 by 64 pixels and fed to the regression model. The model consisted of four convolutional layers followed by max pooling. Then, global average pooling was applied, followed by a fully connected layer. We used an Adam optimizer and trained the network for 100 epochs or until convergence. To optimize the learning rate hyperparameter we monitored the validation loss during the training process. When the metric stopped improving for 10 continuous epochs, we reduced the learning rate value by a factor 0.2. To optimize the training time, we also monitored the validation loss. If it did not decrease for 20 continuous epochs, we terminated the training process. The data were randomly split into training (80%) and testing (20%) subsets. Hence, 20% of the training data were used for validation purposes. To increase the number of training samples, we applied the rotation augmentation technique with the following angles: -25,-20, -10, -5, 5, 10, 20,25. The outcomes of the predictive algorithms were the results of mental status tests such as MMSE, RAVLT, DSST, ADAS-cog, and TMT (Part B). We compared the distribution of the DMNA absolute values in the healthy population and patients with MCI and Dementia. Moreover, we calculated 95% confidence intervals (CIs) for DMNA values using the t-test. To control the familywise error rate related to multiple comparisons we employed the Bonferroni correction. All statistical tests were performed in Python v. 3.6.9 with SciPy v. 1.16.4 library [219].

To determine a diagnosis from DMNA values, we employed nine conventional ML classifiers (SVM linear and non-linear, Gaussian NB,

Extra Trees, Bagging, Random Forest, Logistic Regression, Ridge Regression, Neural Network). DMNA values were obtained from (i) skull-stripped brain images averaged along the axial, coronal, and sagittal axes; (ii) skull-stripped 3D brain images. The ML models were evaluated with the ROC AUC metric.

The experimental work was performed on a Linux Ubuntu 18.04 Nvidia DGX-1 deep learning server with 40 CPU cores and 8x NVIDIA Tesla V100 GPU with 32 GB memory each, accessed with a web-based multi-user concurrent job scheduling system [220]. The tensorflow-gpu v.2.3.1 library was utilized to implement the proposed solution.

## Chapter 3: Results and Discussions

### 3.1 ML Models of Age-Related Cognitive Decline

#### 3.1.1 *Estimates of the Proportional and Disproportional Changes in Cognitive Domains*

We introduce the index of simple reaction time to decision-making time (ISD), which is derived from the analysis described in section 2.2.1 [77]. The index represented the proportion of processing speed to decision-making time (see Formula 3.1). The time estimates were susceptible to age-related neurocognitive loss; nevertheless, there is no convincing evidence that the rate of decrease is equal across cognitive areas. As a result, the derivative variable might be used to track any disproportional deterioration.

$$ISD = \frac{SVMR\_mean}{DMT} \quad (3.1)$$

The ISD index takes into account two markers that make up the visual-motor task's reaction time under the switching situation. It is inherently flawed in that it fails to take performance accuracy into account. As a result, we presented a supplemental derivate variable, the index of simple reaction time to decision-making time with accuracy performance (ISDA) [77]. The proposed index, in comparison to the previous one, includes the fraction of accurate responses in the denominator (see Formula 3.2).

$$ISDA = \frac{SVMR\_mean}{DMT \times (1 - CVMR\_mistakes, \%)} \quad (3.2)$$

Calculating the inverse efficiency score (IES) for each of the tests independently and then computing the ratio between these tests represents a further technique to integrate the speed and accuracy estimations of SVMR and CVMR. As a result of this solution, we determine the index of performance in simple and complex visual-motor reactions with account for accuracy (ISCA) per Formula 3.3 [77].

$$ISCA = \frac{IES_{SVMR}}{IES_{CVMR}} = \frac{SVMR\_mean \times (1 - CVMR\_mistakes, \%)}{CVMR\_mean \times (1 - SVMR\_mistakes, \%)} \quad (3.3)$$

Index of Simple Reaction Time to Decision-Making Time: We did not plan to evaluate all potential ratios of performance indicators in distinct cognitive tasks in this current research. Our objective was to demonstrate the approach's efficacy when testing multiple domains and estimating their correlated divergent changes.

From the encoding of a provided stimulus to the execution of a response, reaction time covers a sequence of linked processing activities. Regrettably, response time does not display each of these transactions individually; instead, it is limited to a total time length. Some researchers have proposed that the transactions can be measured sequentially utilizing the time latency of evoked potentials [221]. Our strategy was to employ a battery of tasks with the following characteristics. We created a range of tests in which the testing modalities (SVMR and CVMR) contain the identical perceptual and motor response components, but the central processing differs. We adopted this approach as opposed to assessing reaction time in a single task or utilizing divergent tasks (DMT). This allowed us to investigate Birren et al.'s complexity hypothesis, which states

that neurocognitive degradation is limited to central nervous system processing. The extent of deterioration increases as the task complexity increases [181, 182]. However, this is true for non-lexical activities, but not for word processing tasks, where slowing is unrelated to complexity [77, 221].

The strong form of the complexity theory is supported by the findings of the current study. According to the strong version, all aspects of information processing (such as reasoning, perception, and response) diminish in the same pace. The ISD index remains steady as the amount of time spent thinking in CVMR decreases over time at the same rate as the total of the receiving, encoding, and reacting elements. On a population basis, this keeps the the proportion of DMT and SVMR\_mean steady throughout lifespan on a population scale.

The strong form of the complexity theory offers several advantages. It backs up the theory that age-related impairment is linked to a general slowing of processing speed rather than specific information processing components aspects. It also makes it much easier for neuroscientists to identify brain structure-functional correlations as individuals age [221]. This is consistent with prior research [221] that used reaction time as an aggregate measure of processing speed.

The complexity hypothesis's weak version asserts that the severity of the deterioration in perceptual, motor, decision-making, or attentional processes might vary. Some researchers have found that "age-related slowing in simple repetitive tasks is mainly related to slowing at the stage of perceptuomotor processes, and after 60 years, to additional decline in attention" [222]. The length of the transactions linked to acquisition of

stimulus and processing of response should be measured using an event-related potentials approach in future studies.

Supplying ISD with Performance Accuracy (ISDA): In the CVMR test, DMT stands for the time it takes to inhibit an automatized activity and transition between tasks. The percentage of choosing and perceptive motor elements of choice RT is indicated by the SVMR to DMT ratio. The cognitive demands of the decision and perceptive-motor components of CVMR are distinct. We can ascertain whether age-related neurocognitive impairment begins with cognitively demanding behaviours (task switching) or includes both intellectual and nonintellectual processes (generalized slowing) by comparing them.

We provided the ISD index with the accuracy metric to acquire the total efficiency of the examinee in the test (see Figure 3.2). The index's goal is to look at the ratio of cognitively demanding to non-demanding tasks' processing speed while also taking performance accuracy into account.

Ratio of IES for Simple and Choice Reactions (ISCA): The IES ratio between SVMR and CVMR reflexes is shown in the final index. The entire efficiency of decision-making is summarised by the IES score. IES takes into consideration several cognitive subdomains and may represent their disproportional changes over time [77]. Some researchers have found disparities in SVMR and CVMR evolve over time [223], but none have found the same is the case with IES scores. The process for generating the IES score could be one of the reasons why this has yet been done. Neuroscientists primarily employ choice errors produced while doing "go/no-go" tests (e.g., CVMR\_false\_reaction) to determine performance accuracy. Two more types of errors were recorded by the equipment we

used: (i) missing the desired events (e.g., SVMR\_passes) and (ii) reacting prematurely (e.g., SVMR\_falstart). By adopting this approach, we were able to compute IES for the basic visioal-motor reaction and contrast it with the equivalent data for the complex reaction.

We believe that examining the link of IES for strongly correlated simple and choice reactions is more informative than researching the association of reaction time. Simple reaction time is responsible for 45% of the variance in choice reaction time [223].

### *3.1.2 Optimal Number of Age Cohorts*

We employed used two dependent variables (age and a novel index) in the cluster analysis and the K-means approach to divide the data points into groups. To identify the optimal number of homogenous clusters, we adopted the K-means method. We discovered the most acceptable number of groups using the elbow approach, and it was further validated by a distortion score (the separability measure). The sum of squared distances between each location and its allocated centroid determines the score. Iteratively, all cluster centers (centroids) are found by optimizing intracuster proximity while increasing the distance between data points from different clusters. The elbow approach was applied to data points made up of the participants' ages and related index values (ISD, ISDA, or ISCA).

For each proposed index, the knee point detection method [224] returns the ideal value of clusters equal to four. The optimal number is marked with a black dashed line in Figure 3.1, which was created for two attributes (age and ISCA). The line in blue on the graph represents the



distortion score values as a function of cluster number, whilst the dashed line in green represents the time required to train the unsupervised model per  $k$ .

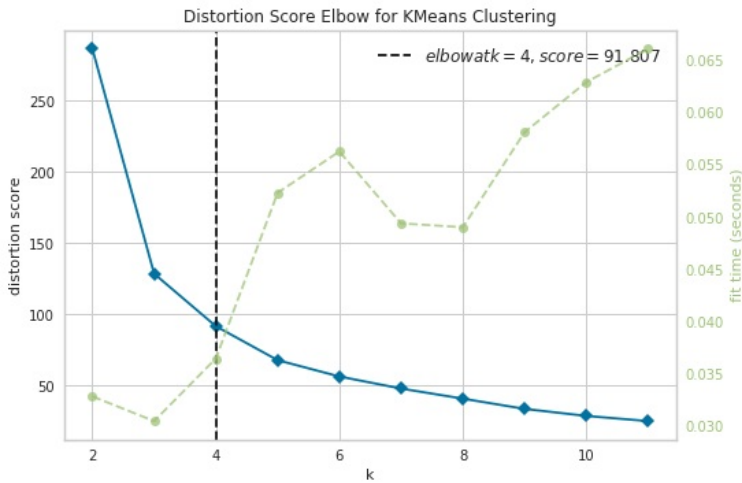


Figure 3.1: Elbow approach with the knee point detection algorithm to select the best number of clusters for the ISCA index

The age distribution of the participants in our sample was not uniform; nevertheless, with the appropriate selection of bin width, the age histogram can come very near to being uniform. Another source of concern is the comparatively small number of patients above the age of 75 compared to the number of participants under 15. To ensure that each group had a roughly similar number of participants, we opted to count the 20-year intervals from birth as opposed to the youngest examinee’s age.

We evaluated how accurate the clustering method is by observing the values of the indices (ISD, ISDA, ISCA) as age-group determinants. We investigated the age values of the points obtained by the clustering approach by plotting them with their centroids. On the age axis, the centroids were

relatively equally spread, with a step of around 20 years (see Table 3.1). Because the cluster center coordinates were determined as the average value of all the points in the particular cluster, we used the resulting age granulation to create our groupings.

Table 3.1: Clusters based on distribution of samples over age and proposed indices

Group	Capacity (females:males)	ISD Index			ISDA Index			ISCA Index		
		Centroid	In	Out	Centroid	In	Out	Centroid	In	Out
Adolescent	48 (19-29)	11.853	48	0	12.047	48	0	11.661	48	0
Young adults	64 (36-28)	31.302	62	2	31.600	60	4	30.075	64	0
Midlife adults	64 (39-25)	53.089	57	7	53.529	56	8	49.908	59	5
Older adults	55 (40-15)	70.647	46	9	71.018	46	9	68.274	55	0

As a result, we divided our sample into four groups: Adolescents (below 20 years), Young adults (from 20 to 40), Midlife adults (from 40 to 60), and Older adults (above 60 years). We reported the number of points properly identified by the clustering approach (classified column) vs. misclassified points in Table 3.1. The best results were achieved on the ISCA. Only five examples of adults in their forties and fifties were misclassified as teenagers. In the POBA dataset that we collected, the ISCA index accurately captures age-related psycho-physiological shifts [77].

We used a heuristic technique and clustering approach to choose and justify the age cohort ranges. We subsequently ran a review to see what biological alterations might be at play in the selection of such subcohorts. The time intervals between the end of neurodevelopment and the appearance and the acceleration of cognitive decline are represented by the group boundaries.

Healthy educated adults begin to experience age-related cognitive

changes during their 20s-30s [225]. Before the age of 20, there is a period of rapid neurodevelopment, during which people exhibit skill acquisition, knowledge development, and a growth in intellect. Cognitive functions exhibit conflicting developments during the next 20 years of life. Early in life, basic physiological cognitive functions deteriorate. As a result, early lowering of fluid intelligence, memory, and processing speed may appear in young adults. Simultaneously, crystallized intelligence rises [226]. The authors of a study on simple reaction time found that consistency of response increases with age from 8 to around 30, after which it begins to diminish. The fastest response was recorded in people over the age of 20, but the most consistent response in terms of time variance was observed in people over the age of 30 [227]. Another study found a roughly similar chronology of changes: the shortest reaction time occurs in the mid-20s of the participants [228].

The total volume of the brain WM increases until early middle adulthood (age 35 years or more) [229, 230]. Then there is a subsequent period when WM volume and cognitive performance are plateaued [229, 230]. Midlife adults' cognitive capacities may be harmed by neurocognitive slowdown throughout this stage of life. Neuroplasticity induced by physical and mental exercise has been shown to reduce alterations and improve cognitive function [231, 232]. Nevertheless, in the middle-aged population, cognitive deterioration is already discernible [233]. However, the precise timing of its commencement remains a point of contention [233]. After late middle age (55–60 years), accelerated cognitive decline commences [229, 230]. It is characterized by a significant decrease in WM volume, while the GM volume decreases at a consistent rate

throughout life.

3.1.3 Proportional Changes in the Cognitive Domains with Age

Figures 3.2-3.4 show a pairwise distribution of age with each proposed index. The linear horizontal trendlines for the linear regression model estimates with a 95% confidence interval reflect inclinations toward maintaining a balance between cognitive functions pertaining to several connected domains.

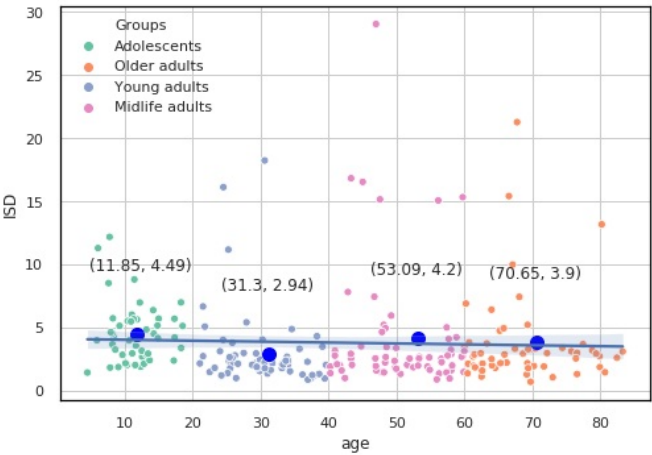


Figure 3.2: Distribution of ISD values throughout life

We used statistical significance tests to examine the indices’ distribution across age groups. We resorted to nonparametric statistics because none of the indices data per the Gaussian distribution exhibited in the Shapiro-Wilk test ( $p < 0.05$ ). The Kruskal-Wallis test, which revealed significant changes in the distribution of the four age cohorts ( $p < 0.05$ ), was used to test the null hypothesis that the cluster medians were equal.

We followed the step-down procedure to run a post hoc Dunn test to ascertain which groups had different medians. To control the familywise

error rate, we employed Bonferroni corrections (Holm’s step-down approach). The median of the Adolescents group differed from the other three cohorts’ indices values. The distribution patterns of the three remaining groups were similar ( $p > 0.01$ ). The indices maintained nearly constant values during a period of neurodevelopmental alterations and maturation, with a modest trend toward functional deterioration.

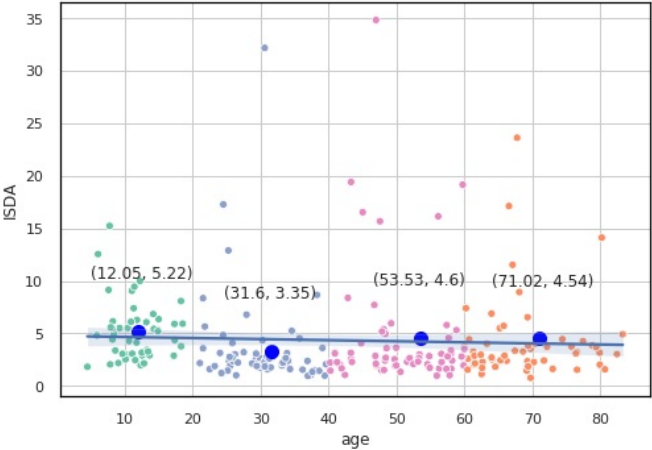


Figure 3.3: Distribution of ISDA values throughout life

However, the RMO test revealed a further tendency. Pairwise comparisons of RMO\_mean data revealed that the median of Midlife adults’ group differed significantly from the remaining three age cohorts ( $p < 0.01$ ). There was no discernible trend in this dependent variable’s age-related variations (see Figure 3.5).

Finally, the variances of the proposed indices were explored, as well as selected psychophysiological characteristic values for various groups. For the abovementioned values, Levene’s test demonstrated no significant difference ( $p > 0.05$ ) in the variances across age ranges.

Homoscedasticity also backed up our theory of a steady linear relationship between observed traits and age.

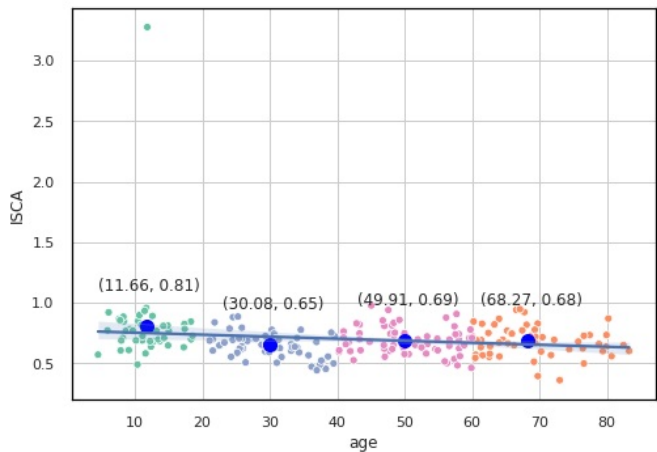


Figure 3.4: Distribution of ISCA values throughout life

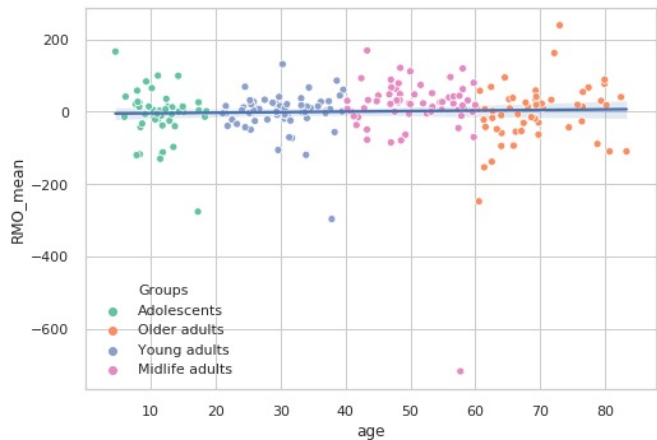


Figure 3.5: Pairwise distribution of reaction time and age in RMO test

Trends in Cognitive Subdomains with Age and Proportionality of their Changes: Table 3.2 shows the statistically significant differences in PT performance across age groups. The study aimed to assess the possible

association between ISD, ISDA, and ISCA; the participant’s general psychophysiological condition; and his or her age. Furthermore, we used a machine learning approach to estimate the examinee’s age group, i.e., whether he or she was under or over 40 years old. We aimed to ascertain how well the variables produced from the test results could reflect the individual’s whole psychophysiological state. As an individual’s psychophysiological status changes with age, one may anticipate the derivative indices to reflect this change as well. Our recent study [32] has previously justified the cutoff level utilized. We investigated the latter’s information value for such a forecast by feeding the models with values of the novel indices. The models’ performance measures are listed on the left side of Table 3.3.

Table 3.2: Comparative analysis of results in PTs

	Total n=231	Adolescent n <sub>1</sub> =48(20.78%)	Young adults n <sub>2</sub> =64(27.71%)	Midlife adults n <sub>3</sub> =64(27.71%)	Older adults n <sub>4</sub> =55(23.81%)	P1 -4
Psychophysiological tests (performance)						
SVMR_mean	260.51[219.63-285.83]	282.03 ± 70.91*	221.03 ± 28.92*	259.76 ± 55.48	288.52 ± 53.75*	1.61005e-14
SVMR_variance	69.88[41.09-80.82]	89.01 ± 73.36	49.41 ± 22.39*	67.69 ± 36.54	79.54 ± 42.92*	7.05157e-06
SVMR_mistakes	1.32[0.0-2.0]	2.69 ± 3.83*	0.83 ± 1.32*	0.62 ± 1.11*	1.49 ± 1.54*	2.8462e-06
SVMR_IES	280.06[224.94-304.73]	339.43 ± 236.3*	227.9 ± 32.9*	265.77 ± 59.02	305.56 ± 64.35*	7.00503e-15
CVMR_mean	360.77[307.45-395.57]	360.8 ± 107.74	324.89 ± 56.55*	362.64 ± 65.15	400.32 ± 71.9*	9.41694e-08
CVMR_variance	108.91[70.7-118.64]	121.55 ± 94.58	91.82 ± 80.43*	92.65 ± 30.46	136.69 ± 74.86*	2.0683e-07
CVMR_mistakes	2.87[1.0-4.0]	3.65 ± 2.45*	2.58 ± 2.81*	2.14 ± 1.75*	3.4 ± 2.26*	0.000253234
CVMR_IES	402.91[336.52-448.65]	416.17 ± 143.57	359.93 ± 81.36*	390.66 ± 66.29	455.62 ± 95.44*	5.88309e-09
DMT	100.26[63.6-122.43]	78.76 ± 52.97*	103.86 ± 48.64	102.88 ± 51.65	111.79 ± 57.81	0.00056484
RMO_mean	0.32[-18.5-31.35]	-8.99 ± 69.28	-2.14 ± 54.25	12.73 ± 104.22*	-3.12 ± 75.59	0.00646979
RMO_variance	167.86[84.7-224.35]	168.85 ± 103.5	111.84 ± 67.33*	158.75 ± 93.83	242.81 ± 105.18*	5.6846e-12
RMO_errors	20.95[18.0-24.0]	19.96 ± 5.22	18.14 ± 4.14*	22.22 ± 3.82*	23.62 ± 3.34*	5.24218e-11
Proportionality of changes in cognitive subdomains						
ISD	3.82[1.97-4.13]	4.53 ± 2.29*	3.02 ± 2.98*	4.14 ± 4.9	3.76 ± 3.59	5.53179e-06
ISDA	4.35[2.15-4.87]	5.22 ± 2.75*	3.57 ± 4.48*	4.55 ± 5.65	4.26 ± 3.99	8.10003e-07
ISCA	0.7[0.61-0.77]	0.81 ± 0.37*	0.65 ± 0.1*	0.68 ± 0.11	0.68 ± 0.12	1.82596e-05

\*Data for various age groups are provided as *Mean* ± *SD*. If the distribution of performance metrics differs considerably ( $p < 0.05$ ) from the other instances combined, its *Mean* ± *SD* is denoted with an asterisk.

Identification of the proposed indices values and their predictive potential: In this case, we intended to ascertain if the variables derived from the test results could accurately describe the individual’s overall

psychophysiological state. We constructed a regression model to forecast the values of the suggested indices based on the array of PTs which illustrates the individual psychophysiological status. The performance metrics are shown in Table 3.3 (see on the right side). Figure 3.6 shows the accuracy of the forecast with regard to the ratio of MAE divided by the range of the index values in different age groups in the form of a notched boxplot.

Table 3.3: Outcomes of the classification and regression models on POBA dataset

Binary classification models two age groups (cutoff value set to 40 years)					Regression models			
Index predictor	<i>Sens.</i>	<i>Spec.</i>	<i>ROCAUC</i>	<i>ACC</i>	Predicted feature	<i>MAE</i>	<i>RMSE</i>	<i>MAE</i> <i>range</i> , %
ISD	0.7 ± 0.056	0.73 ± 0.03	0.78 ± 0.04	0.715 ± 0.29	ISD	2.15 ± 0.14	3.56 ± 0.31	7.62 ± 0.5
ISDA	0.72 ± 0.06	0.73 ± 0.04	0.8 ± 0.03	0.727 ± 0.28	ISDA	2.58 ± 0.19	4.34 ± 0.44	7.56 ± 0.55
ISCA	0.73 ± 0.04	0.73 ± 0.03	0.8 ± 0.02	0.73 ± 0.024	ISCA	0.102 ± 0.004*	0.18 ± 0.013*	3.49 ± 0.14*

\*The model outcomes are represented as *Mean* ± *SD* values among the following classifiers and regressors: Gradient Boosting, Random Forest, AdaBoost, Gaussian NB, Ridge, Lasso, LR, SVM linear and non-linear. If the distribution of metrics differs significantly (*p* < 0.05) from the other instances combined, its *Mean* ± *SD* is denoted with an asterisk.

The distribution of the indices across age cohorts supports the premise that ISCA more accurately reflects psychophysiological status than ISDA or ISD. According to Table 3.3, the proportion of MAE to a range of values in ISCA is significantly smaller ( $7.57 \pm 0.55\%$  in ISDA and  $3.49 \pm 0.14\%$  vs  $7.62 \pm 0.5\%$  in ISD; *p* < 0.05). In Figure 3.6, the CI and IQR are considerably lower in all age group for ISCA compared to ISD or ISDA.

We anticipated that one index (e.g., ISDA) might replace the PT battery’s dependent variables. In this case, the proposed index may reflect the psychophysiological status and serve as its marker. If this is the case, ML algorithms can calculate its value from other PT outcomes. In Table 3.3, the ability of PTs to predict ISCA values is demonstrated. The quality of



models’ outcomes are excellent; the MAE to a range of values proportion is modest ( $3.49 \pm 0.14\%$ ). From our analysis, all of the ML models that were constructed are reliable. In this example, the Random Forest regressor performed the best (3.36%). The suggested model’s accuracy was higher than that of a previously developed model for predicting IES scores from PT features (3.36 – 3.77% vs 3.37 – 5.15%) [77].

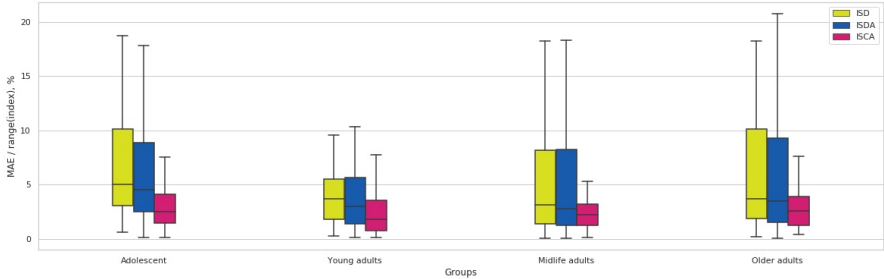


Figure 3.6: Distribution of MAE to range of index values in different age cohorts

All of the age groups analyzed exhibited relatively similar prediction accuracy. In contrast, the accuracy of forecasting IES varied with age, with the maximum accuracy for Adolescents and a somewhat reduced accuracy for Older adults [77]. This diminishes the IES’s dependability, making ISCA the best index for evaluating performance in PTs and comparing results regardless of the examinees’ age. Because it is difficult to distinguish between normal versus accelerated aging, the index which is not susceptible to aging may enhance current screening tools fro dementia.

Strengths and limitations of ML models of age-related cognitive decline: The study’s known disadvantage - a relatively low number of participants - is very usual in this type of investigation. In general, there is a trade-off seen between the quantity of examinees in an aging study and the

precision with which participants are chosen. The study cohort will be smaller if the inclusion criteria are more stringent. As a result, studies on normal aging exhibit limitations in terms of cohort size and evidence. No providers can cover the costs of MRI, which is the gold standard of non-invasive dementia screening in population-scale research. Some neuroscientists use low-strength magnetic field MRI to save money on research [234]. We presented a balanced approach based on the use of a high-field MRI and a careful selection of research participants in this investigation (see exclusion criteria in subsection 3.2). The study cohort was kept small due to the need to carefully select participants who met the inclusion criteria. At the same time, its analysis produced a degree of proof that a population-scale survey with less stringent inclusion criteria could never achieve [223]. Most of the existing work are done based on low number of participants [235, 236, 237, 238, 239, 240, 241, 242] or similar to the number of participants we considered in our experimental work [227, 243].

In our study, we were fortunate in that each age group had a similar number of individuals. This enabled us to construct plots that spanned the whole population without the need for years of approximation. Previous longitudinal studies have exhibited certain drawbacks, such as focusing on the onset of cognitive decline and omitting people younger than middle age [233]. People of all ages are rarely included in equal proportion in studies with a higher number of participants [244, 245, 246].

In this circumstance, we did not evaluate the participants' educational level beyond ensuring they met the inclusion requirements (e.g., literate). In the literature, there is no consensus on the subject. While some

researchers looked at the length of time spent in school, others argued that education, rather than other cognitive capacities, slowed the decline of crystallized intelligence. This is why, in tests, a lower educational level does not indicate a decrease in cognitive speed, memory, or reaction time [247]. As a result, the lack of control over years of education cannot be seen as a drawback in the current study, which is concerned with reaction time and accuracy.

**3.2 Patterns of Structural Changes in Normal Aging**

*3.2.1 Age Related Brain Morphometry Changes*

Figures 3.7-3.8 show a distribution of the major brain compartments across time using regression trendlines of ordinary least squares (OLS). Figures 3.8E-3.8H, and 3.9 demonstrate the brain anatomical changes for each age cohort using linear regression trendlines. The total intracranial volume (TIV) decreases steadily from adolescents to young and middle-aged adults to older individuals ( $p = 0.0068$ ). Growth in the size of the head and body across generations is thought to be the cause. The significant difference warrants adjusting individual brain volume to TIV. We were able to compare the age groupings as a result of this.

Table 3.4 shows the average data and Kruskal-Wallis test findings for four age groups. Asterisks indicate group data with a distribution that appears to deviate from the overall cohort. The P-values in the table’s right column indicate whether there is a significant variation between all of the age groups studied. The rate of the CSF (*CSF%*) steadily increases over time, and its accumulation implies brain parenchyma atrophy. The pace of growth of the cerebral subarachnoid space is faster than that of the brain ventricles

during all life stages [188].

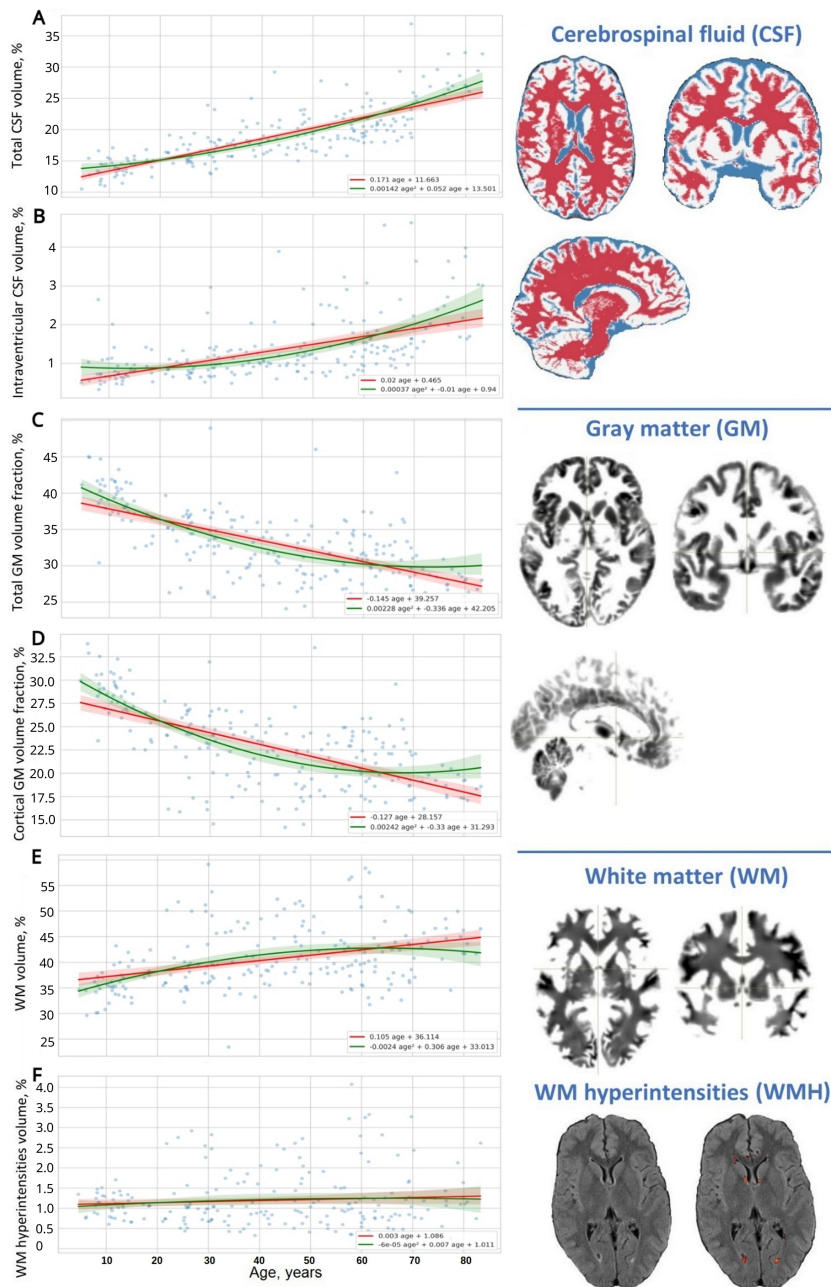


Figure 3.7: Voxel-based brain morphometry results throughout lifespan. Linear trends with 95% CI highlighted in red, second-order trends are drawn in green

Throughout life, there is a decline in the ratio of GM (GM%) to TIV. A reversed slope for GM% loss throughout lifespan in adolescents is significantly steeper than an incline for CSF% buildup. A buildup of WM during active neurodevelopment and myelination may be able to compensate for the GM loss. A slope for CSF% buildup in older persons is substantially shallower than a reversed incline for GM% loss. This can be attributed to the rapid accumulation of WM in minors which slows down as they get older. With aging, the proportion of cGM (cGM%) in TIV decreases. In contrast to GM percent, the percentage of total WM (WM%) follows an age-related pattern of change. It increases throughout time; however, the pace of change varies depending on the age group. Adolescents exhibit a significant rise in WM. There is a little increase in WM% from 20 years to the end of life. After the age of 60–65 years, the non-linear model of the WM volume distribution across time shows a modest decline in volume.

The major predictor of life-long structural alterations in the brain is not WM vascular lesions. We can consider them as a symptom of brain illness rather than a normal part of the aging process. The percentage of the TIV occupied by CSF% increases throughout life and peaks in Older adults, but the percentage of the TIV occupied by WMHs (WMH%) remains nearly stable in normal brain aging. The linear trendlines for WMH% are shallower than CSF% in all age categories. The relative sizes of the brain compartments (e.g., CSF%, WM%, GM%, etc.) do not differ significantly between sexes in Adolescents and Young adults when corrected for skull volume. After the age of 40, the tendency shifts. The sex-related discrepancies can be explained by variations in the rate or start of atrophic alterations in GM. In men, it begins sooner or moves more quickly. A

significant difference in the proportions of iCSF and total CSF demonstrates that elderly males are predisposed to age-related brain shrinkage [188].

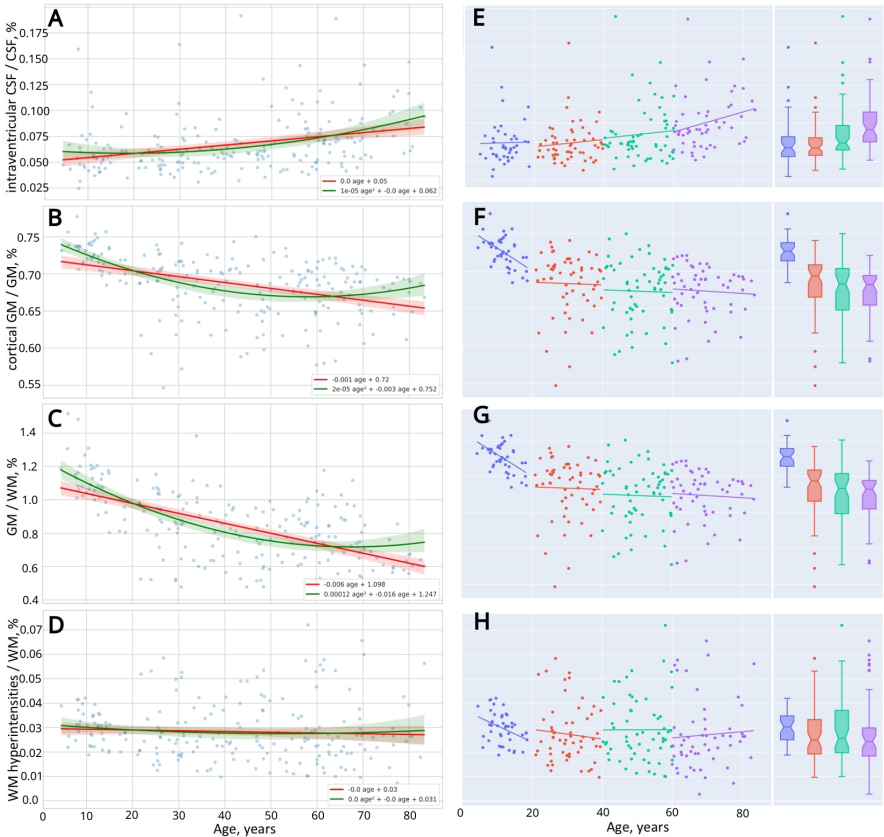


Figure 3.8: Changes in indices of brain morphometry throughout lifespan (A-D) and in four age groups (E-H). Linear trends with 95% CI highlighted in red, second-order trends are drawn in green

Various studies dedicated to neuroimages of degenerative disease are far higher than those focused on normal brain development. Neurobiologists and neurophysiologists use alterations in the structure or function of the brain to describe clinical groups. The lack of data about the baseline morphology and physiology of the "normal" brain during aging

makes clinical data explanation much more difficult [248]. To fill this knowledge gap, we sought to draw conclusions about the natural patterns of brain structure and function in a healthy population.

Figures 3.10A-3.10D, 3.11A-3.11D show how the dependent variables that measure speed of information processing in PTs using different task paradigms develop with age. The parabolic trendline shown in green shows a better fit to the distribution of test results across time than the linear trendline indicated in red. Figures 3.10E and 3.11E present the distribution of the derivative variables that reflect the time spent on task switching and inhibitory control (i.e., inhibiting an automatic response, making a decision, selecting the proper respond, etc.) [188]. The data on these scatterplots have almost linear distribution that is close to the linear trendline in red.

The findings support the existence of unique patterns of cognitive function variations related to age. The explanation for this is that cognitive domains in the brain lack a common structural representation, and structural correlates change at different rates as people age. The majority of studies that have been performed to date have focused on the rate at which cognitive function improves or declines; however, the pattern of age-related changes is unique to the cognitive domain and is in need of further investigation.

The findings of the psychophysiological tests show a "U-shaped" trend of changes in information processing speed. Polynomial kernel ML models adequately describe the variability in RT in SVMR, CVMR, IRT, and AST tests throughout lifespan.

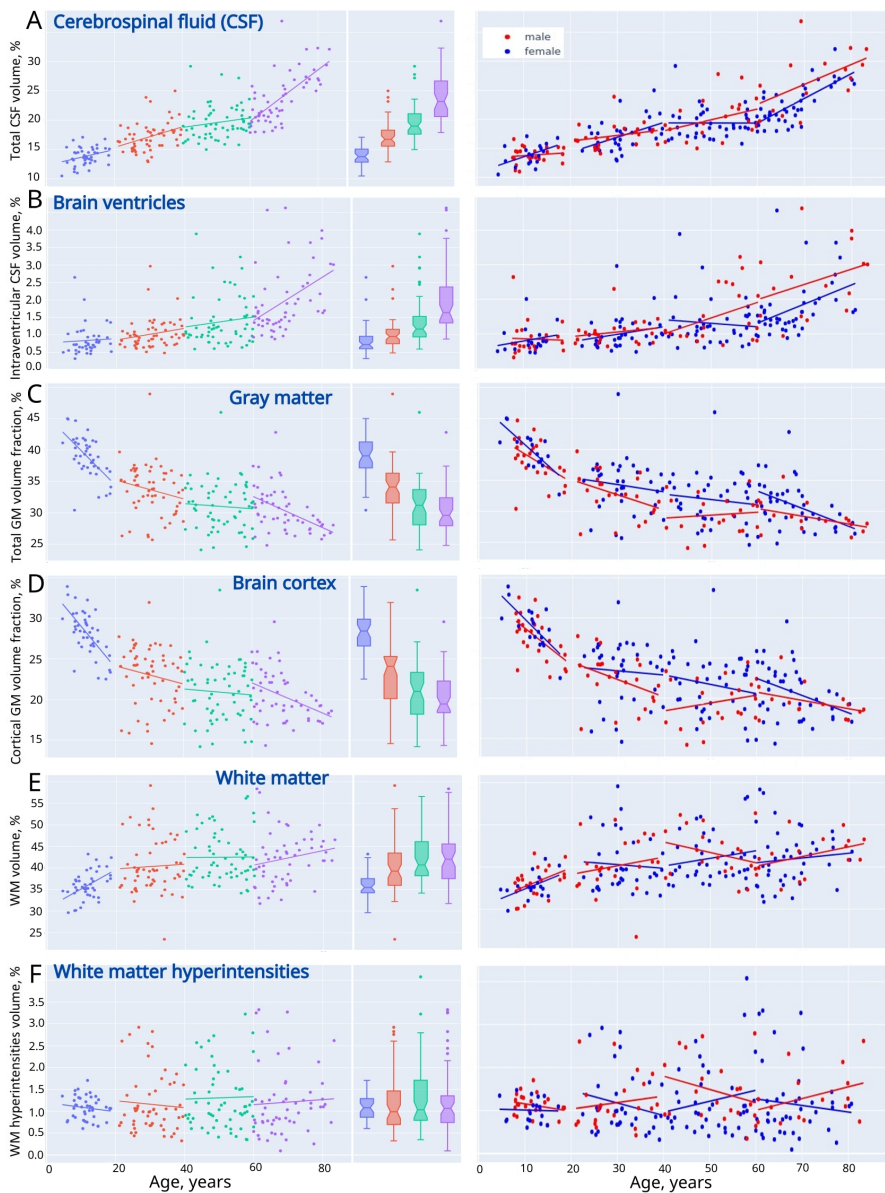


Figure 3.9: Trendlines displaying differences in voxel-based brain morphometry across four age groups



Table 3.4: Brain morphometry with regard to the age group and sex

	<i>All</i>		<i>Adolescents</i>				<i>Young adults</i>				
	mean	CI	Mean $\pm$ SD	female	male	p	Mean $\pm$ SD	female	male	p	
TIV	1614.42	[1515.99-1724.63]	1653.39 $\pm$ 151.51	1555.01 $\pm$ 130.92	1724.22 $\pm$ 123.11	0.0002	1649.87 $\pm$ 211.35*	1561.71 $\pm$ 192.26	1784.03 $\pm$ 162.99	<0.001	
CSF	304.51	[249.28-343.44]	229.93 $\pm$ 36.1*	217.33 $\pm$ 39.12	239.0 $\pm$ 30.71	0.0298	282.31 $\pm$ 52.47*	266.68 $\pm$ 48.91	306.08 $\pm$ 48.64	0.0012	
iCSF	21.54	[12.51-24.56]	14.07 $\pm$ 7.59*	12.99 $\pm$ 6.41	14.84 $\pm$ 8.25	0.178	16.74 $\pm$ 6.62*	15.39 $\pm$ 5.77	18.78 $\pm$ 7.28	0.0173	
GM	533.15	[462.62-603.28]	640.98 $\pm$ 47.03*	616.3 $\pm$ 35.47	658.74 $\pm$ 46.31	0.0012	551.91 $\pm$ 76.92*	529.66 $\pm$ 69.12	585.76 $\pm$ 75.84	0.0028	
cGM	366.93	[306.94-426.57]	463.22 $\pm$ 37.73*	446.42 $\pm$ 28.16	475.31 $\pm$ 39.1	0.0077	377.75 $\pm$ 66.71	362.6 $\pm$ 65.1	400.81 $\pm$ 62.38	0.0086	
WM	652.5	[566.76-719.3]	595.06 $\pm$ 83.52*	551.51 $\pm$ 63.94	626.41 $\pm$ 81.89	0.0022	662.41 $\pm$ 122.08	627.54 $\pm$ 107.18	715.46 $\pm$ 124.25	0.0034	
WMH	19.26	[11.81-23.28]	17.8 $\pm$ 4.67	15.6 $\pm$ 4.1	19.39 $\pm$ 4.41	0.0047	19.01 $\pm$ 10.69	17.87 $\pm$ 11.08	20.74 $\pm$ 9.82	0.0492	
CSF,%	18.88	[15.54-21.25]	13.87 $\pm$ 1.53*	13.91 $\pm$ 1.8	13.84 $\pm$ 1.3	0.4171	17.15 $\pm$ 2.44*	17.15 $\pm$ 2.68	17.14 $\pm$ 2.04	0.3753	
iCSF,%	1.33	[0.79-1.51]	0.84 $\pm$ 0.42*	0.83 $\pm$ 0.38	0.85 $\pm$ 0.45	0.4559	1.02 $\pm$ 0.42*	1.01 $\pm$ 0.46	1.04 $\pm$ 0.35	0.1508	
GM,%	33.15	[29.18-36.46]	38.97 $\pm$ 3.24*	39.82 $\pm$ 2.87	38.36 $\pm$ 3.36	0.0715	33.66 $\pm$ 4.0	34.19 $\pm$ 4.25	32.86 $\pm$ 3.44	0.0935	
cGM,%	22.8	[19.26-25.86]	28.18 $\pm$ 2.7*	28.87 $\pm$ 2.53	27.68 $\pm$ 2.71	0.0981	23.0 $\pm$ 3.55	23.35 $\pm$ 3.79	22.48 $\pm$ 3.09	0.1046	
WM,%	40.52	[35.98-43.85]	35.93 $\pm$ 3.18*	35.46 $\pm$ 2.85	36.26 $\pm$ 3.35	0.1211	42.21 $\pm$ 5.89*	41.91 $\pm$ 6.29	43.01 $\pm$ 4.56	0.1847	
WMH,%	1.19	[0.75-1.39]	1.08 $\pm$ 0.26	1.01 $\pm$ 0.27	1.12 $\pm$ 0.24	0.1366	1.16 $\pm$ 0.66	1.15 $\pm$ 0.71	1.17 $\pm$ 0.58	0.2422	
iCSF/CSF	6.73	[4.94-7.53]	5.95 $\pm$ 2.39*	5.77 $\pm$ 1.87	6.09 $\pm$ 2.69	0.3885	5.92 $\pm$ 2.07*	5.85 $\pm$ 2.39	6.02 $\pm$ 1.45	0.1075	
cGM/GM	68.66	[66.48-71.58]	72.61 $\pm$ 1.97*	72.76 $\pm$ 1.81	72.51 $\pm$ 2.08	0.2415	68.34 $\pm$ 4.01	68.26 $\pm$ 4.63	68.47 $\pm$ 2.82	0.2227	
GM/WM	84.61	[66.5-100.54]	109.53 $\pm$ 15.05*	113.29 $\pm$ 14.76	106.82 $\pm$ 14.67	0.0785	86.12 $\pm$ 19.05	86.91 $\pm$ 17.98	84.92 $\pm$ 20.52	0.2323	
WMH/WM	2.83	[2.0-3.41]	2.98 $\pm$ 0.64*	2.82 $\pm$ 0.65	3.1 $\pm$ 0.6	0.0785	2.74 $\pm$ 1.16	2.7 $\pm$ 1.26	2.8 $\pm$ 0.98	0.2134	

Structural features are expressed as *Mean  $\pm$  SD* in *cm<sup>3</sup>* or % of TIV. The variables with the distribution significantly different (*p* < 0.05) in the age group compared to the overall study cohort are marked with an asterisk. Data expressed as *Mean  $\pm$  SD*.

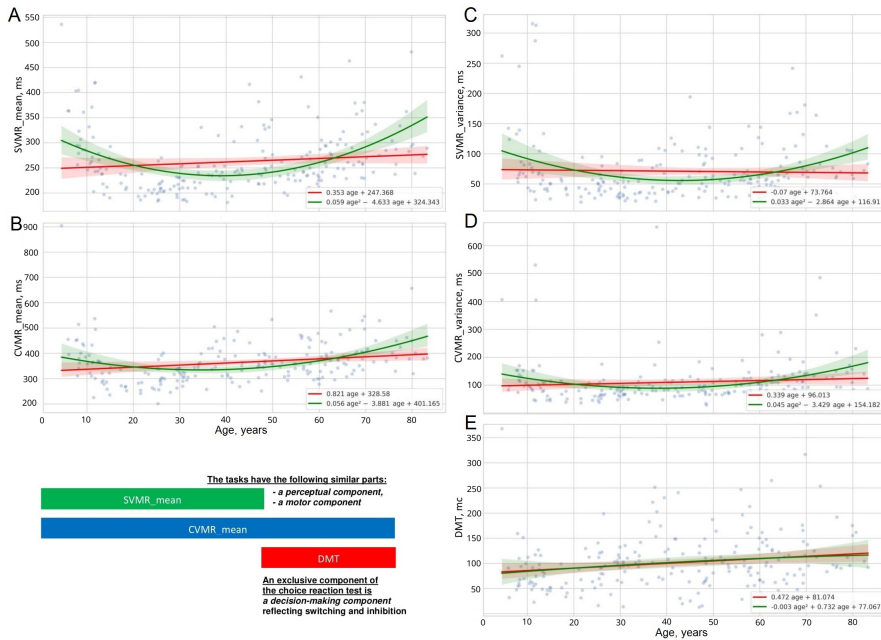


Figure 3.10: Distribution of DMT and RT with its variance in SVMR and CVMR tasks

As the first power of age increases, so too does the psychophysiological measurements that reflect task switching and inhibitory control (e.g., DMT, the temporal delay due to visual interference). Linear machine learning models fit the age dependency of these test outcomes. The linear distribution of the RMO test results throughout lifespan is depicted in scatter plot 3.12A. After the age of 20, age has no effect on reaction time in the RMO test. One possible explanation for this stems from the fact that RMO is tested using a completely different paradigm than the other activities. During the RMO test, the individual is instructed to reply to stimuli which come at specified intervals. Tester asks the participant to await for an unexpected event (e.g., an presentation of a targeted stimulus in IRT and AST or a light flash in

SVMR and CVMR tests) before taking the remaining tests. However, the RMO test's accuracy varies with age. As a result, in Figure 3.12B, the variation of response time (RMO\_variance) fits a parabola trendline in green. Participants between the ages of 35 and 40 have the best performance.

Figures 3.12C and 3.13 show linear regression trendlines that reflect changes in psychophysiological performance across lifespan. The findings in PTs follow a consistent age-related trend. After the age of 20, the participants' performance begins to deteriorate.

Skull morphometry: TIV variations with age have been the subject of research in the past, and they are still being debated. The study findings may differ due to inconsistency in the following settings: (i) population selection, (ii) the study design (e.g., longitudinal or cross-sectional), and (iii) methodology. For instance, TIV did not change between generations in another cross-sectional investigation of persons aged 24 to 80 years. The results of the studies are allegedly incongruent due to social-economic aspects that could explain the inconsistencies [249, 250]. A cross-sectional survey of individuals born within a 40-year period demonstrated that younger participants had bigger mean TIV. The size of the individual's skull was also directly related to their height [251].

Our research was conducted in a cross-sectional manner. We were able to identify the highest mean value of TIV among members of the adolescent population. This explains why growth in volume of skull is in line with the natural trend of human body enlargement in the following generations.

Subarachnoid space: A rise in the proportion of the CSF compartment to the brain parenchyma has been associated with cerebral

atrophy in older people [244]. The increase in CSF volume has resulted in a reduction in liquor turnover to three times per day from four to five times per day [252]. The time it takes to replace the expanded volume is longer [253].

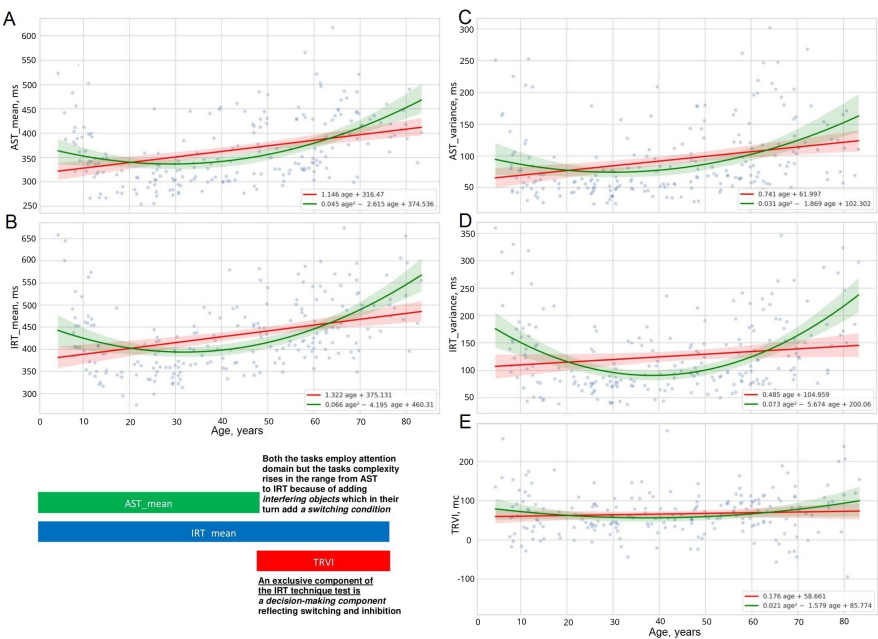


Figure 3.11: Studies of attention with (B, D) and without interference (A,C). Distribution of mean reaction time with its variance and time delay because of distraction

CSF turnover decreases in the elderly for a variety of causes. The first explanation is, as previously stated, an increase in subarachnoid space volume. Another reason is that the choroid plexus produces a smaller amount of CSF [188]. The amount produced drops by nearly twice in animals and humans [254]. The final explanation is in a reduction in the capacity of lymphatic outflow channels to filter both small and large molecules in elderly [255]. In a study of brain morphology changes from

birth to late adulthood, volume of sulcal CSF remained steady until the age of 20 years, and increased curvilinearly throughout maturity. After 50 years, the acceleration was higher [256]. It's possible that the rise in CSF volume as people get older is due to atrophic processes such as cell shrinking. Another investigation found that the proportion of volume of sulcal CSF to intracranial volume was shown to be higher in seniors (above 55 years) than in younger adults [241]. Other authors [236] found a linear decrease in brain volume and a rise in CSF [236].

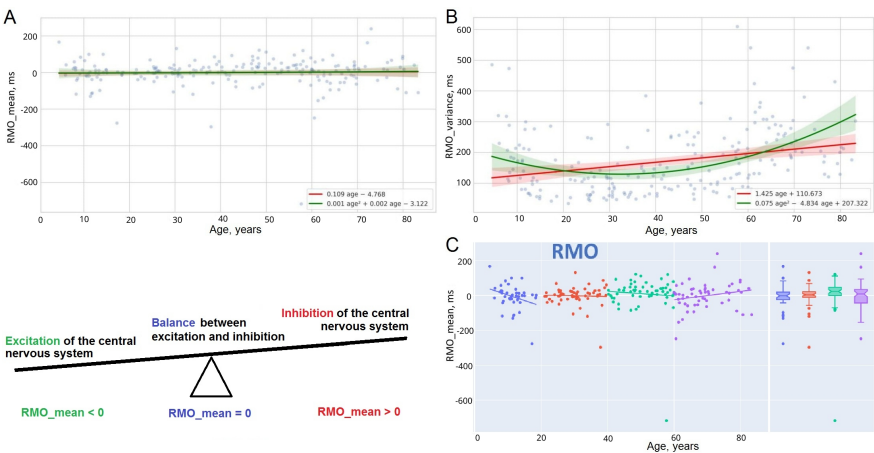


Figure 3.12: Distribution of RT and its variance in responding to moving object test (A-B). Linear trendlines of performance in responding to moving object in age groups (C)

An earlier study looked at the global and regional effects of age on CSF volume in people aged 18 to 79. The researchers found that the volume of CSF gradually increased ( $R^2 = 0.377$ ). The CSF components distributed between sulci and inside ventricles were the same. Researchers discovered a relatively small increase of the CSF volume in the pontine cistern, including its caudal reach around the medulla, in regional effects of age.

The supracerebellar and chiasmatic cisterns, cisterna magna, Sylvian, third ventricle, and interhemispheric fissures all showed the greatest symmetrical increase in the CSF space. The regional effects tended to follow a linear pattern. When they employed the second and third-order polynomial expansion of age, the data fit showed no improvement. They found no evidence of a relationship between CSF volume and gender, either generally or in localized effects [245]. A nonplanimetric approach for assessing intracranial CSF volume in senior volunteers aged 60–84 found a substantial association between age and CSF but a modest correlation between TIV and CSF. This finding demonstrated that the normal brain volume shrinks over time [238].

Brain ventricles: Researchers have gained fresh insight into the neurobiological underpinning for cognitive changes related to age and their impact on cognitive function by studying the brains of healthy people. The bulk of prior studies has found that as people age, their brain volume decreases and their ventricle volume increases, implying that brain shrinkage in humans is linked to aging. The shrinkage of periventricular brain tissue is thought to cause age-related ventricular hypertrophy [257]. With the help of a CT scan, other researchers were able to validate this finding by tracking the ventricles of healthy people aged 60 to 99 [258]. Between the ages of 80 and 99, a more noticeable growth was observed. This backs up other researchers' results that the expansion of the lateral ventricles peaks in the ninth decade. According to their findings, the volume climbed steadily from the adolescence to the seventh decade but rose more rapidly after the age of 70 [259]. This outcome helps to explain why a ventricular volume abnormality is easier to detect in younger people.

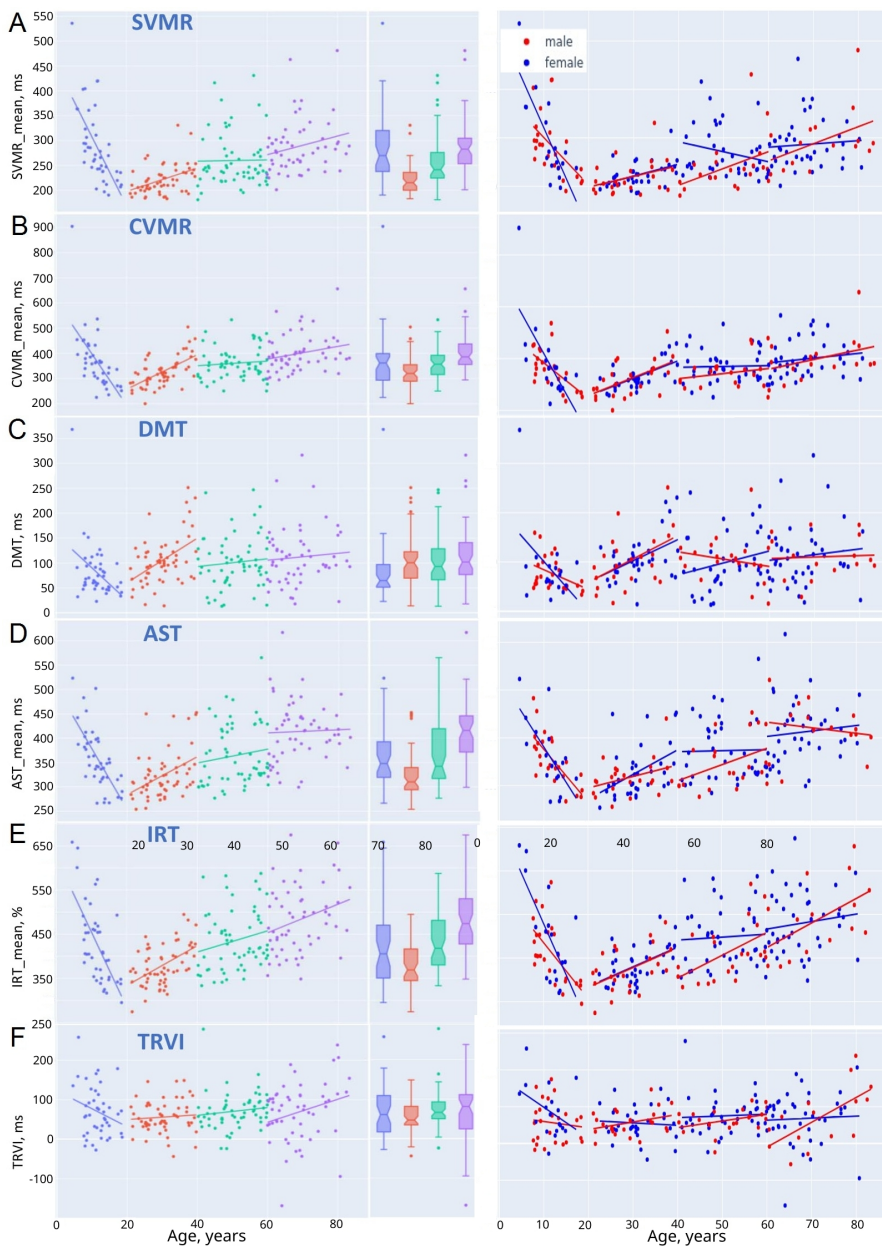


Figure 3.13: Linear dependencies of performance in PTs across lifespan

Subjects in two age groups (16–40 and beyond 60 years) exhibited varying diameters of ventricles and sulci, according to data from prior studies. The ventricles were larger in the elderly [260]. The earlier CT findings were validated by an MRI-based analysis of the lifetime dynamics of the lateral ventricles and CSF volume. The ventricular capacity rose in a linear fashion until the age of 40, then skyrocketed after 60 [242].

The authors concurred that the pace of change in ventricular size observed across longitudinal studies may be of great relevance. For instance, the mean rate of ventricular enlargement was  $650 \text{ mm}^3/\text{y}$  in a longitudinal study of participants between the ages of 31 and 84. After 60 years of age, the enlargement of the ventricles regularly accelerated. Over time, some investigations found a significant increase in ventricular, and frontal lobe measurements [237].

In healthy adult men between the ages of 19 and 92, the right temporal lobe was larger than the left one. This rise in volume of the temporal horn of the lateral ventricle supports the notion of a smaller volume of the hippocampus in the older group [256]. A previous study found that ventricular CSF volume grew significantly, with substantial linear and quadratic increases in the left and right lateral ventricle. It also found pronounced linear trends in the third ventricle and left temporal horn, with a 17 percent variance in volume. Investigators discovered a significant rise in the steepness of the lateral ventricle curve in the elderly population [261].

Several researchers established normal age-related values for brain morphometrics in healthy males between ages of 21 and 80 [262]. They discovered a positive relationship between CSF volume and age, as well as



an increase in the volumes of the third and lateral ventricles in the senior people [262]. These findings corroborate data from postmortem material, in which linear measures in pneumoencephalograms and CT scans revealed a rise in volume of ventricles and an overall increase in volume of CSF in the elderly [259].

Gray matter: Past research has produced findings that confirm our conclusions about a progressive reduction in the volume of GM throughout lifespan.

Total gray matter: The volume of GM begins to decrease at a very young age and proceed changing throughout maturity. Within 2.5 years of birth, there is evidence of a rise in GM volume [263]. From early childhood through the age of 6–9 years, the GM volume expands by 13%. After first decade of life, there is a steady decrease in the volume of GM by approximately 5% per 10 years [263]. Another research study involving healthy, well-developed children between ages of 5 and 18 years (IQ-score > 80) verified this. GM levels grew until 9 years old, both in absolute and normalized terms. After that, there was a fall until the age of 15 and then a minor gain [264]. In conflict, a study of children aged 4.5 to 18 years found that the GM volume decreased by  $6.56 \text{ cm}^3$  every year [265].

The normalized GM volume decreases at a rate of 0.183 percent per year after age 55, compared to  $2.37 \text{ cm}^3$  for the absolute volume of GM [266]. Another study found a  $0.40 \text{ cm}^3$  annual reduction in GM volume in persons aged 59–89 years [240]. To our knowledge, there is no strong agreement on the pace of the changes. Such disparities in findings could be explained by differences in study methods. A study that used both a cross-sectional and longitudinal design yielded mixed results. In participants over

35, a longitudinal phase of the study found that an insignificant proportion of change in volume of GM ( $p > 0.05$ ) remained steady over 3.5 years. A cross-sectional research study, on the other hand, found a substantial link between advancing age and a loss in all brain sizes, including GM [267].

Cortical gray matter: Absolute cGM increases and peaks throughout early childhood, much like total GM. The volume of GM then falls in the second decade before stabilizing in the third [268]. A research of cortical regions showed that GM atrophy begins in the dorsal parietal cortex and progresses in the temporal and frontal cortex [269].

The current study generated evidence of GM volumetric changes as people age. cGM atrophy has been studied extensively as a cause of NDs and mental illnesses. In chronic schizophrenia, for example, there is evidence of a rapid decrease in cGM [270]. Researchers have focused on the thickness of cGM rather than the volume while studying this phenomenon [271, 272, 273, 274].

White matter: The pattern of WM volume change with age differs from that of GM volume change. This is supported by our findings and previous research. However, there is no clear agreement on whether WM lesions are due to normal aging or are caused by age-related disease.

Total WM: The quantities of WM and GM increase during childhood and during puberty, albeit at distinct rates. Before 12–15 years, the volume of GM rises by 13%, whereas the volume of WM changes by 74%. The WM volume increases less dramatically in adolescence than it does in childhood, peaking in the fourth decade of life. The average annual rate of WM volume expansion from 4 to 20 years is 0.77% [275]. The WM volume is steady between 40 and nearly 50. Some scholars claim that the

volume of the WM begins to decline at the age of 50 [276], while others claim that it begins at the age of 60 [245]. According to our findings, after 60–65 years, the volume of the WM decreases slightly (see Figure 3.7E, the green curve). Over time, the detrimental effects of aging on the WM volume accumulate. Between the ages of 40 and 70, the volume of the WM diminishes by 13% [263]. A postmortem study found a 15% decline in WM volume in the cohort between ages of 62 and 90 vs. 18 and 57, corroborating in vivo findings [277]. In adulthood, the volume drop for WM is less than that observed for GM [278].

A comparative analysis of different age cohorts revealed a significant difference in volume of WM between group of young (from 22 to 40 years) and middle-aged (from 41 to 59 years) subjects. Furthermore, the volume of WM in most brain regions was lower in the young group than in the middle-aged cohort. In comparison to middle-aged adults, the volume of WM was decreased in the older generation (60–78 years). In this study, a linear regression analysis revealed a progressive rise in volume of WM before the age of 40, a peak around the age of 50, and a rapid fall beyond the age of 60 [279].

WMHs are among the most typical findings in the brain of elderly. In older persons, the severity of WM lesions differ greatly. WMHs can be evaluated using a volumetric approach or visually using the Fazekas rating scale. When WMHs progressions were evaluated using a volumetric technique, the connection with age was two times higher [280]. Some research has found a link between the distribution of WMHs and the findings of electrophysiologic testing and several frontal lobe functional measurements [281]. However, we cannot verify this based on the current

study's findings. The PTs we used are representative of EF, which includes representations of the frontal lobe. However, there were no significant relationships between psychophysiological performance and age or functional performance in the assessments.

The relationship between the occurrence of lesions and ageing in a healthy population is still being debated. Because the lesions usually represent ischemia insult, the creation of WMHs may represent an indirect signal of pathogenic alterations [281]. Gliosis, myelin pallor, subclinical ischemia, neuropil atrophy, and other variables have been linked to WMHs [282].

WMHs are more commonly found in older people. In one study, 100% of people from 71 to 80 years had WMHs, whereas only 20 percent of young persons from 21 to 30 years had them. Furthermore, there was a positive correlation between the size of lesions and age [283]. WMHs have been found in 92 percent of patients over 60 years old and 22 percent of those aged 0 to 20 years old [284]. A study of healthy adults found that WM lesions were not common in individuals under the age of 55, but after that age, lesions appeared 10-fold more frequently. WMHs were found to be present in 5.3% of the population. WMHs in the periventricular region were detected in 3.7% of the participants, while WMHs in the centrum semiovale were found in 3.7% cases. The participants between the ages of 16 and 25 had the fewest WMHs, while those between the ages of 56 and 65 had the highest prevalence of the lesions [285]. It took a long time for a new WMH to emerge [286].

In addition to assessing the severity (size) of the lesions, radiologists also record the location and evolution of WMHs in follow-up

examinations. The goal of one study was to determine the number and magnitude of lesions in three geriatric age cohorts. The WMHs in all of the cohorts were predominantly tiny (1 - 3 mm). Notably, the number of lesions rose dramatically between the 6th and 7th decades of life, but only marginally between the 7th and 8th. In each age subgroup, 1–2 large (> 10 mm) and 2–5 medium (3 - 10 mm) lesions were found on average [286].

Additional studies looked at periventricular WMH (PVWMH) and deep WMH (DWMH) injuries independently. The results revealed that PVWMH accounts for 2/3 of overall WMH. In adults over 60, both DWMH and PVWMH are related with a drop in GM. The relationship between volume of GM and WMH load is regionally unique; for example, DWMH corresponds with a lower cGM level to a larger extent than PVWMH [287].

WMHs were found to have a weaker correlation with superficial atrophy than with global deep brain atrophy in a study of  $73 \pm 1$  year old. The size of the lesions had a negative relationship with total brain volume but a positive relationship with intraventricular volume. WMHs increase at the same time as WM and GM volumes decrease [288].

Different methods of selecting the study cohorts can account for the disparities between the results of prior studies. Some of the studies may have been limited to clinical population with a history of vascular pathology, according to reports. We followed the inclusion criteria mentioned in subsection 2.1.2 and analyzed subjects representative of the healthy community. We analyzed the influence of age on structure of the brain while minimising an additive effect of confounders (cardiovascular pathology, etc.).

### 3.2.2 *Mathematical Models of Age-Related Changes*

As previously noted, we were able to construct two approximation functions for different qualities. We applied ridge regression model to the linear and non-linear functions of age (see Formulae 2.7-2.8). A straight line and a parabola (second-order line) are two of these forms. Figures 3.7, 3.8-3.12 show scatter plots with trendlines for linear and second degree non-linear models, as well as their 95 percent confidence intervals. This resulted in a more accurate visual selection of the model which fits best.

From Figures 3.7, 3.8A-3.8D, the data for psychophysiological variables are scattered less than the voxel-based morphometry data over lifespan. As a result, selecting a good mathematical model based on a visual trajectory of changes throughout lifespan is difficult.

The scatter plots for the PTs can be divided into two categories, as shown by the scatter plots (Figures 3.10-3.12). The first category includes RT variables in SVMR, CVMR, IRT, and AST tests, as well as time variability in all tests, including RMO. The polynomial kernel regression model matches this category better because it exhibits a U-shaped distribution across time. The features which indicate task switching (DMT, TRVI) and the equilibrium of processes in the central nervous system (RMO\_mean) fall into the second category. The first-order models accurately capture variations in these variables.

Performance of the linear and non-linear models: We analyzed the models' ability to predict anatomical and functional changes in the brain to explain our choice of preferred mathematical models. We used performance measurements to achieve this objective (see Table 3.5). The number of years

can be employed as an independent variable in regression models because the relationship between the aforementioned components and age is statistically relevant ( $p < 0.05$ ).

Table 3.5: Prediction quality of the first-order and second-order ML regression models for predicting results of psychophysiological tests out of age

	First-order regression model				Second-order regression model				Distance
	MAE	RMSE	R2	$\frac{MAE}{range}, \%$	MAE	RMSE	R2	$\frac{MAE}{range}, \%$	
Voxel-based morphometry									
GM, %	2.78	13.82	0.41	11.19	2.72	12.89	0.45	10.95	0.24
cGM / GM	2.81	13.58	0.18	12.2	2.68	12.5	0.24	11.64	0.56
WM, %	4.2	31.24	0.14	11.74	4.19	30.22	0.17	11.74	0.00
WMH / WM	0.92	1.46	0.003	13.3	0.91	1.45	0.005	13.2	0.10
CSF, %	2.06	7.56	0.64	7.8	1.99	7.2	0.66	7.54	0.26
intraventricular CSF / total CSF	1.78	6.58	0.1	10.6	1.75	6.44	0.12	10.39	0.21
Psychophysiological tests									
SVMR_mean	43.65	3466.29	0.02	12.11	39.53	2890.73	0.18	10.97	1.14
CVMR_mean	55.39	6068.92	0.06	7.87	53.03	5585.68	0.13	7.54	0.33
DMT	38.32	2786.15	0.04	10.80	38.14	2782.11	0.04	10.75	0.05
AST_mean	49.67	3745.09	0.14	13.66	45.90	3382.66	0.22	12.63	1.03
IRT_mean	58.21	5414.28	0.13	14.53	54.53	4697.82	0.25	13.61	0.92
TRVI	40.92	3089.75	0.01	9.15	40.15	3030.01	0.03	8.98	0.17
RMO_mean	45.26	6237.70	0.00	4.73	45.22	6236.17	0.00	4.73	0.00

The prediction models’ low R-squared ( $R^2$ ) values imply that there is a lot of variability around the regression line. The nature of our data explains this: psychophysiological performance is unstable, and it reflects an individual’s adjustment to their living environment [32, 68, 289]. Nonetheless, the reproducibility of the PTs and their informative value allows us to consider the tests as a tool for screening psychological misadjustment and cognitive decline [180].

The variables with the trendlines (SVMR\_mean, CVMR\_mean, IRT\_mean, AST\_mean) show rise in the quality of forecast obtained with the second-order regression model. The parabola curvature increases as the gap in accuracy between the linear and non-linear models grows. The

percentage of MAE to the range of the examined data (MAE/range) was used to compare the performance of different models with the underlying objective of ranking the models’ performance (refer to Table 3.6).

Table 3.6: Importance of psychophysiological and morphological variables based on performance of the linear and quadratic models

Psychophysiological performance		Morphological variables	
Distance	Variable	Distance	Variable
1.14	SVMR_mean	0.56	cGM / GM
1.03	AST_mean	0.26	CSF%
0.92	IRT_mean	0.24	GM%
0.33	CVMR_mean	0.21	iCSF / CSF
0.17	TRVI	0.1	WMH / WM
0.05	DMT	0	WM%
0	RMO_mean		

We listed the following psychophysiological variables in the left column of Table 3.6, ranked according to the difference in performance between the first-degree and second-degree functions: SVMR, AST, IRT, CVMR, TRVI, DMT, and RMO. The top factors in the list indicate a cognitive domain known as informative processing speed. Polynomial trendlines considerably better suit the life-long changes in the tests than linear trendlines. The factors in the end of the list (DMT, TRVI) represent task switching and inhibitory control performance, which is another cognitive subdomain. The linear model almost fits their age-related distribution. For RMO\_mean values, both the linear and non-linear polynomial function models have similar performance, since the RMO test’s results are not affected by age.

We ordered morphological factors in the left column of Table 3.6



according to the distance between model performance: cGM/GM, CSF%, GM%, iCSF/CSF, WMH/WM, and WM%. The overall GM (GM%) and its cortical component (cGM/GM) show a quadratic retardation trend as people become older. The same can be said for the total CSF (CSF percent) and the intraventricular portion of it (iCSF/CSF). Because a second-order function does not show advanced performance, linear models can be used to represent the spread of total WM (WM%) and its lesions (WMH/WM) over time.

The comparative analysis of Figures 3.10 and 3.11 reveals two distinct trends of age-related variation in PT performance. There is a clear "U-shaped" tendency in the findings of PTs that measure information processing speed. In comparison to a first-order function, a second-degree function of age enhances data fit. Figures 3.10E, 3.11E demonstrate the dependent features for task switching and inhibitory control. The change trend is linear. Furthermore, using a second-order function of age does not improve the data fit. To clarify this, we contrasted aging's functional consequences to volumetric changes in the brain's primary regions.

Linear dependency: The linear equations can be employed to estimate the regional effects of age on volume of CSF (e.g., the growth of the Sylvian and interhemispheric fissures) [245]. According to our findings, the volume of WM and the rate of WMHs in total WM fluctuate virtually linearly across time (refer to Table 3.6). As the first power of age increases, so do psychophysiological measurements that represent task switching and inhibitory control (DMT, TRVI). The cortical GM and the overall GM have different age-related alterations.

The linear slowing of DMT throughout the lifespan can be explained by the interhemispheric fissure's tendency to grow. Task

switching and inhibitory control may be morphologic correlates of the enlargement. This cognitive subdomain's neuronal centre is located in the medial wall of the frontal cortex, specifically in the supplementary motor region. The results of the "go/no-go" test imply that the premotor areas of the frontal lobe's medial wall play a critical role in delaying response [290]. As a result, the expansion of the interhemispheric fissure is due to the atrophy of these brain centres. Researchers warn, however, that approaches based on the assumption of linearity or even monotonicity of the compared age functions should be utilized with appropriate caution [188, 291].

Second-degree equation: Researchers have assessed how the volume of brain structures changes as people get older [291]. After plotting the dependency between volume and age as a parabola, the effects can be seen as a U-shaped or inverted U-shape line.

The inverted parabola is indicative of the WM bundles' age-related alterations. As a result, cellular piles and WM fibres are characteristic of the WM and hippocampus [143]. WM buildup exceeds its concealed atrophic alterations till around the age of 60–65 years. The interval is followed by WM loss due to myelin breakdown and gradual WM fibre degeneration. Myelin breakdown has been reported to be linked to processing speed in previous studies [292]. Demyelination and other WM alterations are at the root of age-related slowdown [229].

The U-shaped line represents age-related variations in GM volume and structures with patches of neuronal cells. The current research found a link between the GM cortex and overall GM volume. An earlier study found that deep GM structures, such as the thalamus, accumbens, lenticular, and caudate nuclei, were justified in this way [143]. The formations are

dense with cell bodies that cannot grow as large as neural fibres. The loss of neuronal cells is permanent. As a result, interpreting an increase in a polynomial second-degree trendline in advanced age as GM atrophy leading to cell disintegration is impossible. This implies that quadratic functions do not accurately describe GM atrophy.

Third-degree equation: The cubic function of GM nuclei volume as age-related function describes the data better than the second-order curve in [143]. In senior age, no expansion of the GM structures was seen.

### *3.2.3 Comparison of Dynamics of Psychophysiological Performance with Brain Structural Changes*

The correlation coefficients between volumetric brain data and the RT in the array of PTs are shown in Figure 3.14. The CSF volume and the reaction delay in SVMR, CVMR, AST, and IRT tests exhibited a strong positive relationship, as shown in this diagram. In the experiments, the volume of brain ventricles and reaction time revealed a favourable relationship. CSF percentage and iCSF percentage both have a positive relationship with age ( $r = 0.8$  for CSF% and  $r = 0.56$  for iCSF%). As a result, the indices can be used as indicators of brain atrophy across lifespan. Because the highest association (maximal r-value) exists between CSF percent and age, the latter can be regarded the most sensitive measure of atrophy related to aging.

Surprisingly, the total CSF percent and average RT in the IRT exhibited the strongest link between brain anatomical data and functional outcomes ( $r = 0.36$ ). Switching and inhibitory control, information processing, and attention were among the cognitive domains and subdomains used in the test.

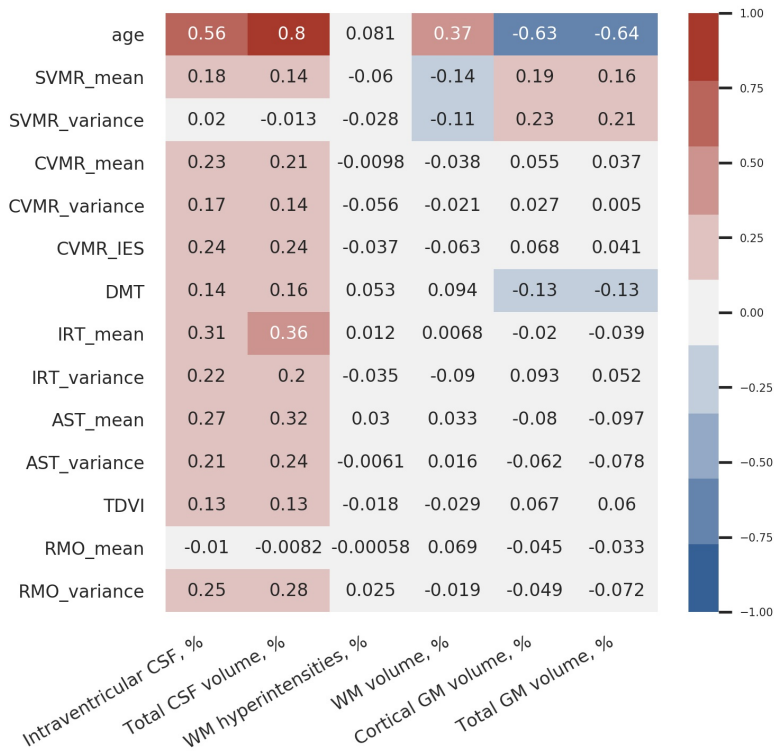


Figure 3.14: Coefficients of correlation between PTs results and volumes of major brain compartments

We also discovered that the SVMR test's variance of RT (SVMR\_variance feature) showed no relation to age; however, it did exhibit a negative relationship with the portion of WM in TIV (WM%;  $r = -0.11$ ). The relative volume of GM ( $r = 0.21$ ), specifically the GM cortical component (cGM%;  $r = 0.23$ ), revealed a moderate positive relationship with SVMR variance.

SVMR test was the most basic within our battery of tests since it focused solely on information processing while putting little strain on other cognitive functions. The relative volumes of the GM ( $r = 0.16$  for GM%;  $r = 0.19$  for cGM%) and CSF ( $r = 0.14$  for CSF%;  $r = 0.18$  for iCSF%)

have moderate relationship with the mean reaction time (SVMR\_mean) in SVMR test. Furthermore, SVMR\_mean shows a moderately negative statistical connection ( $r = -0.14$ ) with the proportion of WM%. The faster reaction could be due to improved brain connections in people with a large relative volume of WM. Because the SVMR test does not need DMT like the "go/no-go" test and does not demand attention like the AST and IRT tests, the link is clear. As a result, the link between brain connection and this test is straightforward.

The relative volumes of CSF are positively associated with decision-making time ( $r = 0.16$  for CSF%;  $r = 0.14$  for iCSF%) and negatively associated with the rate of GM in TIV ( $r = -0.13$  for GM%;  $r = -0.13$  for cGM%). Because judgments are made in the GM cortex, these findings demonstrate the dependability of the PTs utilized. Despite the tests' validity, DMT's utility as a biomarker of brain atrophy alterations is limited by its modest relationships ( $r \leq 0.16$ ).

There is no link between psychophysiological performance and the number of WM lesions (WMH%). Nor is there a link between age and WMH%. The RMO test's average RT (RMO\_mean) has no relation to age or the major brain compartments' volumes.

Strengths and limitations of descriptive model of brain structural changes in normal aging: Instead of investigating all of the probable regional consequences of brain aging, we focused on the major brain compartments. Before engaging in a more extensive investigation, the goal was to link psychophysiological performance with brain atrophy parameters. The reason we chose this method was due to the fact that segmentation of brain can yield a large amount of data. Dealing with

regional effects could be difficult because no one knows which brain areas are involved in the psychophysiological tasks that were performed in this study. The structural correlates of cognitive performance are not empirically supported in today's neuroscience. In our investigations, we integrated findings from MRI and PTs on the neurobiology of aging to solve the outstanding problem. On the plus side, we used statistical tests to determine that the effects of age vary among cognitive subdomains and brain compartments. We considered the non-negative compositional character of brain volumes, which add up to the TIV. Because the loss in absolute volume was less severe in a small structure than in a large one, we utilized a uniform percent loss each year as a measure to compare the pace of change. Other researchers agree that ratios are valuable for describing compositional data, especially while comparing structures with various scales of volume [291]. The PTs we used addressed several cognitive functions. The methodology that underpinned our study was built to identify changes in EF and brain morphology. We were able to support the outcomes with the entire collection of solutions.

### **3.3 Patterns of Brain Structure-Function Association Indicative of MCI and Dementia**

#### *3.3.1 Dynamics of Performance in Cognitive and Neurophysiological Tests in Patients with MCI and Dementia*

We explored the age-related variability of cognitive scores in the tests that are most commonly used either to diagnose MCI and dementia or to improve the accuracy of multimodal diagnostics. We started with the tests of global cognitive functioning: MMSE and ADAS-cog. The

distribution of the test results over age is shown in Figures 3.15-3.16. As ADNI dataset contains follow-up studies of healthy people and patients with cognitive impairment, one can judge on the disease progression by looking at the diagrams. The trends are horizontal for the performance in MMSE and ADAS-cog in all study groups. This means that the global cognitive functioning changes slightly with age in the cognitively normal population. It also remains stable across the disease course. Though there are patients with reversible or progressive MCI, the number of such cases is quite low.

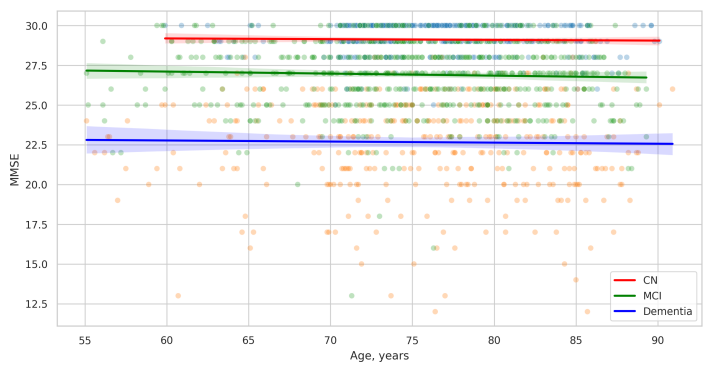


Figure 3.15: MMSE scores in the group of cognitively normal adults and patients with MCI or dementia

ADAS-cog is a very informative tool for monitoring the progression of ND in clinical routine practice [196]. According to recent findings, the test distinguishes between MCI and mild AD with sensitivity of 0.86 and specificity – 0.89 [197]. It can also identify “questionable dementia” because its results in immediate recall and object naming tasks correlate with performance in Category Verbal Fluency Test [198]. MMSE is the most common method for diagnosing cognitive impairment in a

single or multiple domains [199]. Although it detects various types of dementia with a high sensitivity and specificity of over 90%, the test should be accompanied by a full and detailed assessment of the patients [200]. For this, clinicians use neurophysiological tests (e.g., TMT, DSST) [201].

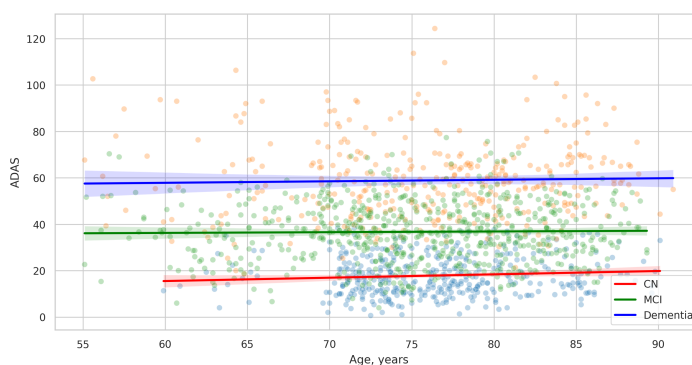


Figure 3.16: ADAS13 in the group of cognitively normal adults and patients with MCI or dementia

The second group of tests covers a few cognitive domains, i.e., information processing in DSST, memory in RAVLT, information processing in TMT. Scores in RAVLT test are quite stable throughout life in normal aging and across the disease course with a slight trend towards lowering in all the study groups (see Figures 3.17). The pace of neurocognitive slowing is moderately higher in the CN group and MCI patients. Thus, the average result for all the groups would reach a common value if the observation lasted several more decades. RAVLT examines verbal learning and memory. It is capable of detecting cognitive impairment in multiple sclerosis [206]. The test differentiates between AD dementia and behavioral variant of fronto-temporal dementia [207] with high sensitivity and specificity of over 81%. It also helps physicians to



distinguish AD from Lewy bodies dementia [208].

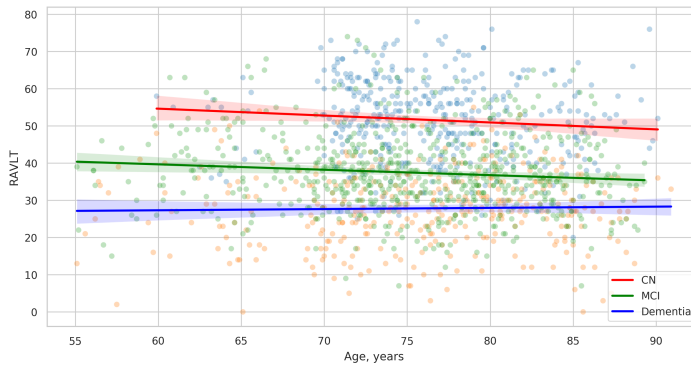


Figure 3.17: Results in RAVLT test in the group of cognitively normal adults and patients with MCI or dementia

The trendlines on Figures 3.18-3.19 show clear signs of malfunctioning in several cognitive domains assessed with DSST and TMT tests. The performance worsens with time. For this reason, the trendlines of CN, MCI and AD groups converge at the approximated point of 100 years of age. DSST identifies early stages of dementia [209] and MCI by detecting working memory impairment and multimodal amnesia [210]. It also shows significantly impaired performance in early Lewy Bodies dementia [211]. TMT provides information on neurophysiological conditions; therefore it is used for diagnosing NDs in combination with other diagnostic modalities [202, 203, 201]. Its clinical implication is multifold. First, TMT helps to define the impaired cognitive domain and improves the assessment with MMSE or MoCA [201]. Second, there is evidence that the inclusion of TMT (part B) boosts the performance of the models that use CSF and structural biomarkers to discriminate between AD and non-AD MCI [204]. Third, the test can sensitively distinguish a case of

mild AD from amnesic MCI and healthy aging [205].

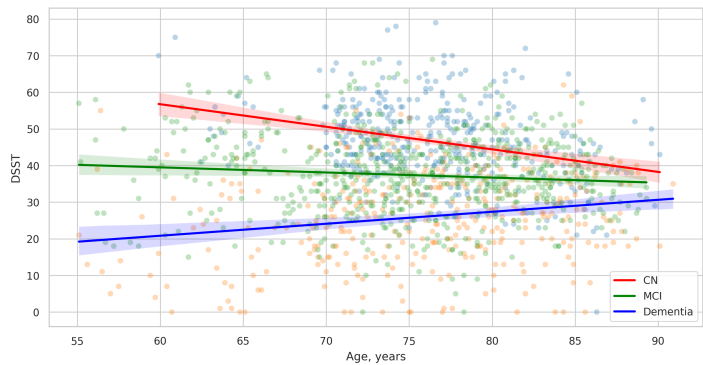


Figure 3.18: Performance in DSST in the group of cognitively normal adults and patients with MCI or dementia

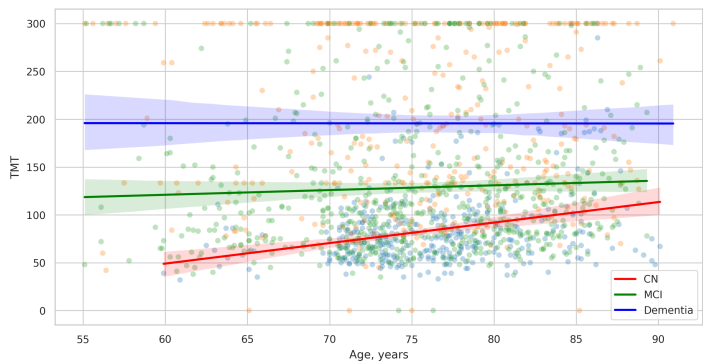


Figure 3.19: Executive functioning assessed with TMT test in the group of cognitively normal adults and patients with MCI or dementia

As seen from the diagrams 3.18-3.19 the trendlines of the performance in neurophysiological tests (TMT and DSST) and the degeneration of the GM show the same dynamics in the correspondent cohorts (see Figure 3.20). But the slopes for the GM volume adjusted to the TIV are steeper than the trendlines for the results in DSST or TMT. Presumably, brain plasticity helps an individual to adjust to aging and

disease and compensates for the loss of the GM volume.

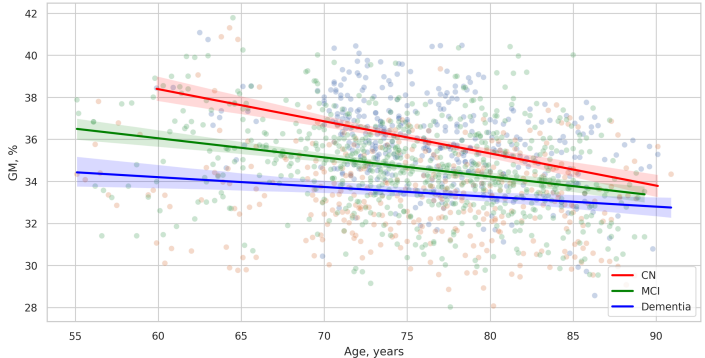


Figure 3.20: Gray matter volume in the group of cognitively normal adults and patients with MCI or dementia

### 3.3.2 Models of Brain Structure-Function Associations in Cognitively Normal Individuals, Patients with MCI or Dementia

Examining the feasibility of employing brain morphometry for predicting neurofunctional performance in CN, MCI, and dementia cohorts, we designed an ML regression model. The performance of these algorithms is presented in Table 3.7. As the test scales differ in size, we adjusted MAE to the range of results in each test. This allowed us to compare the accuracy of the algorithms trained on MMSE, ADAS-cog, RAVLT, TMT and DSST. The test results in MMSE can be predicted much more accurately than in other tests (MAE/range =  $4.5 \pm 0.23$  in the CN group). Despite a markedly higher mistake of the model for the ADAS-cog score ( $p = 1.84e - 95$ ), its prediction also has credible performance (MAE/range =  $5.04 \pm 0.22\%$  in the CN group). The error of the RAVLT, TMT and DSST score prediction is significantly higher ( $10.62 \pm 0.5$ ,  $10.57 \pm 0.68$  and  $10.81 \pm 0.51\%$ ). The dissimilarity in the accuracy of the model goes in line with the trends

described in the previous subsection. In MMSE and ADAS-cog the trendlines are parallel and do not intersect. The same trends for RAVLT, TMT and DSST merge if approximated to future life.

Table 3.7: Performance of models trained on cognitively preserved population, subjects diagnosed with MCI or dementia with adjustment to the maximal score of the scales (MAE/range, %)

DX	Data	MMSE	ADAS	p-value	RAVLT	TMT	DSST	p-value
CN	VBM	4.5 ± 0.23	5.04 ± 0.22	1.84e-95	10.62 ± 0.5	10.57 ± 0.68	10.81 ± 0.51	2.99e-142
	SBM	4.61 ± 0.23	4.96 ± 0.22	1.84e-95	10.38 ± 0.49	10.75 ± 0.67	10.24 ± 0.53	4.15e-131
	VBM+SBM	4.61 ± 0.23	4.94 ± 0.22	1.84e-95	10.07 ± 0.48	10.62 ± 0.66	10.23 ± 0.51	1.92e-129
MCI	VBM	9.28 ± 0.29	7.62 ± 0.22	3.63e-211	9.52 ± 0.3	20.13 ± 0.65	10.95 ± 0.33	1.43e-212
	SBM	9.0 ± 0.28	7.48 ± 0.21	2.46e-206	9.59 ± 0.31	18.8 ± 0.59	10.12 ± 0.33	9.38e-210
	VBM+SBM	9.06 ± 0.28	7.41 ± 0.21	1.65e-206	9.46 ± 0.3	18.81 ± 0.59	10.03 ± 0.32	1.01e-209
Dementia	VBM	13.22 ± 0.54	10.3 ± 0.42	6.98e-121	8.65 ± 0.33	26.97 ± 0.75	12.67 ± 0.46	2.14e-187
	SBM	12.67 ± 0.54	9.09 ± 0.42	3.27e-99	7.97 ± 0.34	25.75 ± 0.76	11.03 ± 0.42	3.43e-172
	VBM+SBM	12.78 ± 0.55	9.11 ± 0.41	1.75e-92	7.9 ± 0.33	25.9 ± 0.77	10.85 ± 0.42	1.94e-171

VBM - voxel-based morphometry; SBM - surface-based morphometry.

We ranked the structural predictors according to the information gain value. The top valuable predictors of MMSE score are the volumes of the total brain, cerebral cortex, accumbens, cerebral WM, inferior lateral ventricles, and hippocampus. However, the results in TMT have a weaker association with the brain structures listed above.

In each study cohort we found clusters of cortical parcellations closely associated with performance in cognitive tests. The volume, surface area of the clusters and their number differ evidently among the studied cohorts. This is because each of the SBM metrics provides unique information regarding cortical anatomy and possibly different SFA patterns [293].

From Table 3.8 one can observe the variations in the capacity of projecting cognitive scores among CN, MCI and dementia groups. The majority dementia cases arise from protein aggregation disorders (e.g., the

accumulation of  $\beta$ -amyloid,  $\tau$ -protein, etc.). Genetic variability in the expression level of the deposited protein is important in pathogenesis of neuronal diseases [294]. It accounts for different solubility of the aggregation-prone protein and the efficiency of clearance mechanisms that keep misfolded proteins in check. Besides this, the clinical appearance of dementia varies because of selective neuronal and regional vulnerability that differs among misfolding diseases [294].

In all the tests, the informative value of brain structures in the prediction of cognitive scores differs by the study group (CN, MCI, dementia). This justifies the presence of different SFA patterns in the healthy cohort and patients with a pathology. We analyzed the SFA patterns in the demented patients of ADNI dataset and discussed the findings. As AD accounts for the majority of dementia cases, we pointed out the structures vulnerable for change in  $\beta$ -amyloidopathy. Other NDs selectively damage different groups of neuronal cells and brain regions, which would result in another SFA patterns.

Table 3.8: Metrics of models trained on cognitively preserved population, subjects diagnosed with MCI or dementia (MAE)

Test	Data	CN		MCI		Dementia		p-value
		Mean $\pm$ Std	CI	Mean $\pm$ Std	CI	Mean $\pm$ Std	CI	
MMSE	VBM	0.81 $\pm$ 0.04	[0.73 - 0.89]	1.67 $\pm$ 0.05	[1.57 - 1.77]	2.38 $\pm$ 0.1	[2.19 - 2.57]	3.97e-239
	SBM	0.83 $\pm$ 0.04	[0.75 - 0.92]	1.62 $\pm$ 0.05	[1.52 - 1.72]	2.28 $\pm$ 0.1	[2.09 - 2.47]	1.34e-234
	VBM+SBM	0.83 $\pm$ 0.04	[0.75 - 0.91]	1.63 $\pm$ 0.05	[1.53 - 1.73]	2.3 $\pm$ 0.1	[2.11 - 2.49]	8.23e-232
ADAS-cog	VBM	3.24 $\pm$ 0.14	[2.96 - 3.51]	4.9 $\pm$ 0.14	[4.62 - 5.17]	6.63 $\pm$ 0.27	[6.09 - 7.16]	6.53e-239
	SBM	3.19 $\pm$ 0.14	[2.91 - 3.46]	4.81 $\pm$ 0.14	[4.53 - 5.08]	5.85 $\pm$ 0.27	[5.32 - 6.38]	5.12e-230
	VBM+SBM	3.18 $\pm$ 0.14	[2.9 - 3.45]	4.77 $\pm$ 0.14	[4.5 - 5.03]	5.86 $\pm$ 0.26	[5.35 - 6.38]	1.44e-227
RAVLT	VBM	7.33 $\pm$ 0.35	[6.65 - 8.01]	6.57 $\pm$ 0.21	[6.16 - 6.98]	5.97 $\pm$ 0.23	[5.52 - 6.42]	2.86e-231
	SBM	7.16 $\pm$ 0.34	[6.5 - 7.82]	6.62 $\pm$ 0.21	[6.2 - 7.04]	5.5 $\pm$ 0.23	[5.04 - 5.96]	4.14e-220
	VBM+SBM	6.95 $\pm$ 0.33	[6.31 - 7.6]	6.53 $\pm$ 0.21	[6.12 - 6.93]	5.45 $\pm$ 0.23	[5.0 - 5.9]	2.48e-213
TMT(part B)	VBM	28.32 $\pm$ 1.83	[24.73 - 31.9]	53.94 $\pm$ 1.73	[50.55 - 57.33]	72.28 $\pm$ 2.02	[68.32 - 76.24]	2.26e-229
	SBM	28.81 $\pm$ 1.81	[25.26 - 32.35]	50.38 $\pm$ 1.57	[47.29 - 53.46]	69.0 $\pm$ 2.03	[65.01 - 72.99]	5.56e-184
	VBM+SBM	28.47 $\pm$ 1.77	[25.0 - 31.95]	50.4 $\pm$ 1.58	[47.3 - 53.49]	69.41 $\pm$ 2.07	[65.36 - 73.47]	1.38e-180
DSST	VBM	8.43 $\pm$ 0.4	[7.65 - 9.21]	8.54 $\pm$ 0.26	[8.03 - 9.04]	9.88 $\pm$ 0.36	[9.18 - 10.57]	4.88e-230
	SBM	7.99 $\pm$ 0.41	[7.19 - 8.79]	7.89 $\pm$ 0.25	[7.4 - 8.39]	8.6 $\pm$ 0.33	[7.95 - 9.24]	3.28e-192
	VBM+SBM	7.98 $\pm$ 0.4	[7.19 - 8.77]	7.82 $\pm$ 0.25	[7.32 - 8.31]	8.46 $\pm$ 0.33	[7.81 - 9.1]	6.89e-187

VBM - voxel-based morphometry; SBM - surface-based morphometry.

### 3.3.2.1 *MMSE*

The test is one of the most frequent tools for screening cognitive impairment in older adults. It is also used to evaluate cognitive impairment progression in follow-up visits. MMSE examines various cognitive domains: temporo-spatial orientation, memory recall, concentration, language, visuospatial function, and working memory. The top valuable structural predictors of MMSE results are listed in Figure 3.21 and described below.

Precuneus volume is the most informative predictor. It is a cortical region located in the posterior portion of the medial parietal cortex. Recent functional imaging findings in healthy subjects suggest its involvement in a wide spectrum of highly complex functions, including visuo-spatial imagery, episodic memory retrieval, working memory, and orientation [295, 296]. Consequently, its integrity determines successful achievement of several MMSE tasks, such as the intersecting pentagon copying test, short-term memory recall, and orientation to time and place. The relative volume of intracranial arteries is the second in the list of structural parameters with the greatest prognostic gain. The lumen of the vessels decreases in atherosclerosis which is associated with impaired cognitive function due to reduced cerebral blood flow and ischemic damage. Recent studies reported that intracranial stenosis of arteries and increased plaque number correlate with more lacunes, larger volume of WM lesions and memory decline [297, 298]. Hence, the decreased total volume of intracranial arteries is implicated in the performance deficiency in the word registration-repetition task and short-term memory recall of MMSE test.

The pars triangularis relative volume is the third index that produces the most informative input. The structure refers to the triangular shaped cortical region of the inferior frontal gyrus in the frontal lobe. It is a segment of Broca's area which takes part in expressive aspects of the spoken and written language. More characteristically, the pars triangularis is involved in the semantic processing of language and syntax. The relatively high predictive value of the pars triangularis in MMSE can be explained by its essential participation in the language tasks: sentence repetition, instructions comprehension, reading sentences and doing as they say, writing short sentences, recognition and naming of two common objects.

MMSE in patients with MCI: In the MCI cohort, the hippocampus contributes the most to the information gain. Its involvement in working memory, memory recall and language processing and production might affect the successful fulfillment of the following tasks: repetition, instruction comprehension, recognition and naming of objects, spelling "WORLD" backward, and short term memory recall. The superior parietal lobule is the next best estimator for MMSE test scores. It is topographically close to the occipital lobe and is employed in some aspects of concentration and visuospatial perception. Its participation in the tasks of copying pentagons and spelling "WORLD" backward might explain the high informative value.

MMSE in patients with dementia: MMSE test scores in the dementia patients are best forecasted from the volumes of the brain parts different from those observed in the CN and MCI cohorts. The fusiform gyrus has the greatest informative potential in the dementia group. Its

function mainly comprises visual processing, i.e., word and object recognition, visuospatial perception. Hence, it's a key partaker in the tasks of copying of intersecting pentagons, reading a sentence, recognising and naming common objects. Next, the transverse temporal gyrus, caudal middle frontal cortex, and cGM have the highest information gain value. The transverse temporal gyrus is the first cortical region to process incoming auditory information. Thus, its impairment could be associated with less efficient processing of speech-related stimuli, which could, in turn, impede learning and perceiving speech sounds thus affecting the performance in sentence repetition and instruction comprehension tasks of MMSE. The caudal portion of the middle frontal gyrus contains the frontal eye fields which control saccadic eye movements. It is these movements which make it possible to scan numerous details within a scene. The role of the structure in visual attention might be relevant to the visuospatial and language tasks including recognition of common objects, reading a sentence and doing as it says, copying intersecting pentagons. Finally, the GM of the cerebral cortex also has a relatively high information gain value. Since it comprises the four lobes, i.e., frontal, parietal, temporal, and occipital, it is involved in a wide range of cognitive processes. cGM participates in memory and learning, sensory perception such as seeing, hearing, speech, language comprehension, concentration, visuospatial processing, orientation, spatial attention and mapping. Hence, its integrity is required for the successful completion of all MMSE tasks.



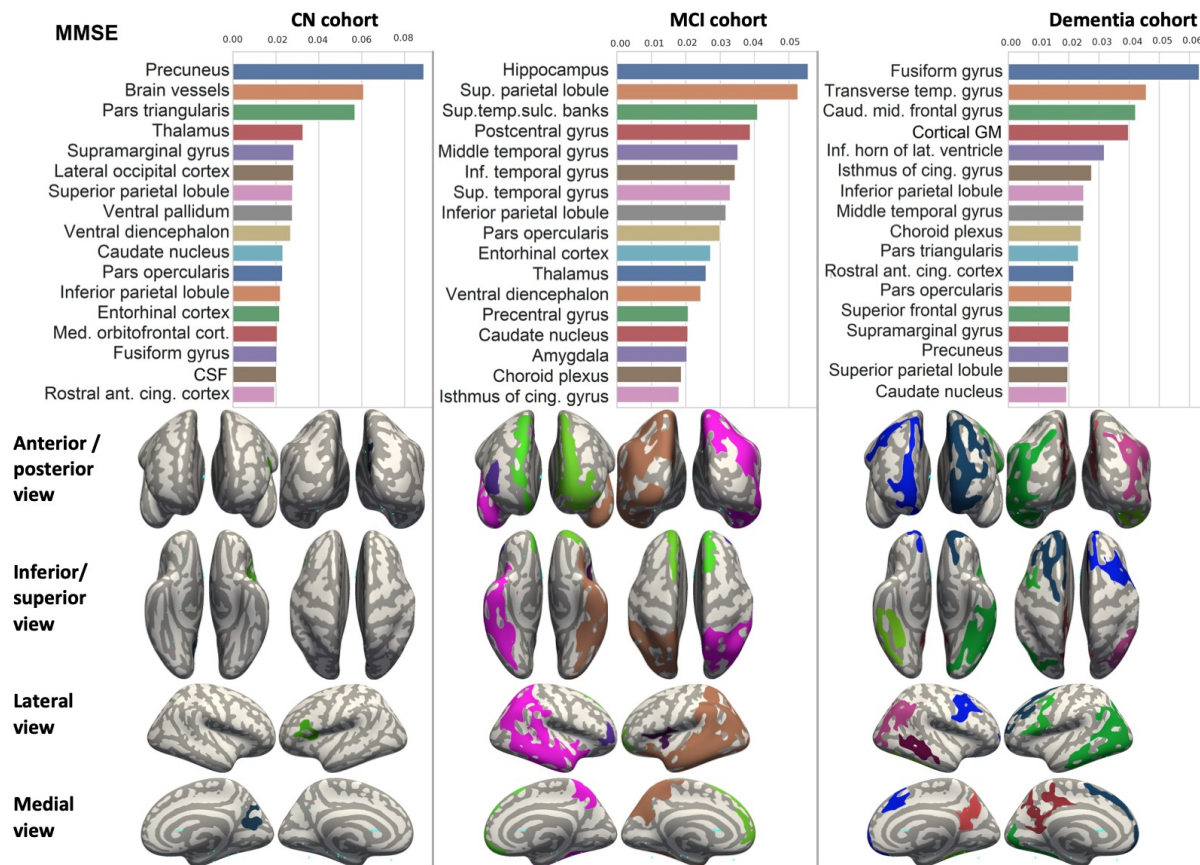


Figure 3.21: Brain structures ranked according to information gain value for MMSE score prediction. Inflated cortical representations showing significant correlations between cortical volumes and test score

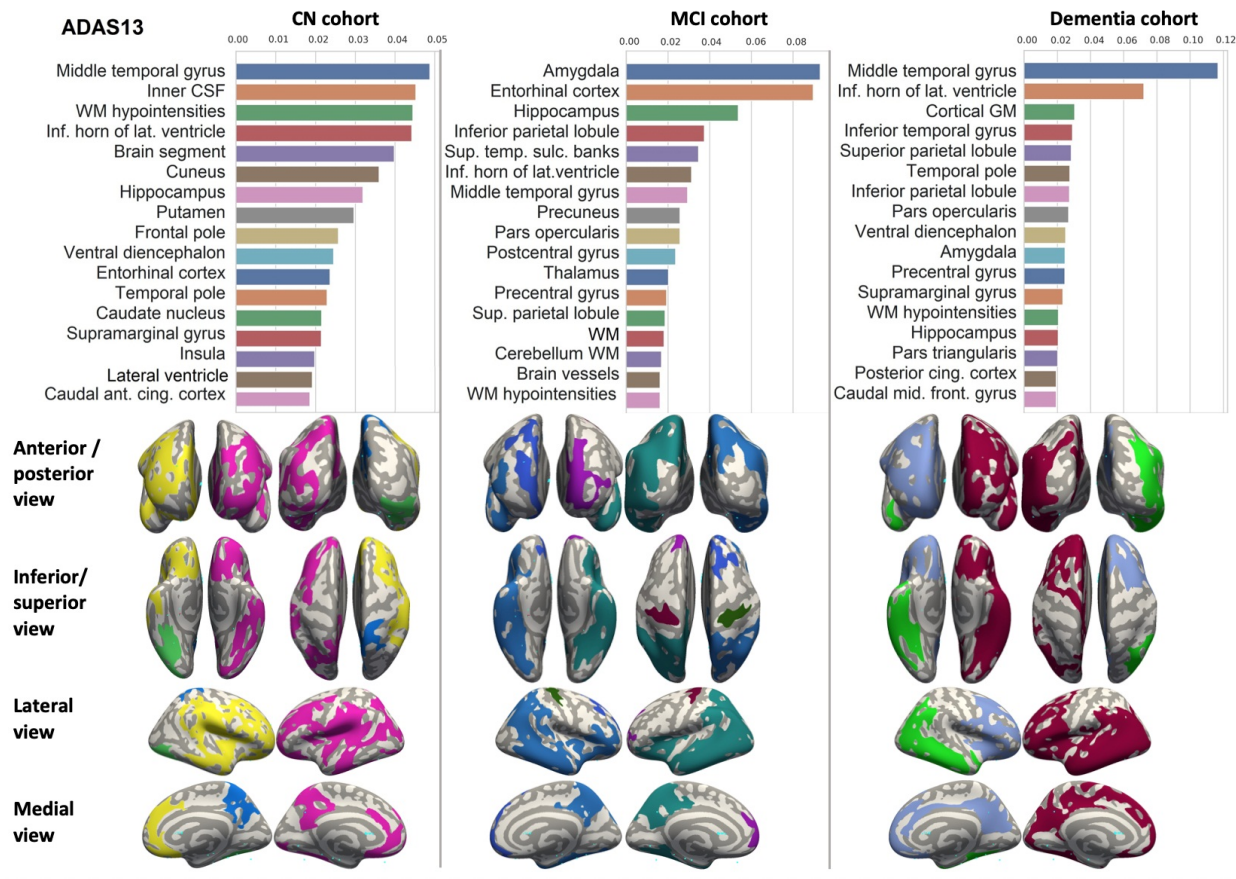


Figure 3.22: Brain structures ranked according to information gain value for ADAS13 score prediction. Inflated cortical representations showing significant correlations between cortical volumes and test score

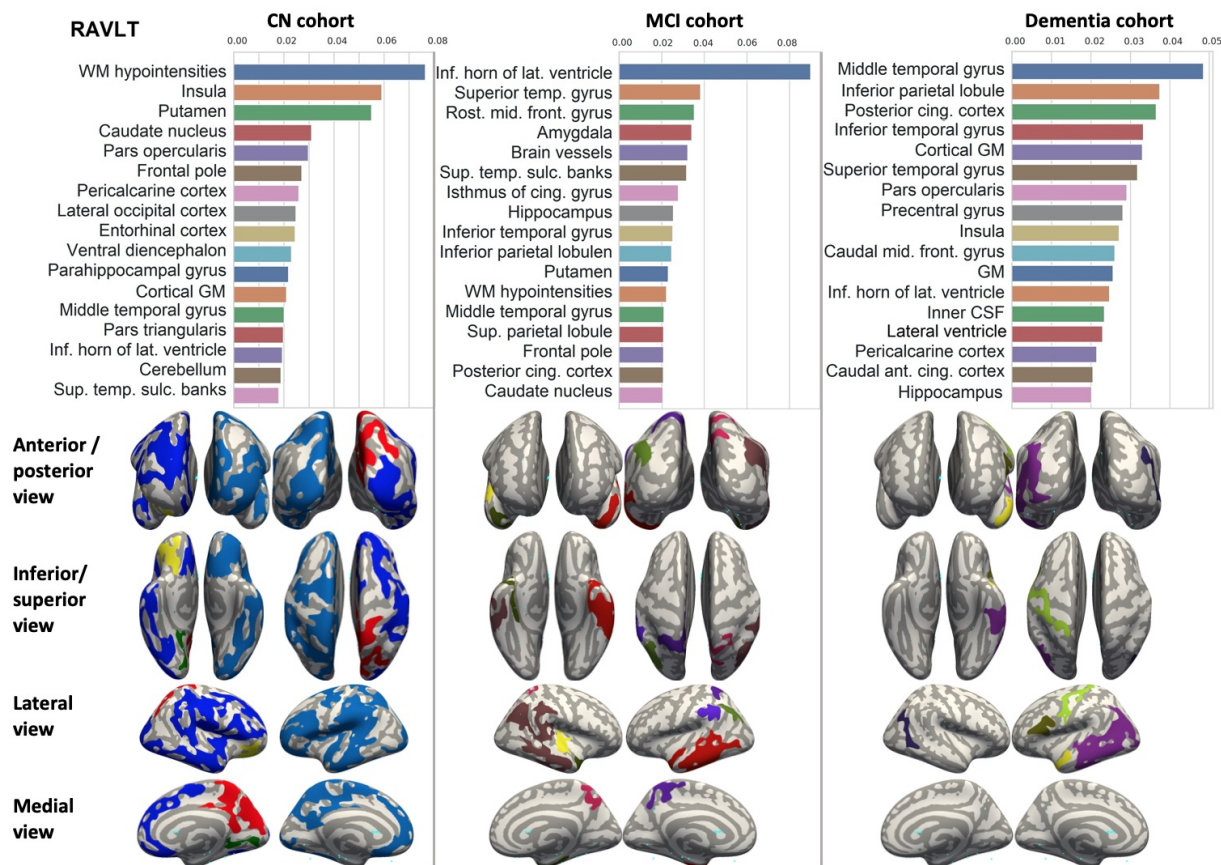


Figure 3.23: Brain structures ranked according to information gain value for RAVLT score prediction. Inflated cortical representations showing significant correlations between cortical volumes and test score

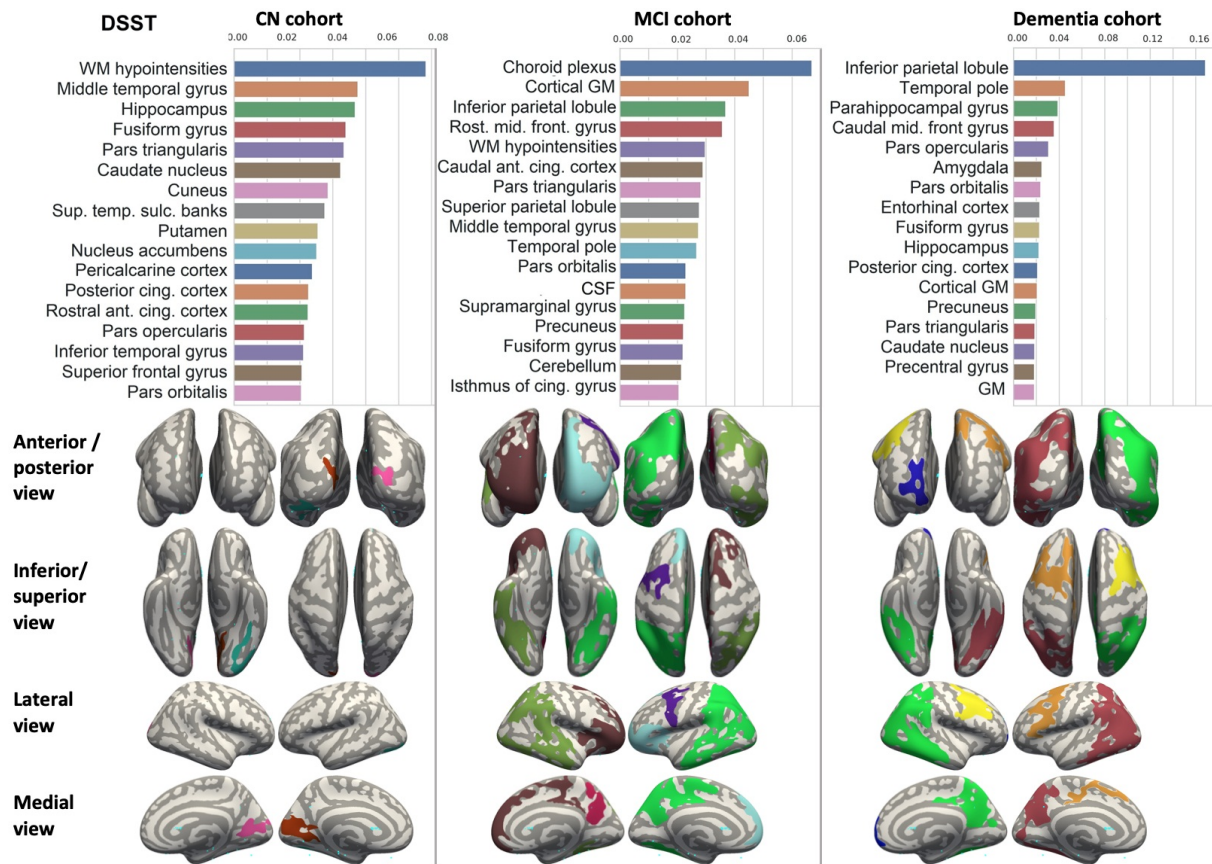


Figure 3.24: Brain structures ranked according to information gain value for DSST score prediction. Inflated cortical representations showing significant correlations between cortical volumes and test score



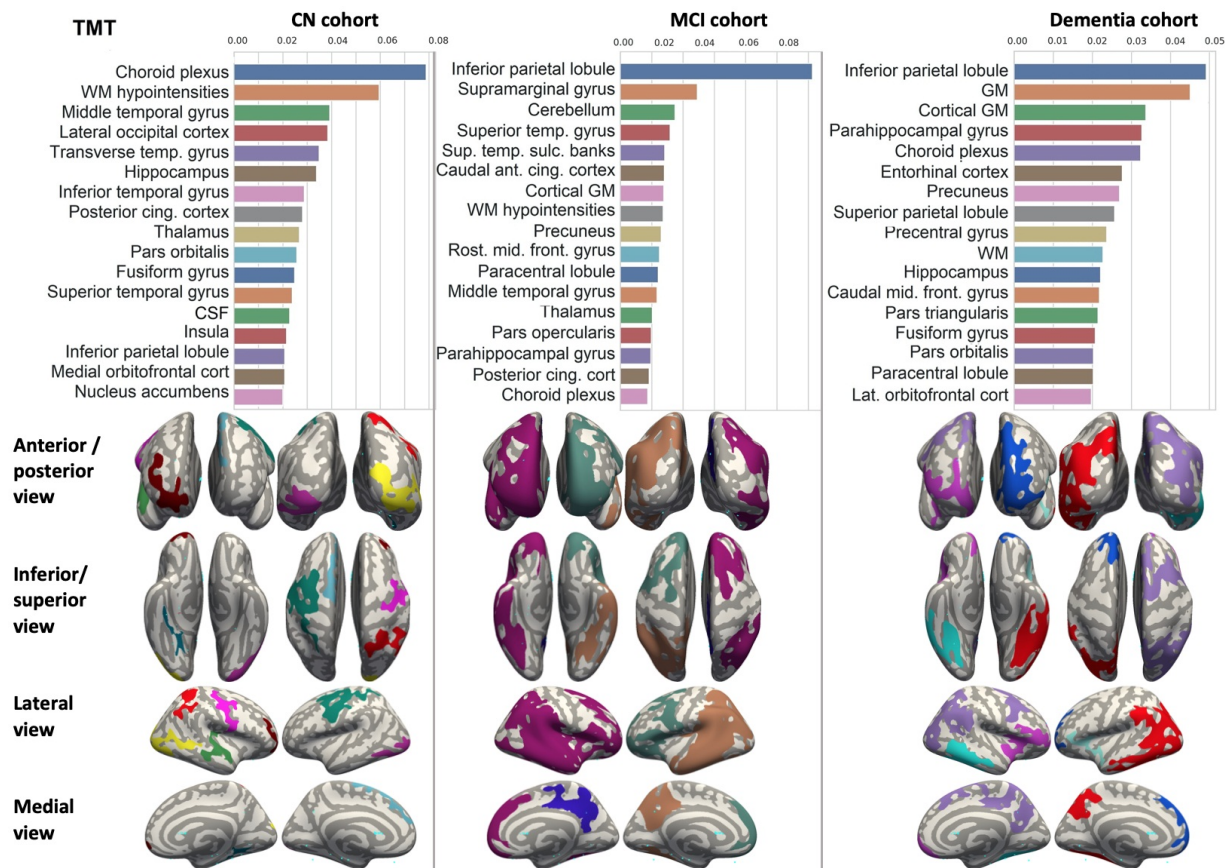


Figure 3.25: Brain structures ranked according to information gain value for TMT score prediction. Inflated cortical representations showing significant correlations between cortical volumes and test score.

### 3.3.2.2 ADAS

ADAS is a brief cognitive test battery that evaluates learning and memory, language production, language comprehension, constructional and ideational praxis, etc. In this study we resorted to average values of ADAS - ADAS13. The reason for the choice of this dependent variable is explained in Subsection 3.4.1. The information gain value of the brain volumes in predicting ADAS13 in the CN, MCI and dementia cohorts is illustrated in Figure 3.22. For the CN subjects, the middle temporal volume provides the highest information gain value. The hippocampus, amygdala and other structures constitute the medial temporal lobe which is essential for episodic memory. Encoding, consolidation, and retrieval are the processes composing the memory function of the lobe while word recall and remembering test instructions are among the tasks assessing memory in the ADAS-cog test.

Intraventricular CSF is the second top-informative predictor of performance in ADAS-cog in the CN cohort. The rise in the volume suggests larger ventricles and indicates brain atrophy which hampers cognitive abilities. Larger ventricles are strongly correlated with lower WM integrity due to the small vessel disease [299]. Increasing intraventricular CSF volume is significantly associated with increasing severity of cognitive impairment and reaction time in the tests.

WM hypointensities and the inner CSF are predictors of roughly the same informative value. The hypointensities are areas of attenuated signal on T1-weighted MRI scans. Pathological lesions in these regions include myelin pallor, tissue rarefaction associated with a loss of myelin and axons, and mild gliosis [300]. They are also associated with a faster

deterioration in global cognitive performance as well as in memory, learning, praxis, and language [188]. These functions are believed to depend on some brain structures including subcortical neural networks and cortical-subcortical circuits. The latter can be damaged while passing through WM. Reasonably, the WM integrity is the key index to predict ADAS13.

Inferior horns of the lateral ventricles have the information gain value almost identical to that of the inner CSF and WM hypointensities. Inferior lateral ventriculomegaly is caused by passive enlargement of the inferior (temporal) horns of the lateral ventricles. Typically, the enlargement follows neuronal loss and brain parenchymal atrophy in the temporal lobe. Therefore the temporal horns have been repeatedly used as the index for middle temporal lobe atrophy [301] which is the top informative biomarker in our study. They may also reflect the level of cognitive impairment. Accordingly, subjects who suffer from cognitive decline exhibit greater temporal horn enlargement compared to their cognitively stable counterparts. Notably, the information gain of the inferior horns is twice as high as that of the total lateral ventricles. This can be explained by the fact that the temporal horn volume is a measurement of the middle temporal lobe atrophy while the size of lateral ventricles is indicative of the global cerebral atrophy. Consequently, it is less specific for neuropsychological decline compared to the temporal horns and has lower significance in projecting ADAS.

The fifth most informative predictor is the ratio of the brain segment to the TIV. The brain segment includes voxels of all intracranial structures with the exception of the brain stem and background. It also includes vessels,

the optic chiasm and CSF.

The information gain of the cuneus is approximately 75% bigger than that of the lateral ventricles. The cuneus is a wedge-shaped area on the medial surface of the occipital lobe. It is most known for its role in primary visual processing (receipt, segmentation, and integration of visual input) and secondary visual processing (analysis and discrimination of visual information in terms of motion, shape, and position). These functions are necessary for the accurate and prompt completion of ADAS tasks such as naming and word recognition. The cuneus is also involved in reward response, anticipation, attention, and working memory manipulations. Thus, it contributes to higher cognitive functions involving visual information.

The information value of the hippocampus is two times lower than that of the total middle temporal lobe. The hippocampus is a complex brain region crucial to semantic, episodic, and spatial memory, learning, and language comprehension and production. A decrease in hippocampal volumes is strongly associated with worse ADAS scores. To accomplish pattern recognition and memory encoding tasks of ADAS-cog, the hippocampus acquires an input from the entorhinal cortex. It is better to combine the volumetric analysis of these substructures that comprise the middle temporal lobe than to explore each of them individually.

The next information valuable structure is the putamen - a deep brain nucleus and a component of the basal ganglia. Through the cortico-striato-thalamocortical neural pathways, the putamen is involved in language learning functions and motor execution, including speech articulation. Its impairment leads to hindered fluency, dysarthria with



clumsy hands and other clinical manifestations. ADAS requires intact motor responses, language and cognition to successfully fulfil different tasks including constructional praxis and spoken language ability. Therefore, the putamen is related to the ADAS-cog score.

The volumes of the frontal lobe, ventral diencephalon, entorhinal and temporal lobe also provide information for the prediction of ADAS13, since they contain neuro-centres for language, voluntary movement, object and language recognition. Although the parahippocampal gyrus volume correlates significantly with language and praxis subscale scores, it has a relatively low information gain value in our models predicting ADAS13.

ADAS-cog in patients with MCI: The middle temporal lobe volume is not high informative in the MCI group. Instead, each of its three main components - the amygdala, the entorhinal cortex and the hippocampus - achieves the highest values of the parameter. The middle temporal lobe is composed of several structures that can disproportionately contribute to the forecast of ADAS results. In our study, the amygdala is the strongest predictor of ADAS13 in the MCI group. It is known for the key role in regulating emotions and encoding memory of them. The predictive value of the amygdala volume can be justified by the fact that emotions impact several cognitive processes, including memory and learning. The entorhinal cortex has the second greatest predictive gain in the performance of the model. Working memory, spatial learning and memory are among the functions of the entorhinal cortex. Injury to it can impact efficiency in such ADAS-cog tasks as word recall, remembering test instructions and orientation. The hippocampus ranks third among the best estimators in the MCI cohort. Its contribution to learning; language comprehension and

production; semantic, working and spatial memory makes it crucial for fulfilling multiple ADAS tasks.

ADAS-cog in patients with dementia: In demented patients, the volume of the middle temporal lobe and the inferior lateral ventricles are the top predictors of ADAS13 in our models.

### 3.3.2.3 *RAVLT*

RAVLT is a powerful neuropsychological instrument for assessing episodic memory and attention. It evaluates the ability to learn 15 words in five immediate trials, to remember the words after an intervening interference list, then to recall and recognize the words after a 30-minute latency interval. RAVLT is commonly used to test cognitive abilities in dementia and pre-dementia patients. Figure 3.23 exhibits the rank of different brain regions in predicting RAVLT values.

In the cognitively preserved subjects, the best predictor is WM hypointensities. According to previous neuroimaging studies, WM damage increases with aging and cerebrovascular disease, and is linked to episodic memory impairment in CN older individuals [302, 303]. Age-related episodic memory deficits are caused by network disruption because injury to various pathways leads to the disconnection between the frontal and temporal cortex and frontal-subcortical WM tracts. Next, the volume of the insula is the second best estimator of the RAVLT score. The insular cortex is a slender band of GM that is located just beneath the lateral brain surface, connecting the temporal lobe to the inferior parietal cortex. The structure is linked to verbal episodic memory tasks, which justifies our findings. The putamen is the ensuing strongest predictor in CN cohorts. Although our

understanding of the putamen's role in cognitive functioning is still limited, recent discoveries suggest that its damage results in poorer attention [304]. The assumed reason for this is its involvement in the cortico-striatal-thalamo-cortical pathway that consists of connections between the basal ganglia, thalamus and multiple brain regions involved in cognitive control in the prefrontal, parietal and temporal lobes. Therefore, alterations to this region can be accountable for the impeded execution of the three tasks in RAVLT neurofunctional test.

RAVLT in patients with MCI: The inferior lateral ventricles exceed all analyzed brain structures in estimating RAVLT scores in the MCI cohort. Since they reflect the temporal lobe volume, the ventricles can be used as indicators of episodic memory and attention.

RAVLT in patients with dementia: The middle temporal lobe outperforms all other brain areas in calculating RAVLT scores. The inferior parietal lobe and its part - the posterior cingulate cortex - take second place in the list of predictors. The involvement of the aforementioned structures in episodic memory and attention helps us to explain the findings.

#### 3.3.2.4 *DSST*

This is a psychomotor test that requires the participant to match symbols to numbers according to the key at the top of the page. The DSST is short and valid, that is why it is widely used in neuropsychology. It assesses a variety of cognitive functions. Motor speed, working memory, associative learning, and visuoperceptual functions are required for good DSST performance.

The structural parameter with the most pronounced information

gain is WM hypointensities. Lower scores in the pencil and paper DSST are substantially correlated with a greater volume of WM lesions [305]. A study showed a notable interaction between WM lesion and accuracy, working memory, associative learning, psychomotor speed, attention, and visuospatial functioning [305, 306]. The middle temporal lobe and hippocampus have the next highest ranking. They play a crucial role in learning coordination, working memory, attention, and spatial perception which are essential for satisfactory performance in the DSST [307].

The next informative predictor is the fusiform gyrus - a vast structure in the inferior temporal cortex. Its role is higher-level processing of visual information, including identification and differentiation of objects, word recognition, and perception. Therefore, the successful completion of the DSST partially depends on the fusiform gyrus integrity.

The pars triangularis receives a rank equal to that of the middle temporal lobe and hippocampus. It is challenging to justify this result since the pars triangularis is involved in the language functions irrelevant to the DSST. The caudate nucleus ranks lower than the pars triangularis. This is supported by multiple studies that revealed correlations between the decreased volumes of the caudate nucleus, reduced attention and motor speed [211].

DSST in patients with MCI: In the MCI cohort, the choroid plexus is the metric that provides most information for anticipating DSST scores. It is involved in producing the CSF and certain proteins as well as transporting solutes to the brain. The choroid plexus volume has been reported to increase with advancing age. The supposed reasons for this are, first, modifications in the choroid plexus microstructure or function and,

second, ventriculomegaly [308]. These lead to dysfunction in CSF synthesis and clearance as well as reduce the levels of anti-inflammatory proteins. The disruption of the neuroimmune axis eventually hampers brain homeostasis and leads to cognitive deterioration [309, 310]. Due to scarcity of research in this topic, it is challenging to pinpoint which cognitive domains are impaired with structural alterations to the choroid plexus. Therefore, it is difficult to identify the DSST tasks that are affected by change in the volume of the structure.

The brain structures that receive the next rank are the cGM and inferior parietal lobe. The cGM is critical for all the cognitive domains assessed by DSST. The inferior parietal cortex plays a crucial role in auditory-spatial working memory, motor speed, attention, and visuospatial processing. The rostral middle frontal gyrus - the fourth most informative region - is associated with working memory and visual attention.

DSST in patients with dementia: The inferior parietal gyrus is the highest ranking predictor in the model of DSST scores in the demented patients.

#### *3.3.2.5 TMT*

TMT is a neuropsychological test that reflects visuospatial abilities, information processing speed, sustained attention, motor speed, working and rote memory. The dependent variable of the TMT shows the time spent on taking the test. Choroid plexus volume ranks first in forecasting TMT scores in the cognitively preserved population. Since the role of this structure in cognition has not been fully described, it's challenging to identify the tasks that are affected by structural alterations to the choroid

plexus. The volume of WM hypointensities takes second place as a TMT performance predictor. Since the WM lesions reduce motor and processing speed, impair memory, visuospatial function and attention, it's plausible that they rank high in prognosing the test scores. The middle temporal lobe is the next valuable structure in the list. It is involved in working memory, attention and visuospatial perception. The lateral occipital cortex is a neural center for visual recognition. It also has a high predictive value for the TMT scores.

TMT in patients with MCI: In the MCI group, the inferior parietal cortex is the strongest predictor because of its role in working memory, attention, visuospatial processing, and motor speed. The second best predictor for TMT scores is the superior marginal cortex which is involved in information processing.

TMT in patients with dementia: Finally, the inferior parietal cortex and the GM outperform all other analysed brain regions in detecting TMT scores among the demented patients.

### *3.3.3 Classification of Examinees Into Cohorts According to the Pattern of SFA Association*

We tried to classify individual findings according to the model which describes the case best. The idea was that the ML model, when trained on the cases of this of that group, describes a disease-specific SFA pattern. The pattern serves as a "stamp" of the disease on which the model was trained. Therefore, one can find the "stamp" which fits the case best. We used Random Forest model as a regression algorithm to predict results of cognitive tests. Then we employed the majority voting technique to assess the performance of the multigroup classification by looking at the

smallest absolute error in prediction between three regression models.

The highest classification accuracy is achieved with the model trained to predict MMSE from VBM (see Figure 3.26). In the cognitively normal cohort, the model identifies 83.91% of individuals as healthy subjects, and a relatively small portion (14.94%) is misclassified as patients with MCI. The true prediction rate reaches 86.96% in the MCI group. The least accurate classification is observed in the group of the demented patients: it misclassifies over 26% of them. This is the major limitation of the constructed classification system.

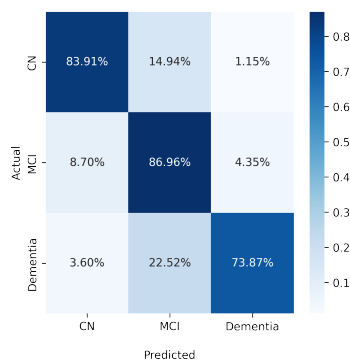


Figure 3.26: Confusion matrix of multigroup classification based on MMSE prediction from VBM data

The diagnostic algorithm based on ML prediction of MMSE from SBM is almost as accurate as the previous classification (see Figure 3.27). The percentage of misclassified cases in the normal cohort is slightly higher. Still, none of the cognitively preserved individuals are misclassified as demented. When VBM and SBM predictors are used in combination, the performance does not increase (see Figure 3.28). Unexpectedly, the true predictive rate drops to 79.31% and 72.07% for the cognitively normal and

demented population respectively. The inclusion of SBM predictors to the model does not boost the accuracy.

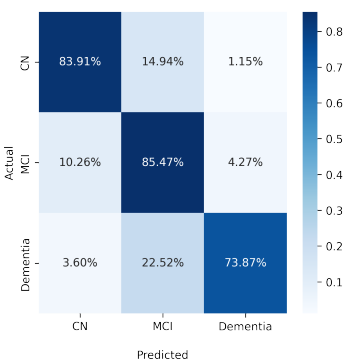


Figure 3.27: Confusion matrix of multigroup classification based on MMSE prediction from SBM data

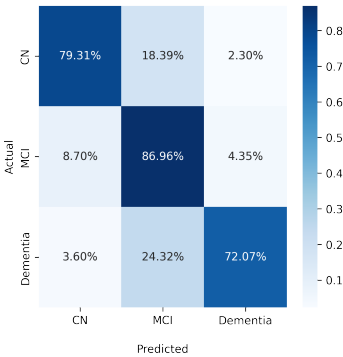


Figure 3.28: Confusion matrix of multigroup classification based on MMSE prediction from SBM and VBM data

Classification based on the model trained to predict ADAS13 from VBM detects the demented patients more accurately than the other considered models at the level of 78.38% true prediction rate. The performance for the CN class is weaker in all the models predicting ADAS13.



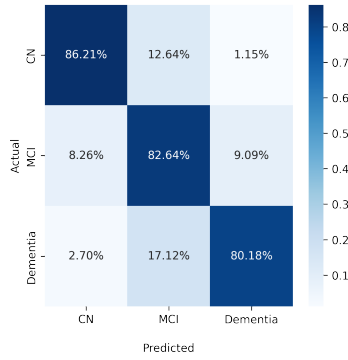


Figure 3.29: Confusion matrix of multigroup classification based on MMSE, ADAS and RAVLT prediction from VBM data

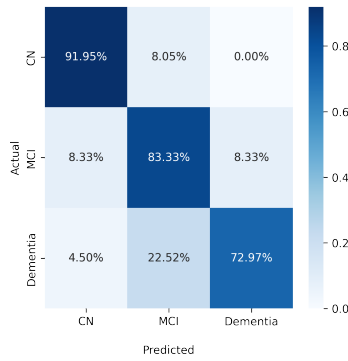


Figure 3.30: Confusion matrix of multigroup classification based on MMSE, ADAS and RAVLT prediction from SBM data

The application of the majority voting technique to models predicting results in MMSE, ADAS and RAVLT improved the classification performance (see Figures 3.29-3.31). We observed the highest classification performance of the algorithm trained on SBM data for the CN group (TPR=91.95%, see Figure 3.30). The accuracy of identifying MCI was 83.33%. The model trained on VBM data showed the best performance for dementia cases (TPR=80.18%, see Figure 3.29).

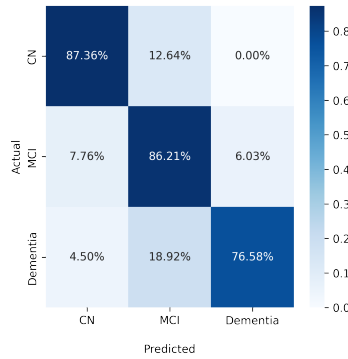


Figure 3.31: Confusion matrix of multigroup classification based on MMSE, ADAS and RAVLT prediction from SBM and VBM data

### 3.4 Deviation From Model of Normal Aging: Application of Deep Learning to Structural MRI and Cognitive Scores

#### 3.4.1 Association of Cognitive Tests and Structural Data

The structural data are presented in terms of percentage of the volume of a specific brain area to the total intracranial volume. There are significant differences among the studied cohorts in the structures most vulnerable to change in ND (see Table 3.9). The data reveal shrinkage of the brain parts (the hippocampus, entorhinal cortex, fusiform gyrus, medial temporal lobe) and enlargement of the ventricles in accelerated aging. No significant differences in age among CN, MCI and AD groups was detected ( $p = 0.1109$ ).

In the MCI cohort, the ADAS-cog score is negatively associated with the major part of the analyzed relative volumes. The exception is the relative volume of WM and its lesions, CSF and caudate nucleus. The association of performance in ADAS-cog with the relative volume of caudate nucleus is almost significant ( $p = 0.061$ ). The portion of TIV

occupied by WM lesions does not correlate with ADAS-cog scores in this group ( $r = 0.03$ ;  $p = 0.38$ ). WM lesions are a typical sign of brain aging. They result from chronic small vessel disease and can be seen well as foci or areas hypointensive on T1-weighted images and hyperintensive on T2-weighted images including FLAIR. There are different patterns of the emergence of the WM lesions in MCI and AD groups.

Table 3.9: Demographics, cognitive performance and volumes of brain parts in studied groups

	Total N= 1302	CN 287(22.04%)	MCI 646(49.62%)	Dementia 369(28.34%)	p-value
Age	75.74[71.7-80.7]	76.62 $\pm$ 5.62	75.25 $\pm$ 7.16	75.93 $\pm$ 7.37	0.0933785
Gender					4.19707e-06
Female	522(40.09%)	134(46.69%)	215(33.28%)	173(46.88%)	
Male	780(59.91%)	153(53.31%)	431(66.72%)	196(53.12%)	
Education, years	15.58[13.0-18.0]	16.13 $\pm$ 2.91	15.76 $\pm$ 2.99	14.85 $\pm$ 3.21*	9.08991e-08
Ethnicity					0.198438
White	1210(92.93%)	261(90.94%)	603(93.34%)	346(93.77%)	
Black	60(4.61%)	21(7.32%)	22(3.41%)	17(4.61%)	
Asian	30(2.3%)	5(1.74%)	19(2.94%)	6(1.63%)	
Indian/Alaskan	1(0.08%)	0(0.0%)	1(0.15%)	0(0.0%)	
More than one	1(0.08%)	0(0.0%)	1(0.15%)	0(0.0%)	
Marital status					4.1773e-08
Married	1035(79.49%)	196(68.29%)	532(82.35%)	307(83.2%)	
Never married	31(2.38%)	13(4.53%)	6(0.93%)	12(3.25%)	
Divorced	79(6.07%)	21(7.32%)	42(6.5%)	16(4.34%)	
Widowed	154(11.83%)	54(18.82%)	66(10.22%)	34(9.21%)	
Unknown	3(0.23%)	3(1.05%)	0(0.0%)	0(0.0%)	
Cognitive tests					
ADAS-cog	19.87[11.67-26.33]	8.73 $\pm$ 4.14	18.82 $\pm$ 6.6	30.37 $\pm$ 8.97	2.2404e-165
MMSE	26.18[24.0-29.0]	29.06 $\pm$ 1.09	26.91 $\pm$ 2.2	22.66 $\pm$ 3.03	2.1560e-155
RAVLT	30.44[23.0-37.0]	43.2 $\pm$ 9.76	29.79 $\pm$ 8.86	21.67 $\pm$ 7.77	3.7071e-120
DSST	36.24[27.0-45.0]	46.77 $\pm$ 11.06	37.37 $\pm$ 11.1	26.05 $\pm$ 12.41	2.72808e-83
TMT(part B)	138.13[75.0-187.0]	85.03 $\pm$ 43.18	128.48 $\pm$ 72.56	200.96 $\pm$ 88.57	2.20487e-73
Morphometry					
Ventricles	2.93[1.82-3.67]	2.52 $\pm$ 3.73	2.86 $\pm$ 1.35	3.37 $\pm$ 1.46	1.13635e-23
Hippocampus	0.41[0.35-0.46]	0.47 $\pm$ 0.06	0.4 $\pm$ 0.07	0.36 $\pm$ 0.07	1.93988e-65
Putamen	0.53[0.48-0.57]	0.55 $\pm$ 0.06	0.52 $\pm$ 0.06	0.51 $\pm$ 0.08	1.54782e-17
Amygdala	0.15[0.13-0.17]	0.18 $\pm$ 0.02	0.15 $\pm$ 0.03	0.14 $\pm$ 0.03	8.82095e-64
WM lesions	0.41[0.17-0.47]	0.32 $\pm$ 0.31	0.38 $\pm$ 0.38	0.54 $\pm$ 0.5	2.23640e-17
Entorhinal cortex	0.21[0.17-0.25]	0.25 $\pm$ 0.04	0.21 $\pm$ 0.05	0.18 $\pm$ 0.05	2.14294e-58
Fusiform gyrus	1.03[0.93-1.13]	1.1 $\pm$ 0.13	1.04 $\pm$ 0.14	0.95 $\pm$ 0.14	2.06811e-30
Middle temporal lobe	1.18[1.06-1.29]	1.28 $\pm$ 0.13	1.18 $\pm$ 0.16	1.07 $\pm$ 0.15	8.55332e-48
Whole brain	63.19[60.16-65.83]	65.51 $\pm$ 4.54	63.29 $\pm$ 3.92	61.21 $\pm$ 3.89	1.84928e-36

P-value is marked in bold if difference among groups is statistically significant ( $p < 0.05$ ).  
Structural features are reported in % to TIV. Statistical data are expressed as *IQR*, *Mean*  $\pm$  *SD*, or the absolute number of cases and their percentage in studied cohort.

The functional data in ADNI1 are obtained with cognitive tests such as MMSE, ADAS-cog ( $ADAS_{Q4}$ ,  $ADAS_{11}$ ,  $ADAS_{13}$ ), DSST, TMT (part B), and RAVLT ( $RAVLT_{immediate}$ ,  $RAVLT_{learning}$ ,  $RAVLT_{forgetting}$ ) [178]. The association between the major marker of brain atrophy - CSF% - and performance in ADAS-cog tests is stronger for  $ADAS_{13}$  ( $r = 0.18$ ;  $p < 0.05$ ) than for  $ADAS_{Q4}$  ( $r = 0.15$ ;  $p < 0.05$ ) and  $ADAS_{11}$  ( $r = 0.15$ ;  $p < 0.05$ ). This goes in line with a research which evidenced a more pronounced annual decline in  $ADAS_{13}$  than in  $ADAS_{11}$  in AD patients [311]. Similarly, the association of CSF% score with  $RAVLT_{immediate}$  is stronger than with  $RAVLT_{learning}$  and  $RAVLT_{forgetting}$  scores ( $r = -0.19$  vs  $-0.10$  and  $0.12$ ;  $p < 0.05$ ). Other authors also showed that the accuracy of the model predicting RAVLT scores from GM density is higher for  $RAVLT_{immediate}$  score than for  $RAVLT_{forgetting}$  [312]. Therefore, we used  $ADAS_{13}$  and  $RAVLT_{immediate}$  in this study. Figure 3.32 shows the associations of the test results with age and structural data.

SFA: ADAS-cog and MMSE are primary cognitive tests required in all recent Food and Drug Administration clinical drug trials for AD in the USA [313]. From our data, the results in ADAS-cog and RAVLT have the strongest association with the structural markers of brain atrophy in the CN group. For instance, the coefficient of correlation between hippocampal volume and  $ADAS_{13}$  score is  $-0.18$  in the CN cohort,  $-0.34$  in patients with MCI, and  $-0.20$  in the AD group. The same coefficient in  $RAVLT_{immediate}$  is  $0.13$ ,  $0.24$ , and  $0.18$  in the correspondent cohorts (see Figure 3.32).

In our study the structural markers of brain aging demonstrate a stronger correlation with the results in ADAS-cog than in the other tests. Other authors also justified the informative value of ADAS-cog by

predicting its score with a regression model from morphometric features [314, 137]. We found an obvious correlation of the MMSE score with the hippocampal volume ( $r = 0.44; p = 7.25e - 86$ ). This goes in line with another study that showed their close association ( $r = 0.51; p < 0.001$ ) [165].

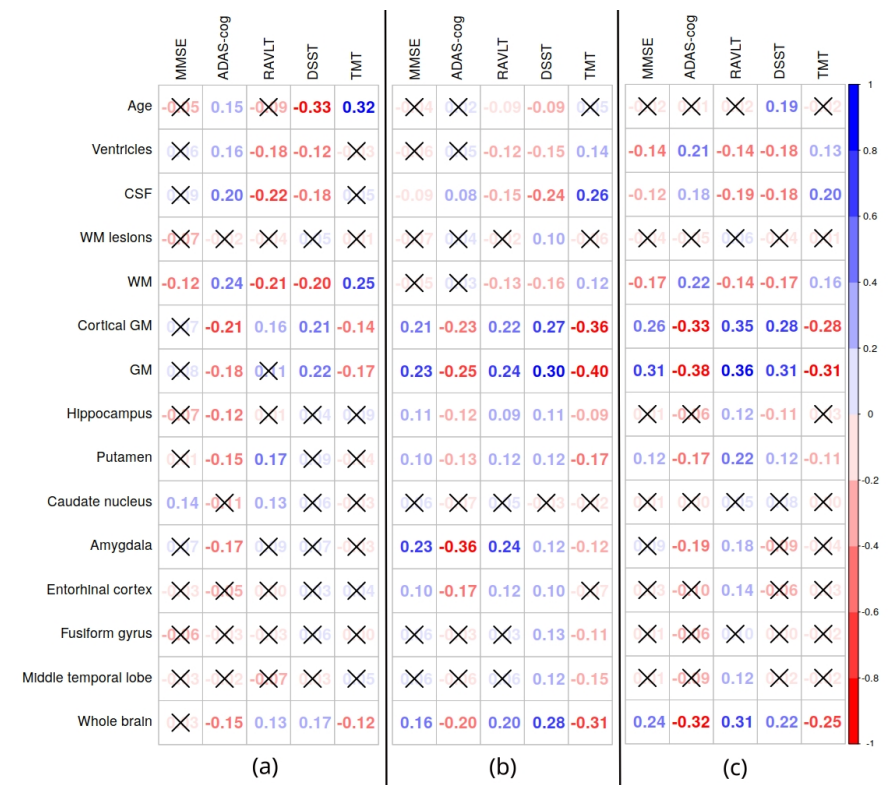


Figure 3.32: Associations of results in cognitive tests with age, functional and structural features in healthy cohort (a), patients with MCI (b) and AD (c). Association is reported in terms of Pearson's correlation coefficient. Cross-mark overlays non-significant relationships between features ( $p > 0.05$ ).

The results we received suggest the presence of different SFA in healthy aging and ND. For instance, the proportion of WM lesions to TIV does not show a linear association with ADAS-cog score in subjects

diagnosed with MCI. In contrast to this, the relationship is strong in AD patients ( $r = 0.22$ ;  $p = 2.61e - 05$ ). Other authors showed that WM lesions enlarged with age and with the development of dementia [315, 146]. It remains unclear why the emergence of WM lesions has a common pattern in the CN adults and patients with AD.

We reported a prominent relationship between cognitive functioning and the volumes of the hippocampus, amygdala, entorhinal cortex, and middle temporal lobe. Other studies also justified the importance of the hippocampal area, amygdala and the middle temporal lobe for intellectual activities [316, 317, 318, 319, 320, 321, 322, 323, 324].

#### *3.4.2 Proposed Marker of Disease-Related Cognitive Decline*

When applied to distinct cognitive test scores, the proposed 3D CNN model shows the best prediction performance in the CN cohort. The worst performance is monitored in the AD group. Data-blending does not boost the performance considerably, i.e., there is no evident advantage in using several image reconstructions. In contrast to this, the model-blending approach shows the top accuracy. It allows us to retrieve maximum data for assessing SFA (see Figure 3.33). The variability of the results in the studied cohorts is most apparent in ADAS-cog and MMSE tests and less evident in RAVLT, DSST, and TMT. The distribution of MAE differs significantly among the cohorts (see Table 3.10). This justifies that cognitively-normal people and patients with NDs have different SFA patterns, which can aid to diagnostics of MCI and AD.

Some authors found marked correlations between the predicted and actual scores in MMSE ( $r = 0.44$ ;  $p < 0.0001$ ) and ADAS-cog tests

( $r = 0.57; p < 0.0001$ ) [136, 137]. We also observed a significant linear association between the predicted and actual values in the combined group of the CN subjects, MCI, and AD patients (MMSE  $r = 0.09, p = 2.28e - 4$ ; ADAS  $r = 0.05, p = 2.87e - 2$ ; RAVLT  $r = 0.11, p = 2.24e - 05$ ; TMT  $r = 0.22, p = 2.34e - 18$ ). We recorded conflicting findings (a non-correlation) in the CN group due to distinct study design. Stonington et. al [136] trained the model on three cohorts (CN, MCI, and AD), while we fed the predictive model exceptionally with the CN cases. Other researchers managed to predict MMSE results from fMRI data accurately [135].

Table 3.10: Mean absolute error of voting regression ensemble model trained on structural brain images averaged along axial, coronal and sagittal axes

	CN group		MCI group		AD group		p-value
	Mean $\pm$ SD	95%CI	Mean $\pm$ SD	95%CI	Mean $\pm$ SD	95%CI	
MMSE	0.84 $\pm$ 0.73	[0.75 - 0.92]	2.38 $\pm$ 2.08	[2.23 - 2.54]	6.46 $\pm$ 3.04	[6.15 - 6.77]	4.8422e-142
ADAS-cog	3.44 $\pm$ 2.42	[3.16 - 3.72]	10.29 $\pm$ 6.15	[9.82 - 10.77]	21.56 $\pm$ 8.94	[20.64 - 22.47]	4.3343e-150
RAVLT	7.94 $\pm$ 5.86	[7.26 - 8.62]	14.63 $\pm$ 7.21	[14.07 - 15.18]	21.78 $\pm$ 7.84	[20.98 - 22.58]	1.08195e-91
TMT(part B)	29.67 $\pm$ 31.42	[26.03 - 33.31]	55.74 $\pm$ 62.73	[50.9 - 60.58]	120.08 $\pm$ 79.28	[111.98 - 128.18]	8.91918e-53
DSST	8.67 $\pm$ 7.0	[7.86 - 9.48]	11.93 $\pm$ 8.51	[11.27 - 12.58]	21.26 $\pm$ 11.73	[20.06 - 22.45]	3.51058e-54

Table 3.11: Performance of models trained on cognitively preserved population and tested on three different cohorts (MAE)

Data	Method	MMSE			ADAS-cog			RAVLT			TMT(part B)			DSST		
		CN	MCI	AD	CN	MCI	AD	CN	MCI	AD	CN	MCI	AD	CN	MCI	AD
Axial(A)	CNN	1.12	2.54	6.54	5.74	10.54	21.95	8.74	14.41	21.4	44.39	109.44	183.62	9.5	12.39	20.8
Coronal (C)	CNN	1.09	2.5	6.08	3.69	12.51	24.19	8.4	12.84	19.42	47.09	114.97	189.33	9.06	11.34	18.3
Sagittal (S)	CNN	1.17	2.46	6.37	3.56	10.89	22.15	9.9	14.31	21.18	47.6	58.08	123.65	9.51	11.84	20.24
3D	3DCNN	0.95	2.25	4.09	3.52	10.96	22.33	7.24	11.25	17.4	25.06	65.14	136.02	8.21	9.56	16.65
VR(C+S)	ensemble	1.13	2.48	6.23	3.63	11.7	23.17	9.15	13.58	20.3	47.34	86.52	156.49	9.28	11.59	19.27
VR(A+C)	ensemble	1.11	2.52	6.31	4.72	11.53	23.07	8.57	13.63	20.41	45.74	112.21	186.47	9.28	11.86	19.55
VR(A+S)	ensemble	1.15	2.5	6.45	4.65	10.72	22.05	9.32	14.36	21.29	46.0	83.76	153.64	9.51	12.11	20.52
VR(A+C+S)	ensemble	1.13	2.5	6.33	4.33	11.32	22.76	9.02	13.85	20.67	46.36	94.16	165.54	9.36	11.85	19.78
MB(A+C+S)	CNN+LR	0.84	2.38	6.46	3.44	10.29	21.56	7.94	14.63	21.78	29.67	55.74	120.08	8.67	11.93	21.26

A, S and C correspond to skull stripped images averaged along appropriate axis; VR - Voting Regression meta-estimator; MB - Model Blending; LR - Linear Regression; RR - Ridge Regression.

The calculation of cognitive scores is more precise from the radiomics data than from the images (see Table 3.11). The first reason for

this is the noise of the 2D images averaged along axes. The second reason is the relatively low number of cases used for training the deep learning model. The high-dimensional computational model needs a larger number of training samples because of the dimensionally cursed phenomena [325].

The idea of using the deviation between the model and actual values is not new for diagnostics. There is a large body of evidence that the difference between the computed and actual age - biological age gap - is a reliable marker of dementia [326, 327, 328]. A study suggested an association between the gap and cognitive performance. It also reported that BAG is related to worsening in performance on the DSST and TMT tests [329]. We applied the same idea to prediction of cognitive performance.

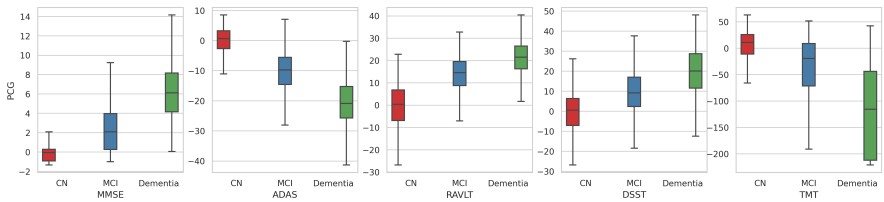


Figure 3.33: Distribution of deviation from model of normal aging among study cohorts

### 3.4.3 Justification of DMNA as Marker of Dementia

Diagnosing from DMNA values is most accurate with Random Forest classifier jointly trained on DMNA MMSE and DMNA ADAS-cog (see Table 3.10, Figures 3.34 and 3.35). The performance of the CN-versus-AD classification model ( $AUC = 1.0$ ) is comparable to the accuracy of state-of-the-art models trained on ADNI dataset (see Table 3.12). From the table, DMNA can accurately distinguish CN subjects from MCI patients ( $AUC = 0.9957$ ). We also achieved creditable



performance in the MCI-versus-AD classification ( $AUC = 0.9793$ ). Therefore, DMNA can be potentially used as a marker of dementia and can help to identify the disease.

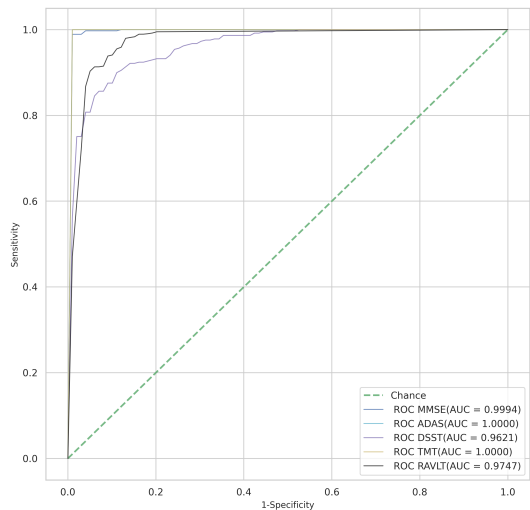


Figure 3.34: Performance of Random Forest model classifying cases into healthy and AD groups. DMNA values are input to the model

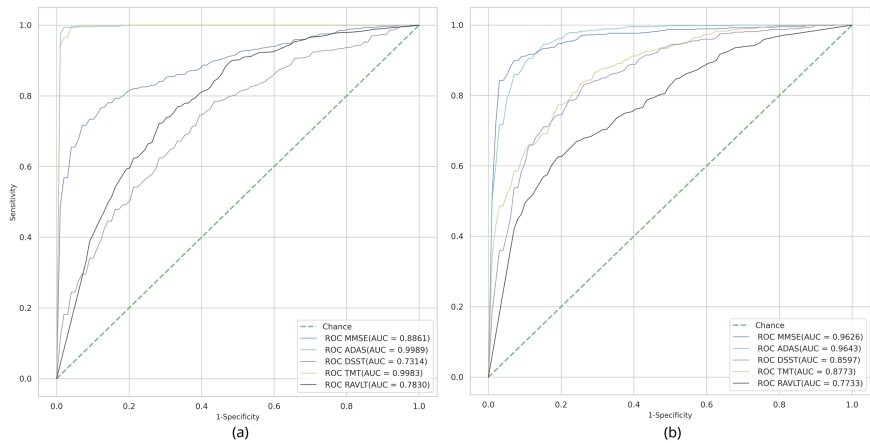


Figure 3.35: Performance of Random Forest model classifying cases into CN and MCI cohorts (a); patients with MCI and AD (b). DMNA values are input to model

Table 3.12: Classification model performance reported in recent studies

Reference, Year	Dataset (CN+MCI+AD)	CN vs AD					MCI vs AD					CN vs MCI				
		Sens	Spec	BAC	AUC	Acc	Sens	Spec	BAC	AUC	Acc	Sens	Spec	BAC	AUC	Acc
Gupta [151], 2013	232+411+200	0.9524	0.9426	0.9475	-	0.9474	0.8407	0.9211	0.8809	-	0.881	0.9223	0.8145	0.8684	-	0.8635
Payan [152], 2015	755+755+755	-	-	-	-	0.9547	-	-	-	-	0.8684	-	-	-	-	0.9211
Ahmed [149], 2015	251+299+347	0.804	0.882	0.843	-	0.8377	0.4902	0.7515	0.62085	-	0.6208	0.6252	0.748	0.6866	-	0.6945
Khedher [150], 2015	229+401+188	0.9127	0.8511	0.8819	-	0.8849	0.8865	0.8541	0.8703	-	0.8703	0.8216	0.8162	0.8189	-	0.8189
Suk [170], 2016	52+99+51	0.92	0.98	0.95	-	0.9509	0.505	0.9267	0.7159	-	0.7415	0.9389	0.5367	0.7378	-	0.8011
Korolev [157], 2017	61+120+50	-	-	-	0.8	0.89	-	-	-	0.66	0.64	-	-	-	0.67	0.63
Cui [156], 2018	223+396+192	0.9063	0.9372	0.92175	0.9695	0.9229	-	-	-	-	-	0.7727	0.6996	0.73615	0.777	0.7464
Billones [160], 2017	300+300+300	0.9889	0.9778	0.9834	-	0.9833	0.9	0.9778	0.9389	-	0.9389	0.9111	0.9222	0.9167	-	0.9167
Altaf [148], 2018	90+105+92	1.0	0.9565	0.97825	-	0.978	0.75	0.9429	0.84645	-	0.853	0.9	0.9333	0.9167	-	0.918
Lee [153], 2019	229+398+192	0.9632	0.9778	0.9705	-	0.9874	-	-	-	-	-	-	-	-	-	-
Basiaa [158], 2019	352+763+294	0.989	0.995	0.992	-	0.992	0.836	0.883	0.8595	-	0.859	0.873	0.865	0.869	-	0.871
Fang [174], 2019	101+204+93	0.9826	0.983	0.9828	-	0.9858	0.8922	0.9067	0.89945	-	0.8998	0.8633	0.9188	0.89105	-	0.8893
Liu [155], 2020	119+233+97	0.866	0.908	0.887	0.925	0.889	-	-	-	-	-	0.795	0.698	0.7465	0.775	0.762
Wang [159], 2020	315+297+221	0.987	-	-	-	0.9883	0.9245	-	-	-	0.9361	0.9834	-	-	-	0.9842
Proposed	287+646+369	1.0	1.0	1.0	1.0	1.0	0.8969	0.9428	0.9199	0.9793	0.9261	0.9756	0.9876	0.9816	0.9957	0.9839

To use the proposed approach in clinics we assessed the possible threshold values of DMNA markers. We undertake sequential values of DMNA and calculated the accuracy of binary classification tasks (CN vs MCI, MCI vs AD). Table 3.13 lists the thresholds of DMNA markers in the binary classification models. The optimal performance is noted on ADAS-cog scores. It allowed us to distinguish normal aging from MCI and the latter from AD with a high-level accuracy (above 90%).

Table 3.13: Threshold values of the DMNA markers in binary classification

Cognitive test	CN vs MCI		MCI vs AD	
	Threshold	Accuracy	Threshold	Accuracy
MMSE	1.0298	0.7889	4.2011	0.9153
ADAS-cog	5.0856	0.9068	18.1063	0.9172
RAVLT	6.2389	0.7921	18.1036	0.7862
TMT(part B)	37.8308	0.8435	146.1889	0.8079
DSST	1.8726	0.7085	15.747	0.802

\*Threshold values are expressed as absolute values of DMNA

Many papers reported a high accuracy of the models that classify healthy and demented subjects [148, 149, 151, 152, 155, 156, 158, 159]. All the deep learning models were trained on pre-processed MRI images of the cognitively preserved and those with cognitive deterioration. In contrast to

the studies, we trained the model exclusively on CN people.

From our data, the predictive power of an SFA model depends on the complexity of the cognitive test used for its training. The accuracy is higher for the tests covering several cognitive domains (MMSE, ADAS, TMT vs information processing in DSST, memory in RAVLT). This supports the results of a study by Stonnington et al. [136]. We report that the model classifying MCI and AD patients has the lowest accuracy (Acc = 0.9261). Recently different authors received the same results [148, 151, 170, 174].

A limitation of the current research is that we did not study convertible and non-convertible to AD MCI cases separately, although some researchers suggest this [158]. Advances in DL technology allowed neuroscientists to improve the classification accuracy of CN-versus-MCI and MCI-versus-AD models [159]. However, the models were biased because of the data leakage related to the late split [330]. Thus, substantial work is required to use such algorithms as a diagnostic tool.

*3.4.4 Prediction of Progressive MCI. Differentiation Between Alzheimer's Disease and Other Neurodegenerative Diseases*

Table 3.14 shows the sensitivity and specificity of the conventional model that classifies MCI cases into stable and progressive ones. As seen from the table, there is no considerable difference in DMNA values between the groups ( $p=0.16\div0.21$ ). Though the balanced accuracy of binary classification is above 80%, low specificity can be considered as a strong limitation of the models. We also identified the difference in DMNA between demented individuals with A+ and A- subjects (see Table 3.15). Only in the MMSE test the distinction in DMNA is considerable

( $6.27 \pm 1.82$  vs  $5.32 \pm 1.9$ ;  $p < 0.05$ ). At the same time, there is no difference between A+ and A– patients with MCI ( $p = 0.75 - 0.98$ ).

Table 3.14: Performance of binary classification model to distinguish between stable and progressive MCI

		DMNA			stable vs progressive MCI				
		stable MCI ( <i>N</i> = 114)	progressive MCI ( <i>N</i> = 518)	<i>p</i>	Sens	Spec	BAC	AUC	Acc
MMSE	2.19[1.15-2.94]	2.21 ± 1.41	2.09 ± 1.3	0.21	0.95	0.71	0.83	0.8547	0.82
ADAS	11.1[8.32-13.63]	11.16 ± 4.02	10.82 ± 3.79	0.16	0.96	0.75	0.855	0.8605	0.85
MMSE + ADAS					0.96	0.67	0.815	0.9475	0.81

Table 3.15: Absolute values of DMNA according to A/T/N classification system

Test		A-T-N-	A-T-N+	A-T+N-	A-T+N+	A+T-N-	A+T-N+	A+T+N-	A+T+N+	p-value
MCI	MMSE ADAS	MCI due to other pathology ( <i>N</i> = 95) 2.29 ± 1.41 11.22 ± 3.85				MCI due to accumulation of $\beta$ amyloid ( <i>N</i> = 26) 2.23 ± 1.12 11.47 ± 3.45				0.98 0.75
Dementia	MMSE ADAS	Non-Alzheimer's disease dementia ( <i>N</i> = 43) 6.27 ± 1.82 23.87 ± 5.42				Dementia due to Alzheimer's disease ( <i>N</i> = 17) 5.32 ± 1.9 21.17 ± 4.81				$p < 0.05$ 0.1

From our data, DMNA cannot be recommended as a tool for predicting the conversion of MCI to dementia because of its low specificity (up to 75%). Other existing CSF markers of progressive MCI also do not ensure the necessary level of prediction: mean diffusivity (average accuracy of 77%),  $\tau$ -protein concentration (74%), volumetry data retrieved from the brain MRI (66%) [331]. There is a considerable difference in DMNA between demented individuals with Alzheimer's continuum (A+) and those with either normal AD biomarkers or non-AD pathologic change (A–). Hence, the proposed marker can be potentially used for distinguishing between dementia due to AD and non-AD. To find and justify a reliable threshold level, further research is required. We failed to identify a strong distinction between MCI due to the accumulation of  $\beta$ -amyloid and because of other pathologies ( $p > 0.05$ ). From our data, the biomarker is not

applicable for discriminating MCI cases by underlying pathology (AD vs non-AD).

Strengths and limitations of DMNA: There is no agreement between researchers on which non-invasive diagnostic modality is more promising for screening purposes. The strength of our study is that we chose to focus on multimodal diagnostics to benefit from both types of data. A limitation of the current research is that we did not study convertible and non-convertible to AD MCI cases separately, although some researchers suggest this [158]. DMNA as a prognostic criterium of progressive MCI has strong limitation. Both the proposed and the existing markers of progressive MCI do not ensure the necessary level of prediction.

## Chapter 4: Conclusion

1.a. We propose estimates of disproportional changes in cognitive functions to extend the applicability of ML classification in cognitive studies (ISD, ISDA, and ISCA). The distribution of the indices and RMO test values over time shows that different cognitive functions degrade at the same rate throughout life. The RT variable of the battery of PTs we utilized was less stable than the major dependent variable of the ISD, ISDA, and ISCA values throughout lifespan. The indicators preserve fairly constant values after neurodevelopment and maturation, with a modest trend toward functional deterioration. Further research is required to determine the ratios' value in distinguishing between normal and accelerated brain aging.

1.b. The optimal number of homogenous age groups, according to unsupervised ML clustering, is four. Starting at birth, we divided the research participants into 20-year age groups: Adolescents aged below 20, Young adults aged 20 to 40, Midlife adults aged 40 to 60, and Older adults aged above 60.

1.c. The ISCA index for PT reflects the overall status of an examinee. We forecasted ISCA values from the results of PTs with high performance metrics (MAE to range of index values is  $3.49 \pm 0.14\%$  vs  $7.57 \pm 0.55\%$  for ISDA and  $7.62 \pm 0.5\%$  for ISD;  $p < 0.05$ ). Proportional age-related developments can be observed in temporal estimates of information processing speed and inhibitory control in task switching in normal brain aging.

2.a. WM changes almost linearly throughout life, as does the percentage of WMHs to total WM. Total GM and its cortical part exhibit

varied age-related alteration patterns. The linear slowdown in decision-making across the lifespan could be explained by a widening of the interhemispheric fissure. Response inhibition is largely controlled by the premotor areas of the frontal lobe's medial wall. The expansion of the interhemispheric fissure is due to the atrophy of these brain regions.

2.b. Following the presentation of WM brain volume as a second-degree function of age, the effects can be seen as a U-shaped or inverted parabola curve. The inverted parabola indicates that the WM bundles are changing. The U-shaped line represents GM volume variation and the structures that penetrate into patches of neuronal cells. It is not possible to interpret a climb in the second-order curve as irreversible GM atrophy in advanced age. As a result, the third-order function of age matches the data better than the second-order function in terms of GM nuclei volume.

2.c. There is a strong association of total CSF volume (*CSF%*) and RT in the IRT (*IRT\_mean*), which is the most cognitively demanding activity in our battery ( $r = 0.36, p < 0.05$ ). It represents the best link between brain anatomical data and functional outcomes. Switching and inhibitory control, information processing, and attention are among the cognitive domains and subdomains tested in this study. The relative volumes of the CSF and GM are strongly positively correlated with decision-making time, which represents switching and inhibitory control. The accuracy of the PTs we utilized is supported by these findings.

3.a. In the healthy population, global cognitive functioning changes slightly with age. It also remains stable across the disease course. Though there are patients with reversible or progressive MCI, the real number of

such cases is quite low. RAVLT scores test are quite stable throughout life in normal aging and across the disease course with a slight trend towards lowering in all the study groups. The pace of neurocognitive slowing was moderately higher in the CN group and MCI patients. Thus, the average result for all the groups would reach a common value if the observation lasted several more decades. There are clear signs of malfunctioning in several cognitive domains assessed with DSST and TMT and the performance worsens within time. For this reason, the trendlines of test performance among the CN, MCI, and AD groups converge at the approximated point of 100 years of age.

3.b. We constructed regression models predicting functional performance in cognitive tests from brain radiomics. The vulnerability of distinct neuronal cells to atrophy in accelerated aging differs among distinct cell groups and brain regions. Logically, the SFA has features specific to the pathology. The feature selection technique allows us to identify the most informative structural neuroimaging measures. The models reflect SFA patterns unique for each study cohort. We analyzed the SFA patterns in the demented patients of ADNI dataset. As AD accounts for the majority of dementia cases, we pointed out the structures vulnerable for change in  $\beta$ -amyloidopathy. Other NDs selectively damage certain neuronal cells and brain regions, which results in another SFA pattern.

3.c. We classified examinees with the majority voting technique. According to the pattern of SFA association we distinguished three cohorts: the cognitively normal elderly, patients with MCI and dementia patients. The highest accuracy was achieved with the model trained to predict MMSE from voxel-based morphometry data. In the cognitively normal



cohort, the model identified 85.06% of individuals as healthy subjects, and a relatively small portion (14.94%) is misclassified as patients with MCI. The true prediction rate reached 81.30% in the MCI group. The major limitation of the constructed classification system was the least accurate classification of the demented patients (73% accuracy). The classification based on the model trained to predict ADAS13 from VBM detected demented patients more accurately than the other considered models (78.38% true prediction rate).

4.a. There is a strong association between the brain structure of a subject and their performance in cognitive tests. However, the patterns of the SFA differ among cognitively preserved people, patients with MCI and dementia patients. For instance, the coefficient of correlation between the hippocampal volume and  $ADAS_{13}$  score is  $-0.18$  in the CN cohort,  $-0.34$  in patients with MCI, and  $-0.20$  in the AD group. The same coefficient in  $RAVLT_{immediate}$  is 0.13, 0.24, and 0.18 in the correspondent cohorts.

4.b. To work out a new marker of neurodegeneration, we predict the cognitive status of the cognitively preserved examinees from the brain MRI data. This is an SFA model of normal aging. A big deviation from the model of normal aging suggests a high risk of accelerated cognitive decline, i.e., a high level of the error of cognitive score prediction should rise awareness of a ND.

4.c. The results in the tests reflecting global cognitive functioning - ADAS-cog and RAVLT - had the strongest association with the structural markers of brain atrophy. In line with this, the variability of the deviation from the model of normal aging in the cognitively preserved subjects, and patients with MCI and dementia was most apparent in the ADAS-cog and

MMSE tests and less evident in the tests covering several cognitive subdomains, namely RAVLT, DSST, and TMT. Diagnosing dementia from DMNA values is most accurate with a Random Forest classifier jointly trained on DMNA MMSE and DMNA ADAS-cog. DMNA can accurately distinguish CN subjects from MCI patients ( $AUC = 0.9957$ ). We also achieved a creditable performance in the MCI-versus-AD classification ( $AUC = 0.9793$ ). Therefore, DMNA has potential for use as a marker of dementia and can help to identify the disease.

4.d. There is no marked difference in DMNA values between stable and progressive MCI cases. DMNA as a prognostic criterium of progressive MCI has strong limitations. Both the proposed and the existing markers of progressive MCI do not ensure the necessary level of prediction. The proposed marker has potential for use in differentiating dementia due to AD from that not due to AD. We identified a considerable difference in DMNA in the MMSE test between demented individuals with (A+) and (A-) according to the ATN-classification ( $6.27 \pm 1.82$  vs  $5.32 \pm 1.9$ ;  $p < 0.05$ ). To find and justify a reliable threshold level, further research is required.

## References

- [1] P. Y. Takahashi, A. Chandra, S. Cha, and A. Borrud, "The relationship between elder risk assessment index score and 30-day readmission from the nursing home," *Hospital Practice*, vol. 39, no. 1, pp. 91–96, 2011.
- [2] J. M. Naessens, R. J. Stroebel, D. M. Finnie, N. D. Shah, A. E. Wagie, W. J. Litchy, P. Killinger, T. O'Byrne, D. L. Wood, and R. E. Nesse, "Effect of multiple chronic conditions among working-age adults." *The American Journal of Managed Care*, vol. 17, no. 2, pp. 118–122, 2011.
- [3] I. O. Korolev, L. L. Symonds, A. C. Bozoki, and A. D. N. Initiative, "Predicting progression from mild cognitive impairment to alzheimer's dementia using clinical, mri, and plasma biomarkers via probabilistic pattern classification," *PloS One*, vol. 11, no. 2, p. e0138866, 2016. doi: 10.1371/journal.pone.0138866
- [4] R. Casanova, F.-C. Hsu, K. M. Sink, S. R. Rapp, J. D. Williamson, S. M. Resnick, M. A. Espeland, A. D. N. Initiative *et al.*, "Alzheimer's disease risk assessment using large-scale machine learning methods," *PloS One*, vol. 8, no. 11, p. e77949, 2013. doi: 10.1371/journal.pone.0077949
- [5] C. Davatzikos, F. Xu, Y. An, Y. Fan, and S. M. Resnick, "Longitudinal progression of alzheimer's-like patterns of atrophy in normal older adults: the spare-ad index," *Brain*, vol. 132, no. 8, pp. 2026–2035, 2009.
- [6] G. . D. F. Collaborators *et al.*, "Estimation of the global prevalence of dementia in 2019 and forecasted prevalence in 2050: an analysis for the global burden of disease study 2019," *The Lancet Public Health*, vol. 7, pp. 105–25, 2022.
- [7] "Uae life expectancy 1950-2021," <https://www.macrotrends.net/countries/ARE/uae/life-expectancy>, [Accessed: 2021-03-29].
- [8] T. Habuza, A. N. Navaz, F. Hashim, F. Alnajjar, N. Zaki, M. A. Serhani, and Y. Statsenko, "Ai applications in robotics, precision medicine, and medical image analysis: an overview and future trends," *Informatics in Medicine Unlocked*, no. 24, p. 100596, 2021. doi: 10.1016/j.imu.2021.100596
- [9] A. Milne, "Dementia screening and early diagnosis: The case for and against," *Health, Risk & Society*, vol. 12, no. 1, pp. 65–76, 2010.
- [10] P. K. Panegyres, R. Berry, and J. Burchell, "Early dementia screening," *Diagnostics*, vol. 6, no. 1, p. 6, 2016. doi: 10.3390/diagnostics6010006

- [11] P. Verhaeghen, “Working memory and cognitive aging,” in *Oxford Research Encyclopedia of Psychology*. Oxford University Press, 2018.
- [12] W. J. Chai, A. I. Abd Hamid, and J. M. Abdullah, “Working memory from the psychological and neurosciences perspectives: a review,” *Frontiers in Psychology*, vol. 9, p. 401, 2018. doi: 10.3389/fpsyg.2018.00401
- [13] M. K. Nyongesa, D. Ssewanyana, A. M. Mutua, E. Chongwo, G. Scerif, C. R. Newton, and A. Abubakar, “Assessing executive function in adolescence: A scoping review of existing measures and their psychometric robustness,” *Frontiers in Psychology*, vol. 10, p. 311, 2019. doi: 10.3389/fpsyg.2019.00311
- [14] C. Rosado-Artalejo, J. Carnicero, J. Losa-Reyna, C. Castillo, B. Cobos-Antoranz, A. Alfaro-Acha, L. Rodríguez-Mañas, and F. J. García-García, “Global performance of executive function is predictor of risk of frailty and disability in older adults,” *The Journal of Nutrition, Health & Aging*, vol. 21, no. 9, pp. 980–987, 2017.
- [15] J. E. Peelle, *The Oxford Handbook of Neurolinguistics*. Oxford University Press Oxford, UK, 2019, pp. 295–216.
- [16] M. Antoniou and S. M. Wright, “Uncovering the mechanisms responsible for why language learning may promote healthy cognitive aging,” *Frontiers in Psychology*, vol. 8, p. 2217, 2017. doi: 10.3389/fpsyg.2017.02217
- [17] J. D. Medaglia, F. Pasqualetti, R. H. Hamilton, S. L. Thompson-Schill, and D. S. Bassett, “Brain and cognitive reserve: translation via network control theory,” *Neuroscience & Biobehavioral Reviews*, vol. 75, pp. 53–64, 2017.
- [18] A. M. Brickman, K. L. Siedlecki, J. Muraskin, J. J. Manly, J. A. Luchsinger, L.-K. Yeung, T. R. Brown, C. DeCarli, and Y. Stern, “White matter hyperintensities and cognition: testing the reserve hypothesis,” *Neurobiology of Aging*, vol. 32, no. 9, pp. 1588–1598, 2011.
- [19] S. Cullati, M. Kliegel, and E. Widmer, “Development of reserves over the life course and onset of vulnerability in later life,” *Nature Human Behaviour*, vol. 2, no. 8, pp. 551–558, 2018.
- [20] D. H. Lee, P. Lee, S. W. Seo, J. H. Roh, M. Oh, J. S. Oh, S. J. Oh, J. S. Kim, and Y. Jeong, “Neural substrates of cognitive reserve in alzheimer’s disease spectrum and normal aging,” *Neuroimage*, vol. 186, pp. 690–702, 2019.
- [21] A. C. Van Loenhoud, C. Groot, J. W. Vogel, W. M. Van Der Flier, and R. Ossenkoppele, “Is intracranial volume a suitable proxy for brain reserve?” *Alzheimer’s Research & Therapy*, vol. 10, no. 1, pp. 1–12, 2018.

- [22] G. Giovacchini, E. Giovannini, E. Borsò, P. Lazzeri, M. Riondato, R. Leoncini, V. Duce, L. Mansi, and A. Ciarmiello, "The brain cognitive reserve hypothesis: A review with emphasis on the contribution of nuclear medicine neuroimaging techniques," *Journal of Cellular Physiology*, vol. 234, no. 9, pp. 14 865–14 872, 2019.
- [23] C. Groot, A. C. van Loenhoud, F. Barkhof, B. N. van Berckel, T. Koene, C. C. Teunissen, P. Scheltens, W. M. van der Flier, and R. Ossenkoppele, "Differential effects of cognitive reserve and brain reserve on cognition in alzheimer disease," *Neurology*, vol. 90, no. 2, pp. e149–e156, 2018.
- [24] A. Breton, D. Casey, and N. A. Arnaoutoglou, "Cognitive tests for the detection of mild cognitive impairment (mci), the prodromal stage of dementia: Meta-analysis of diagnostic accuracy studies," *International Journal of Geriatric Psychiatry*, vol. 34, no. 2, pp. 233–242, 2019.
- [25] K. K. Tsoi, J. Y. Chan, H. W. Hirai, A. Wong, V. C. Mok, L. C. Lam, T. C. Kwok, and S. Y. Wong, "Recall tests are effective to detect mild cognitive impairment: a systematic review and meta-analysis of 108 diagnostic studies," *Journal of the American Medical Directors Association*, vol. 18, no. 9, pp. 807–e17, 2017.
- [26] F. Nemmi, A. Pavy-Le Traon, O. Phillips, M. Galitzky, W. Meissner, O. Rascol, and P. Péran, "A totally data-driven whole-brain multimodal pipeline for the discrimination of parkinson's disease, multiple system atrophy and healthy control," *NeuroImage: Clinical*, vol. 23, p. 101858, 2019. doi: 10.1016/j.nicl.2019.101858
- [27] R. Z. U. Rehman, S. Del Din, Y. Guan, A. J. Yarnall, J. Q. Shi, and L. Rochester, "Selecting clinically relevant gait characteristics for classification of early parkinson's disease: A comprehensive machine learning approach," *Scientific Reports*, vol. 9, no. 1, pp. 1–12, 2019.
- [28] P. Boyle, L. Yu, R. Wilson, J. Schneider, and D. A. Bennett, "Relation of neuropathology with cognitive decline among older persons without dementia," *Frontiers in Aging Neuroscience*, vol. 5, p. 50, 2013. doi: 10.3389/fnagi.2013.00050
- [29] T. Hedden, A. P. Schultz, A. Rieckmann, E. C. Mormino, K. A. Johnson, R. A. Sperling, and R. L. Buckner, "Multiple brain markers are linked to age-related variation in cognition," *Cerebral Cortex*, vol. 26, no. 4, pp. 1388–1400, 2016.

- [30] D. L. Murman, “The impact of age on cognition,” in *Seminars in Hearing*, vol. 36, no. 3. Thieme Medical Publishers, 2015, pp. 111–121.
- [31] J. Hassenstab, R. Chasse, P. Grabow, T. L. Benzinger, A. M. Fagan, C. Xiong, M. Jasielec, E. Grant, and J. C. Morris, “Certified normal: Alzheimer’s disease biomarkers and normative estimates of cognitive functioning,” *Neurobiology of Aging*, vol. 43, pp. 23–33, 2016.
- [32] Y. Statsenko, T. Habuza, I. Charykova, K. N.-V. Gorkom, N. Zaki, G. Baylis, M. Ljubisavljevic, T. M. Almansoor, and M. Belghali, “Predicting age from behavioral test performance for screening early onset of cognitive decline,” *Frontiers in Aging Neuroscience*, vol. 5, p. 661514, 2021. doi: 10.3389/fnagi.2021.661514
- [33] Y. Statsenko, E. Fursa, V. Laver, N. Altakarli, T. Almansoori, F. Al Zahmi, K. Gorkom, M. Sheek-Hussein, A. Ponomareva, G. Simiyu *et al.*, “Risk stratification and prediction of severity of hemorrhagic stroke in dry desert climate-a retrospective cohort study in eastern region of abu dhabi emirate,” *Journal of the Neurological Sciences*, vol. 429, 2021. doi: 10.1016/j.jns.2021.117760
- [34] R. S. Desikan, H. J. Cabral, F. Settecase, C. P. Hess, W. P. Dillon, C. M. Glastonbury, M. W. Weiner, N. J. Schmansky, D. H. Salat, B. Fischl *et al.*, “Automated mri measures predict progression to alzheimer’s disease,” *Neurobiology of Aging*, vol. 31, no. 8, pp. 1364–1374, 2010.
- [35] F. Gaillard, “Neurodegenerative mri brain (an approach): Radiology reference article,” <https://radiopaedia.org/articles/neurodegenerative-mri-brain-an-approach?lang=us>, 2021, [Accessed: 2021-07-09].
- [36] F. Eitel, E. Soehler, J. Bellmann-Strobl, A. U. Brandt, K. Ruprecht, R. M. Giess, J. Kuchling, S. Asseyer, M. Weygandt, J.-D. Haynes *et al.*, “Uncovering convolutional neural network decisions for diagnosing multiple sclerosis on conventional mri using layer-wise relevance propagation,” *NeuroImage: Clinical*, vol. 24, p. 102003, 2019. doi: 10.1016/j.nicl.2019.102003
- [37] W. S. Jung, Y. H. Um, D. W. Kang, C. U. Lee, Y. S. Woo, W.-M. Bahk, and H. K. Lim, “Diagnostic validity of an automated probabilistic tractography in amnesic mild cognitive impairment,” *Clinical Psychopharmacology and Neuroscience*, vol. 16, no. 2, pp. 144–152, 2018.

- [38] K. Kamagata, H. Tomiyama, Y. Motoi, M. Kano, O. Abe, K. Ito, K. Shimoji, M. Suzuki, M. Hori, A. Nakanishi *et al.*, “Diffusional kurtosis imaging of cingulate fibers in parkinson disease: comparison with conventional diffusion tensor imaging,” *Magnetic Resonance Imaging*, vol. 31, no. 9, pp. 1501–1506, 2013.
- [39] M. L. F. Balthazar, B. M. de Campos, A. R. Franco, B. P. Damasceno, and F. Cendes, “Whole cortical and default mode network mean functional connectivity as potential biomarkers for mild alzheimer’s disease,” *Psychiatry Research: Neuroimaging*, vol. 221, no. 1, pp. 37–42, 2014.
- [40] J. Göttler, C. Preibisch, I. Riederer, L. Pasquini, P. Alexopoulos, K. P. Bohn, I. Yakushev, E. Beller, S. Kaczmarz, C. Zimmer *et al.*, “Reduced blood oxygenation level dependent connectivity is related to hypoperfusion in alzheimer’s disease,” *Journal of Cerebral Blood Flow & Metabolism*, vol. 39, no. 7, pp. 1314–1325, 2019.
- [41] J. P. Kim, J. Kim, Y. H. Park, S. B. Park, J. San Lee, S. Yoo, E.-J. Kim, H. J. Kim, D. L. Na, J. A. Brown *et al.*, “Machine learning based hierarchical classification of frontotemporal dementia and alzheimer’s disease,” *NeuroImage: Clinical*, vol. 23, p. 101811, 2019. doi: 10.1016/j.nicl.2019.101811
- [42] N. Lorking, A. D. Murray, and J. T. O’Brien, “The use of positron emission tomography/magnetic resonance imaging in dementia: A literature review,” *Int J Geriatr Psychiatry*, vol. 36, no. 10, pp. 1501–1513, 2021.
- [43] J. Arbizu, E. Prieto, P. Martínez-Lage, J. Martí-Climent, M. García-Granero, I. Lamet, P. Pastor, M. Riverol, M. Gómez-Isla, I. Peñuelas *et al.*, “Automated analysis of fdg pet as a tool for single-subject probabilistic prediction and detection of alzheimer’s disease dementia,” *European Journal of Nuclear Medicine and Molecular Imaging*, vol. 40, no. 9, pp. 1394–1405, 2013.
- [44] K. Van Laere, A. Vanhee, J. Verschueren, L. De Coster, A. Driesen, P. Dupont, W. Robberecht, and P. Van Damme, “Value of 18fluorodeoxyglucose–positron-emission tomography in amyotrophic lateral sclerosis: a prospective study,” *JAMA Neurology*, vol. 71, no. 5, pp. 553–561, 2014.

- [45] K. Kamagata, T. Nakatsuka, R. Sakakibara, Y. Tsuyusaki, T. Takamura, K. Sato, M. Suzuki, M. Hori, K. K. Kumamaru, and T. Inaoka, “Diagnostic imaging of dementia with lewy bodies by susceptibility-weighted imaging of nigrosomes versus striatal dopamine transporter single-photon emission computed tomography: a retrospective observational study,” *Neuroradiology*, vol. 59, no. 1, pp. 89–98, 2017.
- [46] R. M. Steketee, E. E. Bron, R. Meijboom, G. C. Houston, S. Klein, H. J. Mutsaerts, C. P. M. Orellana, F. J. de Jong, J. C. van Swieten, A. van der Lugt *et al.*, “Early-stage differentiation between presenile alzheimer’s disease and frontotemporal dementia using arterial spin labeling mri,” *European Radiology*, vol. 26, no. 1, pp. 244–253, 2016.
- [47] S. Shimizu, Y. Zhang, J. Laxamana, B. L. Miller, J. H. Kramer, M. W. Weiner, and N. Schuff, “Concordance and discordance between brain perfusion and atrophy in frontotemporal dementia,” *Brain Imaging and Behavior*, vol. 4, no. 1, pp. 46–54, 2010.
- [48] Y. Uchida, S. Minoshima, S. Okada, T. Kawata, and H. Ito, “Diagnosis of dementia using perfusion spect imaging at the patient’s initial visit to a cognitive disorder clinic,” *Clinical Nuclear Medicine*, vol. 31, no. 12, pp. 764–773, 2006.
- [49] D. Roquet, M. Sourty, A. Botzung, J.-P. Armspach, and F. Blanc, “Brain perfusion in dementia with lewy bodies and alzheimer’s disease: an arterial spin labeling mri study on prodromal and mild dementia stages,” *Alzheimer’s Research & Therapy*, vol. 8, no. 1, pp. 1–13, 2016.
- [50] H. Hanyu, S. Shimizu, K. Hirao, H. Kanetaka, H. Sakurai, T. Iwamoto, K. Koizumi, and K. Abe, “Differentiation of dementia with lewy bodies from alzheimer’s disease using mini-mental state examination and brain perfusion spect,” *Journal of the Neurological Sciences*, vol. 250, no. 1-2, pp. 97–102, 2006.
- [51] A. Kertesz, W. Davidson, P. McCabe, and D. Munoz, “Behavioral quantitation is more sensitive than cognitive testing in frontotemporal dementia,” *Alzheimer Disease & Associated Disorders*, vol. 17, no. 4, pp. 223–229, 2003.



- [52] R. J. Spencer, C. R. Wendell, P. P. Giggey, L. I. Katzel, D. M. Lefkowitz, E. L. Siegel, and S. R. Waldstein, "Psychometric limitations of the mini-mental state examination among nondemented older adults: an evaluation of neurocognitive and magnetic resonance imaging correlates," *Experimental Aging Research*, vol. 39, no. 4, pp. 382–397, 2013.
- [53] S. Freitas, M. R. Simoes, L. Alves, M. Vicente, and I. Santana, "Montreal cognitive assessment (moca): validation study for vascular dementia," *Journal of the International Neuropsychological Society*, vol. 18, no. 6, pp. 1031–1040, 2012.
- [54] C. Carnero-Pardo, I. Cruz-Orduña, B. Espejo-Martínez, C. Martos-Aparicio, S. López-Alcalde, and J. Olazarán, "Utility of the mini-cog for detection of cognitive impairment in primary care: data from two spanish studies," *International Journal of Alzheimer's Disease*, vol. 2013, 2013. doi: 10.1155/2013/285462
- [55] J.-C. Tsai, C.-W. Chen, H. Chu, H.-L. Yang, M.-H. Chung, Y.-M. Liao, and K.-R. Chou, "Comparing the sensitivity, specificity, and predictive values of the montreal cognitive assessment and mini-mental state examination when screening people for mild cognitive impairment and dementia in chinese population," *Archives of Psychiatric Nursing*, vol. 30, no. 4, pp. 486–491, 2016.
- [56] A. Spiro III and C. B. Brady, "Integrating health into cognitive aging: Toward a preventive cognitive neuroscience of aging," *Journals of Gerontology Series B: Psychological Sciences and Social Sciences*, vol. 66, no. suppl\_1, pp. i17–i25, 2011.
- [57] A. Kaufman, T. Salthouse, C. Scheiber, and H. Chen, "Age differences and educational attainment across the life span on three generations of wechsler adult scales," *Journal of Psychoeducational Assessment*, vol. 34, no. 5, pp. 421–441, 2016.
- [58] T. Salthouse, "Trajectories of normal cognitive aging," *Psychology and Aging*, vol. 34, no. 1, pp. 17–24, 2019.
- [59] M. Rönnlund, L. Nyberg, L. Bäckman, and L.-G. Nilsson, "Stability, growth, and decline in adult life span development of declarative memory: cross-sectional and longitudinal data from a population-based study," *Psychology and Aging*, vol. 20, no. 1, pp. 3–18, 2005.

- [60] T. Salthouse, "Aging cognition unconfounded by prior test experience." *Journals of Gerontology Series B: Psychological Sciences and Social Sciences*, vol. 71, no. 1, pp. 49–58, 2016.
- [61] R. A. Armstrong, "On the 'classification' of neurodegenerative disorders: discrete entities, overlap or continuum?" *Folia Neuropathologica*, vol. 50, no. 3, pp. 201–218, 2012.
- [62] G. G. Kovacs, "Molecular pathology of neurodegenerative diseases: principles and practice," *Journal of Clinical Pathology*, vol. 72, no. 11, pp. 725–735, 2019.
- [63] Y. Chen, X. Zhao, X. Zhang, Y. Liu, P. Zhou, H. Ni, J. Ma, and D. Ming, "Age-related early/late variations of functional connectivity across the human lifespan," *Neuroradiology*, vol. 60, no. 4, pp. 403–412, 2018.
- [64] R. P. Viviano, N. Raz, P. Yuan, and J. S. Damoiseaux, "Associations between dynamic functional connectivity and age, metabolic risk, and cognitive performance," *Neurobiology of Aging*, vol. 59, pp. 135–143, 2017.
- [65] A. B. Storsve, A. M. Fjell, C. K. Tamnes, L. T. Westlye, K. Overbye, H. W. Aasland, and K. B. Walhovd, "Differential longitudinal changes in cortical thickness, surface area and volume across the adult life span: regions of accelerating and decelerating change," *Journal of Neuroscience*, vol. 34, no. 25, pp. 8488–8498, 2014.
- [66] C. K. Tamnes, K. B. Walhovd, A. M. Dale, Y. Østby, H. Grydeland, G. Richardson, L. T. Westlye, J. C. Roddey, D. J. Hagler Jr, P. Due-Tønnessen *et al.*, "Brain development and aging: overlapping and unique patterns of change," *Neuroimage*, vol. 68, pp. 63–74, 2013.
- [67] T. A. Salthouse, T. M. Atkinson, and D. E. Berish, "Executive functioning as a potential mediator of age-related cognitive decline in normal adults." *Journal of Experimental Psychology: General*, vol. 132, no. 4, pp. 566–594, 2003.
- [68] T. Habuza, N. Zaki, Y. Statsenko, and S. Elyassami, "Mri and cognitive tests-based screening tool for dementia," *Journal of the Neurological Sciences*, vol. 429, p. 118964, 2021. doi: 10.1016/j.jns.2021.118964
- [69] K. Gorkom, Y. Statsenko, T. Habuza, L. Uzianbaeva, M. Belghali, I. Charykova *et al.*, "Comparison of brain volumetric changes with functional outcomes in physiologic brain aging. esnr 2021," *Neuroradiology*, vol. 63, pp. 43–44, 2021.

- [70] Y. Statsenko, T. Habuza, I. Charykova, K. Gorkom, N. Zaki, T. Almansoori, M. Ljubisavljevic, M. Szolics, J. Al Koteesh, A. Ponomareva *et al.*, “Ai models of age-associated changes in cns composition identified by mri,” *Journal of the Neurological Sciences*, vol. 429, p. 118303, 2021. doi: 10.1016/j.jns.2021.118303
- [71] Y. Statsenko, T. Habuza, L. Uzianbaeva, K. Gorkom, M. Belghali, I. Charykova *et al.*, “Correlation between lifelong dynamics of psychophysiological performance and brain morphology. esnr 2021,” *Neuroradiology*, vol. 63, pp. 41–42, 2021.
- [72] L. Uzianbaeva, Y. Statsenko, T. Habuza, K. Gorkom, M. Belghali, I. Charykova *et al.*, “Effects of sex age-related changes in brain morphology. esnr 2021,” *Neuroradiology*, vol. 63, pp. 42–43, 2021.
- [73] S. Adólfssdóttir, D. Wollschlaeger, E. Wehling, and A. J. Lundervold, “Inhibition and switching in healthy aging: a longitudinal study,” *Journal of the International Neuropsychological Society*, vol. 23, no. 1, pp. 90–97, 2017.
- [74] D. Finkel, M. Ernst-Bravell, and N. L. Pedersen, “Temporal dynamics of motor functioning and cognitive aging,” *Journals of Gerontology Series A: Biomedical Sciences and Medical Sciences*, vol. 71, no. 1, pp. 109–116, 2016.
- [75] Z. Hong, K. K. Ng, S. K. Sim, M. Y. Ngeow, H. Zheng, J. C. Lo, M. W. Chee, and J. Zhou, “Differential age-dependent associations of gray matter volume and white matter integrity with processing speed in healthy older adults,” *Neuroimage*, vol. 123, pp. 42–50, 2015.
- [76] H.-W. Wahl, M. Schmitt, D. Danner, and A. Coppin, “Is the emergence of functional ability decline in early old age related to change in speed of cognitive processing and also to change in personality?” *Journal of Aging and Health*, vol. 22, no. 6, pp. 691–712, 2010.
- [77] Y. Statsenko, T. Habuza, K. Neidl-Van Gorkom, N. Zaki, and T. M. Almansoori, “Applying the inverse efficiency score to visual–motor task for studying speed-accuracy performance while aging,” *Frontiers in Aging Neuroscience*, vol. 12, 2020. doi: 10.3389/fnagi.2020.574401
- [78] B. M. Bettcher, C. L. Watson, C. M. Walsh, I. V. Lobach, J. Neuhaus, J. W. Miller, R. Green, N. Patel, S. Dutt, E. Busovaca *et al.*, “Interleukin-6, age, and corpus callosum integrity,” *PloS One*, vol. 9, no. 9, p. e106521, 2014. doi: 10.1371/journal.pone.0106521

- [79] N. T. Bott, B. M. Bettcher, J. S. Yokoyama, D. T. Frazier, M. Wynn, A. Karydas, K. Yaffe, and J. H. Kramer, "Youthful processing speed in older adults: genetic, biological, and behavioral predictors of cognitive processing speed trajectories in aging," *Frontiers in Aging Neuroscience*, vol. 9, p. 55, 2017. doi: 10.3389/fnagi.2017.00055
- [80] G. A. Kerchner, C. A. Racine, S. Hale, R. Wilhelm, V. Laluz, B. L. Miller, and J. H. Kramer, "Cognitive processing speed in older adults: relationship with white matter integrity," *PloS One*, vol. 7, no. 11, p. e50425, 2012. doi: 10.1371/journal.pone.0050425
- [81] A. Salami, J. Eriksson, L.-G. Nilsson, and L. Nyberg, "Age-related white matter microstructural differences partly mediate age-related decline in processing speed but not cognition," *Biochimica et Biophysica Acta (BBA)-Molecular Basis of Disease*, vol. 1822, no. 3, pp. 408–415, 2012.
- [82] S.-T. Cheng, P. K. Chow, Y.-Q. Song, C. Edwin, A. C. Chan, T. M. Lee, and J. H. Lam, "Mental and physical activities delay cognitive decline in older persons with dementia," *The American Journal of Geriatric Psychiatry*, vol. 22, no. 1, pp. 63–74, 2014.
- [83] A. F. Hayes, *Introduction to mediation, moderation, and conditional process analysis: A regression-based approach*. Guilford publications, 2017.
- [84] D. Ebaid, S. G. Crewther, K. MacCalman, A. Brown, and D. P. Crewther, "Cognitive processing speed across the lifespan: beyond the influence of motor speed," *Frontiers in Aging Neuroscience*, vol. 9, p. 62, 2017. doi: 10.3389/fnagi.2017.00062
- [85] D. Ebaid and S. G. Crewther, "Visual information processing in young and older adults," *Frontiers in Aging Neuroscience*, vol. 11, p. 116, 2019. doi: 10.3389/fnagi.2019.00116
- [86] H. M. Tam, C. L. Lam, H. Huang, B. Wang, and T. M. Lee, "Age-related difference in relationships between cognitive processing speed and general cognitive status," *Applied Neuropsychology: Adult*, vol. 22, no. 2, pp. 94–99, 2015.
- [87] L. Ji, H. Peng, and X. Mao, "The role of sensory function in processing speed and working memory aging," *Experimental Aging Research*, vol. 45, no. 3, pp. 234–251, 2019.
- [88] E. Zelinski, S. Dalton, and S. Hindin, "Cognitive changes in healthy older adults," *Generations*, vol. 35, no. 2, pp. 13–20, 2011.

- [89] A. J. Borja, E. C. Hancin, V. Zhang, M.-E. Revheim, and A. Alavi, “Potential of pet/ct in assessing dementias with emphasis on cerebrovascular disorders,” *European Journal of Nuclear Medicine and Molecular Imaging*, vol. 47, no. 11, pp. 2493–2498, 2020.
- [90] R. Alkasir, J. Li, X. Li, M. Jin, and B. Zhu, “Human gut microbiota: the links with dementia development,” *Protein & Cell*, vol. 8, no. 2, pp. 90–102, 2017.
- [91] S. Seetharaman, “The influences of dietary sugar and related metabolic disorders on cognitive aging and dementia,” in *Molecular Basis of Nutrition and Aging*. Elsevier, 2016, pp. 331–344.
- [92] Y. Komuro, K. Oyama, L. Hu, and K. Sakatani, “Relationship between cognitive dysfunction and systemic metabolic disorders in elderly: Dementia might be a systematic disease,” in *Oxygen Transport to Tissue XLI*. Springer, 2020, pp. 91–97.
- [93] T. A. Salthouse, “The processing-speed theory of adult age differences in cognition,” *Psychological Review*, vol. 103, no. 3, pp. 403–428, 1996.
- [94] N. D. Anderson and F. I. Craik, “50 years of cognitive aging theory,” *The Journals of Gerontology: Series B*, vol. 72, no. 1, pp. 1–6, 2017.
- [95] A. Miyake and N. P. Friedman, “The nature and organization of individual differences in executive functions: Four general conclusions,” *Current Directions in Psychological Science*, vol. 21, no. 1, pp. 8–14, 2012.
- [96] T. Maldonado, J. M. Orr, J. R. Goen, and J. A. Bernard, “Age differences in the subcomponents of executive functioning,” *The Journals of Gerontology: Series B*, vol. 75, no. 6, pp. e31–e55, 2020.
- [97] P. S. Moreira, N. Santos, T. Castanho, L. Amorim, C. Portugal-Nunes, N. Sousa, and P. Costa, “Longitudinal measurement invariance of memory performance and executive functioning in healthy aging,” *PloS One*, vol. 13, no. 9, 2018. doi: 10.1371/journal.pone.0204012
- [98] A. J. Aschenbrenner and D. A. Balota, “Interactive effects of working memory and trial history on stroop interference in cognitively healthy aging,” *Psychology and Aging*, vol. 30, no. 1, pp. 1–8, 2015.
- [99] P. D. Harvey, “Domains of cognition and their assessment,” *Dialogues in Clinical Neuroscience*, vol. 21, no. 3, pp. 227–237, 2019.
- [100] T. P. Zanto and A. Gazzaley, *Selective attention and inhibitory control in the aging brain*. Oxford University Press, 2017, pp. 207–234.

- [101] E. L. Twedell, W. Koutstaal, and Y. V. Jiang, "Aging affects the balance between goal-guided and habitual spatial attention," *Psychonomic Bulletin & Review*, vol. 24, no. 4, pp. 1135–1141, 2017.
- [102] D. A. Balota, P. O. Dolan, and J. M. Duchek, "Memory changes in healthy older adults," *The Oxford Handbook of Memory*, pp. 395–409, 2000.
- [103] L. K. Obler and M. L. Albert, "Language and aging: A neurobehavioral analysis," *Aging: Communication Processes and Disorders*, pp. 107–121, 1981.
- [104] C. S. Herrington, *Muir's Textbook of Pathology*. CRC Press, 2020.
- [105] D. Erten-Lyons, H. H. Dodge, R. Woltjer, L. C. Silbert, D. B. Howieson, P. Kramer, and J. A. Kaye, "Neuropathologic basis of age-associated brain atrophy," *JAMA Neurology*, vol. 70, no. 5, pp. 616–622, 2013.
- [106] L. Pini, M. Pievani, M. Bocchetta, D. Altomare, P. Bosco, E. Cavedo, S. Galluzzi, M. Marizzoni, and G. B. Frisoni, "Brain atrophy in alzheimer's disease and aging," *Ageing Research Reviews*, vol. 30, pp. 25–48, 2016.
- [107] T. Gorbach, S. Pudas, A. Lundquist, G. Orädd, M. Josefsson, A. Salami, X. de Luna, and L. Nyberg, "Longitudinal association between hippocampus atrophy and episodic-memory decline," *Neurobiology of Aging*, vol. 51, pp. 167–176, 2017.
- [108] M. Josefsson, X. de Luna, S. Pudas, L.-G. Nilsson, and L. Nyberg, "Genetic and lifestyle predictors of 15-year longitudinal change in episodic memory," *Journal of the American Geriatrics Society*, vol. 60, no. 12, pp. 2308–2312, 2012.
- [109] X. Li, F. Pu, Y. Fan, H. Niu, S. Li, and D. Li, "Age-related changes in brain structural covariance networks," *Frontiers in Human Neuroscience*, vol. 7, p. 98, 2013. doi: 10.3389/fnhum.2013.00098
- [110] M. G. Spillantini and M. Goedert, "Tau pathology and neurodegeneration," *The Lancet Neurology*, vol. 12, no. 6, pp. 609–622, 2013.
- [111] D. J. Irwin, "Tauopathies as clinicopathological entities," *Parkinsonism & Related Disorders*, vol. 22, pp. S29–S33, 2016.
- [112] Y. T. Quiroz, "Event-related potentials for early detection of alzheimer's disease," *International Journal of Psychophysiology*, vol. 108, p. 50, 2016. doi: 10.1016/j.ijpsycho.2016.07.168

- [113] F. Nelson, M. A. Akhtar, E. Zúñiga, C. A. Perez, K. M. Hasan, J. Wilken, J. S. Wolinsky, P. A. Narayana, and J. L. Steinberg, “Novel fmri working memory paradigm accurately detects cognitive impairment in multiple sclerosis,” *Multiple Sclerosis Journal*, vol. 23, no. 6, pp. 836–847, 2017.
- [114] “Lewy body dementia,” <https://www.mayoclinic.org/diseases-conditions/lewy-body-dementia/symptoms-causes/syc-20352025>, [Accessed: 2019-03-29].
- [115] S.-M. Fereshtehnejad, K. Vosoughi, P. Heydarpour, S. G. Sepanlou, F. Farzadfar, A. Tehrani-Banihashemi, R. Malekzadeh, M. A. Sahraian, S. E. Vollset, M. Naghavi *et al.*, “Burden of neurodegenerative diseases in the eastern mediterranean region, 1990–2016: findings from the global burden of disease study 2016,” *European Journal of Neurology*, vol. 26, no. 10, pp. 1252–1265, 2019.
- [116] E. Nichols, C. E. Szoeki, S. E. Vollset, N. Abbasi, F. Abd-Allah, J. Abdela, M. T. E. Aichour, R. O. Akinyemi, F. Alahdab, S. W. Asgedom *et al.*, “Global, regional, and national burden of alzheimer’s disease and other dementias, 1990–2016: a systematic analysis for the global burden of disease study 2016,” *The Lancet Neurology*, vol. 18, no. 1, pp. 88–106, 2019.
- [117] E. R. Dorsey, A. Elbaz, E. Nichols, N. Abbasi, F. Abd-Allah, A. Abdelalim, J. C. Adsuar, M. G. Ansha, C. Brayne, J.-Y. J. Choi *et al.*, “Global, regional, and national burden of parkinson’s disease, 1990–2016: a systematic analysis for the global burden of disease study 2016,” *The Lancet Neurology*, vol. 17, no. 11, pp. 939–953, 2018.
- [118] “Uae life expectancy 1950-2016,” <https://www.macrotrends.net/countries/ARE/uae/life-expectancy>, [Accessed: 2019-03-29].
- [119] H. Ritchie and M. Roser, “Causes of death,” <https://ourworldindata.org/causes-of-death>, 2018, [Accessed: 2021-03-29].
- [120] “Frontotemporal dementia,” <https://www.mayoclinic.org/diseases-conditions/frontotemporal-dementia/symptoms-causes/syc-20354737>, [Accessed: 2019-03-29].
- [121] I. D. Duncan and A. B. Radcliff, “Inherited and acquired disorders of myelin: the underlying myelin pathology,” *Experimental Neurology*, vol. 283, pp. 452–475, 2016.
- [122] S. Shively, A. I. Scher, D. P. Perl, and R. Diaz-Arrastia, “Dementia resulting from traumatic brain injury: what is the pathology?” *Archives of Neurology*, vol. 69, no. 10, pp. 1245–1251, 2012.

- [123] Y. Statsenko, T. Habuza, D. Smetanina, G. L. Simiya, L. Uzianbaeva, N.-V. Gorkom, N. Zaki, I. Charikova, J. AlKoteesh, M. R. Ljubisavljevic *et al.*, “Brain morphometry and cognitive performance in normal brain aging: age-and sex-related structural and functional changes,” *Frontiers in Aging Neuroscience*, p. 687, 2021. doi: 0.3389/fnagi.2021.713680
- [124] K. Furukawa, A. Ishiki, N. Tomita, Y. Onaka, H. Saito, T. Nakamichi, K. Hara, Y. Kusano, M. Ebara, Y. Arata *et al.*, “Introduction and overview of the special issue “brain imaging and aging”: The new era of neuroimaging in aging research,” *Ageing Research Reviews*, vol. 30, pp. 1–3, 2016.
- [125] X.-H. Hou, L. Feng, C. Zhang, X.-P. Cao, L. Tan, and J.-T. Yu, “Models for predicting risk of dementia: a systematic review,” *J Neurol Neurosurg Psychiatry*, vol. 90, no. 4, pp. 373–379, 2019.
- [126] M. F. Folstein, L. N. Robins, and J. E. Helzer, “The mini-mental state examination,” *Archives of General Psychiatry*, vol. 40, no. 7, pp. 812–812, 1983.
- [127] R. C. Mohs, “Administration and scoring manual for the alzheimer’s disease assessment scale, 1994 revised edition,” *New York: The Mount Sinai School of Medicine*, 1994.
- [128] A. Rey, “L’examen clinique en psychologie [the clinical psychological examination],” *Paris: Presses Universitaires de France*, 1964.
- [129] D. Wechsler, *WAIS-R manual: Wechsler adult intelligence scale-revised*. Psychological Corporation, 1981.
- [130] O. Spreen, E. Strauss *et al.*, *A compendium of neuropsychological tests: Administration, norms, and commentary*. Oxford University Press, 1998.
- [131] J. C. Morris, “Clinical dementia rating: a reliable and valid diagnostic and staging measure for dementia of the alzheimer type,” *International Psychogeriatrics*, vol. 9, no. S1, pp. 173–176, 1997.
- [132] D. Wechsler, *Wechsler memory scale-revised (WMS-R)*. Psychological Corporation, 1987.
- [133] E. Pellegrini, L. Ballerini, M. d. C. V. Hernandez, F. M. Chappell, V. González-Castro, D. Anblagan, S. Danso, S. Muñoz-Maniega, D. Job, C. Pernet *et al.*, “Machine learning of neuroimaging for assisted diagnosis of cognitive impairment and dementia: A systematic review,” *Alzheimer’s & Dementia: Diagnosis, Assessment & Disease Monitoring*, vol. 10, pp. 519–535, 2018.



- [134] S. Lahmiri and A. Shmuel, “Performance of machine learning methods applied to structural mri and adas cognitive scores in diagnosing alzheimer’s disease,” *Biomedical Signal Processing and Control*, vol. 52, pp. 414–419, 2019.
- [135] N. T. Duc, S. Ryu, M. N. I. Qureshi, M. Choi, K. H. Lee, and B. Lee, “3d-deep learning based automatic diagnosis of alzheimer’s disease with joint mmse prediction using resting-state fmri,” *Neuroinformatics*, vol. 18, no. 1, pp. 71–86, 2020.
- [136] C. M. Stonnington, C. Chu, S. Klöppel, C. R. Jack Jr, J. Ashburner, R. S. Frackowiak, A. D. N. Initiative *et al.*, “Predicting clinical scores from magnetic resonance scans in alzheimer’s disease,” *Neuroimage*, vol. 51, no. 4, pp. 1405–1413, 2010.
- [137] B. Lei, W. Hou, W. Zou, X. Li, C. Zhang, and T. Wang, “Longitudinal score prediction for alzheimer’s disease based on ensemble correntropy and spatial-temporal constraint,” *Brain Imaging and Behavior*, vol. 13, no. 1, pp. 126–137, 2019.
- [138] S. Walter, C. Dufouil, A. L. Gross, R. N. Jones, D. Mungas, T. J. Filshtein, J. J. Manly, T. E. Arpawong, and M. M. Glymour, “Neuropsychological test performance and mri markers of dementia risk,” *Alzheimer Disease & Associated Disorders*, vol. 33, no. 3, pp. 179–185, 2019.
- [139] R. Rodríguez-Labrada, L. Velázquez-Pérez, R. Ortega-Sánchez, A. Peña-Acosta, Y. Vázquez-Mojena, N. Canales-Ochoa, J. Medrano-Montero, R. Torres-Vega, and Y. González-Zaldivar, “Insights into cognitive decline in spinocerebellar ataxia type 2: a p300 event-related brain potential study,” *Cerebellum & Ataxias*, vol. 6, no. 1, p. 3, 2019. doi: 10.1186/s40673-019-0097-2
- [140] C. R. Jack Jr, D. S. Knopman, W. J. Jagust, R. C. Petersen, M. W. Weiner, P. S. Aisen, L. M. Shaw, P. Vemuri, H. J. Wiste, S. D. Weigand *et al.*, “Tracking pathophysiological processes in alzheimer’s disease: an updated hypothetical model of dynamic biomarkers,” *The Lancet Neurology*, vol. 12, no. 2, pp. 207–216, 2013.
- [141] H. Matsuda, “Mri morphometry in alzheimer’s disease,” *Ageing Research Reviews*, vol. 30, pp. 17–24, 2016.

- [142] M. Vernooij, F. Pizzini, R. Schmidt, M. Smits, T. Yousry, N. Bargallo, G. Frisoni, S. Haller, and F. Barkhof, "Dementia imaging in clinical practice: a european-wide survey of 193 centres and conclusions by the esnr working group," *Neuroradiology*, vol. 61, no. 6, pp. 633–642, 2019.
- [143] P. Coupé, J. V. Manjón, E. Lanuza, and G. Catheline, "Lifespan changes of the human brain in alzheimer's disease," *Scientific Reports*, vol. 9, no. 1, pp. 1–12, 2019.
- [144] T. M. Hughes, L. H. Kuller, E. J. Barinas-Mitchell, R. H. Mackey, E. M. McDade, W. E. Klunk, H. J. Aizenstein, A. D. Cohen, B. E. Snitz, C. A. Mathis *et al.*, "Pulse wave velocity is associated with  $\beta$ -amyloid deposition in the brains of very elderly adults," *Neurology*, vol. 81, no. 19, pp. 1711–1718, 2013.
- [145] A. M. Pietroboni, M. Scarioni, T. Carandini, P. Basilico, M. Cadioli, G. Giulietti, A. Arighi, M. Caprioli, L. Serra, C. Sina *et al.*, "Csf  $\beta$ -amyloid and white matter damage: a new perspective on alzheimer's disease," *Journal of Neurology, Neurosurgery & Psychiatry*, vol. 89, no. 4, pp. 352–357, 2018.
- [146] K. Wei, T. Tran, K. Chu, M. T. Borzage, M. N. Braskie, M. G. Harrington, and K. S. King, "White matter hypointensities and hyperintensities have equivalent correlations with age and csf  $\beta$ -amyloid in the nondemented elderly," *Brain and Behavior*, vol. 9, no. 12, p. e01457, 2019. doi: 10.1002/brb3.1457
- [147] M. R. Ahmed, Y. Zhang, Z. Feng, B. Lo, O. T. Inan, and H. Liao, "Neuroimaging and machine learning for dementia diagnosis: Recent advancements and future prospects," *IEEE Reviews in Biomedical Engineering*, vol. 12, pp. 19–33, 2018.
- [148] T. Altaf, S. M. Anwar, N. Gul, M. N. Majeed, and M. Majid, "Multi-class alzheimer's disease classification using image and clinical features," *Biomedical Signal Processing and Control*, vol. 43, pp. 64–74, 2018.
- [149] O. B. Ahmed, M. Mizotin, J. Benois-Pineau, M. Allard, G. Catheline, C. B. Amar, A. D. N. Initiative *et al.*, "Alzheimer's disease diagnosis on structural mr images using circular harmonic functions descriptors on hippocampus and posterior cingulate cortex," *Computerized Medical Imaging and Graphics*, vol. 44, pp. 13–25, 2015.

- [150] L. Khedher, J. Ramírez, J. M. Górriz, A. Brahim, F. Segovia, A. D. N. Initiative *et al.*, “Early diagnosis of alzheimer’s disease based on partial least squares, principal component analysis and support vector machine using segmented mri images,” *Neurocomputing*, vol. 151, pp. 139–150, 2015.
- [151] A. Gupta, M. Ayhan, and A. Maida, “Natural image bases to represent neuroimaging data,” in *International Conference on Machine Learning*, vol. 28, no. 3, 2013, pp. 987–994.
- [152] A. Payan and G. Montana, “Predicting alzheimer’s disease: a neuroimaging study with 3d convolutional neural networks,” *ArXiv Preprint ArXiv:1502.02506*, 2015. doi: 10.48550/arXiv.1502.02506
- [153] B. Lee, W. Ellahi, and J. Y. Choi, “Using deep cnn with data permutation scheme for classification of alzheimer’s disease in structural magnetic resonance imaging (smri),” *IEICE TRANSACTIONS on Information and Systems*, vol. 102, no. 7, pp. 1384–1395, 2019.
- [154] T. Habuza, N. Zaki, Y. Statsenko, F. Alnajjar, and S. Elyassami, “Predicting the diagnosis of dementia from mri data: added value to cognitive tests,” in *The 7th Annual International Conference on Arab Women in Computing in Conjunction with the 2nd Forum of Women in Research*, 2021, pp. 1–7.
- [155] M. Liu, F. Li, H. Yan, K. Wang, Y. Ma, L. Shen, M. Xu, A. D. N. Initiative *et al.*, “A multi-model deep convolutional neural network for automatic hippocampus segmentation and classification in alzheimer’s disease,” *NeuroImage*, vol. 208, p. 116459, 2020. doi: 10.1016/j.neuroimage.2019.116459
- [156] R. Cui and M. Liu, “Hippocampus analysis by combination of 3-d densenet and shapes for alzheimer’s disease diagnosis,” *IEEE journal of Biomedical and Health Informatics*, vol. 23, no. 5, pp. 2099–2107, 2018.
- [157] S. Korolev, A. Safiullin, M. Belyaev, and Y. Dodonova, “Residual and plain convolutional neural networks for 3d brain mri classification,” in *2017 IEEE 14th International Symposium on Biomedical Imaging (ISBI 2017)*. IEEE, 2017, pp. 835–838.
- [158] S. Basaia, F. Agosta, L. Wagner, E. Canu, G. Magnani, R. Santangelo, M. Filippi, A. D. N. Initiative *et al.*, “Automated classification of alzheimer’s disease and mild cognitive impairment using a single mri and deep neural networks,” *NeuroImage: Clinical*, vol. 21, p. 101645, 2019. doi: 10.1016/j.nicl.2018.101645

- [159] S. Wang, H. Wang, A. C. Cheung, Y. Shen, and M. Gan, "Ensemble of 3d densely connected convolutional network for diagnosis of mild cognitive impairment and alzheimer's disease," in *Deep Learning Applications*. Springer, 2020, pp. 53–73.
- [160] C. D. Billones, O. J. L. D. Demetria, D. E. D. Hostallero, and P. C. Naval, "Demnet: A convolutional neural network for the detection of alzheimer's disease and mild cognitive impairment," in *2016 IEEE Region 10 Conference (TENCON)*. IEEE, 2016, pp. 3724–3727.
- [161] S. A. Soliman, E.-S. A. El-Dahshan, and A.-B. M. Salem, "Deep learning 3d convolutional neural networks for predicting alzheimer's disease (ald)," in *New Approaches for Multidimensional Signal Processing*. Springer, 2022, vol. 270, pp. 151–162.
- [162] H. Qiao, L. Chen, and F. Zhu, "Ranking convolutional neural network for alzheimer's disease mini-mental state examination prediction at multiple time-points," *Computer Methods and Programs in Biomedicine*, vol. 213, p. 106503, 2022. doi: 10.1016/j.cmpb.2021.106503
- [163] Y. Gao, H. Huang, and L. Zhang, "Predicting alzheimer's disease using 3dmagnet," *ArXiv Preprint ArXiv:2201.04370*, 2022. doi: 10.48550/arXiv.2201.04370
- [164] X. Liu, D. Tosun, M. W. Weiner, N. Schuff, A. D. N. Initiative *et al.*, "Locally linear embedding (lle) for mri based alzheimer's disease classification," *Neuroimage*, vol. 83, pp. 148–157, 2013.
- [165] L. Sørensen, C. Igel, N. Liv Hansen, M. Osler, M. Lauritzen, E. Rostrup, M. Nielsen, A. D. N. Initiative, the Australian Imaging Biomarkers, and L. F. S. of Ageing, "Early detection of alzheimer's disease using m ri hippocampal texture," *Human Brain Mapping*, vol. 37, no. 3, pp. 1148–1161, 2016.
- [166] K. Ellis, A. Bush, D. Darby, D. De Fazio, J. Foster, P. Hudson, N. Lautenschlager, N. Lenzo, R. Martins, P. Maruff *et al.*, "The australian imaging, biomarkers and lifestyle (aibl) study of aging: methodology and baseline characteristics of 1112 individuals recruited for a longitudinal study of alzheimer's disease," *International Psychogeriatrics*, vol. 21, no. 4, pp. 672–687, 2009.
- [167] M. Osler, R. Lund, M. Kriegbaum, U. Christensen, and A.-M. N. Andersen, "Cohort profile: the metropolit 1953 danish male birth cohort," *International Journal of Epidemiology*, vol. 35, no. 3, pp. 541–545, 2006.

- [168] F. Li, L. Tran, K.-H. Thung, S. Ji, D. Shen, and J. Li, "A robust deep model for improved classification of ad/mci patients," *IEEE Journal of Biomedical and Health Informatics*, vol. 19, no. 5, pp. 1610–1616, 2015.
- [169] E. Hosseini-Asl, R. Keynton, and A. El-Baz, "Alzheimer's disease diagnostics by adaptation of 3d convolutional network," in *2016 IEEE International Conference on Image Processing (ICIP)*. IEEE, 2016, pp. 126–130.
- [170] H.-I. Suk, S.-W. Lee, D. Shen, A. D. N. Initiative *et al.*, "Deep sparse multi-task learning for feature selection in alzheimer's disease diagnosis," *Brain Structure and Function*, vol. 221, no. 5, pp. 2569–2587, 2016.
- [171] X. W. Gao, R. Hui, and Z. Tian, "Classification of ct brain images based on deep learning networks," *Computer Methods and Programs in Biomedicine*, vol. 138, pp. 49–56, 2017.
- [172] J. Zhang, M. Liu, L. An, Y. Gao, and D. Shen, "Alzheimer's disease diagnosis using landmark-based features from longitudinal structural mr images," *IEEE journal of Biomedical and Health Informatics*, vol. 21, no. 6, pp. 1607–1616, 2017.
- [173] M. Liu, D. Cheng, K. Wang, and Y. Wang, "Multi-modality cascaded convolutional neural networks for alzheimer's disease diagnosis," *Neuroinformatics*, vol. 16, no. 3, pp. 295–308, 2018.
- [174] X. Fang, Z. Liu, and M. Xu, "Ensemble of deep convolutional neural networks based multi-modality images for alzheimer's disease diagnosis," *IET Image Processing*, vol. 14, no. 2, pp. 318–326, 2019.
- [175] J. Zhang, B. Zheng, A. Gao, X. Feng, D. Liang, and X. Long, "A 3d densely connected convolution neural network with connection-wise attention mechanism for alzheimer's disease classification," *Magnetic Resonance Imaging*, vol. 78, pp. 119–126, 2021.
- [176] V. Sathiyamoorthi, A. Ilavarasi, K. Murugeswari, S. T. Ahmed, B. A. Devi, and M. Kalipindi, "A deep convolutional neural network based computer aided diagnosis system for the prediction of alzheimer's disease in mri images," *Measurement*, vol. 171, p. 108838, 2021. doi: 10.1016/j.measurement.2020.108838
- [177] A. Qiu, L. Xu, and C. Liu, "Predicting diagnosis 4 years prior to alzheimer's disease incident," *NeuroImage: Clinical*, vol. 34, p. 102993, 2022. doi: 10.1016/j.nicl.2022.102993

- [178] “Adni1 dataset,” <https://ida.loni.usc.edu/login.jsp>, 2022, [Accessed: 2021-11-09].
- [179] “Adni general procedures manual,” *"https://adni.loni.usc.edu/wp-content/uploads/2010/09/ADNI\_GeneralProceduresManual.pdf"*, pp. 20–21, 2021, [Accessed: 2021-11-12].
- [180] E. Statsenko and I. Charykova, “Psycho-physiological criteria for overtraining in athletes,” *Voprosy Kurortologii, Fizioterapii, i Lechebnoi Fizicheskoi Kultury*, no. 2, pp. 50–54, 2010.
- [181] J. E. Birren, A. M. Woods, and M. Williams, “Speed of behavior as an indicator of age changes and the integrity of the nervous system,” in *Brain Function in Old Age*. Springer, 1979, pp. 10–44.
- [182] J. E. Birren, A. M. Woods, and M. V. Williams, “Behavioral slowing with age: Causes, organization, and consequences.” *Aging in the 1980s: Psychological Issues*, pp. 293–308, 1980.
- [183] C. R. Jack Jr, D. A. Bennett, K. Blennow, M. C. Carrillo, B. Dunn, S. B. Haeberlein, D. M. Holtzman, W. Jagust, F. Jessen, J. Karlawish *et al.*, “Nia-aa research framework: toward a biological definition of alzheimer’s disease,” *Alzheimer’s & Dementia*, vol. 14, no. 4, pp. 535–562, 2018.
- [184] J. L. Ebenau, T. Timmers, L. M. Wesselman, I. M. Verberk, S. C. Verfaillie, R. E. Slot, A. C. Van Harten, C. E. Teunissen, F. Barkhof, K. A. Van Den Bosch *et al.*, “Atn classification and clinical progression in subjective cognitive decline: The science project,” *Neurology*, vol. 95, no. 1, pp. e46–e58, 2020.
- [185] B. M. Tijms, E. A. Willemse, M. D. Zwan, S. D. Mulder, P. J. Visser, B. N. van Berckel, W. M. van der Flier, P. Scheltens, and C. E. Teunissen, “Unbiased approach to counteract upward drift in cerebrospinal fluid amyloid- $\beta$  1–42 analysis results,” *Clinical Chemistry*, vol. 64, no. 3, pp. 576–585, 2018.
- [186] C. Mulder, N. A. Verwey, W. M. van der Flier, F. H. Bouwman, A. Kok, E. J. van Elk, P. Scheltens, and M. A. Blankenstein, “Amyloid- $\beta$  (1–42), total tau, and phosphorylated tau as cerebrospinal fluid biomarkers for the diagnosis of alzheimer disease,” *Clinical Chemistry*, vol. 56, no. 2, pp. 248–253, 2010.
- [187] Y.-N. Ou, W. Xu, J.-Q. Li, Y. Guo, M. Cui, K.-L. Chen, Y.-Y. Huang, Q. Dong, L. Tan, and J.-T. Yu, “Fdg-pet as an independent biomarker for alzheimer’s biological diagnosis: a longitudinal study,” *Alzheimer’s Research & Therapy*, vol. 11, no. 1, pp. 1–11, 2019.

- [188] Y. Statsenko, T. Habuza, D. Smetanina, G. L. Simiyu, L. Uzianbaeva, K. Neidl-Van Gorkom, N. Zaki, I. Charykova, J. Al Koteesh, T. M. Almansoori *et al.*, “Brain morphometry and cognitive performance in normal brain aging: Age-and sex-related structural and functional changes,” *Frontiers in Aging Neuroscience*, vol. 13, 2021. doi: 10.3389/fnagi.2021.713680
- [189] P. Schmidt, C. Gaser, M. Arsic, D. Buck, A. Förschler, A. Berthele, M. Hoshi, R. Ilg, V. J. Schmid, C. Zimmer *et al.*, “An automated tool for detection of flair-hyperintense white-matter lesions in multiple sclerosis,” *Neuroimage*, vol. 59, no. 4, pp. 3774–3783, 2012.
- [190] P. Schmidt and L. Wink, “Lst: A lesion segmentation tool for spm,” *Manual/Documentation for Version*, vol. 2, p. 15, 2017.
- [191] “Freesurfer software suite,” <https://surfer.nmr.mgh.harvard.edu/fswiki/FreeSurferWiki>, [Accessed: 2020-09-29].
- [192] M. Jenkinson, C. F. Beckmann, T. E. Behrens, M. W. Woolrich, and S. M. Smith, “Fsl,” *Neuroimage*, vol. 62, no. 2, pp. 782–790, 2012.
- [193] N. J. Tustison, B. B. Avants, P. A. Cook, Y. Zheng, A. Egan, P. A. Yushkevich, and J. C. Gee, “N4itk: improved n3 bias correction,” *IEEE Transactions on Medical Imaging*, vol. 29, no. 6, pp. 1310–1320, 2010.
- [194] X. Zhu, H.-I. Suk, L. Wang, S.-W. Lee, D. Shen, A. D. N. Initiative *et al.*, “A novel relational regularization feature selection method for joint regression and classification in ad diagnosis,” *Medical Image Analysis*, vol. 38, pp. 205–214, 2017.
- [195] K. Gorgolewski, C. D. Burns, C. Madison, D. Clark, Y. O. Halchenko, M. L. Waskom, and S. S. Ghosh, “Nipype: a flexible, lightweight and extensible neuroimaging data processing framework in python,” *Frontiers in Neuroinformatics*, vol. 5, p. 13, 2011. doi: 10.3389/fninf.2011.00013
- [196] Y. Zhu, X. Zhu, M. Kim, J. Yan, D. Kaufer, and G. Wu, “Dynamic hyper-graph inference framework for computer-assisted diagnosis of neurodegenerative diseases,” *IEEE Transactions on Medical Imaging*, vol. 38, no. 2, pp. 608–616, 2018.
- [197] N. H. Zainal, E. Silva, L. L. Lim, and N. Kandiah, “Psychometric properties of alzheimer’s disease assessment scale-cognitive subscale for mild cognitive impairment and mild alzheimer’s disease patients in an asian context,” *Ann Acad Med Singapore*, vol. 45, no. 7, pp. 273–283, 2016.

- [198] L. C. W. Lam, P. Ho, V. W. C. Lui, and C. W. C. Tam, “Reduced semantic fluency as an additional screening tool for subjects with questionable dementia,” *Dementia and Geriatric Cognitive Disorders*, vol. 22, no. 2, pp. 159–164, 2006.
- [199] T. Foley, A. McKinlay, N. Warren, and R. Stolwyk, “Assessing the sensitivity and specificity of cognitive screening measures for people with parkinson’s disease,” *NeuroRehabilitation*, vol. 43, no. 4, pp. 491–500, 2018.
- [200] K. N. Fountoulakis, M. Tsolaki, H. Chantzi, and A. Kazis, “Mini mental state examination (mmse): a validation study in greece,” *American Journal of Alzheimer’s Disease & Other Dementias®*, vol. 15, no. 6, pp. 342–345, 2000.
- [201] O. Godefroy, A. Fickl, M. Roussel, C. Auribault, J. M. Bugnicourt, C. Lamy, S. Canaple, and G. Petitnicolas, “Is the montreal cognitive assessment superior to the mini-mental state examination to detect poststroke cognitive impairment? a study with neuropsychological evaluation,” *Stroke*, vol. 42, no. 6, pp. 1712–1716, 2011.
- [202] S. Ciulli, L. Citi, E. Salvadori, R. Valenti, A. Poggesi, D. Inzitari, M. Mascalchi, N. Toschi, L. Pantoni, and S. Diciotti, “Prediction of impaired performance in trail making test in mci patients with small vessel disease using dti data,” *IEEE Journal of Biomedical and Health Informatics*, vol. 20, no. 4, pp. 1026–1033, 2016.
- [203] M. R. Olchik, M. Ghisi, A. M. Freiry, A. Ayres, A. F. S. Schuh, C. R. d. M. Rieder, and A. R. Teixeira, “Comparison trail making test between individuals with parkinson’s disease and health controls: Suggestions of cutoff point,” *Psychology & Neuroscience*, vol. 10, no. 1, p. 77, 2017.
- [204] M. Ewers, C. Walsh, J. Q. Trojanowski, L. M. Shaw, R. C. Petersen, C. R. Jack Jr, H. H. Feldman, A. L. Bokde, G. E. Alexander, P. Scheltens *et al.*, “Prediction of conversion from mild cognitive impairment to alzheimer’s disease dementia based upon biomarkers and neuropsychological test performance,” *Neurobiology of Aging*, vol. 33, no. 7, pp. 1203–1214, 2012.
- [205] S. Bottiroli, S. Bernini, E. Cavallini, E. Sinforiani, C. Zucchella, S. Pazzi, P. Cristiani, T. Vecchi, D. Tost, G. Sandrini *et al.*, “The smart aging platform for assessing early phases of cognitive impairment in patients with neurodegenerative diseases,” *Frontiers in Psychology*, vol. 12, 2021. doi: 10.3389/fpsyg.2021.635410



- [206] M. Beier, A. J. Hughes, M. W. Williams, and E. S. Gromisch, “Brief and cost-effective tool for assessing verbal learning in multiple sclerosis: Comparison of the rey auditory verbal learning test (ravlt) to the california verbal learning test–ii (cvlt-ii),” *Journal of the Neurological Sciences*, vol. 400, pp. 104–109, 2019.
- [207] M. Ricci, S. Graef, C. Blundo, and L. A. Miller, “Using the rey auditory verbal learning test (ravlt) to differentiate alzheimer’s dementia and behavioural variant fronto-temporal dementia,” *The Clinical Neuropsychologist*, vol. 26, no. 6, pp. 926–941, 2012.
- [208] C. Bussè, P. Anselmi, S. Pompanin, G. Zorzi, F. Fragiaco, G. Camporese, G. A. Di Bernardo, C. Semenza, P. Caffarra, and A. Cagnin, “Specific verbal memory measures may distinguish alzheimer’s disease from dementia with lewy bodies,” *Journal of Alzheimer’s Disease*, vol. 59, no. 3, pp. 1009–1015, 2017.
- [209] C. Proust-Lima, H. Amieva, J.-F. Dartigues, and H. Jacqmin-Gadda, “Sensitivity of four psychometric tests to measure cognitive changes in brain aging-population-based studies,” *American Journal of Epidemiology*, vol. 165, no. 3, pp. 344–350, 2007.
- [210] J. Ciafone, A. Thomas, R. Durcan, P. C. Donaghy, C. A. Hamilton, S. Lawley, G. Roberts, S. Colloby, M. J. Firbank, L. Allan *et al.*, “Neuropsychological impairments and their cognitive architecture in mild cognitive impairment (mci) with lewy bodies and mci-alzheimer’s disease,” *Journal of the International Neuropsychological Society*, pp. 1–11, 2021.
- [211] A. Botzung, N. Philippi, V. Noblet, P. Loureiro de Sousa, and F. Blanc, “Pay attention to the basal ganglia: a volumetric study in early dementia with lewy bodies,” *Alzheimer’s Research & Therapy*, vol. 11, no. 1, pp. 1–9, 2019.
- [212] J. C. Platt, “Probabilistic outputs for support vector machines and comparisons to regularized likelihood methods,” in *Advances in Large Margin Classifiers*. MIT Press, 1999, pp. 61–74.
- [213] G. H. John and P. Langley, “Estimating continuous distributions in bayesian classifiers,” *ArXiv Preprint ArXiv:1302.4964*, 2013. doi: 10.48550/arXiv.1302.4964
- [214] G. Louppe and P. Geurts, “Ensembles on random patches,” in *Joint European Conference on Machine Learning and Knowledge Discovery in Databases*. Springer, 2012, pp. 346–361.

- [215] P. Geurts, D. Ernst, and L. Wehenkel, "Extremely randomized trees," *Machine Learning*, vol. 63, no. 1, pp. 3–42, 2006.
- [216] L. Breiman, "Random forests," *Machine Learning*, vol. 45, no. 1, pp. 5–32, 2001.
- [217] J. H. Friedman, "Greedy function approximation: a gradient boosting machine," *Annals of Statistics*, pp. 1189–1232, 2001.
- [218] Y. Freund and R. E. Schapire, "A decision-theoretic generalization of on-line learning and an application to boosting," *Journal of Computer and System Sciences*, vol. 55, no. 1, pp. 119–139, 1997.
- [219] "Scipy is open-source software for mathematics, science, and engineering," *Numpy and Scipy Documentation*, 2021, [Accessed: 2021-11-12]. [Online]. Available: <https://docs.scipy.org/doc/scipy/reference/index.html>
- [220] T. Habuza, K. Khalil, N. Zaki, F. Alnajjar, and M. Gochoo, "Web-based multi-user concurrent job scheduling system on the shared computing resource objects," in *2020 14th International Conference on Innovations in Information Technology (IIT)*. IEEE, 2020, pp. 221–226.
- [221] T. R. Bashore, K. R. Ridderinkhof, and M. W. van der Molen, "The decline of cognitive processing speed in old age," *Current Directions in Psychological Science*, vol. 6, no. 6, pp. 163–169, 1997.
- [222] O. Godefroy, M. Roussel, P. Despretz, V. Quaglino, and M. Boucart, "Age-related slowing: perceptuomotor, decision, or attention decline?" *Experimental Aging Research*, vol. 36, no. 2, pp. 169–189, 2010.
- [223] G. Der and I. J. Deary, "Age and sex differences in reaction time in adulthood: results from the united kingdom health and lifestyle survey." *Psychology and Aging*, vol. 21, no. 1, pp. 62–73, 2006.
- [224] V. Satopaa, J. Albrecht, D. Irwin, and B. Raghavan, "Finding a" kneedle" in a haystack: Detecting knee points in system behavior," in *2011 31st international conference on distributed computing systems workshops*. IEEE, 2011, pp. 166–171.
- [225] T. A. Salthouse, "When does age-related cognitive decline begin?" *Neurobiology of Aging*, vol. 30, no. 4, pp. 507–514, 2009.
- [226] D. Zimprich and A. Mascherek, "Five views of a secret: does cognition change during middle adulthood?" *European Journal of Ageing*, vol. 7, no. 3, pp. 135–146, 2010.
- [227] W. R. Pierson and H. J. Montoye, "Movement time, reaction time and age," *Journal of Gerontology*, vol. 13, no. 4, pp. 418–421, 1958.

- [228] P. Rabbitt, "Crystal quest: A search for the basis of maintenance of practised skills into old age." *Attention: Selection, Awareness, and Control: a Tribute to Donald Broadbent*, pp. 188–230, 1993.
- [229] J. Nilsson, A. J. Thomas, J. T O'Brien, and P. Gallagher, "White matter and cognitive decline in aging: A focus on processing speed and variability," *Journal of the International Neuropsychological Society: JINS*, vol. 20, no. 3, pp. 262–267, 2014.
- [230] D. Ferreira, Y. Molina, A. Machado, E. Westman, L.-O. Wahlund, A. Nieto, R. Correia, C. Junqué, L. Díaz-Flores, and J. Barroso, "Cognitive decline is mediated by gray matter changes during middle age," *Neurobiology of Aging*, vol. 35, no. 5, pp. 1086–1094, 2014.
- [231] S. Bauermeister and D. Bunce, "Aerobic fitness and intraindividual reaction time variability in middle and old age," *Journals of Gerontology Series B: Psychological Sciences and Social Sciences*, vol. 71, no. 3, pp. 431–438, 2016.
- [232] B. I. Haynes, S. Bauermeister, and D. Bunce, "A systematic review of longitudinal associations between reaction time intraindividual variability and age-related cognitive decline or impairment, dementia, and mortality," *Journal of the International Neuropsychological Society*, vol. 23, no. 5, pp. 431–445, 2017.
- [233] A. Singh-Manoux, M. Kivimaki, M. M. Glymour, A. Elbaz, C. Berr, K. P. Ebmeier, J. E. Ferrie, and A. Dugravot, "Timing of onset of cognitive decline: results from whitehall ii prospective cohort study," *Bmj*, vol. 344, p. d7622, 2012. doi: 10.1136/bmj.d7622
- [234] Y. Taki, S. Kinomura, K. Sato, K. Inoue, R. Goto, K. Okada, S. Uchida, R. Kawashima, and H. Fukuda, "Relationship between body mass index and gray matter volume in 1,428 healthy individuals," *Obesity*, vol. 16, no. 1, pp. 119–124, 2008.
- [235] S.-C. Li, U. Lindenberger, B. Hommel, G. Aschersleben, W. Prinz, and P. B. Baltes, "Transformations in the couplings among intellectual abilities and constituent cognitive processes across the life span," *Psychological Science*, vol. 15, no. 3, pp. 155–163, 2004.
- [236] T. L. Jernigan, G. A. Press, and J. R. Hesselink, "Methods for measuring brain morphologic features on magnetic resonance images: validation and normal aging," *Archives of Neurology*, vol. 47, no. 1, pp. 27–32, 1990.

- [237] R. I. Scahill, C. Frost, R. Jenkins, J. L. Whitwell, M. N. Rossor, and N. C. Fox, "A longitudinal study of brain volume changes in normal aging using serial registered magnetic resonance imaging," *Archives of Neurology*, vol. 60, no. 7, pp. 989–994, 2003.
- [238] J. A. Malko, J. Hoffman, and R. C. Green, "Mr measurement of intracranial csf volume in 41 elderly normal volunteers." *American Journal of Neuroradiology*, vol. 12, no. 2, pp. 371–374, 1991.
- [239] M. Edsbacke, G. Starck, H. Zetterberg, D. Ziegler, and C. Wikkelso, "Spinal cerebrospinal fluid volume in healthy elderly individuals," *Clinical Anatomy*, vol. 24, no. 6, pp. 733–740, 2011.
- [240] S. M. Resnick, A. F. Goldszal, C. Davatzikos, S. Golski, M. A. Kraut, E. J. Metter, R. N. Bryan, and A. B. Zonderman, "One-year age changes in mri brain volumes in older adults," *Cerebral Cortex*, vol. 10, no. 5, pp. 464–472, 2000.
- [241] R. C. Gur, P. D. Mozley, S. M. Resnick, G. L. Gottlieb, M. Kohn, R. Zimmerman, G. Herman, S. Atlas, R. Grossman, and D. Berretta, "Gender differences in age effect on brain atrophy measured by magnetic resonance imaging." *Proceedings of the National Academy of Sciences*, vol. 88, no. 7, pp. 2845–2849, 1991.
- [242] A. L. Foundas, D. Zipin, and C. A. Browning, "Age-related changes of the insular cortex and lateral ventricles: conventional mri volumetric measures," *Journal of Neuroimaging*, vol. 8, no. 4, pp. 216–221, 1998.
- [243] S. M. Grieve, C. R. Clark, L. M. Williams, A. J. Peduto, and E. Gordon, "Preservation of limbic and paralimbic structures in aging," *Human Brain Mapping*, vol. 25, no. 4, pp. 391–401, 2005.
- [244] C. Coffey, W. Wilkinson, L. Parashos, S. Soady, R. Sullivan, L. Patterson, G. Figiel, M. Webb, C. Spritzer, and W. Djang, "Quantitative cerebral anatomy of the aging human brain: a cross-sectional study using magnetic resonance imaging," *Neurology*, vol. 42, no. 3, pp. 527–527, 1992.
- [245] C. D. Good, I. S. Johnsrude, J. Ashburner, R. N. Henson, K. J. Friston, and R. S. Frackowiak, "A voxel-based morphometric study of ageing in 465 normal adult human brains," *Neuroimage*, vol. 14, no. 1, pp. 21–36, 2001.
- [246] X. Chen, P. S. Sachdev, W. Wen, and K. J. Anstey, "Sex differences in regional gray matter in healthy individuals aged 44–48 years: a voxel-based morphometric study," *Neuroimage*, vol. 36, no. 3, pp. 691–699, 2007.

- [247] H. Christensen, A. E. Korten, A. F. Jorm, A. S. Henderson, P. A. Jacomb, B. Rodgers, and A. J. Mackinnon, "Education and decline in cognitive performance: compensatory but not protective," *International Journal of Geriatric Psychiatry*, vol. 12, no. 3, pp. 323–330, 1997.
- [248] L. Weyandt, A. Swentosky, and B. G. Gudmundsdottir, "Neuroimaging and adhd: fmri, pet, dti findings, and methodological limitations," *Developmental Neuropsychology*, vol. 38, no. 4, pp. 211–225, 2013.
- [249] R. González-José, F. Ramírez-Rozzi, M. Sardi, N. Martínez-Abadías, M. Hernández, and H. M. Pucciarelli, "Functional-cranial approach to the influence of economic strategy on skull morphology," *American Journal of Physical Anthropology: The Official Publication of the American Association of Physical Anthropologists*, vol. 128, no. 4, pp. 757–771, 2005.
- [250] S. H. Bouthoorn, F. J. van Lenthe, A. C. Hokken-Koelega, H. A. Moll, H. Tiemeier, A. Hofman, J. P. Mackenbach, V. W. Jaddoe, and H. Raat, "Head circumference of infants born to mothers with different educational levels; the generation r study," *PloS One*, vol. 7, no. 6, p. e39798, 2012. doi: 10.1371/journal.pone.0039798
- [251] Y. S. Kim, I. S. Park, H. J. Kim, D. Kim, N. J. Lee, and I. J. Rhyu, "Changes in intracranial volume and cranial shape in modern koreans over four decades," *American Journal of Physical Anthropology*, vol. 166, no. 3, pp. 753–759, 2018.
- [252] L. Sakka, G. Coll, and J. Chazal, "Anatomy and physiology of cerebrospinal fluid," *European Annals of Otorhinolaryngology, Head and Neck diseases*, vol. 128, no. 6, pp. 309–316, 2011.
- [253] J. E. Preston, "Ageing choroid plexus-cerebrospinal fluid system," *Microscopy Research and Technique*, vol. 52, no. 1, pp. 31–37, 2001.
- [254] C. Chiu, M. C. Miller, I. N. Caralopoulos, M. S. Worden, T. Brinker, Z. N. Gordon, C. E. Johanson, and G. D. Silverberg, "Temporal course of cerebrospinal fluid dynamics and amyloid accumulation in the aging rat brain from three to thirty months," *Fluids and Barriers of the CNS*, vol. 9, no. 1, pp. 1–8, 2012.
- [255] Q. Ma, B. V. Ineichen, M. Detmar, and S. T. Proulx, "Outflow of cerebrospinal fluid is predominantly through lymphatic vessels and is reduced in aged mice," *Nature Communications*, vol. 8, no. 1, pp. 1–13, 2017.

- [256] A. Pfefferbaum, D. H. Mathalon, E. V. Sullivan, J. M. Rawles, R. B. Zipursky, and K. O. Lim, "A quantitative magnetic resonance imaging study of changes in brain morphology from infancy to late adulthood," *Archives of Neurology*, vol. 51, no. 9, pp. 874–887, 1994.
- [257] Y. H. Kwon, S. H. Jang, and S. S. Yeo, "Age-related changes of lateral ventricular width and periventricular white matter in the human brain: a diffusion tensor imaging study," *Neural Regeneration Research*, vol. 9, no. 9, pp. 986–989, 2014.
- [258] M. P. Earnest, R. K. Heaton, W. E. Wilkinson, and W. F. Manke, "Cortical atrophy, ventricular enlargement and intellectual impairment in the aged," *Neurology*, vol. 29, no. 8, pp. 1138–1138, 1979.
- [259] S. A. Barron, L. Jacobs, and W. R. Kinkel, "Changes in size of normal lateral ventricles during aging determined by computerized tomography," *Neurology*, vol. 26, no. 11, pp. 1011–1011, 1976.
- [260] C. Preul, M. Hund-Georgiadis, B. U. Forstmann, and G. Lohmann, "Characterization of cortical thickness and ventricular width in normal aging: a morphometric study at 3 tesla," *Journal of Magnetic Resonance Imaging: An Official Journal of the International Society for Magnetic Resonance in Medicine*, vol. 24, no. 3, pp. 513–519, 2006.
- [261] E. V. Sullivan, L. Marsh, D. H. Mathalon, K. O. Lim, and A. Pfefferbaum, "Age-related decline in mri volumes of temporal lobe gray matter but not hippocampus," *Neurobiology of Aging*, vol. 16, no. 4, pp. 591–606, 1995.
- [262] M. Schwartz, H. Creasey, C. L. Grady, J. M. DeLeo, H. A. Frederickson, N. R. Cutler, and S. I. Rapoport, "Computed tomographic analysis of brain morphometrics in 30 healthy men, aged 21 to 81 years," *Annals of Neurology: Official Journal of the American Neurological Association and the Child Neurology Society*, vol. 17, no. 2, pp. 146–157, 1985.
- [263] E. Courchesne, H. J. Chisum, J. Townsend, A. Cowles, J. Covington, B. Egaas, M. Harwood, S. Hinds, and G. A. Press, "Normal brain development and aging: quantitative analysis at in vivo mr imaging in healthy volunteers," *Radiology*, vol. 216, no. 3, pp. 672–682, 2000.
- [264] M. Wilke, I. Krägeloh-Mann, and S. K. Holland, "Global and local development of gray and white matter volume in normal children and adolescents," *Experimental Brain Research*, vol. 178, no. 3, pp. 296–307, 2007.

- [265] B. D. C. Group, "Total and regional brain volumes in a population-based normative sample from 4 to 18 years: the nih mri study of normal brain development," *Cerebral Cortex*, vol. 22, no. 1, pp. 1–12, 2012.
- [266] C. D. Smith, H. Chebrolu, D. R. Wekstein, F. A. Schmitt, and W. R. Markesbery, "Age and gender effects on human brain anatomy: a voxel-based morphometric study in healthy elderly," *Neurobiology of Aging*, vol. 28, no. 7, pp. 1075–1087, 2007.
- [267] R. Liu, L. Lemieux, G. Bell, S. Sisodiya, S. Shorvon, J. Sander, and J. Duncan, "A longitudinal study of brain morphometrics using quantitative magnetic resonance imaging and difference image analysis," *Neuroimage*, vol. 20, no. 1, pp. 22–33, 2003.
- [268] K. L. Mills, A.-L. Goddings, M. M. Herting, R. Meuwese, S.-J. Blakemore, E. A. Crone, R. E. Dahl, B. Güroğlu, A. Raznahan, E. R. Sowell *et al.*, "Structural brain development between childhood and adulthood: Convergence across four longitudinal samples," *Neuroimage*, vol. 141, pp. 273–281, 2016.
- [269] N. Gogtay, J. N. Giedd, L. Lusk, K. M. Hayashi, D. Greenstein, A. C. Vaituzis, T. F. Nugent, D. H. Herman, L. S. Clasen, A. W. Toga *et al.*, "Dynamic mapping of human cortical development during childhood through early adulthood," *Proceedings of the National Academy of Sciences*, vol. 101, no. 21, pp. 8174–8179, 2004.
- [270] D. H. Mathalon, E. V. Sullivan, K. O. Lim, and A. Pfefferbaum, "Progressive brain volume changes and the clinical course of schizophrenia in men: a longitudinal magnetic resonance imaging study," *Archives of General Psychiatry*, vol. 58, no. 2, pp. 148–157, 2001.
- [271] E. R. Sowell, P. M. Thompson, C. M. Leonard, S. E. Welcome, E. Kan, and A. W. Toga, "Longitudinal mapping of cortical thickness and brain growth in normal children," *Journal of Neuroscience*, vol. 24, no. 38, pp. 8223–8231, 2004.
- [272] K. Koelkebeck, J. Miyata, M. Kubota, W. Kohl, S. Son, H. Fukuyama, N. Sawamoto, H. Takahashi, and T. Murai, "The contribution of cortical thickness and surface area to gray matter asymmetries in the healthy human brain," *Human Brain Mapping*, vol. 35, no. 12, pp. 6011–6022, 2014.

- [273] O. Profant, A. Škoch, J. Tintěra, V. Svobodová, D. Kuchárová, J. S. Burianová, and J. Syka, “The influence of aging, hearing, and tinnitus on the morphology of cortical gray matter, amygdala, and hippocampus,” *Frontiers in Aging Neuroscience*, vol. 12, 2020. doi: 10.3389/fnagi.2020.553461
- [274] S. O’donnell, M. D. Noseworthy, B. Levine, and M. Dennis, “Cortical thickness of the frontopolar area in typically developing children and adolescents,” *Neuroimage*, vol. 24, no. 4, pp. 948–954, 2005.
- [275] J. N. Giedd, J. Blumenthal, N. O. Jeffries, F. X. Castellanos, H. Liu, A. Zijdenbos, T. Paus, A. C. Evans, and J. L. Rapoport, “Brain development during childhood and adolescence: a longitudinal mri study,” *Nature Neuroscience*, vol. 2, no. 10, pp. 861–863, 1999.
- [276] E. Pagani, F. Agosta, M. A. Rocca, D. Caputo, and M. Filippi, “Voxel-based analysis derived from fractional anisotropy images of white matter volume changes with aging,” *Neuroimage*, vol. 41, no. 3, pp. 657–667, 2008.
- [277] Y. Tang, J. Nyengaard, B. Pakkenberg, and H. Gundersen, “Age-induced white matter changes in the human brain: a stereological investigation,” *Neurobiology of Aging*, vol. 18, no. 6, pp. 609–615, 1997.
- [278] Y. Ge, R. I. Grossman, J. S. Babb, M. L. Rabin, L. J. Mannon, and D. L. Kolson, “Age-related total gray matter and white matter changes in normal adult brain. part i: volumetric mr imaging analysis,” *American Journal of Neuroradiology*, vol. 23, no. 8, pp. 1327–1333, 2002.
- [279] H. Liu, L. Wang, Z. Geng, Q. Zhu, Z. Song, R. Chang, and H. Lv, “A voxel-based morphometric study of age-and sex-related changes in white matter volume in the normal aging brain,” *Neuropsychiatric Disease and Treatment*, vol. 12, pp. 453–465, 2016.
- [280] D. Van den Heuvel, V. Ten Dam, A. De Craen, F. Admiraal-Behloul, A. Van Es, W. Palm, A. Spilt, E. Bollen, G. Blauw, L. Launer *et al.*, “Measuring longitudinal white matter changes: comparison of a visual rating scale with a volumetric measurement,” *American Journal of Neuroradiology*, vol. 27, no. 4, pp. 875–878, 2006.
- [281] D. H. Salat, J. A. Kaye, and J. S. Janowsky, “Prefrontal gray and white matter volumes in healthy aging and alzheimer disease,” *Archives of Neurology*, vol. 56, no. 3, pp. 338–344, 1999.



- [282] N. Raz and K. M. Rodrigue, "Differential aging of the brain: patterns, cognitive correlates and modifiers," *Neuroscience & Biobehavioral Reviews*, vol. 30, no. 6, pp. 730–748, 2006.
- [283] P. Christiansen, H. Larsson, C. Thomsen, S. Wieslander, and O. Henriksen, "Age dependent white matter lesions and brain volume changes in healthy volunteers," *Acta Radiologica*, vol. 35, no. 2, pp. 117–122, 1994.
- [284] I. A. Awad, R. F. Spetzler, J. A. Hodak, C. A. Awad, and R. Carey, "Incidental subcortical lesions identified on magnetic resonance imaging in the elderly. i. correlation with age and cerebrovascular risk factors." *Stroke*, vol. 17, no. 6, pp. 1084–1089, 1986.
- [285] R. O. Hopkins, C. J. Beck, D. L. Burnett, L. K. Weaver, J. Victoroff, and E. D. Bigler, "Prevalence of white matter hyperintensities in a young healthy population," *Journal of Neuroimaging*, vol. 16, no. 3, pp. 243–251, 2006.
- [286] J. Cees De Groot, F.-E. De Leeuw, M. Oudkerk, J. Van Gijn, A. Hofman, J. Jolles, and M. M. Breteler, "Cerebral white matter lesions and cognitive function: the rotterdam scan study," *Annals of Neurology: Official Journal of the American Neurological Association and the Child Neurology Society*, vol. 47, no. 2, pp. 145–151, 2000.
- [287] W. Wen, P. S. Sachdev, X. Chen, and K. Anstey, "Gray matter reduction is correlated with white matter hyperintensity volume: a voxel-based morphometric study in a large epidemiological sample," *Neuroimage*, vol. 29, no. 4, pp. 1031–1039, 2006.
- [288] B. S. Aribisala, M. C. V. Hernández, N. A. Royle, Z. Morris, S. M. Maniega, M. E. Bastin, I. J. Deary, and J. M. Wardlaw, "Brain atrophy associations with white matter lesions in the ageing brain: the lothian birth cohort 1936," *European Radiology*, vol. 23, no. 4, pp. 1084–1092, 2013.
- [289] T. Habuza, Y. Statsenko, L. Uzianbaeva, K. Gorkom, N. Zaki, M. Belghali *et al.*, "Models of brain cognitive and morphological changes across the life: machine learning-based approach. esnr 2021," *Neuroradiology*, vol. 63, p. 42, 2021.
- [290] S. H. Mostofsky and D. J. Simmonds, "Response inhibition and response selection: two sides of the same coin," *Journal of Cognitive Neuroscience*, vol. 20, no. 5, pp. 751–761, 2008.
- [291] T. L. Jernigan and A. C. Gamst, "Changes in volume with age—consistency and interpretation of observed effects." *Neurobiology of Aging*, vol. 26, no. 9, pp. 1271–1274, 2005.

- [292] P. H. Lu, G. J. Lee, T. A. Tishler, M. Meghpara, P. M. Thompson, and G. Bartzokis, “Myelin breakdown mediates age-related slowing in cognitive processing speed in healthy elderly men,” *Brain and Cognition*, vol. 81, no. 1, pp. 131–138, 2013.
- [293] R. Riccelli, N. Toschi, S. Nigro, A. Terracciano, and L. Passamonti, “Surface-based morphometry reveals the neuroanatomical basis of the five-factor model of personality,” *Social Cognitive and Affective Neuroscience*, vol. 12, no. 4, pp. 671–684, 2017.
- [294] H. Fu, J. Hardy, and K. E. Duff, “Selective vulnerability in neurodegenerative diseases,” *Nature Neuroscience*, vol. 21, no. 10, pp. 1350–1358, 2018.
- [295] A. E. Cavanna and M. R. Trimble, “The precuneus: a review of its functional anatomy and behavioural correlates,” *Brain*, vol. 129, no. 3, pp. 564–583, 2006.
- [296] E. Kumral, F. E. Bayam, and H. N. Özdemir, “Cognitive and behavioral disorders in patients with precuneal infarcts,” *European Neurology*, vol. 84, no. 3, pp. 157–167, 2021.
- [297] A. Ruitenbergh, T. Den Heijer, S. L. Bakker, J. C. Van Swieten, P. J. Koudstaal, A. Hofman, and M. M. Breteler, “Cerebral hypoperfusion and clinical onset of dementia: the rotterdam study,” *Annals of Neurology: Official Journal of the American Neurological Association and the Child Neurology Society*, vol. 57, no. 6, pp. 789–794, 2005.
- [298] X.-J. Liu, P. Che, M. Xing, X.-B. Tian, C. Gao, X. Li, and N. Zhang, “Cerebral hemodynamics and carotid atherosclerosis in patients with subcortical ischemic vascular dementia,” *Frontiers in Aging Neuroscience*, vol. 13, 2021. doi: 10.3389/fnagi.2021.741881
- [299] J.-P. Coutu, A. Goldblatt, H. D. Rosas, D. H. Salat, A. D. N. I. (ADNI *et al.*, “White matter changes are associated with ventricular expansion in aging, mild cognitive impairment, and alzheimer’s disease,” *Journal of Alzheimer’s Disease*, vol. 49, no. 2, pp. 329–342, 2016.
- [300] S. Haller, E. Kövari, F. R. Herrmann, V. Cuvinciuc, A.-M. Tömm, G. B. Zulian, K.-O. Lovblad, P. Giannakopoulos, and C. Bouras, “Do brain t2/flair white matter hyperintensities correspond to myelin loss in normal aging? a radiologic-neuropathologic correlation study,” *Acta Neuropathologica Communications*, vol. 1, no. 1, pp. 1–7, 2013.

- [301] J. Min, W.-J. Moon, J. Y. Jeon, J. W. Choi, Y.-S. Moon, and S.-H. Han, "Diagnostic efficacy of structural mri in patients with mild-to-moderate alzheimer disease: automated volumetric assessment versus visual assessment," *American Journal of Roentgenology*, vol. 208, no. 3, pp. 617–623, 2017.
- [302] C. W. Nordahl, C. Ranganath, A. P. Yonelinas, C. DeCarli, E. Fletcher, and W. J. Jagust, "White matter changes compromise prefrontal cortex function in healthy elderly individuals," *Journal of Cognitive Neuroscience*, vol. 18, no. 3, pp. 418–429, 2006.
- [303] S. N. Lockhart, A. B. Mayda, A. E. Roach, E. Fletcher, O. Carmichael, P. Maillard, C. G. Schwarz, A. P. Yonelinas, C. Ranganath, and C. DeCarli, "Episodic memory function is associated with multiple measures of white matter integrity in cognitive aging," *Frontiers in Human Neuroscience*, vol. 6, p. 56, 2012. doi: 10.3389/fnhum.2012.00056
- [304] L. H. T. Fornari, N. da Silva Júnior, C. M. Carpenedo, A. Hilbig, and C. R. de Mello Rieder, "Striatal dopamine correlates to memory and attention in parkinson's disease," *American Journal of Nuclear Medicine and Molecular Imaging*, vol. 11, no. 1, pp. 10–19, 2021.
- [305] V. K. Venkatraman, H. Aizenstein, J. Guralnik, A. B. Newman, N. W. Glynn, C. Taylor, S. Studenski, L. Launer, M. Pahor, J. Williamson *et al.*, "Executive control function, brain activation and white matter hyperintensities in older adults," *Neuroimage*, vol. 49, no. 4, pp. 3436–3442, 2010.
- [306] B. Rizvi, A. Narkhede, B. S. Last, M. Budge, G. Tosto, J. J. Manly, N. Schupf, R. Mayeux, and A. M. Brickman, "The effect of white matter hyperintensities on cognition is mediated by cortical atrophy," *Neurobiology of Aging*, vol. 64, pp. 25–32, 2018.
- [307] N. A. Ruiz, M. R. Meager, S. Agarwal, and M. Aly, "The medial temporal lobe is critical for spatial relational perception," *Journal of Cognitive Neuroscience*, vol. 32, no. 9, pp. 1780–1795, 2020.
- [308] J. S. Alisch, M. Kiely, C. Triebswetter, M. H. Alsameen, Z. Gong, N. Khattar, J. M. Egan, and M. Bouhrara, "Characterization of age-related differences in the human choroid plexus volume, microstructural integrity, and blood perfusion using multiparameter magnetic resonance imaging," *Frontiers in Aging Neuroscience*, p. 613, 2021. doi: 10.3389/fnagi.2021.734992

- [309] P. Lizano, O. Lutz, G. Ling, A. M. Lee, S. Eum, J. R. Bishop, S. Kelly, O. Pasternak, B. Clementz, G. Pearlson *et al.*, “Association of choroid plexus enlargement with cognitive, inflammatory, and structural phenotypes across the psychosis spectrum,” *American Journal of Psychiatry*, vol. 176, no. 7, pp. 564–572, 2019.
- [310] I. Kratzer, J. Ek, and H. Stolp, “The molecular anatomy and functions of the choroid plexus in healthy and diseased brain,” *Biochimica et Biophysica Acta (BBA)-Biomembranes*, vol. 1862, no. 11, p. 183430, 2020. doi: 10.1016/j.bbamem.2020.183430
- [311] W. Debanne, A. H. Diacon, L. John, and C. A. Johnson, “Population pharmacokinetics of azd-5847 in adults with tuberculosis abdullah alsultan1, 2, jennifer j. furin3, jeannine du bois4, elana van brakel4, phalkun chheng3, amour venter5, bonnie thiel3, sara a.” *Population*, vol. 1000, pp. S11–S122, 2016.
- [312] E. Moradi, I. Hallikainen, T. Hänninen, J. Tohka, A. D. N. Initiative *et al.*, “Rey’s auditory verbal learning test scores can be predicted from whole brain mri in alzheimer’s disease,” *NeuroImage: Clinical*, vol. 13, pp. 415–427, 2017.
- [313] M. N. Sabbagh, S. Hendrix, and J. E. Harrison, “Fda position statement “early alzheimer’s disease: Developing drugs for treatment, guidance for industry”,” *Alzheimer’s & Dementia: Translational Research & Clinical Interventions*, vol. 5, pp. 13–19, 2019.
- [314] B. Jie, M. Liu, J. Liu, D. Zhang, and D. Shen, “Temporally constrained group sparse learning for longitudinal data analysis in alzheimer’s disease,” *IEEE Transactions on Biomedical Engineering*, vol. 64, no. 1, pp. 238–249, 2016.
- [315] S. Hatashita and D. Wakebe, “Amyloid- $\beta$  deposition and long-term progression in mild cognitive impairment due to alzheimer’s disease defined with amyloid pet imaging,” *Journal of Alzheimer’s Disease*, vol. 57, no. 3, pp. 765–773, 2017.
- [316] H. Eichenbaum, “Hippocampus: cognitive processes and neural representations that underlie declarative memory,” *Neuron*, vol. 44, no. 1, pp. 109–120, 2004.
- [317] D. Kumaran and E. A. Maguire, “The human hippocampus: cognitive maps or relational memory?” *Journal of Neuroscience*, vol. 25, no. 31, pp. 7254–7259, 2005.

- [318] R. D. Rubin, P. D. Watson, M. C. Duff, and N. J. Cohen, “The role of the hippocampus in flexible cognition and social behavior,” *Frontiers in Human Neuroscience*, vol. 8, p. 742, 2014. doi: 10.3389/fnhum.2014.00742
- [319] I. Driscoll, D. A. Hamilton, H. Petropoulos, R. A. Yeo, W. M. Brooks, R. N. Baumgartner, and R. J. Sutherland, “The aging hippocampus: cognitive, biochemical and structural findings,” *Cerebral Cortex*, vol. 13, no. 12, pp. 1344–1351, 2003.
- [320] J. Lisman, G. Buzsáki, H. Eichenbaum, L. Nadel, C. Ranganath, and A. D. Redish, “Viewpoints: how the hippocampus contributes to memory, navigation and cognition,” *Nature Neuroscience*, vol. 20, no. 11, pp. 1434–1447, 2017.
- [321] A. Bechara, H. Damasio, and A. R. Damasio, “Role of the amygdala in decision-making,” *Annals of the New York Academy of Sciences*, vol. 985, no. 1, pp. 356–369, 2003.
- [322] S. P. Poulin, R. Dautoff, J. C. Morris, L. F. Barrett, B. C. Dickerson, A. D. N. Initiative *et al.*, “Amygdala atrophy is prominent in early alzheimer’s disease and relates to symptom severity,” *Psychiatry Research: Neuroimaging*, vol. 194, no. 1, pp. 7–13, 2011.
- [323] K. M. Gothard, “Multidimensional processing in the amygdala,” *Nature Reviews Neuroscience*, vol. 21, no. 10, pp. 565–575, 2020.
- [324] J. M. van Bergen, X. Li, F. C. Quevenco, A. F. Gietl, V. Treyer, S. E. Leh, R. Meyer, A. Buck, P. A. Kaufmann, R. M. Nitsch *et al.*, “Low cortical iron and high entorhinal cortex volume promote cognitive functioning in the oldest-old,” *Neurobiology of Aging*, vol. 64, pp. 68–75, 2018.
- [325] J. Berner, P. Grohs, and A. Jentzen, “Analysis of the generalization error: Empirical risk minimization over deep artificial neural networks overcomes the curse of dimensionality in the numerical approximation of black–scholes partial differential equations,” *SIAM Journal on Mathematics of Data Science*, vol. 2, no. 3, pp. 631–657, 2020.
- [326] J. H. Cole, R. P. Poudel, D. Tsagkrasoulis, M. W. Caan, C. Steves, T. D. Spector, and G. Montana, “Predicting brain age with deep learning from raw imaging data results in a reliable and heritable biomarker,” *NeuroImage*, vol. 163, pp. 115–124, 2017.

- [327] C. Bermudez, A. J. Plassard, S. Chaganti, Y. Huo, K. E. Aboud, L. E. Cutting, S. M. Resnick, and B. A. Landman, “Anatomical context improves deep learning on the brain age estimation task,” *Magnetic Resonance Imaging*, vol. 62, pp. 70–77, 2019.
- [328] X. Feng, Z. C. Lipton, J. Yang, S. A. Small, F. A. Provenzano, A. D. N. Initiative, F. L. D. N. Initiative *et al.*, “Estimating brain age based on a uniform healthy population with deep learning and structural mri,” *Neurobiology of Aging*, vol. 91, pp. 15–25, 2020.
- [329] B. A. Jónsson, G. Bjornsdottir, T. Thorgeirsson, L. M. Ellingsen, G. B. Walters, D. Gudbjartsson, H. Stefansson, K. Stefansson, and M. Ulfarsson, “Brain age prediction using deep learning uncovers associated sequence variants,” *Nature Communications*, vol. 10, no. 1, pp. 1–10, 2019.
- [330] J. Wen, E. Thibeau-Sutre, M. Diaz-Melo, J. Samper-González, A. Routier, S. Bottani, D. Dormont, S. Durrleman, N. Burgos, O. Colliot *et al.*, “Convolutional neural networks for classification of alzheimer’s disease: Overview and reproducible evaluation,” *Medical Image Analysis*, p. 101694, 2020. doi: 10.1016/j.media.2020.101694
- [331] G. Douaud, R. A. Menke, A. Gass, A. U. Monsch, A. Rao, B. Whitcher, G. Zamboni, P. M. Matthews, M. Sollberger, and S. Smith, “Brain microstructure reveals early abnormalities more than two years prior to clinical progression from mild cognitive impairment to alzheimer’s disease,” *Journal of Neuroscience*, vol. 33, no. 5, pp. 2147–2155, 2013.
- [332] “A computational anatomy toolbox for spm,” <http://www.neuro.uni-jena.de/cat/>, [Accessed: 2021-03-29].
- [333] P. Schmidt, “Bayesian inference for structured additive regression models for large-scale problems with applications to medical imaging,” Ph.D. dissertation, lmu, 2017.
- [334] “Diadem is an automated system for analysing mr brain scans, providing the clinician with an easily interpreted report that aids their diagnosis of dementia.” <https://www.brainminer.co.uk/products.html>, [Accessed: 2021-03-29].
- [335] “Enabling early diagnosis and efficient management of neurodegenerative diseases,” <https://www.cneuro.com/>, [Accessed: 2021-03-29].
- [336] “For the assessment of dementia, alzheimer’s disease and other neurodegenerative conditions.” <https://brainreader.net>, [Accessed: 2021-03-29].

- [337] “Providing an accurate and quantifiable insight to the brain.” <https://www.cortechs.ai/products/neuroquant/dementia/>, [Accessed: 2021-03-29].
- [338] “Fmrib software library,” <https://fsl.fmrib.ox.ac.uk/fsl/fslwiki/FAST>, [Accessed: 2021-03-29].
- [339] “Docker image for the interactive nipy tutorial,” [https://miykael.github.io/nipy/tutorial/notebooks/introduction\\_docker.html](https://miykael.github.io/nipy/tutorial/notebooks/introduction_docker.html), [Accessed: 2021-01-10].

## List of Publications

### Journal Publications

1. T. Habuza, N. Zaki, E. F. Mohamed, Y. Statsenko. "Deviation From Model of Normal Aging in Alzheimer's disease: Application of Deep Learning to Structural MRI data and Cognitive Tests", *IEEE Access*, p. 3174601, 2022. doi:10.1109/ACCESS.2022.3174601
2. T. Habuza, A. N. Navaz, F. Hashim, F. Alnajjar, N. Zaki, M. A. Serhani, and Y. Statsenko. "AI applications in robotics, precision medicine, and medical image analysis: an overview and future trends," *Informatics in Medicine Unlocked*, no. 24, p. 100596, 2021. doi:10.1016/j.imu.2021.100596
3. Y. Statsenko, T. Habuza, I. Charykova, K. N. V. Gorkom, N. Zaki, G. Baylis, M. Ljubisavljevic, T. M. Almansoor, and M. Belghali. "Predicting age from behavioral test performance for screening early onset of cognitive decline," *Frontiers in Aging Neuroscience*, no. 5, p. 661514, 2021. doi:10.3389/fnagi.2021.661514
4. Y. Statsenko, T. Habuza, D. Smetanina, G. L. Simiyu, L. Uziyanbaeva, K. N. V. Gorkom, N. Zaki, I. Charykova, J. Al Koteesh, T. M. Almansoori, et al. "Brain morphometry and cognitive performance in normal brain aging: Age- and sex-related structural and functional changes," *Frontiers in Aging Neuroscience*, no. 13, p. 713680, 2021. doi:10.3389/fnagi.2021.713680
5. Y. Statsenko, T. Habuza, K. N. V. Gorkom, N. Zaki, T. M. Almansoori, F. Al Zahmi, M. R. Ljubisavljevic, and M. Belghali. "Proportional changes in cognitive subdomains during normal brain aging," *Frontiers in Aging Neuroscience*, 673469, 2021. p. doi:10.3389/fnagi.2021.673469
6. Y. Statsenko, T. Habuza, K. N. V. Gorkom, N. Zaki, and T. M. Almansoori. "Applying the inverse efficiency score to visual-motor task for studying speed-accuracy performance while aging," *Frontiers in Aging Neuroscience*, no. 12. p. 574401, 2020. doi:10.3389/fnagi.2020.574401



7. Y. Statsenko, F. Al Zahmi, T. Habuza, K. N. V. Gorkom, and N. Zaki. "Prediction of COVID-19 severity using laboratory findings on admission: informative values, thresholds, ML model performance," *BMJ open*, vol. 11, no. 2, p. e044500, 2021. doi:10.1136/bmjopen-2020-044500
8. Y. Statsenko, F. Al Zahmi, T. Habuza, T. M. Almansoori, D. Smetanina, G. L. Simiyu, K. N. V. Gorkom et al. "Impact of Age and Sex on COVID-19 Severity Assessed From Radiologic and Clinical Findings," *Frontiers in Cellular and Infection Microbiology*, p. 1395, 2022. doi:10.3389/fcimb.2021.777070
9. F. Al Zahmi, T. Habuza, R. Awawdeh, H. Elshekhali, M. Lee, N. Salamin, R. Sajid et al. "Ethnicity-Specific Features of COVID-19 Among Arabs, Africans, South Asians, East Asians, and Caucasians in the United Arab Emirates," *Frontiers in Cellular and Infection Microbiology*, p. 1241, 2022. doi:10.3389/fcimb.2021.773141
10. B. Albreiki, T. Habuza, Z. Shuqfa, M. A. Serhani, N. Zaki, and S. Harous. "Customized Rule-Based Model to Identify At-Risk Students and Propose Rational Remedial Actions," *Big Data and Cognitive Computing*, vol. 5, no. 4, p. 71, 2021. doi:10.3390/bdcc5040071

### **Conference Proceedings Papers**

11. T. Habuza, B. Albreiki, N. Zaki, Y. Statsenko. "Reliability of deep learning MRI-based screening tool for accelerated aging," in *2022 UAE Graduate Student Research Conference (UAE GSRC 2022)*. Dubai, UAE, March, 2022.
12. T. Habuza, N. Zaki, Y. Statsenko, F. Alnajjar, S. Elyassami. "Predicting the diagnosis of dementia from MRI data: added value to cognitive tests," in *2021 7th Annual International Conference on Arab Women in Computing in Conjunction with the 2nd Forum of Women in Research*. August, 2021, pp. 1-7.
13. T. Habuza, N. Zaki, Y. Statsenko, and S. Elyassami. "MRI and cognitive tests-based screening tool for dementia," *Journal of the Neurological Sciences*, no. 429, 2021, p. 118964.

14. T. Habuza, N. Zaki, Y. Statsenko, S. Elyassami. "Early marker of dementia using deep learning," in *2021 3rd World aging & rejuvenation conference (ARC-2021)*. Barcelona, Spain, Sep., 2021. (<https://aging-geriatrics.com/>)
15. Y. Statsenko, T. Habuza, I. Charykova, K. N. V. Gorkom, N. Zaki, T. Almansoori, Milos Ljubisavljevic et al. "AI models of age-associated changes in CNS composition identified by MRI," *Journal of the Neurological Sciences*, no. 429, 2021, p. 118303.
16. T. Habuza, K. Khalil, N. Zaki, F. Alnajjar, and M. Gochoo, "Web-based multi-user concurrent job scheduling system on the shared computing resource objects," in *2020 14th International Conference on Innovations in Information Technology (IIT)*. IEEE, 2020, pp. 221–226.
17. N. Zaki, M. Al Yammahi, T. Habuza. "ProtRet: A Web Server for Retrieving Proteins in a Functional Complex" in *2019 International Conference on Practical Applications of Computational Biology & Bioinformatics*. Springer, Cham, June, 2019, pp. 1-7.

## **Appendices**

### **Appendix A: Definitions**

Cognition is the mental processes involved in gaining knowledge and comprehension. These cognitive processes include thinking, knowing, remembering, judging, perceiving, recognizing, conceiving, reasoning and problem-solving.

Cognitive domains are the domains of cognitive function. They are hierarchical. The bottom of the cognitive construct is responsible for information input and refers to basic sensory and perceptual processes. The top of the construct is higher-order cognitive functioning. It maintains information processing that involves synthesis, accumulation, and retrieval from memory storage. The functions enable goal-driven behavior in an individual. The top-level elements are executive functioning (EF) and cognitive control. The domains are cross-dependent with the prevalence of top-down versus bottom-up regulation. Broadly speaking, EF also encompasses cognitive control and exerts control over the use of more basic cognitive processes. Cognitive domains can be classified into memory, attention, language, and EF (e.g., reasoning and problem solving). EF is further classified into inhibition, task switching, working memory updating, and information speed processing, which are EF domains, or alternatively, cognitive subdomains.

Neuropathology is the study of disease of nervous system tissue, usually in the form of either small surgical biopsies or whole-body autopsies.

Gray matter (GM) is a major component of the central nervous system. It contains most of the brain's neuronal cell bodies, specifically

unmyelinated neurons. It is present in the brain, brainstem and cerebellum, and present throughout the spinal cord. GM includes regions of the brain involved in muscle control, and sensory perception such as seeing and hearing, memory, emotions, speech, decision making, and self-control.

White matter (WM) is an part of the central nervous system. It mainly made up of myelinated axons. White matter is composed of bundles, which connect various GM regions of the brain to each other. WM is responsible for the transmission of the nerve impulses between neurons.

Brain atrophy refers to a loss of brain cells or a loss in the number of connections between brain cells. Brain atrophy is a morphological basis of both aging and Neurodegenerative disorders.

Neurodegenerative disorder is incurable condition that result in death of neurons and a progressive deterioration, i.e. dementia.

Dementia is a syndrome in which there is a disturbance of higher mental function, such as reasoning, planning, judgment, and memorization. Dementia is one of the major causes of disability and dependency among older people worldwide.

Alzheimer's disease is the most common form of dementia and it may contribute to 60–70% of cases.

Mild cognitive impairment causes a slight but noticeable and measurable decline in cognitive abilities, including memory and thinking skills. It can be defined as the transition period from normal aging process to AD or another type of dementia.

## Appendix B: Evaluation measures

The set of methods we proposed in this research work (e.g. deep machine learning, computer vision, etc.) are known to be effective techniques for improving the current diagnostic approaches. In this case, we will consider the performance of the proposed models are satisfactory if the specificity and sensitivity of the classification models are higher than 85% and the fraction of the MAE over the range of the predicted feature is less than 10% based on the regression models.

Mean Absolute Error is used to assess the quality of the regression model. It is a measure of absolute difference between two continuous variables, which gives a clear understanding of the error between actual and predicted values for medical decision making community. Considering this evaluation metric, the MAE is calculated as follow:

$$MAE(y, \hat{y}) = \frac{1}{N} \sum_{i=1}^N |y_i - \hat{y}_i|$$

where  $y_i, \hat{y}_i$  are actual and predicted values of dependent variable respectively,  $i = \overline{1, N}$ ,  $N$  - number of samples.

To assess the quality of the classification models we use sensitivity, specificity, ROC AUC, accuracy and balanced accuracy metrics. The confusion or error matrix is built for each predictive model to show how it can distinguish between classes.

Receiver Operating Characteristic (ROC) curve and its Area Under the Curve (AUC) are used for performance evaluation of the classifiers and memorization of the trade-off between true positive rate (TPR) and false

positive rate (FPR) using different probability thresholds.

Sensitivity is true positive rate. It refers to an ability of a model to identify an individual with disease as positive.

Specificity is true negative rate. It refers to an ability of a model to identify a subject who does not have a disease as negative.

$$TPR(sensitivity) = \frac{TP}{TP + FN} \quad (4.1)$$

$$TNR(specificity) = \frac{TN}{TN + FP} \quad (4.2)$$

$$BAC(Balanced Accuracy) = \frac{Sensitivity + Specificity}{2} \quad (4.3)$$

The overall accuracy of the model is defined as:

$$Accuracy = \frac{TP + TN}{TP + TN + FP + FN} \quad (4.4)$$

where  $TP, TN, FP, FN$  are the true positive, true negative, false positive and false negative values representing the confusion matrix of classification model respectively.

All models are trained using k-fold cross-validation technique. The metrics are calculated for each fold separately and then averaged values are used as final measure.

## **Appendix C: Development of a CAD System for NDs Diagnosis**

The automatic assessment and interpretation of the results of the brain MRI findings may help doctors to provide a better diagnosis of NDs. Such tools may serve as an objective quantitative measurement of ND. CAD may accurately predict the state of the disease and its outcomes. There are plenty of algorithms available to analyze neuroimaging, however, they require a heterogeneous collection of specialized applications. There is no transparent way to incorporate results into one pipeline. The majority of the existing tools use and assess morphometry features extracted from MRI such as subcortical volume measurements. Morphometry features may be extracted from the structural MRI images utilising e.g., the Computational Anatomy Toolbox CAT12 for SPM [332], FreeSurfer[191], lesion prediction algorithm (LPA) [333] just to name a few. There are also a few proprietary solutions [334, 335, 336, 337] related to the assessment of the MRI images. All the mentioned solutions may help physicians to evaluate the level of cognitive impairments and memory loss indirectly. However, NDs are diagnosed with the help of cognitive assessments and this aspect should be taken in consideration. The incorporation of such tests into the pipeline of diagnosis may significantly improve the value of such CAD systems. The literature search for existing CAD systems that allow using cognitive tests results in their pipeline, revealed only one tool [335]. The cNeuro combines findings from brain MRI T1w and FLAIR modalities with results of cognitive tests. Its use is limited to the subscribed users only.

The availability of a tool that provides multi-modal analysis of findings is desired. The overall diagnosis process may be improved if online

cognitive tests and quantitative and qualitative analysis of the MRI findings can be incorporated in one pipeline. A comprehensive view of the patients' data will reduce the burden on the doctors. Such a data blending approach implemented in the CAD system will lead to more powerful solutions for healthcare professionals. The strengths and limitations of the available CAD systems are summarized in Table A1.

The development of the proposed CAD consists of three tasks:

- Design and implement of algorithms to visualize the areas of the brain which is affected by ND.
- Compose and deploy online version of psychophysiological and cognitive tests.
- Develop a predictive model to prognosticate the potential diagnosis of the ND.

The high-level pipeline of the proposed tool is described in Figure A1 and Figure A2. To solve the first task we will segment brain areas and highlight the structure with different color similar to Figure A3. Then we will look at the deviation of the brain structures volumes from normal aging assessed on our in-house dataset. These deviations may indicate an accelerated ageing.

To assess the separability measures between two groups and predict the final diagnosis we will conduct few steps. We propose to use a similarity measure by conducting the t-test and finding if there is significant differences between groups. This will allow us to show the potential of the reviewed attribute to be used as marker of the disease.



Table A1: Strengths and limitations of CAD systems to assist doctors in diagnosis of NDs

Product	Segmentation Cognitive tests Prediction Online Stand-alone app	Strengths	Limitations
FAST, FSL[338]	✓	<ul style="list-style-type: none"> <li>+ Segments a 3D image of the brain into different tissue types (GM, WM, CSF, etc.)</li> <li>+ It is robust and reliable</li> <li>+ Compared to most finite mixture model-based methods + Tissue volume quantification</li> </ul>	<ul style="list-style-type: none"> <li>- Limited number of tissues segmented</li> <li>- Is not specifically developed for the NDs diagnosis</li> <li>- Sensitive to noise</li> </ul>
CAT12, SPM [332]	✓	<ul style="list-style-type: none"> <li>+ Voxel-wise estimation of the local amount or volume of a specific tissue compartment</li> <li>+ Applied to investigate the local distribution of grey matter</li> <li>+ Permits to use gyrification indices that measure surface complexity in 3D</li> <li>+ Allows to estimate the cortical thickness</li> </ul>	<ul style="list-style-type: none"> <li>- Worse in matching of homologous cortical regions comparing methods that use geometry</li> <li>- Limited number of tissues segmented</li> <li>- No white matter hyperintensities evaluation</li> <li>- Is not specifically developed for the NDs diagnosis</li> </ul>
recon-all, FreeSurfer[191]	✓	<ul style="list-style-type: none"> <li>+ Segmentation and parcellation of brain regions</li> <li>+ FS uses geometry to do inter-subject registration</li> <li>+ Much better matching of homologous cortical regions than VBM techniques</li> <li>+ FS allows you to look at thickness and surface area</li> </ul>	<ul style="list-style-type: none"> <li>- Soft and hard-failure segmentation errors</li> <li>- Sensitive to artifacts due to intensity in homogeneity, head motion, reduced signal to noise ratio, and partial volume effects</li> <li>- Artifacts can all lead to reduced image quality, alterations in intensity values and, ultimately, errors in image segmentation</li> </ul>
LST, SPM [333]	✓	<ul style="list-style-type: none"> <li>+ Segments T2 hyperintense lesions in FLAIR images</li> <li>+ Proven to be useful for the segmentation of brain lesions in the context of Alzheimer's disease</li> </ul>	<ul style="list-style-type: none"> <li>- FLAIR image has to be provided</li> <li>- Limited number of tissues segmented</li> <li>- The choice of the initial threshold lead to different segmentation results</li> </ul>
Diadem, Brainminer [334]	✓	<ul style="list-style-type: none"> <li>+ Developed to aid in diagnosis of dementia</li> <li>+ Can be embedded in the clinical workflow (Connects directly to the hospital PACS)</li> <li>+ Automatically detects new MR scans that are suitable for processing</li> </ul>	<ul style="list-style-type: none"> <li>- The ML learning methods the tool is based on are not properly documented</li> <li>- All reports are based on in-house dataset</li> <li>- Proprietary tool, it is not publicly available</li> <li>- High price of the tool</li> </ul>
cNeuro, Combinostics [335]	✓	<ul style="list-style-type: none"> <li>+ Helps in early diagnosis of neurodegenerative diseases</li> <li>+ Quantitative assessment of brain images for providing clinical decision support in neurological disorders</li> <li>+ Cognitive assessment is incorporated into the tool</li> <li>+ Statistical comparison with a large reference database cognitively normal subjects</li> </ul>	<ul style="list-style-type: none"> <li>- Proprietary tool, it is not publicly available</li> <li>- High price of the tool</li> </ul>
Neuroreader, Brainreader[339]	✓	<ul style="list-style-type: none"> <li>+ Fast processing time</li> <li>+ Fits into clinical workflows with full PACS integration</li> <li>+ Includes list of all the structures showing abnormal volumes</li> </ul>	<ul style="list-style-type: none"> <li>- Is not specifically developed for the NDs diagnosis</li> <li>- Proprietary tool, it is not publicly available</li> <li>- Cognitive assessment is incorporated into the tool</li> <li>- High price of the tool</li> </ul>
NeuroQuant[337]	✓	<ul style="list-style-type: none"> <li>+ Automatic image segmentation from radiographic images</li> <li>+ Fits into clinical workflows with full PACS integration</li> <li>+ Allows monitoring structure volumes and visually evaluate changes</li> <li>+ Accuracy Across All Ages (3-100 y.o)</li> </ul>	<ul style="list-style-type: none"> <li>- The tool is not publicly available</li> <li>- Cognitive tests are not incorporated into the tool</li> <li>- High price of the tool</li> </ul>
Proposed	✓	<ul style="list-style-type: none"> <li>+ Automatic image segmentation from radiographic images</li> <li>+ Cognitive assessment is incorporated into the tool</li> <li>+ Publicly available</li> <li>+ Diversified normative dataset</li> </ul>	<ul style="list-style-type: none"> <li>- No integration into clinical workflows with PACS</li> <li>- No standalone application available</li> <li>- No approval for clinical use</li> </ul>

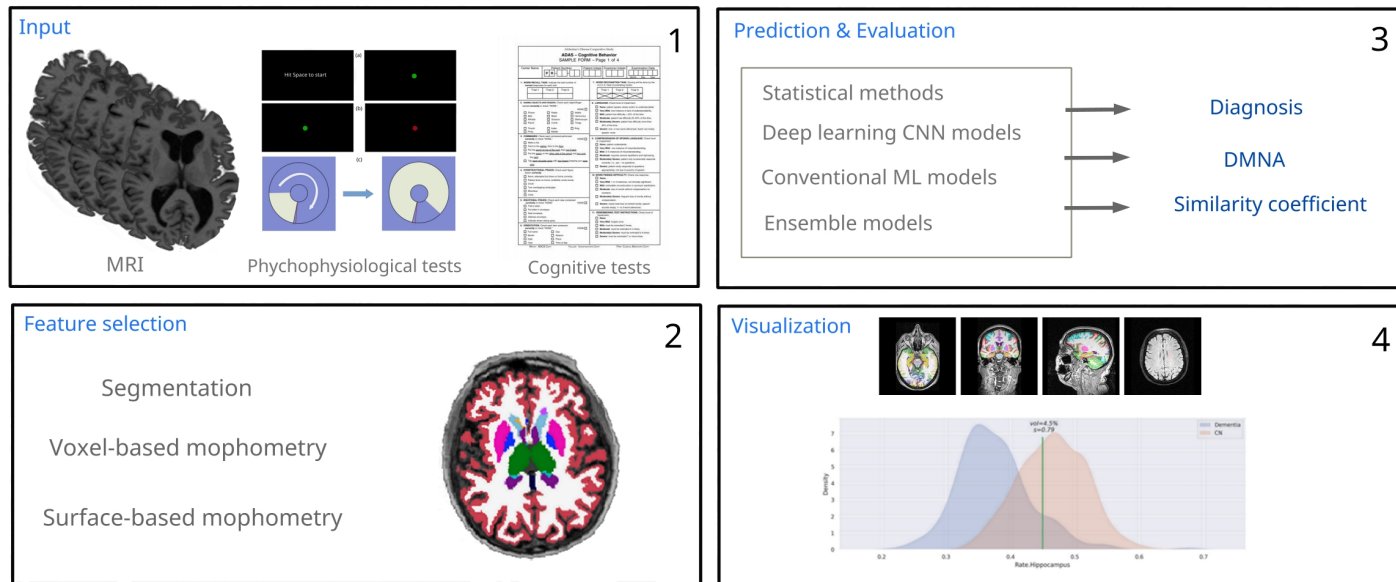


Figure A1: High-level pipeline of the proposed web-based CAD system

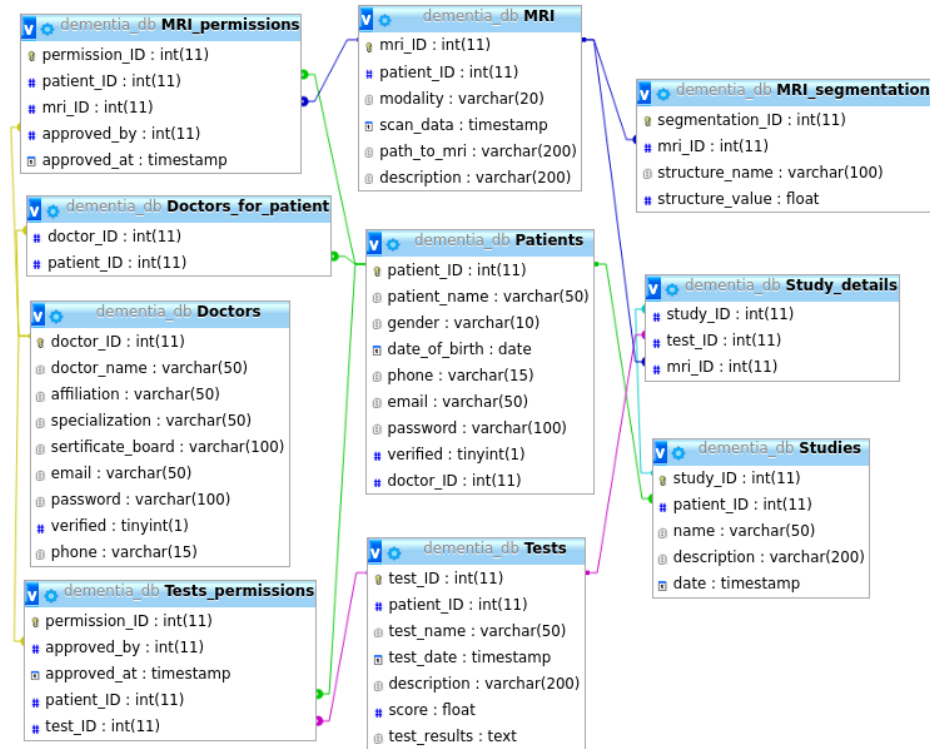


Figure A2: Entity relation diagram of the database of the proposed CAD system

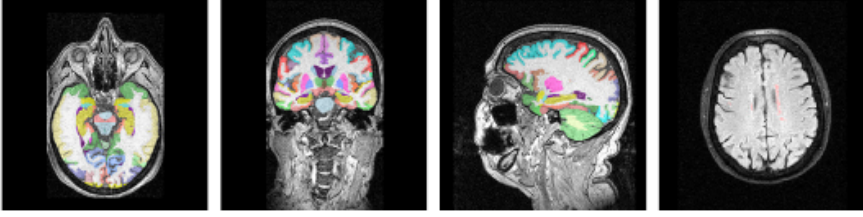


Figure A3: Sample of expected visualization of the brain structures segmented by the proposed CAD tool using T1w images

Next, we will build the probability density functions  $f_{cohort}(x)$  for each group from our dataset as it is shown in Figure A4. The studied subject's value  $e$  will be visualized with the vertical line. We will also calculate the similarity coefficient  $s$  as follows:

$$s = \frac{P_C}{P_C + P_D}, \quad (4.5)$$

where  $P_C$ , and  $P_D$  of are the probabilities that are calculated by formula 4.6 if expected value  $\mu_C$  for group C is smaller than  $\mu_D$  and with formula 4.7 otherwise. Here  $C$  corresponds to Control normal, and  $D$  to Dementia cohort.

$$\begin{aligned} P_C &= P_C(x \leq e) = \int_{-\infty}^e f_C(x) dx \\ P_D &= P_D(x \geq e) = \int_e^{\infty} f_D(x) dx \end{aligned} \quad (4.6)$$

$$\begin{aligned} P_C &= P_C(x \geq e) = \int_e^{\infty} f_C(x) dx \\ P_D &= P_D(x \leq e) = \int_{-\infty}^e f_D(x) dx \end{aligned} \quad (4.7)$$

The similarity coefficient  $s$  can obtain values between 0 and 1. If  $s$

is zero it means that there is no similarity between control normal group  $C$  and our examinee. Meanwhile, when  $s$  is one the subject is most probably belongs to the control normal group. The smaller the value of  $s$  ( $s < 0.5$ ) the higher the probability of disease state.

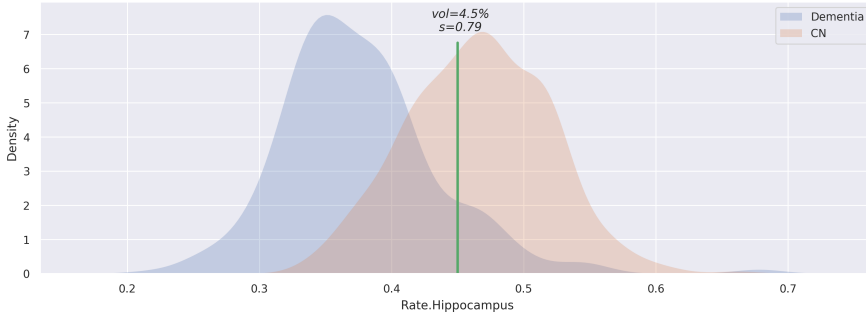


Figure A4: Sample of the expected output from proposed web-based CAD tool for relative hippocampus volume to show the separability measure between cognitively normal group and cohort diagnosed with dementia

The second task is related to design and implementation of web-based tool composed from cognitive tests for early detection of NDs.

To solve the third task the deep learning model will be developed to predict the cognitive status from structural data and prognosticate the diagnosis. As an input, the model may consist of images and numerical features, we will utilize ensemble modeling approach to enhance the model's performance and accuracy. Specifically, we will design the feedforward deep learning model. The feedforward regression algorithm will map an structural images  $x$  to a cognitive tests results  $y$  as follows:

$$y = f(x, w) \quad (4.8)$$

where  $w$  correspond to the parameters, that need to be optimized in order to reach the best approximation of function  $f(x, w)$ . We may present equation 4.8 in a form of:

$$y = f^{(n)}(f^{(n-1)}(\dots(f^{(1)}(x, w))))$$

where  $f^{(i)}$  represents the  $i^{th}$  layer out of  $n$  layers in NN.



## UAE UNIVERSITY DOCTORATE DISSERTATION NO. 2022: 9

Psychophysiological and cognitive tests as well as other functional studies can detect pre-symptomatic stages of dementia. When assembled with structural data, cognitive tests diagnose neurodegenerative disorders more reliably thus becoming a multimodal diagnostic tool. Screening for dementia can be improved by studying an association between the brain structure and its function.

**Tetiana Habuza** received her PhD from the Department of Computer Science and Software Engineering, College of Information Technology at UAE University, UAE. She received her MSc in Informatics from the College of Computer Science, Chernivtsi National University, Ukraine. She received her BSc in Applied Mathematics from the College of Computer Science, Chernivtsi National University, Ukraine.

[www.uaeu.ac.ae](http://www.uaeu.ac.ae)